RESPONSES OF VASCULAR CELLS TO SHEAR STRESS AND DIABETES-ASSOCIATED METABOLIC DYSFUNCTION

By

FARZANA ROUF

Bachelor of Science in Mechanical Engineering
Bangladesh University of Engineering and Technology
Dhaka, Bangladesh
2008

Master of Science in Mechanical and Aerospace Engineering
Oklahoma State University
Stillwater, OK
2011

Submitted to the Faculty of the
Graduate College of the
Oklahoma State University
in partial fulfillment of
the requirements for
the Degree of
DOCTOR OF PHILOSOPHY
December, 2016

RESPONSES OF VASCULAR CELLS TO SHEAR STRESS AND DIABETES-ASSOCIATED METABOLIC DYSFUNCTION

Dissertation Approved:

Dr. Arvind Santhanakrishnan

Dissertation Adviser (MAE)

Dr. Pamela G Lloyd

Dissertation Adviser (Physiological Sciences)

Dr. Kaan A Kalkan

Dr. Véronique Lacombe

ACKNOWLEDGEMENTS

I would like to take this opportunity to give special thanks to Dr. Pamela G Lloyd (my Physiological Science advisor) for her constant guidance, encouragement, and support during my graduate years. When my first PhD advisor left Oklahoma State University, I was unsure of continuing my PhD program. But, after talking to Dr. Lloyd and Dr. Daniel E Fisher (Head of the department, MAE), I found how supportive they are who wishes the very well for me. Therefore, I started fresh for the second part of my PhD. Dr. Fisher has provided me with departmental support and guidance for which I am very grateful to him. Dr. Lloyd not only gave me guidance with research, but also made me love science more and inspired me to try different things regarding my research work. I am grateful to her for giving me the opportunity to work in her lab. I have learned a lot under her supervision and became an inspired independent researcher, that surely will help me in the future. I would like to thank Dr. Arvind Santhanakrishnan (my new MAE advisor) for his suggestions and guidance from time to time. I would also like to thank Dr. Kaan Kalkan and Dr. Véronique Lacombe for serving in my committee and sharing their valuable thoughts with me. I want to thank Dr. Wei Yin (my first MAE advisor) for her guidance and inspiration during the first part of my PhD. I am thankful to all my previous and new lab colleagues, specially to Dr. Saravan Kumar, Dr. Nabil Rashdan, and Dr. Zahra Maria, who spent their valuable time arguing with me, inspiring me, and making the lab environment an enjoyable one. Thanks to all of my school and university friends who directly or indirectly motivated me through their mental support. At last, I would like to acknowledge the contribution of my loving family (mother: Hasina Akhter, husband: Dr. Salah Hamim, father: Abdur Rouf, sister: Fahmida Rouf, brother: Anisur Rouf, and son: Saadat Ahmed), the most important people in my life. My mother has spent endless nights thinking of me and praying for my wellbeing. She gave me comfort, support, and suggestions every single day of my PhD life. Without the sacrifice of my family, I could not have finished my PhD. Special thanks to my dear husband and my son, as they had to bear with me in every ups and downs. With their love, faith, constant support, and inspiration, I am who I am today. Therefore, this PhD degree is dedicated to my loving family.

Name: FARZANA ROUF

Date of Degree: December, 2016

Title of Study: RESPONSES OF VASCULAR CELLS TO SHEAR STRESS AND DIABETES-ASSOCIATED METABOLIC DYSFUNCTION

Major Field: MECHANICAL AND AEROSPACE ENGINEERING

Abstract:

Cardiovascular disease (CVD) is the leading cause of death worldwide, accounting for 30% of all deaths. Coronary artery disease (CAD - narrowing of arteries), most common type of CVD, results in altered shear stress that can affect platelets and endothelial cells (EC). Activated platelets and EC can express/secrete adhesion ligands, and inflammatory molecules, further promoting CVD. Previous functional studies utilized constant shear stress to activate either platelets or EC without considering EC/platelet communication. These conditions are not physiological. Therefore, we exposed platelets and EC together to physiological dynamic shear stress to study platelet and EC responses and signal pathway activation. Our results indicated that platelets showed increased PECAM-1 and decreased GPIbα and GPIIb expression, whereas EC showed increased soluble vWF expression and EMP generation in response to dynamic shear stress. We also found signaling pathway (MAPK and NF-κB) activation. Our results demonstrated that platelets enhance shear induced EC activation, which in turn leads to platelet-EC crosstalk that returns the activation level towards equilibrium by modulating platelet activation.

Arteriogenesis (remodeling of collateral arteries), a natural defense mechanism, attempts to preserve blood flow during CAD. Placental growth factor (PLGF) is a key arteriogenic growth factor. Diabetes is known to inhibit arteriogenesis, but how diabetes affects platelet uptake/release of PLGF, EC PLGF expression, and the underlying molecular mechanisms regulating PLGF has not been studied. Our results demonstrated that 1) platelets can take up PLGF; 2) simulated acute hyperglycemia (glucose treatment) and chronic hyperglycemia (AGE treatment) are the major contributors to impaired PLGF expression in cardiac and skeletal muscle cells; 3) elevated dynamic shear stress increases PLGF production by EC, and AGE can negatively modulate this effect; and 4) Western diet consumption can increase AGE levels in mouse skeletal muscle. We conclude that inhibition of PLGF expression by AGE contributes to impaired arteriogenesis in diabetes.

Findings from this study have advanced our knowledge of how platelets and EC interact in various physiological and pathophysiological settings, suggesting their contribution to CAD development. We also identified a possible mechanism for impaired arteriogenesis in diabetic patients. Thus, our study has the potential to lead to therapeutic innovations.

TABLE OF CONTENTS

Chapter Page

Chapter Page

Chapter Page

LIST OF TABLES

LIST OF FIGURES

Figure Page

Figure Page

Figure Page

LIST OF ABBREVIATIONS

CVD	Cardiovascular diseases
CAD	Coronary artery disease
PAD	Peripheral artery disease
EC	Endothelial cells
MI	Myocardial infarction
VEGF-A	Vascular endothelial growth factor-A
PLGF	Placental growth factor
AGE	Advanced glycation end products
LDL	Low density lipoprotein
vWF	von Willebrand factor
VEGFR	Vascular endothelial growth factor receptor
SMC	Smooth muscle cells
QF	Quadriceps femoris
G-P-S	Gastrocnemius/plantaris/soleus
CD	Control diet
WD	Western diet
Ox-LDL	Oxidize LDL
GPIbα	Glycoprotein Ibα
ECM	Extracellular membrane
LMA	Left main coronary artery
LAD	Left anterior descending
LCA	Left circumflex artery
NO	Nitric oxide
MAPK	Mitogen activated protein kinase
ICAM-1	Intracellular adhesion molecule
TF	Tissue factor
NF-κB	Nuclear factor-kappa B
PECAM-1	Platelet endothelial cell adhesion molecule-1
JNK	Jun amino-terminal kinases
RAGE	Receptor for advanced glycation end products
NOX	NADPH oxidase
HO-1	Heme oxygenase-1
MCP-1	Monocyte chemoattractant protein-1
TNF-α	Tumor necrosis factor-α
EMP	Endothelial microparticles
PMP	Platelet microparticles

CHAPTER I

INTRODUCTION

Cardiovascular diseases (CVD) are the number one cause of death around the world. According to the statistics from American Heart Association, in the USA, CVD accounted for about 31.3% of total deaths and affected approximately 86 million people in 2011[1]. Every year, over $320 billion is spent on direct and indirect medical care costs of CVD treatment and prevention in the USA alone[2]. Coronary artery disease (CAD) is the most common type of CVD and is characterized by localized narrowing (or stenosis) of the coronary arteries, resulting in decreased blood supply to different regions of the heart. Narrowing of arteries mainly occurs by the accumulation of lipids and fats in the inner lining of the endothelium of the blood vessels, induction of inflammatory responses, and formation of localized plaques. The plaques stiffen the blood vessel wall, which is widely known as "hardening of the arteries" or atherosclerosis. Atherosclerotic plaque can form in both large (macro-vessels involving arteries and veins) and small (micro-vessels involving capillaries and collaterals) blood vessels. Macrovascular plaque formation can lead to CAD, peripheral artery disease (PAD), and cerebrovascular diseases, whereas microvascular complications lead to disease conditions such as diabetic retinopathy, and neuropathy. Major determining factors for atherosclerotic plaque formation are 1) the location and 2) the geometry of the blood vessels. In the coronary circulation, the left coronary artery, especially areas near the bifurcation of the left anterior descending artery and the left circumflex artery, are vulnerable to

plaque formation due to their complex geometrical structure. In these regions, altered blood flow generates low recirculatory shear stress or oscillatory shear stress, which are considered to be atherogenic[3].

Peripheral artery disease (PAD) is another chronic circulatory disorder during which fatty substances deposit under the endothelium of the peripheral arteries limiting blood flow in the upper and lower limbs of the body. It is the leading cause of critical limb ischemia and amputation, as PAD often remains undiagnosed until the late stage. PAD affected around 18 million US people in 2010, which is predicted to reach 21 million by the year 2020[4;5]. Diabetic people are predisposed to develop cardiovascular diseases (such as CAD, PAD), at least 2-3 times more, and suffer greater complications. Currently, above 29 million US people have diabetes, and around 40% of them are diagnosed with PAD[6-8].

During both PAD and CAD development, endothelial cells (EC) and platelets, two major cell types of our body, become dysfunctional and undergo activation, further promoting disease progression. EC are the innermost layer of the arteries and platelets are circulating blood cells. Thus, both of these cell types are continuously exposed to blood flow. Hence, any changes in blood flow induced shear stress can greatly affect the normal functions of EC and platelets. Activated EC, stimulated by biochemical or biomechanical changes, express many adhesion ligands, secrete numerous cytokines, inflammatory molecules, and growth factors, and interact with circulating blood cells including platelets. Interaction between activated EC and platelets can induce platelets to secrete different biochemical substances which can further activate EC or nearby quiescent platelets, leading to thrombosis[9]. Studies have demonstrated that local shear stress conditions play a major role in EC and platelet activation, as well as cardiovascular and peripheral disease progression[10;11]. Although many *in vitro* studies have been conducted characterizing functional changes of platelet and EC in response to shear stress, most of these studies used constant shear stress to activate platelets and EC, which is

not physiologically relevant[12-14]. Also, most of these studies have investigated the effect of constant shear stress only on either platelet or EC without considering the effect of platelet-EC communication on modulation of their responses. Therefore, in our studies, we have exposed platelet and EC under physiologically relevant dynamic shear stress, found in healthy and diseased left coronary artery, using a cone-plate shearing device *in vitro* and investigated post shear platelet responses through platelet surface glycoproteins PECAM-1, GPIbα, GPIIb expression, and platelet microparticle generation. EC responses were also assessed through vWF and TF expression, and endothelial microparticle generation. Physiological relevance was further enhanced through an *ex vivo* study where freshly harvested rat aortas were exposed to dynamic shear stress for quantification of EC activation (vWF and ICAM-1) and inflammatory (TF) responses. Since, variation in shear stress can be transmitted from EC cell surface to nucleus via different signaling pathways to change functional responses, we also have investigated the effect of dynamic shear stress on MAPK and NF-κB pathway activation.

Activation and interaction of EC and platelets can narrow arteries through formation of plaques, decreasing oxygen and nutrient supply to distal tissues, which in acute conditions can lead to myocardial infarction (MI) or heart attack. However, the body has a natural defense mechanism that attempts to preserve blood flow in the downstream regions of the occluded blood vessels. This is a bypass mechanism known as arteriogenesis or radial enlargement of small pre-existing interconnecting collateral arteries, which under normal conditions carry little blood due to their high resistance. In the presence of an occlusion in the upstream regions of a main artery, collateral arteries remodel to carry an increased amount of blood, thus reducing ischemic tissue damage. Unfortunately, the extent of arteriogenesis varies greatly among people, and is negatively affected by disease conditions like diabetes. Surgical intervention to reopen or replace blocked arteries is not always feasible in many people with CAD and PAD, due to physical condition or age. Also, statistics show that 25 – 30% of CAD patients fail to revascularize even after coronary or femoral artery bypass surgery and have a

higher occurrence of restenosis[15]. Therefore, therapeutic stimulation of collateral artery growth is potentially a valuable and more desirable treatment for these patients than surgical intervention.

EC and platelets can contribute to arteriogenesis through the production/transportation of growth factors and modulation of growth factor receptor expression. During PAD or CAD development, the pressure gradient across the collateral arteries increases, elevating blood flow induced shear stress on the vessel wall and thus affecting cellular activities. Since shear stress has been shown to be a primary modulator of arteriogenesis, numerous studies have investigated the role of shear stress in activating EC and stimulating arteriogenesis through the release of growth factors[16;17]. However, most studies have focused on vascular endothelial growth factor-A (VEGF-A), which primarily promotes capillary proliferation, not arteriogenesis. Therefore, in our studies, we focused on placental growth factor (PLGF), a growth factor which is more specific for arteriogenesis. We have studied for the first time, how platelets can take up or release PLGF in response to physiologically relevant dynamic changes in shear stress. Our study also investigated how PLGF expression is modulated in different cell types (endothelial cells, cardiac muscle cells, and skeletal muscle cells) by diabetes-associated metabolic dysfunction. Diabetes, a serious metabolic disorder, can cause dysregulated expression of growth factors and receptors[18]. Diabetes is characterized by several metabolic dysfunctions such as hyperglycemia, hyperlipidemia, hyperinsulinemia, and oxidative stress. Sustained hyperglycemia leads to production of advanced glycation end products (AGE), and persistent hyperlipidemia increases low density lipoprotein (LDL) levels. Both of these compounds can greatly affect normal functions of EC and platelets[19].

Results from *in vivo* studies previously conducted in our lab have demonstrated that metabolic dysfunctions induced through 6 mo of Western diet feeding reduces tissue level PLGF expression in mice. Therefore, another goal of this study was to factor out which specific metabolic parameters have the greatest impact on cellular level PLGF expression, and to begin identifying the underlying mechanisms by which these parameters act to reduce PLGF in tissue levels. In addition, we asked

whether metabolic dysfunction would influence shear stress mediated PLGF expression at the molecular level, and which pathways would be involved.

In summary, the major goals of this study were to investigate the effects of physiologically relevant dynamic shear stress, cell-cell communication, and diabetes-associated metabolic factors on platelet and EC activities, and to understand how the changes in their behavior can contribute to 1) CAD progression and 2) arteriogenesis. Signaling pathways involved in modulation of cellular functions were also studied. Findings obtained from this study have provided insight into how dynamic shear stress and diabetes-associated metabolic dysfunction can modulate EC and platelet behavior, and may lead to potential therapeutic approaches to treat CAD progression or diabetic CAD/PAD.

CHAPTER II

SPECIFIC AIMS AND SIGNIFICANCE

The global hypothesis of this study was that blood flow induced pathological dynamic shear stress can regulate platelet and endothelial cell activities and lead to the progression of certain types of cardiovascular disease (CVD). CVD progression in turn can cause increased blood velocity through narrowed vessels, resulting in altered shear stress that can trigger compensatory collateral vessel remodeling (arteriogenesis) through further modulation of platelet and endothelial cell behavior. Presence of disease conditions such as diabetes can inhibit arteriogenesis. Therefore, we further hypothesized that presence of diabetes associated metabolic dysfunction and cell-cell interactions play important roles both in CVD development and in compensatory mechanisms for CVD. These hypotheses were tested through the following specific aims.

Specific aim 1: The goal of this aim was to measure platelet and endothelial cell (EC) responses under physiologically relevant dynamic shear stress conditions *in vitro*, and to determine whether the presence of one cell type affects the responses of the other to shear. In addition, the effects of dynamic shear stress on endothelial cell responses *ex vivo*, in a rat aorta model, was also investigated. Dynamic shear stress was applied on platelets in absence/presence of EC using a cone-plate shearing device *in vitro*. Post-shear, platelet responses were assessed by measuring cell surface PECAM-1, GPIbα, and GPIIb expression, as well as

platelet microparticle generation. EC responses were assessed by measuring cell surface and released von Willebrand factor (vWF) levels and tissue factor (TF) expression, as well as EC microparticle generation. *ex vivo* study was conducted by exposing freshly harvested rat aorta to dynamic shear stress in a perfusion flow chamber, followed by measurement of EC activation and inflammatory responses through vWF, ICAM-1, and TF protein expression.

Specific aim 2: The goal of this aim was to study signaling pathways involved in endothelial cell responses to dynamic shear stress. EC were exposed to dynamic shear stress and MAPK pathway activation was assessed through quantification of p38, JNK, and ERK1/2 protein phosphorylation. NF-κB pathway activation was measured through NF-κB p65 protein phosphorylation.

Specific aim 3: The goal of this aim was to characterize the uptake/release of endothelial growth factors by platelets, and to test the effect of dynamic shear stress on these processes. Platelets were incubated with different concentrations of recombinant human placental growth factor (PLGF) or vascular endothelial growth factor (VEGF-A), after which PLGF and VEGF-A uptake by platelets was quantified. The effect of shear stress, hyperglycemia, or calcium ion chelation on uptake/release of PLGF and VEGF-A was also assessed after exposing platelets to these conditions in the presence of recombinant human PLGF or VEGF-A.

Specific aim 4: The goal of this aim was to quantify the effect of diabetes-associated major metabolic dysfunction on the expression level of PLGF and vascular endothelial growth factor receptor 1 (VEGFR1, the receptor for PLGF) in mouse and human cell. Coronary artery EC, cardiac muscle cells, and skeletal muscle cells from both mouse and human were treated with low density lipoprotein (LDL), oxidized LDL, advanced glycation end products (AGE), and hydrogen peroxide, followed by quantification of PLGF level and cell surface VEGFR1.

Specific aim 5: The goal of this aim was to investigate the effects of glucose, advanced glycation end products (AGE), and the presence of smooth muscle cells (SMC) on dynamic shear stress-stimulated EC PLGF expression, and to identify the signaling pathways involved. EC-SMC co-cultures were exposed to dynamic shear stress in the presence or absence of glucose or AGE, followed by quantification of EC produced PLGF expression levels. Involvement of signaling pathways was investigated by assessing EC RAGE, Nox2 and Nox4, HO-1, MCP-1, and TNF-α levels.

Specific aim 6: The goal of this aim was to discover the key underlying molecular mechanisms by which a Western diet induces dysfunctional PLGF expression in mouse skeletal muscle. Thigh (quadriceps femoris, QF) and calf (gastrocnemius/plantaris/soleus, G-P-S) muscles of control diet (CD) and Western diet (WD) fed C57/BL6J and $ApoE^{-/-}$ mice were collected. Tissue AGE levels were quantified, and the activity of associated signaling pathways was assessed through measuring tissue RAGE, Nox2 and Nox4, HO-1, MCP-1, and TNF-α expression.

Many studies have investigated the effects of shear stress on platelets and EC[20;21]. The major limitations of these studies include 1) use of simplified constant shear stress and 2) lack of consideration of platelet-EC or EC-SMC communication/interaction. In the current studies, we addressed these limitations by exposing cells to physiological and pathological dynamic shear stress. We also tested the effect of cell-cell interaction on platelet and EC activities. In addition, we assessed the effect of Type 2 diabetes associated metabolic dysfunction on modulation of platelet and EC behavior. The physiological relevance of our research was further enhanced through the inclusion of *ex vivo* animal studies. The results obtained from this study have advanced our understanding of how shear stress, cell-cell interactions, and metabolic parameters influence both CVD development and adaptive responses (such as arteriogenesis) to CVD, and may lead to potential therapeutic solutions.

CHAPTER III

REVIEW OF LITERATURE

This study had two sections. In the first section, we have characterized changes in platelet and EC activation responses (through quantification of adhesion ligands and inflammatory molecules expression) under dynamic shear exposure to understand how they can contribute to CAD progression. The second section focused on how the key arteriogenic growth factor uptake/release, production, and growth factor receptor expression by platelet and EC are modulated in presence of diabetes associated metabolic parameters to understand the role of platelet and EC in arteriogenesis during diabetic CAD/PAD. Therefore, the literature review of these two sections are presented separately referring as study 1 and study 2.

3.1 Study 1

Atherosclerosis, a chronic inflammatory disease of the vasculature, is the underlying cause of coronary artery disease, peripheral artery disease, stroke, and heart attack. Arteriosclerosis is a type of atherosclerosis that refers to thickening and stiffening of the arteries. Under normal healthy conditions, the endothelium (the inner lining of the arteries) maintains vascular permeability and provides an atheroprotective environment. During atherosclerosis, this atheroprotective state is disrupted by EC dysfunction, which is characterized by increased permeability of the endothelium to macromolecules such as low density lipoprotein (LDL), increased adhesion of platelets and leukocytes, and upregulation of inflammatory molecules expression. As a result of these changes, LDL passes through the damaged endothelium and accumulates in the subendothelial space. White blood cells (particularly leukocytes and monocytes) transmigrate across the endothelium, after which they release enzymes, oxidize LDL, and initiate inflammatory signal cascades. With time, the accumulating inflammatory cells, cholesterol, and oxidized lipids form plaques that narrow the artery lumen and may eventually completely block the artery. Narrowing of the arteries alters both blood velocity and blood flow induced shear stress, factors that have been found to influence normal vascular cell activities and functions.

3.1.1 Blood vascular system

Blood vessels are blood carrying conduits that are flexible enough to move freely with the underlying tissues, but strong enough to accommodate changes in blood pressure. In the cardiovascular system, blood vessels are classified into five main categories: arteries, arterioles, capillaries, venules, and veins. Blood vessels that carry blood away from the heart are known as arteries and are the primary focus of these studies. The wall of arteries is composed of three distinct layers: the tunica interna, tunica media, and tunica externa. The tunica interna, the innermost layer of an artery, consists of a monolayer of endothelial cells (EC) surrounded by extracellular

membrane (ECM) proteins and a thick underlying elastic fiber layer. The tunica media, the middle layer of an artery, is composed of a concentric layer of smooth muscle cells (SMC) surrounded by extracellular basement membrane, and is separated from the tunica intima and tunica externa by the internal and external elastic laminae. In large arteries, the tunica media contains many layers of SMC. Contraction and relaxation of these SMC modulates the radius of the blood vessel and accommodates changes in blood pressure and/or volume. The tunica externa, the outermost layer of an artery, is composed mainly of collagen fibers and fibroblasts. The connective tissue of this layer blends into the surrounding tissue and provides anchorage and stability of the blood vessel.

3.1.2 Hemodynamics of coronary artery blood flow

Coronary arteries, which originate from the aortic root, supply oxygen- and nutrient- rich blood to the cardiac muscle to support the proper function of the heart. The left main coronary artery (LMA), supplies blood to the left side of the heart and has two major branches: the left anterior descending artery (LAD) and the left circumflex artery (LCA) (shown in Figure 3.1A).

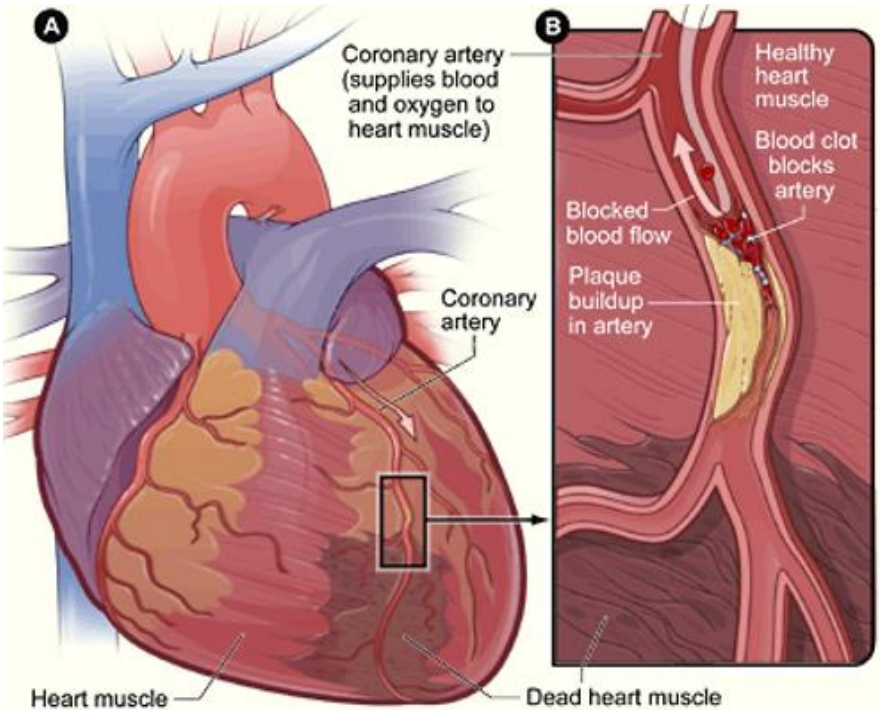

Figure 3.1: (A) Exterior anatomy of the heart. Atherosclerotic plaque formation has caused narrowing of the LAD, resulting in insufficient blood flow eventually leading to heart attack and muscle death in the region downstream of the occlusion. (B) Enlarged schematic representation of the atherosclerotic plaque inside the LAD branch. A blood clot has blocked blood flow completely, causing a heart attack (NIH NHLBI, 2015)[22].

The LMA is characterized by complex vascular geometry (such as bifurcations, twists, and curvature) and varying shear stress regions (due to flow skewing and flow separation). Therefore, the LMA has a high potential to develop atherosclerotic lesions[23]. Likewise, the presence of complex secondary flow (due to the curvature) and a bifurcation in the upstream region makes the LAD vulnerable to atherosclerosis (Figure 3.1B). The formation of atherosclerotic plaque inside the artery narrows the vessel diameter, altering local blood flow conditions and resulting in elevated, low, and/or oscillatory shear stress. It is well established that shear stress levels from 1.5-7 Pa are atheroprotective, whereas low shear stress (below 0.4 Pa) is atherogenic, and elevated shear stress (above 7 Pa) is pro-thrombotic on vascular EC[24-26].

As platelets travel along the blood vessel wall, they are exposed to shear stress at a magnitude similar to that experienced by EC. The large shear stress gradient within the stenotic (narrowed) region of an artery can rapidly activate platelets. Similarly, recirculation shear stress

conditions downstream of the stenosis can promote EC activation, possibly leading to platelet activation. Several studies have reported that platelet and EC activation is dependent on both shear stress magnitude and shear exposure duration[27;28]. Therefore, it is necessary to characterize platelet and EC responses under physiologically relevant dynamic shear stress conditions that replicate both normal and diseased states.

3.1.3 Endothelial cells

The endothelium is the innermost layer of the blood vessels and acts as a barrier between blood and tissues. Endothelium is comprised of endothelial cells (EC) which have a critical role in maintaining normal vascular function. ECs are ~10-20 μm in diameter, flat, cobblestone-like in shape, and have central nuclei. Under physiological conditions, the major function of EC is to maintain hemostasis. The other functions of EC include regulation of vascular permeability, transportation of molecules (nutrients, oxygen, waste) between blood and surrounding tissues, maintenance of an atheroprotective environment through production of nitric oxide (NO) and other mediators, and regulation of angiogenesis/arteriogenesis. EC release various vasoactive compounds (NO, prostaglandin, endothelin) that regulate vascular diameter and blood flow through acute responses such as vasodilation and vasoconstriction. These vasoactive compounds can inhibit platelet adhesion and aggregation as well[29]. However, under pathological conditions, in the presence of biochemical agonists (inflammatory cytokines including tumor necrosis factor-α, interleukin-6, thrombin, and ADP) and biomechanical agonists (shear stress), EC become activated and these normal activities are impaired. Activated EC release various mediators that are pro-coagulant and inflammatory in nature, and express adhesion molecules on their surface to facilitate adherence of platelets and leukocytes which may lead to thrombosis, atherosclerosis, and other inflammatory responses.

3.1.4 Endothelial cells and shear stress

Due to the pulsatile nature of blood flow, vascular EC and SMC are continuously exposed to blood flow induced shear stress and stretch. However, shear stress primarily affects EC, whereas cyclic stretch impacts SMC. Therefore, EC are sensitive to shear stress variation. Alterations in shear stress can be sensed by EC and converted to intracellular signals that can affect gene expression and cause structural and functional changes (such as remodeling, proliferation, migration) in EC.

In the vasculature, shear stress is defined as the tangential frictional force applied by flowing blood on the vessel wall. Assuming blood as a Newtonian fluid (fluid with a constant viscosity and laminar flow pattern), shear stress can be calculated using the following equation:

$$\tau = \mu(\frac{du}{dy}) \text{ (Equation 1)}$$

where τ is shear stress, μ is blood viscosity, u is blood velocity, y is distance from the vasculature surface, and $\left(\frac{du}{dy}\right)$ is the velocity gradient or shear rate.

Another way of quantifying shear stress in the vessel wall is using Hagen-Poiseuille's equation:

$$\tau = \frac{4\mu Q}{\pi r^3} \text{ (Equation 2)}$$

where τ is shear stress, μ is blood viscosity, Q is blood flow rate, and r is the internal radius of the vessel.

This equation is only applicable when the blood vessel is assumed to be a straight, inelastic cylinder where blood flow is laminar, steady, and behaves as a Newtonian fluid. This formula does not strictly replicate the blood flow exerted shear stress environment. However, because of the high

expense of imaging techniques like magnetic resonance imaging (MRI) and the unfeasibility of direct *in vivo* quantification of shear stress, the equation is useful for general approximation.

Detection of shear stress and transformation of mechanical force into intracellular signals has been a fascinating field of study for the last few decades. After years of study, researchers have found that EC can detect and respond to any changes in shear stress using integrins (GPIa/IIa, $\alpha_5\beta_1$), ion channels, receptors (VEGFR1/2/3), and adhesion molecules (PECAM-1) on their surface[30-33]. Blocking these proteins demonstrates that they act as mechanosensors, since a significant reduction in shear stress mediated signaling and corresponding changes in EC responses occurs following their inhibition[34-36]. After detecting a change in mechanical stimuli through these multiple mechanosensors, the EC transmits the signal from its surface to the nucleus via a network of signaling pathways, including the protein kinase C (PKC) pathway, the PI3K pathway, and the mitogen activated protein kinase (MAPK) pathway. Numerous studies confirmed the role of shear stress in activation of these pathways[37;38]. Shear mediated activation of different MAPK family members, such as ERK1/2 and JNK, has been found to regulate various transcription factors including NF-κB, which in turn controls gene expression of various proteins involved in cell activation (TNF-α), adhesion (ICAM-1), and inflammation (interleukins)[39-42].

The effect of shear stress on adhesion molecule expression/activation is of interest, since EC can interact with platelets and leukocytes using different adhesion glycoproteins present on their surface. Increased interaction may facilitate platelet and leukocyte adhesion, activation, and subsequent initiation and formation of atherosclerotic plaques. Some of the major adhesion molecules expressed/released by EC are intracellular adhesion molecule (ICAM-1), vascular cell adhesion molecule (VCAM-1), P-selectin, and von Willebrand Factor (vWF). In addition, the pro-thrombotic protein tissue factor (TF) plays a major role in thrombus formation, which can acutely occlude arteries already narrowed by atherosclerotic plaque and is the immediate cause of many heart attacks and strokes. The expression of all of these proteins can be affected by shear stress.

Nagel *et al*. reported up-regulation of ICAM-1 expression on human umbilical vein endothelial cells (HUVEC) when the cells were exposed to steady shear stress of 0.25-4.6 Pa[13]. Sampath *et al*. observed increased ICAM-1 mRNA expression when HUVEC were exposed to constant shear stress of 2.5 Pa for 12 hr[14]. However, ICAM-1 mRNA expression returned to basal levels with longer shear exposure duration (24 hr). Lin *et al*. reported that 1.2 Pa shear stress could induce a rapid but transient induction of tissue factor (TF) mRNA expression in HUVEC[20]. Beside ICAM-1 and TF, altered shear stress can also affect the expression of vWF by/on EC, as well as generation of endothelial cell microparticles. Results from these studies indicate that EC activated by altered shear stress can play a major role in CAD development.

3.1.4.1 Intracellular adhesion molecule-1 (ICAM-1)

ICAM-1 is a transmembrane glycoprotein of 95 kDa molecular weight, present on the EC and leukocyte cell surface. A low level of ICAM-1 is always present on the resting EC membrane and increases during cell activation. Therefore, ICAM-1 is often used as an activation marker for EC. Many studies have investigated the effects of shear stress on ICAM-1 expression. A study by Tsuboi *et al*. found a 2.7-fold increase in ICAM-1 expression after HUVEC were exposed to shear stress at 1.5 Pa in a parallel plate flow chamber for 4 hr, compared to non-sheared HUVEC[43]. A study by Nagel *et al*. reported a time-dependent and shear stress magnitude-independent upregulation of ICAM-1 expression in HUVEC in response to shear stresses varying between 0.25 to 4.6 Pa for 24 hr[13]. Morigi *et al*. also observed an increase in ICAM-1 expression after exposing HUVEC to 0.8 Pa shear stress[44]. Tsou *et al*.'s study indicated that ICAM-1 expression was enhanced as shear stress magnitude increased when human aortic endothelial cells (HAEC) were simultaneously exposed to TNF-α and shear stress (0 to 1.6 Pa for 4 hr)[45]. In a recent study conducted by Yin *et al*., dynamic shear stress (normal, low, and high) was used to stimulate bone marrow vascular EC[46]. Their results demonstrated a significant increase in ICAM-1 expression under the pathological low shear stress (0-0.4 Pa) condition, compared to the normal (0.05 to 1 Pa)

shear stress condition. A study by Davies *et al*. revealed that ICAM-1 expression was elevated in atherosclerotic regions, which further enhanced disease progression[47]. It is thus clear that EC surface ICAM-1 expression can be regulated by shear stress and can contribute to CVD.

3.1.4.2 Tissue factor (TF)

Tissue factor is a 47 kDa membrane bound glycoprotein that plays crucial role in blood coagulation during blood vessel injury. Activated/injured EC and leukocytes express TF on their surface and release soluble TF that binds to factor VII (coagulation factor, present in plasma) nearly irreversibly to form a TF:VII complex. This enzymatically inactive complex anchors to the TF expressing cells and is quickly (within 20 sec of vessel injury) cleaved to produce an active TF:VIIa complex. The TF:VIIa complex eventually activates factor Xa, leading to insoluble fibrin (a fibrous protein that facilitates blood clotting) formation.

An elevated level of TF is observed in EC under conditions of vascular injury, inflammation, and in the presence of various agonists (including serotonin, histamine, smoke, and shear stress). TF enhances expression of various coagulation factors including FIIa, FVIIa, and FXa. FIIa induces platelet activation through interaction with glycoproteins GPIbα and GPIIb/IIIa, whereas FVIIa and FXa induce MAPK pathway activation and NF-κB activation in EC[48].

Several studies have investigated the effects of shear stress on EC TF expression. Houston *et al*. exposed EC to shear stress of 1.5 Pa for up to 3 hr in a parallel plate flow chamber and found increased TF gene expression with increased shear exposure duration[49]. They also conducted an *in vivo* study where increased TF expression in the stenosed region of the artery wall was observed. Lin *et al*. reported a transient increase (within 4 to 6 hr) in TF activity after exposing HUVEC to shear stress at 1.2 Pa in a flow channel for 12 hr[20]. These studies suggest that TF expression level of EC is regulated by variations in shear stress.

3.1.4.3 von Willebrand factor (vWF)

vWF is a multimeric adhesion glycoprotein that has a major role in thrombus formation initiation. It acts as a bridging molecule between two platelets or between a platelet and exposed sub-endothelium, facilitating platelet-platelet and platelet-EC interaction. vWF multimers are of high molecular weight (>10,000 kDa) as they are composed of many identical subunits (each subunit is 250 kDa)[50]. vWF is exclusively synthesized in EC and megakaryocytes, and therefore is commonly used as an immunohistochemical marker for identifying EC. Depending on the size and location of the blood vessels, the level of vWF expression can vary. It has been observed that EC of larger blood vessels tend to have elevated vWF expression, compared to EC of microvessels[51;52].

vWF is stored in Weibel-Palade bodies of EC and α-granules of platelets. There is also some (~15%) vWF circulating in plasma. Upon cell activation, stored vWF is expressed on the cell surface and secreted into the plasma, increasing the local concentration of vWF[53]. Secreted vWF molecules have high thrombotic potential, as they can efficiently capture circulating platelets through multiple interaction sites. ADAMTS13 (a proteolytic enzyme) limits unnecessary thrombus formation by cleaving vWF, regulating the multimer size[54].

During vascular damage and exposure of the sub-endothelium, vWF is required for platelet adhesion, especially under high shear stress. Through GPIbα, platelets can adhere to the injured vessel wall by binding to vWF[55]. This vWF-GPIbα interaction causes intercellular signaling, platelet activation, and further engagement of other collagen receptors (such as $\alpha_2\beta_1$). In this process, glycoprotein GPIIb/IIIa also becomes activated and binds to fibrinogen or vWF to form platelet aggregates. Under pathological conditions, aggregation may continue, unless regulatory mechanisms are triggered or the blood vessel becomes occluded.

Since shear stress can modulate EC and platelet responses, several studies have investigated the effects of shear stress on expression and function of vWF. A study by Ruggeri *et*

al. reported that platelet adhesion was modulated only by GPIbα-vWF interaction at a shear rate of >500s^{-1} to 1000s^{-1} [56]. At that shear rate, the adhesive function of vWF is essential for the initial attachment of platelets to the thrombogenic blood vessel wall. Galbusera *et al*. found a shear stress magnitude dependent increase in levels of vWF in HUVEC cell supernatants after exposing HUVEC to 0.2, 0.8, and 1.2 Pa shear stress for 6-15 hr[57]. Though these researchers found a shear stress magnitude dependent increase in surface/released vWF expression, altered shear stress did not induce any change in vWF mRNA expression, indicating enhanced expression/secretion of stored vWF without an increase in new protein synthesis.

3.1.4.4 Endothelial microparticle generation

Endothelial microparticles (EMP) are small vesicles (<1.5 μm) shed from the EC membrane upon EC activation, injury, or during apoptosis. Activation/injury induces an increase in the intracellular calcium concentration, which subsequently causes translocation of phosphatidylserine (PS), activation of cytosolic enzymes, and cleavage of the cell membrane leading to membrane budding, i.e., EMP generation. Both biochemical (TNF-α, reactive oxygen species, inflammatory cytokines) and biomechanical (shear stress) stimulation can induce EC activation leading to EMP generation.

EMP contain phospholipids, coagulation proteins (tissue factor, thrombomodulin), and various adhesion molecules (vWF, ICAM-1, PECAM-1), since they are generated from activated EC[58-60]. EMP bind to different coagulation factors using surface phospholipids, and transfer TF to other cells (such as monocytes and platelets) through surface adhesion molecules resulting in pro-coagulant and pro-inflammatory responses[61-63]. EMP can also increase stiffness of arteries, decrease vasodilation by modulating nitric oxide production, and promote thrombus formation[64]. Recent studies demonstrated that EMP contain transcription factors, mRNA, and microRNA, indicating their many possible regulatory roles[65;66]. A gene profiling study reported that EMP generation

induced by thrombin eventually leads to activation of the transcription factor NF-κB[67;68]. Several groups have also studied MP generation upon shear stress exposure[69;70]. A study conducted by Vion *et al*. has reported that alterations in shear stress induce activation of Rho kinase and the ERK1/2 pathway, eventually leading to enhanced EMP release. In this study, HUVEC exposed to 0.2 Pa shear stress for 24 hr demonstrated increased EMP generation in a time dependent manner[70].

Though the presence of EMP in blood is a normal phenomenon, elevated EMP generation can be an indication of endothelial activation and dysfunction. Therefore, EMP generation has been quantified in many clinical studies as a marker of EC activation. Elevated levels of EMP have been correlated with alterations in shear stress under various pathological conditions including end-stage renal disease, acute coronary syndrome, hypertension, and atherosclerosis[71-74].

3.1.5 Signaling pathway

Signaling pathways are complex networks of protein components that transmit biochemical signals from the cell surface to the nucleus, contributing to various cellular functions including cell proliferation, differentiation, and gene expression. Mechanosensors on the EC surface, sense and convert extracellular mechanical (stretch or shear stress) or biochemical (cytokines, growth factors) signals into intracellular signals. The intracellular responses then trigger a chain of biochemical events which are transmitted through the cytoplasm to the nucleus by signaling pathways. Activation of multiple signaling cascades including the protein kinase C (PKC), Akt, and mitogen activated protein kinase (MAPK) pathways have been reported previously[75-77]. Since cellular functions depend greatly on the cell's ability to properly transduce a signal, it is necessary to study how the presence of pathological shear stress can modulate signaling pathway activation.

3.1.5.1 Mitogen activated protein kinase pathway

Mitogen activated protein kinases (MAPK) are serine/threonine specific protein kinases that regulate diverse biological functions including mitosis, cell differentiation, cell proliferation,

and gene expression. MAPK can be activated by extracellular stimulation (biochemical or biomechanical) that induces dual phosphorylation at serine/threonine and tyrosine residues. The MAPK family is composed of three sequentially acting kinase members: MAPK kinase kinase (MAPKKK), MAPK kinase (MAPKK), and MAPK. MAPKKK can phosphorylate and activate MAPKK which subsequently stimulates MAPK through dual phosphorylation. Activated MAPK then phosphorylates target substrates and induces activation of various protein kinases. A variety of stimuli such as growth factors, G-protein coupled receptor activation, and shear stress can activate MAPK. The most important MAPK members identified in mammals include extracellular signal regulated kinases 1 and 2 (ERK1/2), p38 (isoforms α, β, γ, δ), and c-Jun amino terminal kinases (JNKs) 1, 2, and 3. These kinases link extracellular stimuli to diverse cellular responses. Figure 3.2 represents activation of different MAPK family members and their roles in various biological responses.

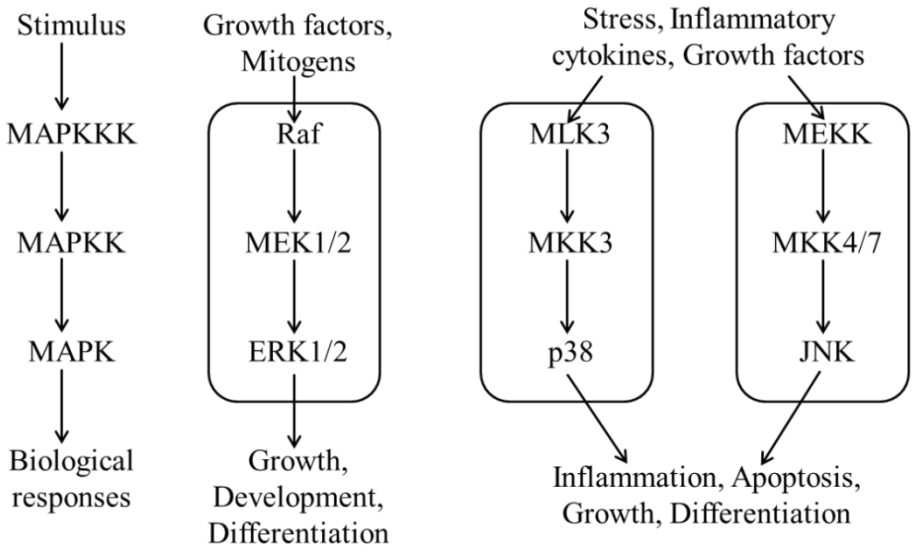

Figure 3.2: Mitogen activated protein kinase (MAPK) pathways.

ERK1/2 (molecular weight 42/44 kDa) is the first identified member of the MAPK cascade. ERK1/2 activation is initiated by the phosphorylation of Raf (a MAPKKK), which can phosphorylate MEK1/2 (MAPKK), leading to ERK1/2 (MAPK) activation[78]. Activated ERK1/2

can modulate cell proliferation, differentiation, and gene expression through phosphorylation of transcription factors, nuclear factors, and other kinases.

p38 is a 38 kDa protein kinase that is activated by stimuli such as cytokines, ultraviolet radiation, and physiological stress. Due to the variation of isoforms' expression, the activation level of p38 differs among tissues. Activated p38 is involved in various cellular functions including cell differentiation, apoptosis, and inflammation.

JNK, with isoforms of 46 and 54 kDa molecular weight, is activated by stimuli similar to those that activate p38. MKK4 and MKK7 are the two major upstream MAPKK that initiate JNK activation. Phosphorylated JNK can regulate inflammatory events by activating pro-inflammatory transcription factors (activator protein 1) and modulating gene expression of cytokine signaling molecules (interleukin 2 and 8).

Stimuli such as shear stress can activate MAPK family members. Many studies have investigated the effects of shear stress on ERK1/2, JNK, and p38 activation. In a study conducted by Li *et al*., ERK1/2 and JNK activation was observed when bovine aortic EC (BAEC) were exposed to shear stress at 1.2 Pa in a rectangular flow channel for up to 60 minutes[40]. Cheng *et al*. observed ERK1/2, p38, and JNK activation after exposing HUVEC to shear stress at 0.42 Pa for 2 hr in a parallel plate flow channel[79]. Shepherd *et al.* investigated the long term (up to 20 hr exposure) effect of pulsatile shear stress (2±1 and 1±0.3 Pa) on MAPK activation in human aortic EC[77]. Their results indicated time- and magnitude-dependent activation of ERK1/2, p38, and JNK by shear stress. Activated members of the MAPK pathway can engage in cross-talk, as they share different upstream and downstream kinase members. Each member can also negatively affect functions of other members[80]. A study by Zhang *et al*. demonstrated that activated p38 can inhibit phosphorylation of ERK1/2[81]. It has been also observed that ERK1/2 can regulate JNK function via MAPK phosphatase 2, indicating cross-talk among the members[82].

Activation of MAPK pathway members leads to phosphorylation of the transcription factor NF-κB, which can eventually lead to modulation of gene expression and protein synthesis of various adhesion molecules, cytokines, and growth factor receptors such as TF, ICAM-1, and VEGFR. Vega-Ostertag *et al*. found a significant increase in TF expression in antiphospholipid antibody-treated HUVEC due to phosphorylation of MAPK (p38) and NF-κB pathway[83]. Involvement of MAPK family members in modulation of EC surface expression of ICAM-1 has also been reported by several groups[84;85]. Tamura *et al*. found that inhibiting MAPK activation caused a decrease in ICAM-1 expression in pulmonary microvascular EC[86]. Curtis *et al*., using TNF-α treated human aortic endothelial cells, reported that MAPK pathway activation can selectively regulate generation and maturation of EMP[87]. Grugel *et al*. reported that oncogenes, associated with the MAPK pathway, can potentiate expression of VEGF which eventually modulates VEGFR expression[88].

3.1.5.2 Nuclear factor-κB (NF-κB)

NF-κB, a transcription factor, plays important roles in expression of various EC growth factors, cytokines (tumor necrosis factor-α), and inflammatory (ICAM-1, VCAM-1, E-selectin) genes[89]. NF-κB is generally sequestered in the cytoplasm by an inhibitory protein, IκB. This regulatory protein non-covalently interacts with NF-κB and prevents its translocation into the nucleus[90]. However, in the presence of certain stimuli (such as cytokines, growth factors, and shear stress), IκB specific kinases (IKK) phosphorylate IκB at its N-terminal residue and degrade the protein. As a result, NF-κB translocates into the nucleus and modulates gene transcription.

Phosphorylation of MAPK proteins plays a major role in activation and nuclear translocation of NF-κB[91]. Yang *et al*., by blocking p38 MAPK with an inhibitor, reported a significant decrease in NF-κB phosphorylation and translocation[92]. Their study also indicated that MAPK and NF-κB pathway activation can induce a pro-inflammatory phenotype in cardiac muscle

cells. Several other studies also reported modulation of transcriptional activity of NF-κB by MAPK members[93;94].

Since various cellular functions are dependent on NF-κB activation, it has been of interest to several researchers to study phosphorylation level of NF-κB with shear stress variation. Lan *et al.* observed NF-κB activation in bovine aortic EC after exposing cells to shear stress of 1.2 Pa for 1 hr[95]. NF-κB activation was reported to occur after 90 minutes by Liang *et al.*, when HUVEC were exposed to 0.42 Pa shear stress for up to 120 min[96]. Mohan *et al*. studied the effect of steady low shear (2 Pa), pulsatile low oscillatory shear (0.2±0.2 Pa), and physiological laminar shear (1.6 Pa) stress on human coronary artery endothelial cell (HCAEC) for up to 24 hr. Their results indicated that physiological laminar shear of 1.6 Pa can cause a rapid and transient increase in NF-κB activation that returns to baseline with longer shear exposure duration[97].

NF-κB activation can induce gene transcription of various immune and inflammatory proteins (including receptors, cytokines, and adhesion molecules) that are involved in EC activation. Read *et al*. indicated that TF expression can be modulated by NF-κB, as the TF gene carries recognition elements for NF-κB[98]. Several studies reported up-regulation of ICAM-1 expression by activated NF-κB[99;100]. Activation of NF-κB can regulate EMP generation as well through the synthesis of several cytokines including TNF-α, interleukin-1β, and interleukin-6[101].

The literature review above demonstrates that shear stress has a profound effect on EC activation as assessed by EC vWF, TF, ICAM-1, and VEGFR expression, EMP generation, as well as activation of MAPK and NF-κB signaling pathways. Since most of these previous studies utilized steady shear stress to activate EC, our goal was to characterize the physiological relevance of these EC responses under simulated blood flow induced dynamic shear stress conditions.

3.1.6 Platelets

Platelets are small non-nucleated cells, shed from megakaryocytes in bone marrow, that circulate through the blood. They are ellipsoidal in shape with a diameter of ~4 μm. Due to this ellipsoidal shape and small size, platelets are forced to travel along the apical surface of the endothelium by the blood flow, allowing platelets to respond rapidly to any vascular damage. The average lifespan of platelets is 10 to 12 days. Though the concentration of platelets in plasma varies among people, the normal physiological concentration is between 150,000-500,000/μL[102].

Resting platelets have a tri-laminate cytoskeletal membrane that gives them the discoid shape described above and allows them to encounter blood flow induced shear stress efficiently. The membrane is composed of a phospholipid bilayer with embedded cholesterol, glycolipids and many glycoproteins[103]. GPIbα and GPIIb/IIIa are the two most important platelet surface glycoproteins that play major role in platelet adhesion (GPIbα – receptor for vWF) and aggregation (GPIIb/IIIa – receptor for vWF or fibrinogen). In quiescent platelets, negatively charged phospholipids are present on the inside of the cell membrane; upon activation, these translocate to the outer surface of the cell membrane, participating in coagulation. Platelets also contain different organelles (peroxisomes, mitochondria) and granules in their cytoplasm that play important roles in platelet activities. There are two types of granules in platelets: α-granules and dense granules. Alpha granules are the most abundant type (50 to 80 per platelet) and the larger of the two types; they contain matrix adhesion molecules (vWF, fibronectin, and fibrinogen), growth factors [VEGF, basic fibroblast growth factor (bFGF)], and coagulation proteins (factor V and XIII). Alpha granules also contain P-selectin (a surface glycoprotein not expressed on quiescent platelets), GPIbα, and GPIIb/IIIa in their membranes that are translocated to the platelet surface upon activation. Dense bodies, another type of granule, contain biochemical mediators such as ADP, serotonin, thrombin, and calcium (Ca^{2+}). Upon stimulation, Ca^{2+} ions are released from dense bodies, raising the intracellular Ca^{2+} concentration from ~100nM to ~2-5 μM[104]. This Ca^{2+} ion

release is central to key platelet functions such as activation and adhesion. Activated platelets release substances from α- and dense granules, which then act as a positive feedback mechanism to induce further activation of nearby quiescent platelets[105].

The major function of platelets is to maintain hemostasis through detection of, and response to, any damage in the blood vessel wall. Platelets accomplish this feat through initial interaction of their specific surface membrane receptors with exposed connective tissue (collagen and laminin) or soluble factors such as plasma vWF released by the damaged endothelium. Interaction induces formation of pseudopods, translocation of negatively charged phospholipids to the outer membrane, secretion of α- and dense granule components, activation of signaling pathways that initiate production and release of platelet agonists (thromboxane, ADP, thrombin, collagen), and activation of surface integrins (GPIbα and GPIIb/IIIa). Under conditions of high shear stress, bound or soluble vWF interacts with the GPIbα complex on activated platelets, facilitating platelet adhesion to the damaged vessel wall[106]. This interaction results in activation of GPIIb/IIIa and GPIa/IIa on the platelet surface. Through GPIIb/IIIa, activated platelets can firmly adhere to the sub-endothelium and initiate platelet aggregation. Along with vWF, fibrinogen (a dimer) can also act as a bridging molecule between the GPIIb/IIIa receptors of two activated platelets[107]. However, in low shear stress regions, activated platelets use their GPIa/IIa receptors to adhere to collagen. Translocation of negatively charged phospholipids promotes the coagulation process by: 1) acting as a catalytic surface, 2) binding circulating coagulation factors, and 3) eventually forming a platelet plug (Figure 3.3) by trapping the platelets in the insoluble fibrin mesh formed at the end of the coagulation cascade.

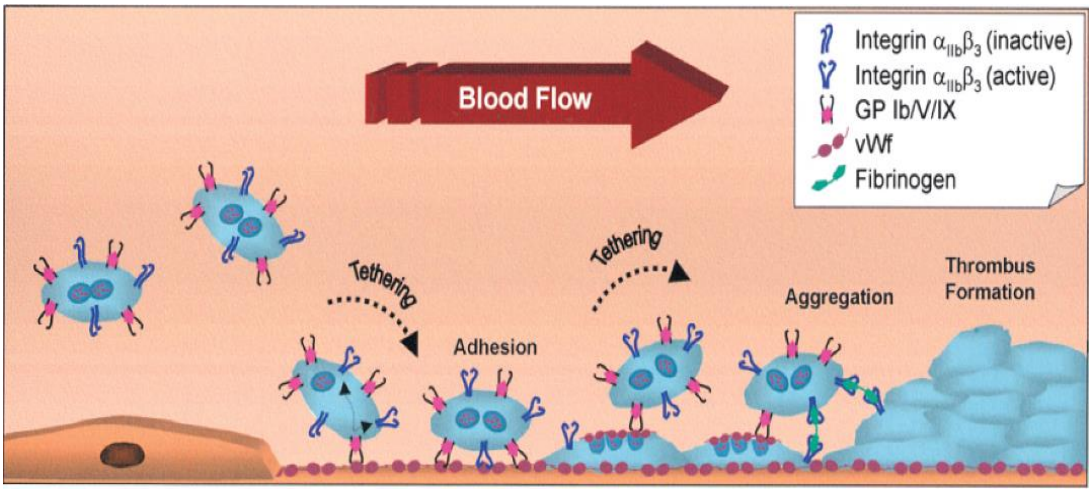

Figure 3.3: Dynamics of platelet dependent thrombus formation[108].

Under physiological conditions, this plug formation remains controlled, and the plug is later dissolved (hemostasis). However, during pathological conditions, unregulated clotting activity can happen, resulting in thrombosis (formation of a clot within a blood vessel). Thrombus formation may narrow the blood vessel lumen and change the local blood flow rate, inducing altered shear stress which can promote disease pathogenesis by further activating platelets and endothelium.

3.1.7 Platelets and shear stress

Blood flow induced shear stress, especially altered shear stress, can induce platelet activation, adhesion, and aggregation. Many investigators have studied the effects of shear stress on platelet responses[109]. Brown *et al*. reported both platelet activation and aggregation when platelets were exposed to shear stress at 5 Pa in a cone-plate shearing system[110]. Their findings also showed platelet lysis at 10 Pa and platelet fragmentation at 25 Pa. A study conducted by Anderson *et al*. demonstrated that platelet lysis occurred when platelets were exposed to shear stress of 16 Pa for 5 min, or 60 Pa for less than 30 sec, indicating the importance of considering shear exposure time as a parameter during platelet functional studies[12]. Yin *et al.* also demonstrated that low shear stress (0.24 Pa) can activate platelets if the shear exposure time is long enough[111]. Apparently,

either a short exposure to high shear stress or a long exposure to low shear stress can both lead to platelet activation[12]. Exposing platelets to various shear stress levels (30, 75, or 100 Pa) for 25-1650 ms, Ramstack *et al*. also reached to this conclusion[21]. A study by Bluestein *et al*. indicated that platelets exposed to high shear (5, 6, or 7 Pa for 5-40 sec) and subsequent low shear stress (0.1 Pa for 14-60 min) activate 20 times faster than platelets not exposed to the initial high shear condition[112].

Platelet activation can lead to expression and activation of various surface glycoproteins (including PECAM-1, GPIbα, and GPIIb/IIIa) which can participate in platelet adhesion and aggregation. Dysregulated expression of these proteins can contribute to atherosclerosis or thrombosis.

3.1.7.1 Platelet endothelial cell adhesion molecule (PECAM-1)

PECAM-1 is a 130 kDa glycoprotein expressed on the membrane of platelets and in the intracellular junctions of EC[113;114]. Upon activation, a significant increase in PECAM-1 expression is observed on the platelet membrane. When platelets were activated by thrombin, Wu *et al*. and Metzelaar *et al*. found a three-fold increase in surface PECAM-1 expression compared to that of resting platelets[115;116]. Whether the increase in PECAM-1 expression was due to the increased exposed surface area of activated platelets or to fusion of α-granules containing PECAM-1 is yet to be elucidated. The presence of PECAM-1 in α-granules is also still controversial as one study reported no PECAM-1, whereas another found a significant amount of PECAM-1 localized in α-granules[115;117].

The major role of PECAM-1 is to mediate cell-cell interaction by acting as an adhesion molecule. PECAM-1 receptors expressed in one cell can interact with both homophilic (PECAM-1) and heterophilic (integrin $\alpha_V\beta3$) ligands of adjacent cells. Other functions of PECAM-1 include up-regulation of integrin functions and participation as a mechanosensing molecule. As PECAM-

1 is expressed on the cell surface or in cell junctions, it can be directly activated by blood flow induced shear stress[118]. The cytoplasmic tail of PECAM-1 has several serine, threonine, and tyrosine residues that are phosphorylated during cell activation. Phosphorylation of PECAM-1 tyrosine residues has been detected in both fluid shear stress stimulated EC and in aggregating platelets[119;120]. Phosphorylated PECAM-1 can activate the MAPK pathway and NF-κB. Thus, PECAM-1 is a major player in signal transduction. Several studies, using PECAM-1 knockout mouse models, have reported the contribution of PECAM-1 to the initiation and progression of atherosclerosis[121;122]. These studies indicated that atherosclerosis developed mainly in the flow reversal regions due to continuous expression and activation of PECAM-1. Interestingly, in the unidirectional flow region, atherosclerotic development was not observed, which the researchers have attributed to the adaptation or desensitization of PECAM-1 with time. Blocking PECAM-1 with an antibody in a rat model, Gumina *et al*. demonstrated a significant reduction in myocardial infarct size as cell adhesion to the myocardium decreased, confirming the role of PECAM-1 in atherosclerotic plaque development[123].

Though PECAM-1 potentially acts as an initiator of EC activation, several studies reported that PECAM-1 also acts as a potent inhibitor of platelet activation[124]. Cicmil *et al*. reported that cross-linking of PECAM-1, in presence of collagen and thrombin, can inhibit platelet activation and aggregation *in vivo*[125]. In another *in vivo* study, conducted by Falati *et al*., large and stable thrombus formation was observed in PECAM-1 deficient mice compared to control mice[126]. Rathore *et al*. indicated that, along with an activation signal, GPIbα-vWF interaction triggers a negative feedback loop involving PECAM-1 that can modulate the rate and extent of platelet function[127]. Since PECAM-1 potentially plays a controversial role in activation of platelets and EC, it is of interest to investigate the effects of dynamic shear stress on PECAM-1 expression and function.

3.1.7.2 GPIIb/IIIa complex

GPIIb/IIIa is the most abundant platelet membrane glycoprotein and plays an important role in platelet aggregation. It is a heterodimer consisting of an α subunit (GPIIb) and a β subunit (GPIIIa)[128]. Resting platelets have ~80,000 inactive GPIIb/IIIa molecules randomly distributed on their surface, which accounts for about 1.5% of the total protein in platelets[129;130]. Along with the randomly distributed GPIIb/IIIa on the platelet membrane, α-granules also contain a pool of GPIIb/IIIa[131].

Activation of platelets initiates signaling events that cause a conformational change in platelet surface GPIIb/IIIa. This change transforms the protein from the inactive to the active state, resulting in increased affinity for receptors such as vWF, fibrinogen, and fibronectin. Fibrinogen and vWF can act as bridging molecules between two GPIIb/IIIa receptors on different platelets and accelerate platelet aggregation. Activation of GPIIb/IIIa can also enhance platelet spreading, procoagulant granules secretion, and clot retraction[132].

Several studies have investigated the effects of various agonists, including shear stress, on GPIIb/IIIa activation. Ikeda *et al*. observed that, under low shear stress, platelet aggregation was induced by the interaction between GPIIb/IIIa and fibrinogen[133]. However, the formed aggregate was unstable and disintegrated under higher shear stress conditions. Their study also demonstrated that interaction of vWF with both GPIbα and GPIIb/IIIa was necessary for stable aggregates to form under high shear stress. Initial interaction between immobilized vWF and platelet GPIbα, under high shear stress, triggers an increase in intracellular calcium concentration, in turn inducing release of various activating factors by platelets, and activation of the GPIIb/IIIa receptor[134-136]. Activated GPIIb/IIIa then interacts primarily with vWF (under high shear stress) and fibrinogen (under low shear stress) to form stable aggregates. However, a recent study reported that GPIIb/IIIa

mediated signaling can regulate both platelet activation and aggregation independent of the vWF-GPIbα interaction[132].

The major function of GPIIb/IIIa is to induce platelet aggregation during hemostasis. Dysfunction of this glycoprotein can lead to disease conditions including mild bleeding disorder, myocardial infarction, and stroke[137;138]. Though GPIIb/IIIa makes a crucial contribution to aggregation and thrombus formation, no study has yet investigated the effects of physiologically relevant dynamic shear stress on platelet GPIIb/IIIa expression.

3.1.7.3 Platelet microparticle generation

Platelet microparticles (PMP) are small plasma membrane vesicles shed by platelets during activation and apoptosis[139]. Due to their small size (0.1 to 1 μm), PMP were first described as "platelet dust"[140]. As PMP are generated by membrane shedding, they contain most of the glycoproteins found in intact platelets, including P-selectin, PECAM-1, GPIbα, and GPIIb/IIIa[141]. PMP also express negatively charged phospholipids on their membrane and have multiple binding sites for coagulation factors including factor Va and Xa. Due to these binding sites, PMP are more procoagulant (~100 times) than activated platelets[142]. The presence of different glycoprotein receptors on the surface of PMP enables them to interact with different cell types (platelets and EC) inducing cell activation and facilitating platelet adhesion to the vascular wall[143;144].

Fracture of pseudopods of activated platelets under high shear stress conditions is one of the mechanisms for PMP generation[145]. Interaction of platelet surface receptor GPIbα with vWF can also lead to PMP generation via an increase in cytosolic calcium concentration which subsequently inhibits phosphatases, activates kinases and calpain (a calcium dependent protease), leading to disruption of the membrane cytoskeleton and formation of PMP[146;147;148]. However, in apoptotic cells, instead of cytosolic calcium, activation of caspases induces PMP generation.

Several studies have investigated the effects of shear stress on PMP generation[149]. Exposing platelets to shear stress of 10.8 Pa, Nomura *et al*. observed an increase in PMP generation[109]. The generated PMP further activated platelets, acting as a positive feedback mechanism, and induced the release of inflammatory cytokines. Holme *et al*. sheared whole blood at 1.3, 8, and 31.5 Pa for 0.075 sec to 3.045 sec using a parallel plate perfusion chamber and found an increase in PMP generation in a shear stress magnitude dependent manner[150].

PMP have been observed to increase in various disease conditions like hypertension, transient ischemic attack, and myocardial infarction, but to decrease in mild bleeding disorder[151;152]. As PMP generation varies with different disease conditions, it can be used as an early predictor of disease development.

3.1.8 Cell-cell interaction

Cell-cell interaction can greatly affect cellular functions, contributing to many physiological and pathological conditions[153]. Both platelet-EC and EC-SMC communication play a vital role in modulation of their individual behavior. Under physiological conditions, healthy EC inhibit platelet activation and adhesion by providing an atheroprotective surface and releasing platelet activation inhibiting substances such as NO and prostacyclin (PGI_2). Although NO can directly activate platelet guanylyl cyclase to synthesize cyclic guanosine monophosphate GMP (cGMP), PGI_2 first binds with platelet surface G-protein coupled receptors to activate platelet adenyl cyclase to produce cyclic adenosine monophosphate (cAMP). cGMP and cAMP inhibit increase in the intracellular Ca^{2+} ion level and, thus prevent any undue activation of platelets. Hence, though platelets travel along the close proximity of the EC of the vasculature, they do not interact with EC under normal conditions, providing natural resistance to thrombus formation. In response to vascular damage, platelets and EC work together to support coagulation, form and dissolve thrombi, and repair damaged tissues. Beside working as platelet activation inhibitors, NO

and PGI_2 can act as potent vasodilators by modulating SMC contractile properties. On the other hand, SMC can modulate EC function through release of different pro-inflammatory molecules such as cyclophilin A.

Generally, platelets, EC, and SMC all stay in a non-activated and non-proliferative state. However, under pathological conditions, the normal function of EC and SMC is disrupted resulting in overexpression of adhesion ligands, upregulation of cytokines and inflammatory molecules, release of platelet activating agents, and a switch of the SMC phenotype from contractile to secretory/proliferative state. These events lead to platelet activation and adhesion to the vascular wall, perpetuating disease progression. It has been established that interaction between platelets and EC is involved at every stage of atherosclerosis, and the interaction is greatly modulated by blood flow induced shear stress[154]. Events associated with platelet and EC activation, platelet-EC interaction, and platelet aggregation are summarized in Figure 3.4. Endothelial cells and activated platelets interact with each other through the expression of many inflammatory and adhesion proteins, including TF, GPIbα, vWF, ICAM-1 and GPIIb/IIIa. Adhesion takes place when activated platelets bind to activated EC or damaged sub-endothelium through GPIbα-vWF interaction. Platelets may also bind to activated EC through P-selectin or PECAM-1 expressed on the surface of both cell types[9;119]. After initial adhesion, platelets start to form aggregates with surrounding activated platelets through GPIIb/IIIa interaction. Fibrinogen and vWF serve as links between two GPIIb/IIIa or GPIIb/IIIa and ICAM-1 receptors, thus facilitating adhesion and aggregation which can contribute to thrombosis or atherosclerotic plaque formation.

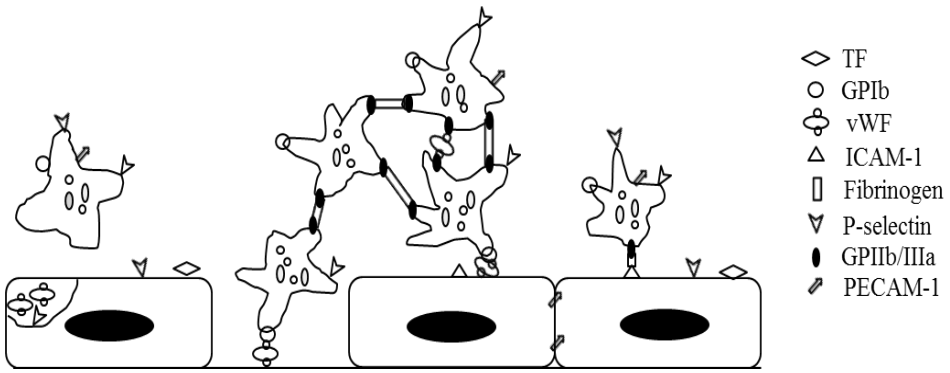

Figure 3.4: Schematic representation of platelet and EC activation, their interaction, and platelet aggregation.

Different studies have investigated the effects of shear stress on platelet and EC responses. However, very few of them focused on how platelet/EC interactions affect platelet and EC behavior in response to shear exposure. Moreover, most of these studies utilized constant shear stress for platelet and EC activation. A study by Martin *et al*. indicated that activated EC express P-selectin glycoprotein ligand-1 (PSGL-1) on their surface, which can mediate platelet tethering and rolling via P-selectin–PSGL-1 binding[155]. Frenette *et al*. showed that this P-selectin–PSGL-1 binding happens in a low shear stress environment. Activated platelets and EC also generate microparticles under high shear stress exposure, which increase cytokine production and induce adhesion molecule expression on both platelets and EC[109,156].

The above literature review indicates that interactions between platelets and EC can affect their functions and activities. Also, different shear stress magnitudes and exposure durations have different effects on platelet and EC behavior. Therefore, the goal of study 1 was to apply physiologically relevant dynamic shear stress mimicking conditions in both healthy and diseased coronary arteries to platelets and EC, in order to better understand how dynamic shear stress and platelet-EC interactions can modulate activation in both cell types. Furthermore, we wished to determine how the corresponding signaling pathways are affected, especially under disease conditions. Our findings demonstrated that dynamic shear stress and platelet-EC communication can affect their activation through modulation of expression/release of different surface adhesion

ligands (platelet PECAM-1, GPIbα, and GPIIb; EC vWF), EMP generation, as well as EC signal transduction pathways (MAPK and NF-κB). Findings from this study may lead to potential therapeutic approaches to treat CAD progression.

3.2 Study 2

In addition to the large arteries, some tissues also contain much smaller (~30 -100 μm diameter) interconnecting blood vessels known as “collateral arteries.”. Collateral arteries are natural bypasses which connect two major arteries that supply neighboring perfusion zones. Due to their narrow diameter and high resistance, collateral arteries carry little blood under physiological conditions. Only during vascular occlusion, when there is a drop in the pressure gradient across the collateral due to a blockage in one of the two major blood vessels, does blood starts re-routing through the collaterals. Under these circumstances, collaterals may increase their local flow capacity up to 200 fold. This increase in blood flow activates signaling pathways that leads to vascular remodeling. This process of collateral growth (or arteriogenesis) enables collateral arteries to accommodate a significantly increased amount of blood flow.

3.2.1 Hemodynamics of coronary collateral artery blood flow

Coronary collateral arteries can carry blood to myocardial areas that are at risk of ischemia when the primary blood supply route is affected by complete or partial occlusion of major coronary arteries. Collateral arteries are a network of small, thin-walled blood vessels, arising from arterioles that radially enlarge and interconnect to maintain an alternate pathway for blood supply. Collateral connections are found even in the absence of CAD, although they carry little blood under physiological conditions. However, during CAD, these pre-existing collaterals become fully functional through an outward remodeling process known as arteriogenesis (Figure 3.5).

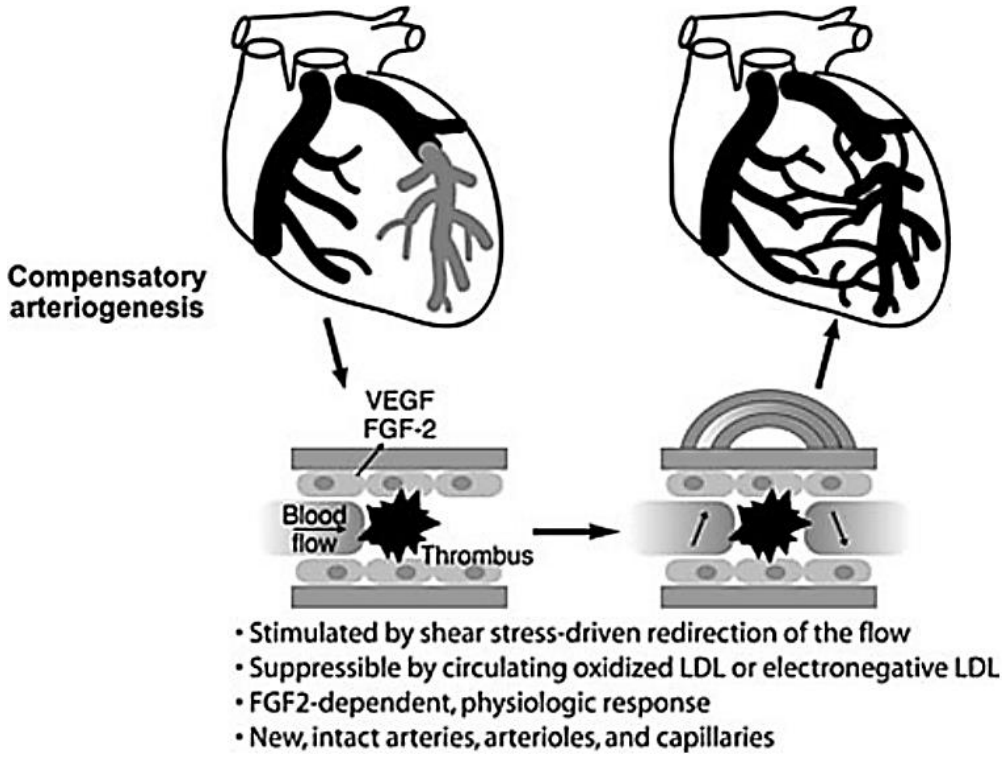

Figure 3.5: Coronary collateral artery remodeling or arteriogenesis[157].

In the presence of a stenosis in the coronary artery, pressure in the post-stenotic region drops, generating a pressure gradient which drives blood flow through the pre-existing collateral arterioles. Over time, this chronic increase in blood flow increases the mean diameter of the collaterals, resulting in a greater capacity for blood flow. However, a key point to keep in mind is that this blood flow increase is not due to vasodilation, but rather to actual structural remodeling of the blood vessel wall.

When collateral blood flow increases, ECs on the collateral vessel wall and circulating blood cells (like platelets) passing through the collaterals are exposed to enhanced shear stress. In a healthy normal coronary collateral artery, the endothelium is exposed to a mean shear stress of ~0.07 Pa. This shear stress level increases to ~1 – 2 Pa, based on the degree of stenosis in the upstream region of the coronary artery[158]. Increased shear stress is considered to be a key stimulus for arteriogenesis, and may act in part by activating pathways leading to the release of growth factors by EC and platelets. Therefore, it is necessary to study how EC and platelet growth factor,

growth factor receptor, and inflammatory molecule levels change in response to physiologically relevant collateral shear stress.

3.2.2 Arteriogenesis

Arteriogenesis is the process by which pre-existing collateral arterioles undergo radial growth to remodel into fully functional collateral arteries. It is an adaptive physiological compensatory mechanism, through which collateral vessels can enlarge their diameter up to 20 times more than their original diameter (usually 30 – 50 μm) to meet increased blood flow demand when supply arteries are stenosed or occluded[159]. In the absence of stenosis or occlusion, there is minimal blood flow through collateral arterioles due to lack of a significant pressure gradient and the presence of high resistance. In presence of an atherosclerotic plaque in an upstream supply artery, blood flow in the downstream regions of the occlusion is limited. Therefore, to maintain normal tissue function and protect tissue from ischemic damage, the body attempts to preserve blood flow downstream of the occlusion by redirecting oxygenated blood through the collaterals.

Due to the sudden increase in blood flow through collaterals, shear stress on the collateral vessel wall increases. Cell surface mechanotransduction receptors on EC of the vessel wall sense this change in shear stress, and transduce the signals inside the cell through various signaling pathways. These events then converge to activate downstream transcription factors modulating the expression of growth factors such as vascular endothelial growth factor (VEGF-A) and placental growth factor (PLGF); cytokines such as monocyte chemoattractant protein (MCP-1) and tumor necrosis factor-α (TNF-α); cell adhesion molecules such as platelet endothelial cell adhesion molecule (PECAM-1) and intracellular adhesion molecule-1 (ICAM-1); and signaling proteins such as endothelial nitric oxide synthase (e-NOS) and NADPH oxidase (NOX). Cytokine and growth factor expression attracts circulating monocytes and platelets to the site of vascular

remodeling, and induces adhesion and transmigration of the cells into the vessel wall through growth factor/growth factor receptor and adhesion molecule interaction.

After invading the vessel wall, monocytes produce a range of proteoglycans and proteases (such as matrix metalloproteinases and plasmin) that remodel the extracellular matrix (ECM). Monocytes also release abundant amounts of growth factors, especially growth factors from the vascular endothelial growth factor (VEGF) and fibroblast growth factor (FGF) families. These growth factors bind to their corresponding receptors on EC and SMC, followed by EC and SMC proliferation. At this point, SMC switch to a secretory phenotype (as opposed to their normal contractile phenotype), which is typical of SMC during an active growth phase. Meanwhile, the internal and external elastic lamina of the tunica media is disrupted by proteases, allowing SMC to migrate through the disrupted internal elastic lamina to form a neointima. The external elastic lamina of the tunica externa is then degraded by proteolytic enzymes, providing space for radial growth of the blood vessels. Additional SMC layers and extracellular matrix start to surround the outer periphery of the vessel wall, increasing luminal diameter and vascular wall thickness. These steps of arteriogenesis are summarized in Figure 3.6. Clearly, collaterals enlarge through an active remodeling process, rather than vasodilation.

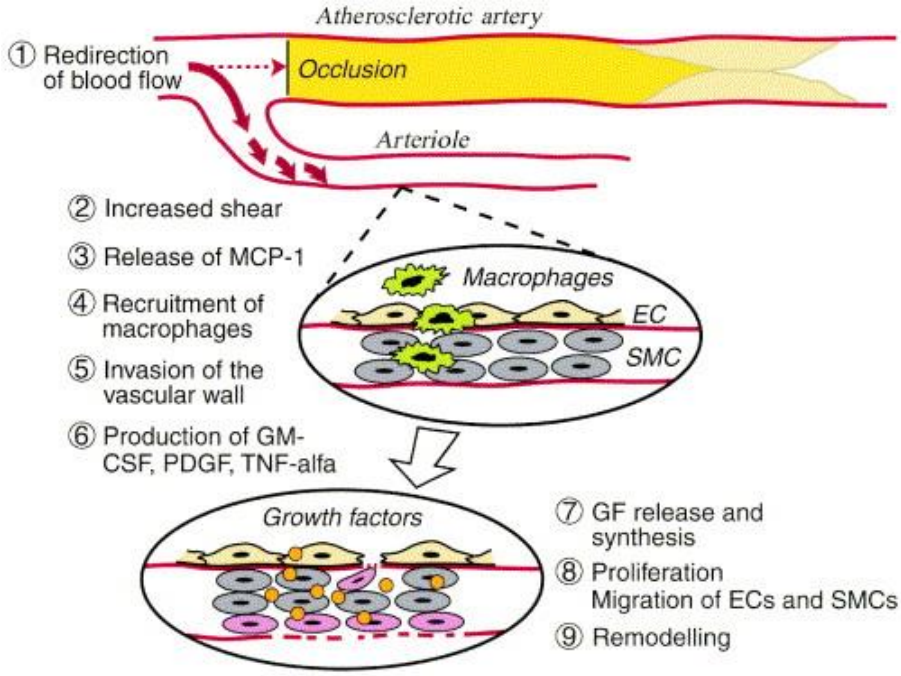

Figure 3.6: Steps associated with arteriogenesis[159].

Circulation through collaterals plays a major role in maintaining viable functioning of the tissue during abrupt or chronic occlusion of supply arteries. Due to its tremendous adaptive power, the collateral circulation can significantly change the outcome of coronary or peripheral artery disease. For example, the presence of collateral arteries can significantly improve the survival rate in patients who are undergoing surgical intervention after suffering from myocardial infarction[160]. This observation demonstrates the importance of collateral arteries in reducing ischemic tissue death and improving blood flow recovery following revascularization therapy.

3.2.3 Diabetes

Diabetes (also referred as diabetes mellitus) is a group of chronic metabolic disorders primarily characterized by hyperglycemia (persistent high blood glucose) for prolonged period of time. When the cells in the body that utilize blood glucose for energy cannot take up glucose properly, glucose accumulates in the blood. Over time, this excessive glucose can be converted into other reactive byproducts such as advanced glycation end products (AGE). Hyperglycemia and

AGE formation have damaging effect on multiple organs including the heart, vasculature, kidney, brain, nerves, and eyes. Around 50% of diabetics die due to cardiovascular complications (including CAD, PAD, and cerebrovascular disease). One reason for this is that diabetes-associated metabolic dysfunction can promote endothelial dysfunction, leading to atherosclerosis in the vasculature.

Diabetes can occur due to either insufficient insulin production (type 1) and/or improper insulin action (type 2). In type 2 diabetes, glucose uptake is impaired due to tissue resistance to insulin activity. Insulin is a hormone that is produced by the beta cells found in the islets of Langerhans of the pancreas. After consumption of food, proteins, fats, and carbohydrates are broken down into amino acids, fatty acids, and glucose by digestive enzymes. Insulin regulates the blood glucose level, preventing unnecessary glucose buildup in the blood. Insulin works like a key to unlock cells by interacting with insulin receptors throughout the body, to allow blood glucose entrance into cells for energy production. Insulin/insulin receptor interaction activates intracellular signaling pathways that stimulate glucose transporters to translocate to the plasma membrane, where they facilitate glucose uptake into the cell. In healthy people, the pancreas releases the right amount of insulin in response to a rise in blood glucose after food consumption. However, in diabetic people, insulin production may be reduced, or insulin may not function effectively (known as insulin resistance).

Diabetes can be diagnosed in several ways. The most common tests are fasting plasma glucose (FPG) and random plasma glucose (RPG). To check FPG, blood is collected in the morning after at least 8 hr of fasting, and the plasma glucose level is quantified. The person is considered nondiabetic if the glucose level is less than 100 mg/dL, prediabetic (showing abnormal glucose levels but not yet diabetic) if the glucose level is between 100 - 125 mg/dL, and diabetic if the glucose level is equal or greater than 126 mg/dL. The RPG test can be conducted by testing the blood glucose level at any time of the day. If the level is greater than 200 mg/dL, the person is

considered diabetic. Other diabetes diagnostic tests include the hemoglobin A1C (HBA1C) test and the oral glucose tolerance test (OGTT). For the HBA1C test, a person's average blood glucose level over a period of 2 to 3 mo is estimated by assessing the amount of glucose linked to red blood cell hemoglobin. The OGTT assesses how well the body can tolerate and process a glucose load. In the OGTT, the blood glucose level is checked before and 2 hr after consuming a drink containing 75 g glucose. The person is considered to be nondiabetic if his/her glucose level is less than 140 mg/dL, and diabetic if the glucose level is equal or greater than 200 mg/dL.

Diabetic people are predisposed to have complications including cardiovascular disease, cerebrovascular disease, kidney disease, retinal damage, and nerve damage. If not treated, patients are at high risk for heart attacks, limb amputations, stroke, blindness, and premature death. According to the Centers for Disease Control and Prevention (CDC), around 29.1 million people in the US (~9.3% of the total population) had diabetes in 2012. Alarmingly, among these 29.1 million people, 8.1 million were unaware that they were diabetic, further increasing the risk of their health[161]. This discrepancy exists because many people suffer silently from diabetes, as there are no particular symptoms initially. The medical expense for treating diabetes is extremely high. In 2012, $244 billion and $78 billion were expended for direct and indirect (associated with disability, early death, work loss) medical care costs of diabetes respectively in the USA alone[162]. Diabetic people have ~2.3 times the medical expenditures of nondiabetic people, creating an economic burden of >$1,000 for each US citizen.

Diabetes is classified into three types: type 1, type 2, and gestational diabetes. Type 1 diabetes, also known as insulin-dependent diabetes or juvenile diabetes, develops when the immune system attacks the insulin-producing pancreatic beta cells and makes them non-functional. Unfortunately, type 1 diabetes is not curable and preventable, and treatment requires taking insulin shots every day to keep the glucose level under control. Type 2 diabetes is called non-insulin dependent diabetes, as the body is capable of producing enough insulin but is unable to use it

properly. This phenomenon arises when cells become insulin resistant or cannot efficiently respond to circulating insulin. Therefore, despite an adequate level of insulin, blood glucose levels increase, sending a signal to the pancreas to release even more insulin. With time, the pancreas becomes incapable of maintaining this increased insulin demand, leading to reduced insulin production. Type 2 diabetes is the most common form of diabetes and has few symptoms, leading to it often going unnoticed until the condition becomes severe. Obesity, high blood pressure, unhealthy food habits, and sedentary behavior can increase the risk of type 2 diabetes. Gestational diabetes is the least common type of diabetes, affecting ~2-10% of pregnant women. Similar to type 2 diabetes, obesity, unhealthy food habits, a family history of diabetes, and high blood pressure increase the risk of this complication during pregnancy. Gestational diabetes affects both the mother and the baby, as babies can be born prematurely or become obese with a higher chance of developing diabetes themselves. Although gestational diabetes may disappear after delivery, these mothers remain at increased risk of eventually developing type 2 diabetes.

3.2.4 Metabolic parameters associated with diabetes

Diabetes is associated with alterations in several metabolic parameters, including hyperglycemia, hyperlipidemia, hyperinsulinemia, and oxidative stress. Type 2 diabetics are predisposed to vascular disease development, especially coronary artery disease or peripheral artery disease, as they are more prone to having multiple abnormal metabolic parameters than type 1 diabetics. In general, compared to nondiabetic people, diabetics have a two- to four-fold higher risk of cardiovascular events. Diabetic cardiovascular morbidity and mortality can be reduced if overall risk factor management is implemented, including weight loss, more physical activity, management of blood pressure and blood glucose level, and normalization of other metabolic parameters.

3.2.4.1 Hyperglycemia

Hyperglycemia (excessive level of glucose), if maintained untreated in the blood plasma for long period, causes various long term complications in diabetic people. Prolonged hyperglycemia results in glycation of plasma lipids and/or proteins via a non-enzymatic process, leading to advanced glycation end product (AGE) formation[163]. In AGE formation, the amino groups of proteins and the carbonyl group of sugars react with each other to generate AGE through the Maillard reaction. In the Maillard reaction, the carbonyl group of glucose (or other reducing sugars) interacts with free amino groups of proteins to form a reversible Schiff base, an unstable compound which forms within a few hours. The labile Schiff base can undergo further rearrangement to form the more stable and practically irreversible Amadori product. Formation of Amadori products usually takes several days. Through further chemical reactions (e.g. dehydration, oxidation), the Amadori product can break down into various reactive bicarbonyl compounds. However, if not broken, Amadori products can undergo further glycation, chemical modifications, and molecular rearrangement to form irreversible AGE. The different steps of AGE formation are illustrated in Figure 3.7. In addition to being formed inside the body, exogenous AGE can also be consumed through AGE enriched foods (such as butter, sesame oil, broiled beef, grilled chicken leg) or tobacco[164].

AGE are complex molecules that can cross-link many different proteins. AGE can modify protein half-life, reduce ligand binding capability, and alter enzyme activity[165]. They can also disrupt normal cellular functions by changing molecular conformations and altering corresponding receptor (RAGE) function. Interaction between AGE-RAGE can activate downstream intracellular signal pathways modulating nuclear factor (NF-κB) activation, gene expression, and cytokines and inflammatory molecules release[166;167]. AGE can accumulate in cells and tissues, where it forms both intracellular and extracellular cross links with other proteins, lipids, and nucleic acids. These cross links can have serious physiological consequences. For example, intermolecular cross linking with

collagen induces systolic hypertension, reduces arterial compliance, and increases vascular stiffness (through cross linkage with other proteins that increases extracellular matrix area)[168]. AGE have been found to contribute in different diabetic complications including diabetic atherosclerosis, retinopathy, nephropathy, and neuropathy.

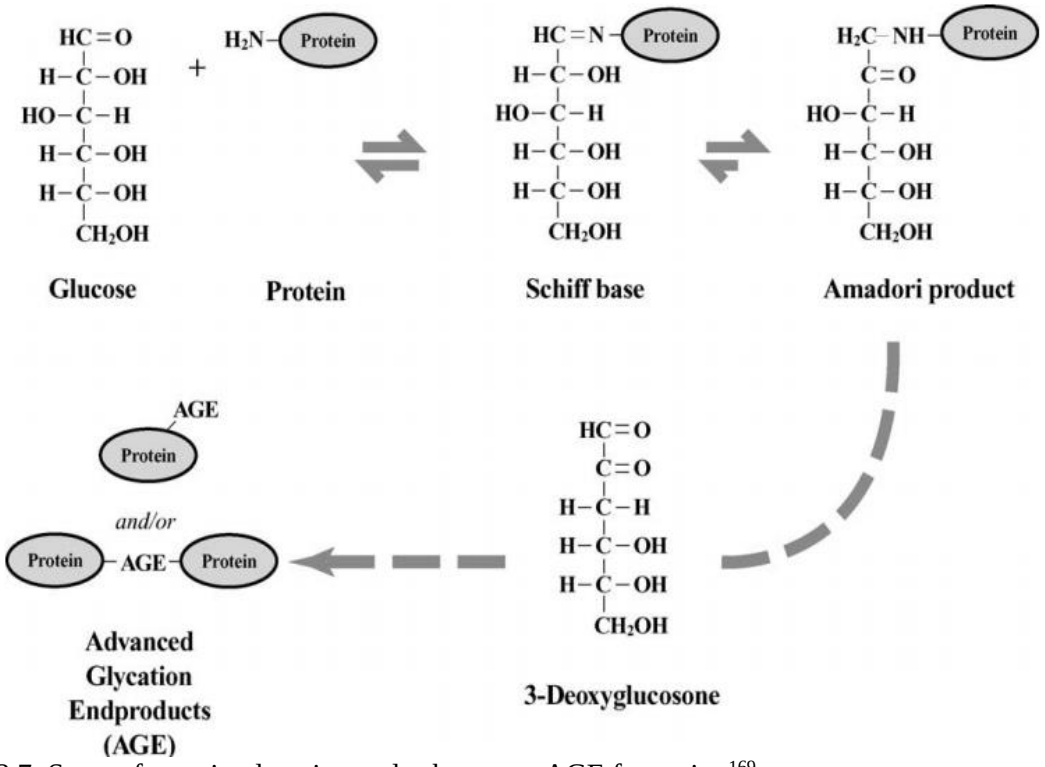

Fig 3.7: Steps of protein glycation and subsequent AGE formation[169].

There are several receptors for AGE, among which the receptor of AGE (RAGE) was the first to be identified. RAGE, a multi-ligand transmembrane signal transduction receptor of 35 kDa molecular weight, can be found on the cell surface of EC, SMC, and macrophages. RAGE has three extracellular domains, among which the V-type domain acts as the ligand binding domain[170]. Increased AGE formation during hyperglycemia also upregulates cellular RAGE expression. AGE-RAGE interaction can cause cellular activation leading to oxidative stress induction, MAPK and NF-κB signaling pathway activation, proinflammatory cytokine (TNF-α, interleukin 1 and 6) release, and adhesion molecule (ICAM-1, VCAM) expression[166;167].

Since AGE can exert many detrimental effects, prevention of AGE formation or breaking of the cross links formed by AGE are desirable outcomes in diabetic people. The most effective way to inhibit diabetic AGE formation in diabetic patients is through limiting or reversing hyperglycemia by diet modification or antihyperglycemic agents. When hyperglycemia cannot be effectively controlled, some pharmacological compounds can inhibit AGE formation or limit its effects. Various compounds have different working principles, including: 1) blocking attachment of amino groups of proteins to sugar (using pyridoxical-5-phosphate); 2) preventing attachment of carbonyl groups of sugars and Amadori products to protein (using aspirin); 3) reducing autooxidative glycation by altering the oxidative environment (using vitamins C and E); 4) preventing AGE crosslinks formation by blocking Amadori product interaction with target molecules (using metformin, aminoguanidine); 5) trapping reactive carbonyl intermediate compounds (using metformin, aminoguanidine); 6) breaking AGE and some existing crosslinkage after their formation (using alagebrium chloride and N-phenacyl thiazolium bromide); or 8) blocking RAGE interaction and signaling[169]. Using soluble RAGE (sRAGE, an isoform of RAGE protein) or RAGE specific antibody, AGE-RAGE interaction can be blocked. Since, sRAGE lacks the transmembrane signaling domain of the full length RAGE protein, it can interact with AGE, but, cannot transduce intracellular signal. Thus, sRAGE, acting as a decoy protein, counteracts the detrimental effects of RAGE protein.

As mentioned above, AGE-RAGE interaction can induce oxidative stress. The main mechanism for oxidative stress is the overproduction of reactive oxygen species (ROS) that can be generated by different enzyme families including NADPH oxidases (Nox), xanthine oxidases (XO), and uncoupled endothelial nitric oxide synthase (eNOS), all of which has been found to be modulated by AGE[171;172]. The Nox family consists of several members (Nox 1-5 and dual oxidase 1-2), each of which is distinctly distributed in different cells and tissues. By transferring electrons from NADPH to oxygen molecules (O_2) across the cell membrane, most Nox isoforms generates

superoxide anion radicals ($O_2^{\cdot-}$) which are then dismutated to H_2O_2 by superoxide dismutase enzymes. In contrast to most Nox family members, Nox4 directly produces hydrogen peroxide (H_2O_2). The activity of Nox4 is regulated by its expression level, and Nox4 only requires regulatory subunit p22phox association to be activated[17]. On the other hand, for activation, Nox2 requires stimulus to induce translocation of its regulatory subunits (such as $p47^{phox}$, $p67^{phox}$, and Rac1) to the membrane[173]. When any agonist stimulates the G-protein coupled receptors of the cell surface, Nox2 regulatory subunits translocate to the membrane to form heterodimers with Nox2. The formed heterodimer is a functionally active complex that initiates $O_2^{\cdot-}$ production[174]. Since H_2O_2 is quite stable and can easily diffuse through the membrane, it is currently considered to be the main ROS for physiological signaling. H_2O_2 can directly or indirectly regulate phosphorylation of specific downstream signaling protein molecules (such as PI3K and p38 MAPK), thereby regulating cell growth, proliferation, and survival[175]. H_2O_2 production by Nox4 has also been found to enhance activity of eNOS and bioactivity of NO[176].

Iron metabolism is another potential source of oxidative stress. Heme proteins are highly toxic, as they can catalyze ROS production. Heme oxygenase-1 (HO-1), an inducible stress protein, protects cells against oxidative stress and programmed cell death by controlling free heme levels and promoting the synthesis of ferritin (an iron binding protein). HO-1 degrades toxic free heme groups to biliverdin, carbon monoxide (CO), and ferrous ion (Fe^{2+}). Ferritin, eliminates the pro-oxidant iron by binding it so that it can be transported into the extracellular space. This mechanism reduces the intracellular iron level, providing cytoprotection against oxidative stress and inhibiting apoptotic compound formation.

Increased oxidative stress leads to further AGE formation and nuclear factor kappa B (NF-κB, a transcription factor) activation[177]. NF-κB activation increases release of proinflammatory cytokine (interleukin 6, TNF-α, MCP-1) and RAGE expression, further intensifying inflammatory cellular responses. MCP-1, the first chemokine discovered due to its high abundance, plays a crucial

role in attracting monocytes/macrophages to sites of inflammation and mediates their migration and infiltration across the vascular wall, increasing vascular permeability[178]. It is produced (either constitutively or in response to oxidative stress) by several different cell types including monocytes, EC, SMC, fibroblasts, epithelial cells. TNF-α exerts the same inflammatory effects as MCP-1, and plays an important role in endothelial cell dysfunction. It enhances the transcription of different cytokine genes that contribute to cell proliferation, inflammatory response, and cell adhesion through further activation of NF-κB. TNF-α increases oxidative stress generation, by inducing NADPH oxidase enzyme expression, which can lead to further TNF-α expression through a positive feedback mechanism (for example, as found in diabetic nephropathy)[179;180]. Thus, chronic hyperglycemia and the resulting AGE formation can induce oxidative stress promoting a pro-inflammatory state through inflammatory cytokine production. This inflammatory state can damage pancreatic β-cells, causing endocrine pancreatic malfunction which further affects intracellular insulin signaling and diabetic complications.

3.2.4.2 Hyperinsulinemia

Hyperinsulinemia happens when insulin receptors become resistant to insulin action, resulting in higher insulin production by the pancreas to exert the usual effects. When the insulin level in blood remains high for a long period, cells and tissues become less responsive to the hormone. For example, a diabetic person may need 10 times more insulin than a healthy person to metabolize the same amount of glucose. With time, the pancreas can no longer keep up with the increased production and secretion of insulin, causing impaired insulin release in response to elevated glucose levels which in turn causes hyperglycemia. Therefore, insulin resistance and hyperinsulinemia are considered to be risk factors for the development of diabetes. When this hyperinsulinemic state is maintained for a long period, cytokine production is elevated, increasing inflammatory responses in the body. Hyperinsulinemia also increases blood pressure and the release of low density lipoprotein (LDL).

3.2.4.3 Hyperlipidemia

Hyperlipidemia is a condition characterized by elevated levels of cholesterol, lipids, and triglycerides in the blood stream. Obesity, unhealthy food habits, and a sedentary lifestyle increase the risk of hyperlipidemia. In addition, diabetics have a higher chance of developing hyperlipidemia than nondiabetics, as diabetes tends to reduce high density lipoprotein (HDL) and increase the low density lipoprotein (LDL) and triglyceride level. Hyperlipidemia arises due to impaired function of the body's systems for transporting and metabolizing cholesterol, lipids, and triglycerides. High cholesterol levels (hypercholesterolemia) are considered to be a major risk factor for cardiovascular disease. Cholesterol must be transported within protein particles known as lipoproteins because of cholesterol's water insolubility. Several types of lipoproteins exist. HDL delivers excess cholesterol to the liver for processing and elimination and is referred to as "good cholesterol". LDL, in contrast, contributes to buildup of excess cholesterol in the blood and to the transport of cholesterol and lipids into the artery wall, and is often called "bad cholesterol." LDL, if present at too high of a level in the blood, can accumulate in the artery wall increasing the risk of early atherosclerosis.

High local concentration of LDL can promote atherogenesis by inducing EC injury and attracting more monocytes and lymphocytes to the intima of the vasculature. LDL is cytotoxic and especially damaging in diabetics as glucose can become linked to LDL. This glucose-LDL complex forms harmful sticky plaques due to increased uptake into the arterial wall and increased susceptibility to oxidative modification. Reacting with transition metal ions and free radicals produced by EC, SMC, or macrophages, LDL particles converts into oxidized LDL (ox-LDL). Meanwhile, attracted monocytes transmigrate into the vascular wall that release cytokines and chemoattractant proteins such as TNF-α and MCP-1[181]. Ox-LDL had been found to induce differentiation of monocytes to macrophages *in vivo* through activation of macrophage stimulating factor receptor[182]. Available LDL and ox-LDL further converts macrophages into lipid-loaded foam

cells which forms the fatty streak beneath the endothelium leading to atherosclerotic plaque formation.

3.2.4.4 Oxidative stress

Oxidative stress is another metabolic disorder that plays a crucial role in the development of diabetic complications. It results from the overproduction of reactive oxygen species (ROS, charged and uncharged molecular species including superoxide, hydroxyl radicals and hydrogen peroxide) and/or reactive nitrogen species (RNS, charged and uncharged species including peroxynitrite radicals and nitric oxide). ROS levels in the cytoplasm can become elevated due to leakage of ROS from mitochondria or by enzymatic/non-enzymatic generation in the cytoplasm. ROS and RNS are generated in all cells in the course of normal metabolism, and are necessary for various physiological activities (such as redox signaling and cellular defense mechanisms). However, their overproduction leads to modification of cellular structure (such as carbohydrates, proteins, lipids) alteration of normal biological functions (such as call activation, proliferation), and formation of cell-damaging toxic products (such as free radicals). Under hyperglycemic conditions, 1) an excess amount of free radicals are generated; 2) gene transcription of proinflammatory cytokines (TNF-α) increases that induces NADPH oxidase expression; 3) AGE synthesis and AGE receptor expression increase; 4) the antioxidant defense system becomes impaired; and 5) auto-oxidation of glucose occurs. All of these factors act to increase cellular oxidative stress, which induces β-cell dysfunction and cellular insulin resistance, thereby playing a role in the pathogenesis of diabetes.

3.2.5 Effects of diabetes on arteriogenesis

Diabetes is a negative modulator of angiogenesis/arteriogenesis, acting through mechanisms that are yet to be elucidated. In studies of the coronary circulation of diabetics and nondiabetics who underwent coronary angiography, collateral development was found to be

impaired in the diabetic group[183]. Results from studies of experimentally induced hindlimb ischemia further demonstrated that blood flow recovery through arteriogenesis was less effective in type 2 (db/db) diabetic mice than control (C57BL/6) mice[184]. Diabetes can affect arteriogenesis through multiple mechanisms, including: 1) interfering with shear stress sensing; 2) inducing EC activation/dysfunction; 3) reducing monocyte growth factor receptor signal transduction capability and migration responses; and 4) increasing vasoconstriction and impairing flow mediated vasodilation.

Shear stress is considered to be the primary stimulus for initiating arteriogenesis. Therefore, any reduction in the shear stress sensing capability of EC mechanoreceptors and the resulting impairment of associated downstream signaling by diabetes compromises arteriogenesis.

EC dysfunction can occur when the normal functional homeostasis of different mediators gets imbalanced. If the generation of a certain mediator is more or less than its elimination level, then the overproduction or underproduction of the mediator alters normal cellular functions. One such example is optimal level of reactive oxygen species (ROS). A certain physiological level of ROS is required for cell to respond properly to extracellular stimuli that modulates normal cell survival, proliferation, and cellular signaling. However, when the homeostasis gets imbalanced, oxidative stress occurs which can lead to cellular death and different disease development. Several studies have reported that oxidative stress can reduce arteriogenesis during diabetes[185;186]. Diabetes reduces eNOS expression and function that has role in different steps of arteriogenesis[187].

Monocyte migration is one of the key steps in arteriogenesis, and is known to be reduced under diabetic conditions. For example, monocytes from rabbits with experimentally induced diabetes had reduced migratory response to VEGF-A and MCP-1 during the acute phase of arteriogenesis (induced by hindlimb ischemia) compared to monocytes from control rabbits[188]. Waltenberger *et al*. found that the migratory response of monocytes isolated from peripheral blood

could be stimulated ~150% by VEGF-A in non-diabetic individuals, but that VEGF-A could not stimulate monocyte migration at all in diabetics[189]. However, a similar level of monocyte migration in response to a peptide-G-protein coupled receptor mediated mechanism was seen in both diabetics and non-diabetics. These results suggest that impairment in growth factor release and activation of the related downstream chemotactic signaling pathways could be a major cause of impaired arteriogenesis during diabetes. These studies examined VEGF-A, which is not specific for arteriogenesis. Therefore, it is important that further studies be conducted to investigate the effects of diabetes on PLGF, a potent arteriogenesis-specific growth factor, to determine whether PLGF expression and/or PLGF dependent monocyte migration in arteriogenic collaterals is also impaired by diabetes.

3.2.6 Role of endothelial cells in arteriogenesis

In the setting of CVD, EC can also participate in the collateral artery remodeling process through production and release of growth factors such as PLGF and VEGF, which act to induce arteriogenesis and maintain blood supply to the distal tissues following upstream vascular occlusion.

3.2.7 Endothelial cells and shear stress

Along with enhanced expression of adhesion and inflammatory molecules, EC exposed to altered shear stress also release growth factors (VEGF-A) and express increased levels of growth factor receptors (VEGFR1/2) on their surface. These changes facilitate compensatory collateral growth and remodeling. Blood flow induced shear stress increases in collaterals during atherosclerotic plaque formation in major arteries, and numerous studies have provided evidence that this increase in shear stress is a major driving force for arteriogenesis[190;191]. Several studies have investigated the effect of shear stress on EC VEGF expression. Dela-Paz *et al*. reported a significant increase in VEGF and VEGFR2 mRNA and protein expression after exposing HUVEC

to orbital shear stress of 0.6 – 4 Pa for 72 hr[192]. Abumiya *et al*. found a 3- and 5-fold increase in VEGFR2 mRNA expression in HUVEC after 8 hr of 1.5 Pa and 4 Pa laminar shear stress, respectively[193]. Results from these studies indicate that EC activated by altered shear stress can play a major role in compensatory vascular remodeling.

3.2.7.1 Placental growth factor (PLGF)

Placental growth factor (PLGF), the second member of the vascular endothelial growth factor (VEGF) family to be discovered, plays a major role in the modulation of arteriogenesis. Though only 42% of the amino acid sequence of human PLGF matches that of VEGF-A (the best characterized VEGF family member), both proteins have remarkable topological similarity. Human PLGF gene encodes four different isoforms of PLGF, among which the primary difference lies in the presence or absence of the heparin binding domain[194]. All the isoforms are secreted as monomers and dimers. Due to the fact that PLGF was first cloned from a human placental cDNA, the growth factor was named PLGF. Though PLGF is indeed abundantly produced by the placenta, it is also produced in heart, lungs, and skeletal muscle by vascular EC, SMC, and activated inflammatory cells. Quiescent EC generally release less PLGF, whereas upon activation they can produce abundant PLGF[195]. However, PLGF does not directly promote angiogenesis (capillary proliferation), due to its lack of effect on EC proliferation[196]. Rather, PLGF stimulates arteriogenesis (enlargement of pre-existing collateral arterioles) by binding to its receptor VEGFR1 on SMC and inflammatory cells like monocytes. VEGFR1 activation stimulates SMC growth, attracts monocyte migration into the vessel wall, induces cytokine (such as TNF-α and MCP-1) and SMC/EC mitogen production, and enhances the angiogenic activity of VEGF-A. The mitogenic response of capillary ECs to VEGF was found to be enhanced ~50% when cells were treated with VEGF and PLGF together, as compared to VEGF treatment alone[197]. PLGF deficiency has also been shown to impair responses to VEGF, but not basic fibroblast growth factor (bFGF), indicating that PLGF is a controlling switch for VEGF activity[198].

PLGF expression also determines how SMC respond to VEGF, as PLGF deficient SMC were reported to proliferate normally only in the presence of both PLGF and VEGF[199]. Modulation of SMC behavior is important, as it is crucial for development of mature, durable, and functional collateral arteries. Indeed, when the angiogenic/arteriogenic stimulus such as increased shear stress reduces, collaterals can undergo rarefaction (diameter reduction and disappearance of some collaterals) and the remodeling process stops. PLGF may induce blood vessel growth in a more balanced way than other growth factors [VEGF or platelet derived growth factor (PDGF)] as it stimulates both EC and SMC behavior simultaneously; whereas, VEGF and PDGF preferentially modulate EC or SMC behavior, respectively[200].

PLGF can stimulate post-ischemic myocardial revascularization as effectively as VEGF, without the negative side effects of VEGF such as edema or hemangioma[199]. The PLGF-VEGF heterodimer has been reported to have more of a mitogenic effect on EC than the PLGF homodimer, but less effect than the VEGF homodimer[201]. The heterodimer has a higher binding affinity toward VEGFR1 that enables VEGFR1 to dimerize with either VEGFR1 or VEGFR2, if both receptors are simultaneously expressed on the cell surface. Depending on the receptor dimerization pattern, the receptor's tyrosine residue phosphorylation level and resulting downstream signal pathway activation may vary[202]. Thus, PLGF directly activates VEGFR1 due to its binding specificity for the receptor and indirectly activates VEGFR2 1) by displacing VEGF-A from VEGFR1 and making more VEGF-A available for binding to VEGFR2, 2) forming heterodimers with VEGF-A that can bind to VEGFR2, and 3) through the VEGFR1/VEGFR2 transphosphorylation mechanism[203].

Mouse models lacking the PLGF gene have been developed for increasing our understanding of the role of PLGF. PLGF knock out ($PLGF^{-/-}$) mice have no apparent defects in blood vessel development, but show reduced angiogenic or arteriogenic capability in response to ischemic insults such as myocardial infarction or hindlimb artery ligation[198]. For example, hindlimb collateral arteries are initially small in both $PLGF^{-/-}$ and wild type mice, but enlarge and become

tortuous post-ligation of the femoral artery only in wild type mice, not in PLGF$^{-/-}$ mice. In wild type mice, the PLGF level increases by ~45% in ligated femoral arteries, compared to non-ligated controls, resulting in attraction and infiltration of more monocytes and macrophages in collateral arteries of wild type mice than PLGF$^{-/-}$ mice. Moreover, fibronectin (which provides extracellular scaffolding for migrating SMC), extravasated or leaked in 70% of wild type mice but only 25% of PLGF$^{-/-}$ mice. These results further demonstrate PLGF's role in increasing vascular permeability and plasma extravasation, which is important for arteriogenesis. Results from high resolution micro-CT scans indicate enhancement of collateral vessel growth after PLGF administration in mouse models of hindlimb ischemia. This increase in number and size of collateral vessels enlarges the total collateral perfusion area, thus restoring blood volume and flow following ischemia[204]. Similarly, Takaoka *et al*. found that administration of recombinant human PLGF for 3 days in a mouse model of acute myocardial infarction (MI) improved survival rate and cardiac function, suggesting an important role for PLGF in the healing process through stimulation of arteriogenesis[205]. Scholz *et al.* found a significant delay at the early stages of collateral enlargement in PLGF$^{-/-}$ mice, implying that PLGF is an important early mediator of arteriogenesis[206]. Luttun *et al*. reported that PLGF release can stimulate stable and mature vessel formation as effectively as VEGF in mouse ischemic heart. Likewise, in mouse ischemic hindlimb, PLGF administration increases perfusion area and improves functionality[199].

Although PLGF is one of the first factors to increase at the onset of arteriogenesis, it has not been studied as extensively as VEGF-A. Therefore, our group set out to investigate how PLGF expression is regulated and to identify molecular mechanisms modulating PLGF under physiological and pathological conditions, especially in the heart and skeletal muscle where arteriogenesis is very important as a compensatory mechanism during diabetic CAD or PAD. Though shear stress is considered as a major modulator of arteriogenesis and PLGF is a key arteriogenic growth factor, the effect of shear stress on PLGF expression has not been directly

investigated. Recently, our lab was the first to report that PLGF protein and mRNA expression in EC is significantly increased after exposure of coronary EC-SMC co-cultures to high dynamic shear exposure (mean time average of 1.24 Pa) mimicking conditions in remodeling collateral arteries. Our group also demonstrated that there is a significant increase in PLGF mRNA expression in mesenteric arterioles following exposure to a pressure gradient of 50 mmHg, compared to 20 mmHg[17].

3.2.7.2 Vascular endothelial growth factor (VEGF)

Vascular endothelial growth factor (VEGF) is a signaling protein that has a potent role in stimulation of vasculogenesis and capillary proliferation. The VEGF family consists of six members: VEGFA, VEGFB, VEGFC, VEGFD, VEGFE, and PLGF. All the six VEGF proteins are found as homodimers or heterodimers, covalently linked by disulfide bonds. Dimeric VEGF molecules act through binding to their tyrosine kinase receptors (VEGFRs).

Before the discovery of the latter family members, VEGF-A was known as VEGF. VEGF-A, a heparin-binding dimeric glycoprotein of 34-42 kDa, acts mainly on EC, although it has effects on SMC and monocytes. VEGF-A contributes to angiogenesis (primarily) and arteriogenesis by increasing cell permeability, survival, proliferation, migration, and signal transduction through stimulating nitric oxide (NO) production and modulating signaling pathways. Gerber *et al*. reported that VEGF-A enhances cell survival in HUVEC via anti-apoptotic signaling through the Akt and PI3 kinase pathways[207]. VEGF-A was reported to enhance EC proliferation via VEGFR2 pathway stimulation and activation of ERK1/2 and JNK members of the MAPK family[208]. VEGF-A was also found to activate several transcription factors and modulate TF, PLGF, and NOS gene expression[209;210]. Vascular permeability is affected by VEGF-A, as the protein stimulates NO and prostacyclin (PGI_2) production by endothelial cells[210;211]. Results from several studies indicated that VEGF-A is required for coronary collateral growth, and that blood flow induced shear stress has a

profound effect on VEGF-A protein and mRNA expression. Toyota *et al*. found that VEGF-A modulate coronary collateral growth in a rat model of repetitive coronary occlusion, as anti-VEGF-A administration diminished collateral growth. dela-Paz *et al*. reported that arterial shear stress can increase VEGF-A expression in HUVEC both *in vitro* and *in vivo*[192]. Likewise, Conklin *et al*. found a significant increase in endothelial cell VEGF-A mRNA and protein expression after exposing porcine carotid arteries to low shear stress for 24 hr[16].

3.2.7.3 Vascular endothelial growth factor receptor (VEGFR)

Vascular endothelial growth factor receptors (VEGFRs) are tyrosine kinase receptors that participate in angiogenesis and arteriogenesis by modulating various cellular functions. Three main isoforms (VEGFR1, VEGFR2, and VEGFR3) have been discovered that are present either as membrane bound proteins or in soluble forms generated by alternative splicing. VEGFR1 was the first VEGF receptor to be discovered on the EC surface of the vasculature. Though both VEGFR1 and VEGFR2 are predominantly expressed by EC, they can also be found in SMC, monocytes, and trophoblasts. Whereas VEGFR1 is the receptor for both PLGF and VEGF-A ligands, VEGFR2 exclusively interacts with VEGF-A. By competing with VEGF-A to bind with VEGFR1, PLGF potentially makes more VEGF-A available to bind with VEGFR2[195].

VEGFR1 and VEGFR2 generally form homodimers upon ligand binding, but can also form heterodimers with each other depending on the ligand's dimer form (homodimeric or heterodimeric). Upon binding with PLGF or VEGF-A homodimers or heterodimers, VEGFRs dimerize resulting in tyrosine kinase activation and autophosphorylation of the tyrosine residues[212]. These events cause attraction of adaptor proteins or kinases to the phosphorylation region, inducing activation of downstream signaling pathways. After blocking VEGFR1 activity using an antibody, EC growth inhibition was observed, suggesting the necessity for PLGF or VEGF-A binding to VEGFR1 for EC proliferation. PLGF binding to VEGFR1 can initiate crosstalk with VEGFR2,

influencing the VEGFR2 activation level and eventually enhancing VEGF-VEGFR2 signaling. Also, soluble VEGFR1 can form complexes with VEGF-A and VEGFR2 which are inactive in nature. In human microvascular EC, this type of complex formation was found to inhibit VEGF-A induced cell migration and proliferation[213]. Thus, VEGFR1 can modulate VEGFR2 signaling either through crosstalk or by acting as a decoy receptor. Activation of VEGFR1 induces monocyte migration, and increases EC production of inflammatory and adhesion molecules; whereas VEGFR2 activation leads to enhanced cell proliferation, migration, and NO release[214;215].

Several studies have investigated the effect of shear stress on EC VEGFR expression. After applying orbital shear stress on HUVEC for 72 hr, dela-Paz *et al*. found a four-fold increase in VEGFR2 protein expression in shear stress stimulated cells compared to static HUVEC[192]. Urbich *et al*. reported a time- and dose-dependent increase in VEGFR2 expression after exposing HUVEC to shear stress of 1.5 Pa for 6-24 hr, and to 0.5-4.5 Pa for 16 hr[216]. These studies suggest that VEGFR expression of EC is modulated by shear stress.

3.2.8 Role of platelets in arteriogenesis

Another important function of platelets is to transport proteins. Platelets can take up proteins from one region of the circulation and release them upon activation in a different/targeted region, helping to localize inflammation and collateral outward remodeling. Platelets take up proteins by diffusion, endocytosis, or through the export transporters present on their surface membrane. They also have the "open canalicular system" of channels, arising on the plasma membrane and leading into the platelet interior, which may facilitate uptake or secretion of protein molecules. Platelets are effective transporters of proteins as they are present in large numbers in blood, have compartments to store proteins, and circulate freely through the body. Thus, by transporting growth factors to collateral blood vessels, platelets can contribute to arteriogenesis. However, during hyperglycemia (fasting plasma glucose level >126 mg/dL or >200 mg/dL after two hours of 75 g oral glucose

intake) or hyperlipidemia (total plasma cholesterol level >200 mg/dL and LDL level >130 mg/dL), associated with coronary artery disease (CAD) in diabetic patients, altered platelet calcium homeostasis can occur, resulting in platelet hyperactivity[217;218]. Evidence has shown that an elevated blood glucose level can increase production and secretion of platelet activation agonists (such as thrombin), platelet activation, and adhesion, suggesting that hyperglycemia may affect uptake/release of growth factors by platelets as well.

To compensate for the reduced arterial blood flow arising from these disease conditions such as CAD, activated platelets can take up or release growth factors like PLGF and VEGF to induce arteriogenesis. Even though several studies have quantified the release/uptake of these proteins by activated platelets in response to shear stress, few have utilized physiologically relevant dynamic shear stress conditions. Therefore, those *in vitro* studies may not accurately replicate *in vivo* conditions.

3.2.9 Cell-cell interaction

The presence of pathological atherosclerotic plaque in major blood carrying arteries reduces blood flow through the arteries, resulting in increased flow through collaterals. Increased blood flow increases shear stress level on the EC of the collateral artery wall. Hence, EC of collateral arteries become activated and release growth factors like PDGF, PLGF and VEGF. EC-released growth factors can be sensed by SMC through tyrosine kinase receptors that modulate SMC's migration, proliferation, and growth factor expression. Thus, paracrine signaling between EC and SMC through released or diffusible mediators plays a major role in blood vessel formation/radial growth and function under both physiological and pathological conditions. Compared to SMC, EC produce and release less VEGF and more PLGF. However, PLGF produced by EC and VEGF released by SMC influence each other in a paracrine manner to enhance each other's mitogenic potential. Activated platelets or platelets adhering to EC can take up these growth factors through endocytosis and via uptake transporters present on platelet plasma membrane.

Circulating activated platelets can then act as a transporter, releasing the growth factors at another site through fusion and exocytosis. Released PLGF and VEGF interact with their corresponding receptors, VEGFR1 and VEGFR2, present either in soluble form or on the platelet and EC surface, initiating signaling cascades for arteriogenesis.

The goal of study 2 was to investigate how levels of the arteriogenic growth factor PLGF are modulated in heart and skeletal muscle cells. Building on previous results from our lab, we characterized molecular mechanisms by which diabetes-associated metabolic dysfunction alters PLGF expression. In further experiments, we tested how high dynamic shear stress mimicking conditions in coronary/peripheral collateral arteries can modulate PLGF production, and how hyperglycemia can alter these effects of shear stress. Our findings suggested a novel mechanism for the impairment of coronary and peripheral collateral artery growth that is observed to occur in diabetes. Further exploration of this mechanism may lead to the development of novel therapeutic treatments that will benefit people suffering from CAD/PAD and diabetes.

CHAPTER IV

RESEARCH DESIGN AND METHODS

4.1 Detailed methods section

Washed platelets

Fresh platelet rich plasma (PRP) was purchased from Oklahoma Blood Institute (Oklahoma City, OK) and centrifuged at 3,000 rpm (1,100x*g*) for 9 min to separate platelets from plasma. The supernatant (or platelet poor plasma, PPP) was collected separately and stored at -80ºC for future use. Platelet pellets were resuspended in HEPES buffered modified Tyrode's solution (HBMT; 137 mM sodium chloride, 2.7 mM potassium chloride, 0.36 mM monobasic sodium phosphate, 12 mM sodium bicarbonate, 2 mM magnesium chloride, 0.2% BSA, 5.5 mM 2% dextrose, and 0.01M HEPES; pH = 7.4) to prepare washed platelets. The platelet number was counted using an optical particle counter (Z1 Coulter particle counter, Beckman Coulter, Brea, CA) and the volume of washed platelets was adjusted to achieve a final platelet concentration of 250,000/μL. This concentration was maintained for all the experiments.

Cell culture – Monoculture model

Human coronary artery endothelial cells (HCAEC) and human skeletal muscle cells (HSKMC) were purchased from LONZA (Walkersville, MD), and, human cardiac muscle cells

(HCM) and mouse cardiac muscle cells (MCM) were purchased from Sciencell Research Laboratories (Carlsbad, CA). Mouse skeletal muscle cells (MSKMC; ATCC, Manassas, VA) were kindly provided to us, for experimental purpose, by Dr. Clarke of OSU. Initially, cells were thawed and cultured in T-75 (75 cm^2 rectangular area) flasks. Cells were maintained in Endothelial cell basal medium (EBM), Skeletal muscle cell basal medium (SKBM), Cardiac muscle cells medium (CMM), and Dulbecco's modified eagle's medium (DMEM) respectively, supplemented with corresponding growth factors and bullet kits as mentioned by the manufacturers and were kept in 5% CO_2 containing, 37 ºC temperature humidified incubator. The culture medium was refreshed in every alternate day. For cardiac muscle cells, T-75 flasks were coated initially with poly-L-lysine solution to enhance cell attachment and growth. Also, HCM and MCM were used directly, without sub-culturing into different passages, as they can terminally differentiate in other cell types in long-term culture. For other cell types, upon confluency, cells were trypsinized and sub-cultured in 6 or 12 well plates/petri dishes according to the need of the experiments. For a particular cell line, equal numbers of viable cells were seeded on each well of the plates or petri-dishes after conducting cell count using hemocytometer.

Cell culture – Co-culture model

Human coronary artery smooth muscle cells (HCASMC) and human iliac artery EC (HIAEC) were purchased from LONZA. After thawing, cells were grown in T-75 flasks and maintained in smooth muscle cell basal medium (SMBM) and endothelial cell basal medium (EBM) respectively, supplemented with the bullet kit components, until reached to confluency. To enhance physiological relevance further through cell-cell interaction, cells were trypsinized, neutralized, and co-cultured on porous Transwell inserts (Corning Costar) of 0.4 µm sized pores. Two different types of co-culture models were developed: HCAEC-HCASMC (for studying CAD) and HIAEC-HCASMC (for studying PAD). Initially, the bottom surface of the inserts was coated with 0.1% gelatin (to enhance cell attachment on the insert surface) and kept in the humidified

incubator (37 ºC and 5% CO_2) for 1 hr. HCASMC were then seeded on the bottom side of the inserts and incubated overnight in the incubator. Next day, inserts with cells were placed in supplemented SMBM containing wells of 6 well plates and returned to the incubator for overnight incubation. Coating the top surface of the inserts with 0.1% gelatin for 1 hr in the following day, HCAEC or HIAEC were seeded with supplemented EBM medium. The plates with the inserts were then put back in the incubator and cells were grown to confluency. Afterwards, confluent co-cultures were serum starved for 24 hr in the corresponding reduced serum medium prior to any shearing experiments.

Cone-Plate shearing device

A modified cone and plate shearing device, based on the original design of Blackman, was used to investigate the effects of shear stress on platelets and EC[219]. Based on the experimental needs, two different types of devices were used in this study to expose platelets and EC layer (both in mono and co-cultures) to different constant and dynamic shear stress waveforms. One device used a single cone (cone angle 2°) and could accommodate a 6 cm diameter polypropylene petri dish (Figure 4.1A). The other had four cones (with two different heights and diameter, 0.5° angle) in the outer side and could fit with a 6-well plate (Figure 4.1B) with or without the inserts. The middle two wells of the 6 well plate were not sheared and were used as static control. The cones were made of ultra-high molecular weight polyethylene (UHMWPE) and were coupled to micro-stepper motors. The motors were connected to a microcontroller (Allegra, Optimal Engineering System, Van Nuys, CA) unit which was guided through BASIC programs to generate specified shear stress waveforms. Both devices were capable of generating uniform laminar shear stress in the flow field. The maximum shear stress the single cone and plate shearing device could achieve was 7.2 Pa, and that for the multi-channel cone and plate shearing device was 12 Pa.

Using the following equation, the generated shear stress values of the cone and plate shearing devices were calculated:

$$\tau = \frac{\mu\omega}{\alpha} \quad \text{(Equation 3)}$$

where τ = shear stress, ω = angular velocity of the cone, α = angle of the cone, and μ = dynamic viscosity of the fluid.

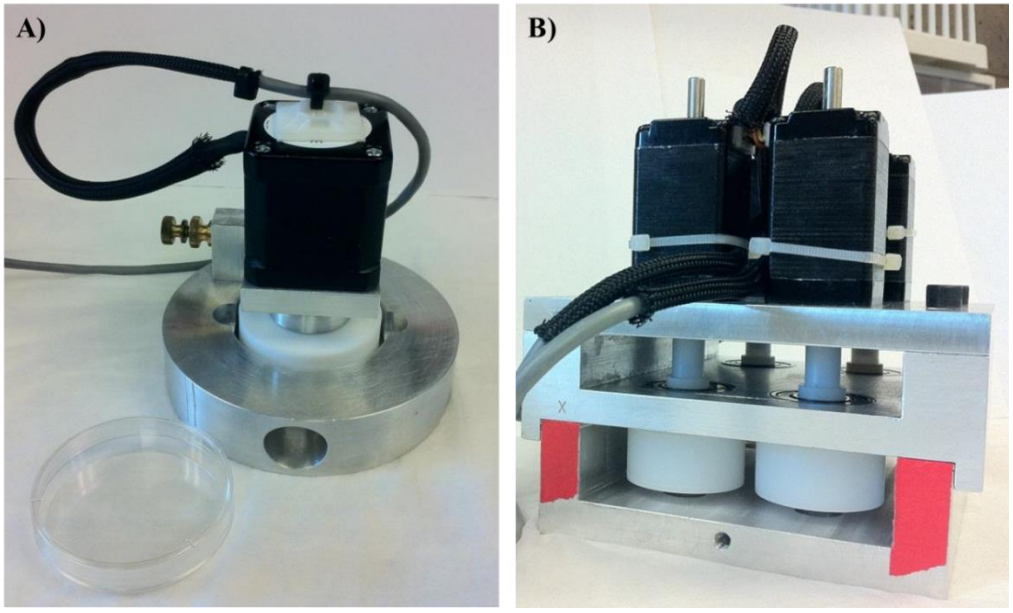

Figure 4.1: The cone and plate shearing devices: A) Single cone-plate, and B) Multi-channel cone-plate.

Coronary artery blood flow induced shear stress

Four constant (0.1 Pa, 0.3 Pa, 1 Pa, and 3 Pa) and three dynamic (normal, low, and elevated) shear stress waveforms were applied to platelets and EC *in vitro* using the cone-plate shearing devices[46].

Constant shear stress of 1 Pa was chosen as it represents shear stress commonly found in healthy left coronary arteries; low shear stress at 0.1 and 0.3 Pa are typical in recirculation zones; whereas elevated shear stress at 3 Pa is often found on stenotic regions. In order to simulate physiologically relevant shear stress conditions, dynamic shear stress (normal, low and elevated)

waveforms were also employed. These dynamic shear stress waveforms were obtained from numerical modeling conducted in our lab[220].

Platelet shear stress (coronary artery blood flow)

The normal shear (NS) waveform (varies between 0.05 to 1 Pa in 0.9 sec) mimics the physiological pulsatile shear stress condition experienced by platelets in the healthy left coronary artery (when platelets travel close to the wall); low shear (LS, varies between 0.06 to 0.4 Pa in 0.9 sec) stress simulates pathological shear conditions occurring in the recirculation zones past a stenosis; and elevated shear (ES) represents pathological shear stress experienced by a platelet as it passes through a 60% stenosis. While passing through the stenosis, the platelet experiences an elevated shear stress of 6.5 Pa for only 0.1 sec, followed by normal shear (0.1 to 1 Pa) stress for rest of the time. For the purposes of this study, it was assumed that platelets pass through the same stenosis once every 90 sec. The three dynamic shear stress waveforms that were applied to platelets are illustrated in Figure 4.2A.

EC shear stress (coronary artery blood flow)

Dynamic shear stress waveforms applied to EC are shown in Figure 4.2B. In a normal left coronary artery, wall shear stress varies between 0.1 and 1 Pa (NS) in 0.9 sec; around a stenosis, wall shear stress can be elevated to 6.5 Pa (ES). In recirculation zones past a stenosis, low unidirectional shear stress can develop, varying between 0 and 0.4 Pa (LS).

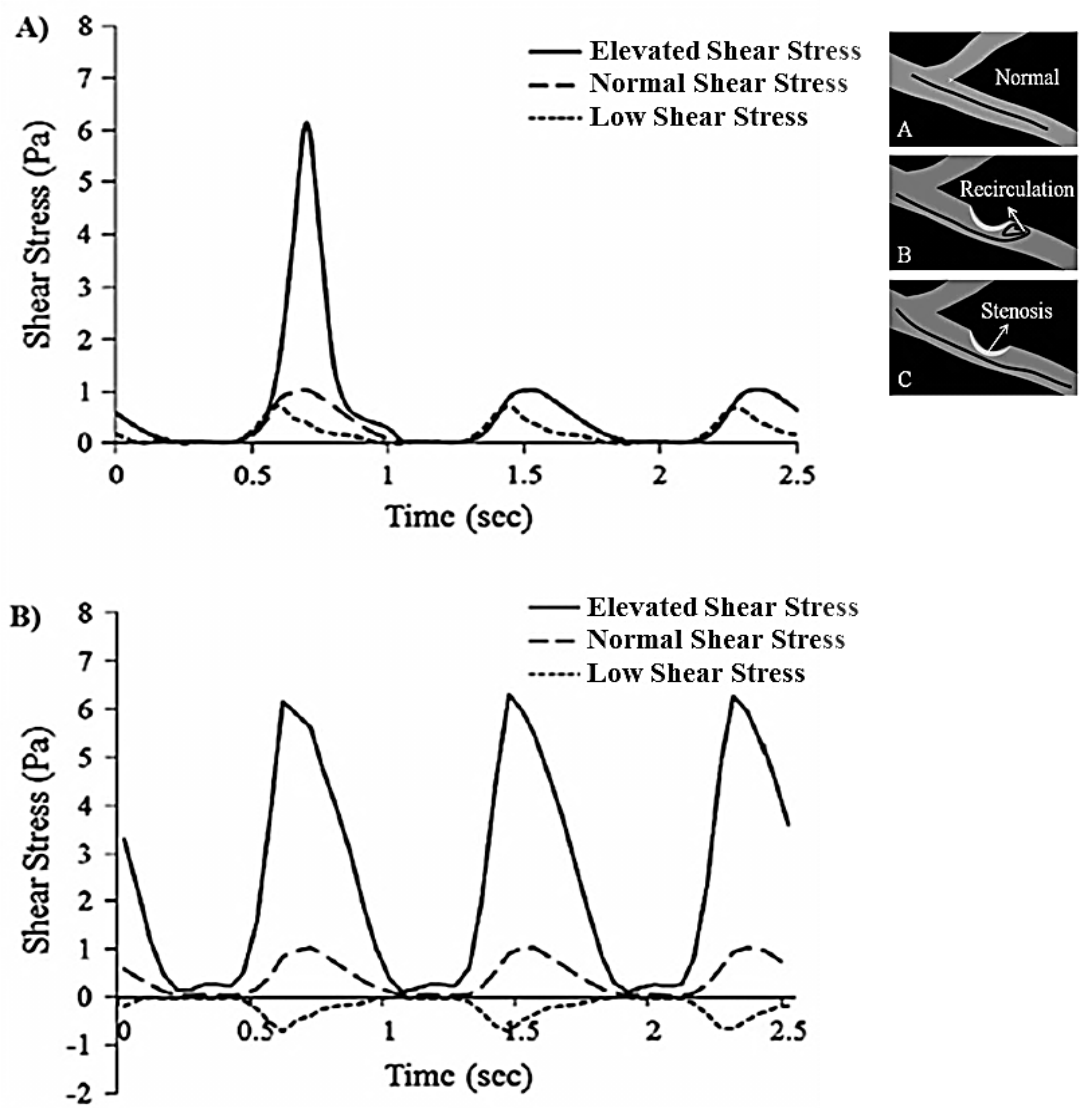

Figure 4.2: A) Shear stress history of platelets passing through the left coronary artery under physiological (normal) and pathological (low and elevated) conditions. Inset A, B, C (at right side) show the corresponding trajectories of platelets passing through healthy left coronary artery, platelets trapped in a recirculation zone past the stenosis region, and platelets passing through a stenosis throat respectively. B) Wall shear stress distribution of EC[46].

Collateral blood flow induced shear stress

Platelets and EC (of both monoculture and co-culture) were exposed to two different dynamic (normal and elevated) shear stress waveforms of coronary/peripheral collateral arteries *in vitro* using the 6 well cone-plate shearing devices. Since coronary/peripheral collateral arteries are small in size (~0.2 mm diameter), it was assumed that both EC and platelets (travelling close to EC) are exposed to the same shear stress waveforms *in vivo*.

The coronary collateral shear stress waveforms were obtained from a previously published paper by Mack *et al*., in which the authors conducted numerical simulation in a lumped parameter model of a coronary collateral artery[158]. The normal shear waveform (NS, time average value of 0.07 Pa) models physiological shear stress conditions experienced by EC in a normal collateral vessel downstream of a healthy coronary artery; whereas, elevated shear stress (ES, time average value of 1.24 Pa) describes the pathological shear stress conditions experienced by platelets or EC in a remodeling collateral vessel downstream of a 60% stenosed coronary artery. Figure 4.3 shows the applied coronary collateral dynamic shear stress waveforms.

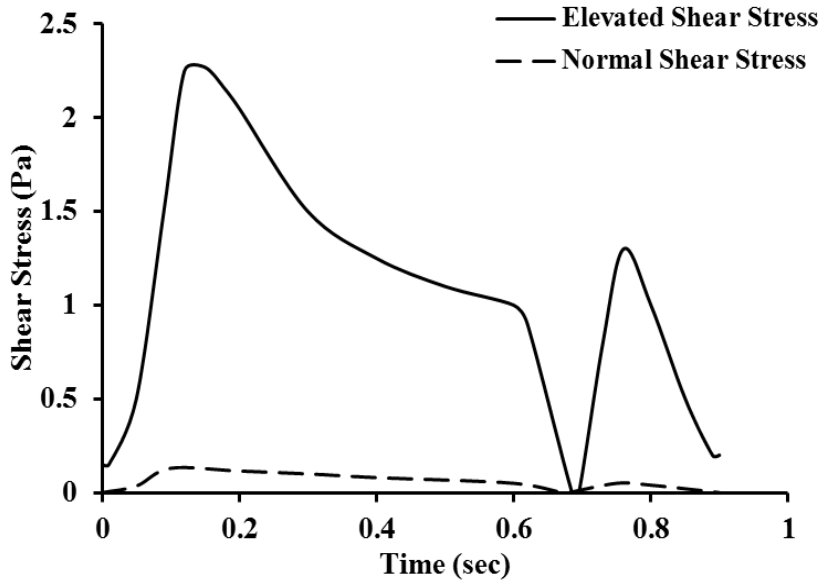

Figure 4.3: Shear stress waveforms (normal and elevated shear) of coronary collateral arteries applied to platelets and EC using a cone and plate shearing device.

The peripheral collateral artery shear stress waveforms were obtained from Watanabe *et al*.'s paper, where the authors developed a distributed-parameter hemodynamic model (a simple and effective blood flow simulation model in deformable blood vessels) of the arm, focusing on the anatomically detailed arterial structure[296]. From their paper, the flow rate waveform of the superior ulnar collateral artery was obtained from which the shear stress waveform was calculated using Hagen-Poiseuille's equation [$\tau = (4\mu Q/\pi r^3)$, τ = shear stress, μ = blood viscosity, Q = blood flow rate, and r = the internal radius of the vasculature (provided in the paper)]. The time average

value of the normal shear stress came as 0.156 Pa that models the physiological shear stress of a healthy superior ulnar collateral artery. As it was found from coronary collateral circulation that the time average value of elevated shear stress was about 17.7 times higher than the normal shear stress time average, the same scaling value was utilized for elevated shear stress (ES) calculation in the remodeling superior ulnar collateral artery downstream of diseased (60% stenosed) main (brachial) artery. This resulted in the time average value of ES as 2.753 Pa. The obtained shear stress waveforms of peripheral collateral artery are shown in Figure 4.4.

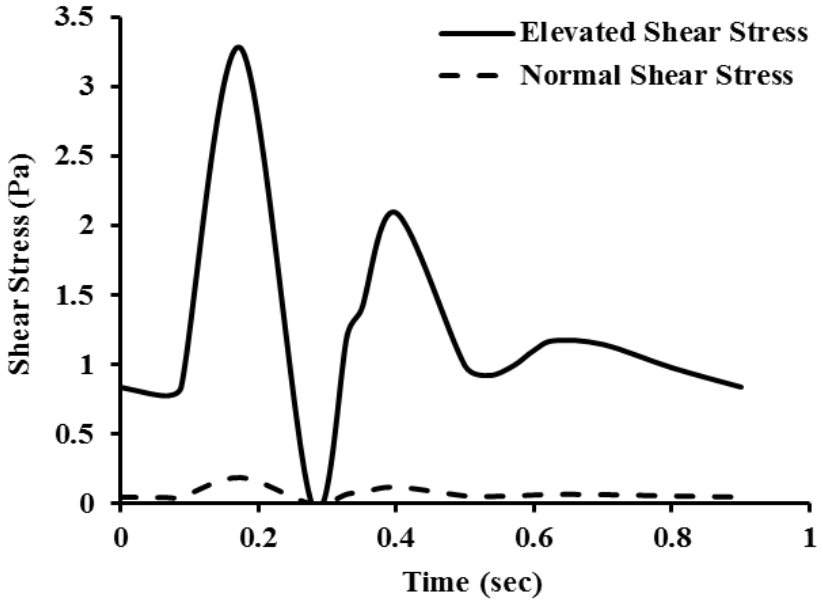

Figure 4.4: Normal (NS) and elevated shear (ES) stress, of peripheral collateral arteries, applied to HIAEC of the co-culture model to mimic healthy/diseased peripheral arterial condition.

Perfusion flow chamber

To further enhance the physiological relevance of our study, a perfusion flow chamber (Figure 4.5) was used to investigate the role of dynamic shear stress (as found in coronary blood vessels) on EC *ex vivo*. The chamber was fabricated using polydimethylsiloxane elastomer (PDMS, Sylgard-184, Dow Corning). Two 16G×2" I.V. catheters were positioned at opposite ends of the chamber. A freshly harvested rat aorta was cannulated to the catheters using suture and kept immersed in HEPES buffered physiological salt solution (NaCl: 142 mM, KCl: 4.7 mM, $MgSO_4$:

1.17 mM, $CaCl_2$ 1.56 mM, glucose: 5.5 mM, HEPES: 10 mM, KH_2PO_4: 1.18 mM, 1% penicillin/streptomycin, pH = 7.4). Aortas were obtained, within 10 min of euthanization of a rat, through a tissue sharing plan at OSU.

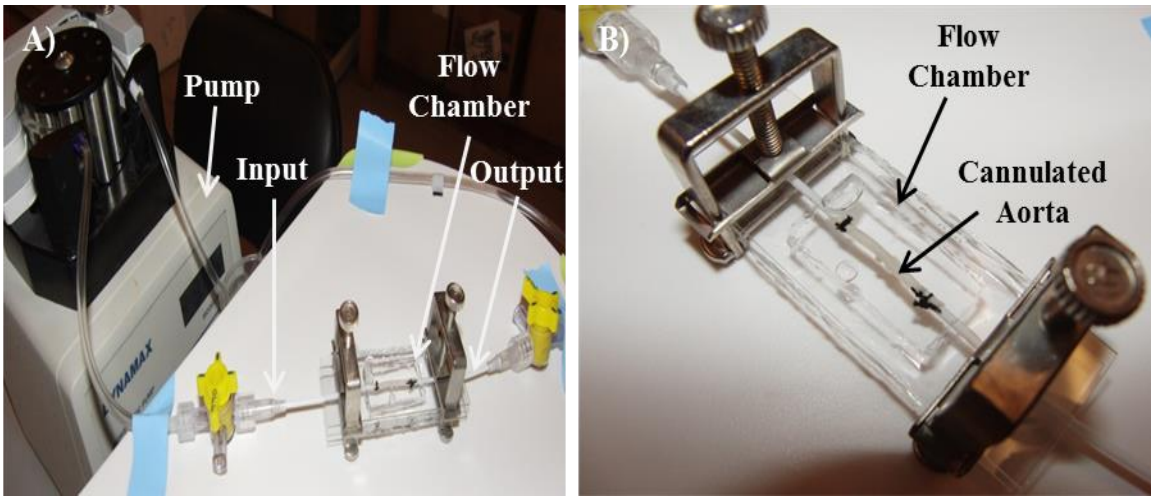

Figure 4.5: A) Flow chamber connected to a pump through silicone tubing to investigate the effects of dynamic shear stress on explanted rat aorta's EC. B) Flow chamber with the cannulated aorta.

Through pump tubing (Inner diameter 1.587 mm and 3.175 mm; Tygon tubing, vWR International, Batavia, IL), the flow chamber (aorta and the catheters) was connected to a programmable peristaltic pump (Manostat Varistallic Compulab 3 Modulus Dispensing System, Thermo Scientific, Waltham, MA). Physiological salt solution was perfused through the aorta at different flow rates using this pump to generate different shear waveforms. Adjusting the pump flow rate, the generated shear stress (obtained using equation 4) could be precisely controlled at the aorta wall.

$$\tau = \frac{4\mu Q}{\pi r^3} \quad \text{(Equation 4)}$$

where, μ = fluid viscosity (1 cP for the physiological salt solution), Q = fluid flow rate, and r = blood vessel diameter. Pulsatile flow at 20 mL/min, 8 mL/min, and 124 mL/min could generate normal (0 to 1 Pa), low (0 to 0.4 Pa), and elevated (0 to 6 Pa) pulsatile wall shear stress within the cannulated aorta.

4.2 Specific aim 1: The goal of this aim was to measure platelet and endothelial cell (EC) responses under physiologically relevant dynamic shear stress conditions *in vitro*, and to determine whether the presence of one cell type affects the responses of the other to shear. In addition, the effects of dynamic shear stress on endothelial cell responses *ex vivo*, in a rat aorta model, was also investigated.

4.2.1 *in vitro* study

Confluent EC and platelets were exposed to constant or dynamic shear stress of the coronary artery, either together or separately, in cone-plate shearing devices for 60 min. Platelet responses were measured through cell surface PECAM-1, GPIbα, and GPIIb expression, as well as PMP generation. EC responses were measured through EC surface and released vWF and TF expression, as well as EMP generation.

4.2.1.1 Platelet surface PECAM-1 expression

After shear exposure (with or without EC), platelet samples were collected and incubated with FITC conjugated murine anti-human PECAM-1 (1:50 dilution, Ancell Corporation, Bayport, MN) antibody for 30 min at room temperature (RT). Post incubation, samples were diluted in HBMT (1:10) and analyzed using flow cytometry (Accuri Cytometers Inc., Ann Arbor, MI). FITC conjugated MOPC (1:100 dilution, Ancell Corporation) antibody (an isotype control) was used to detect non-specific antibody binding. Thrombin receptor activator peptide (TRAP6, 20 μM, 5min, RT) treated platelets were used as the positive control, representing fully activated platelets; whereas resting platelets (alone or with EC) were used as the negative control.

4.2.1.2 Platelet surface GPIbα expression

Platelets were exposed to various shear stress conditions for 60 min. Platelet samples were taken every 15 min and incubated with FITC conjugated mouse anti-human monoclonal GPIbα

(CD42b, 1:10 dilution, Abcam, Cambridge, MA) antibody for 30 min at RT. Samples were then diluted 10-fold in HBMT and analyzed using flow cytometry.

4.2.1.3 Platelet surface GPIIb expression

Timed platelet samples (collected every 15 min during shear exposure) were also examined for cell surface GPIIb expression, using FITC conjugated murine anti-human CD41a (30 min at RT, 1:50 dilution, Ancell Corporation, Bayport, MN) antibody, by flow cytometry.

4.2.1.4 EC surface vWF expression

EC surface vWF expression in response to shear stress was measured using a solid phase ELISA approach. Confluent EC were exposed to various shear stress (constant/dynamic) waveforms in the presence or absence of platelets. After shear exposure, supernatant (cell media or buffer containing platelets) was removed and EC were washed and fixed with 0.5% glutaraldehyde (Sigma Aldrich, St. Louis, MO) for 15 min at 37°C. Following neutralization using glycine-0.1% BSA (30 min at 37°C), EC surface vWF expression was measured using monoclonal mouse anti-human vWF antibody (1 µg/mL, Abcam, Cambridge, MA, 60 min at 37°C). Primary antibody binding was detected using an alkaline phosphatase conjugated goat anti-mouse (Sigma-Aldrich, 1:1000 dilution) secondary antibody (60 min at 37°C), followed by p-nitrophenyl phosphate substrate (pNPP) incubation (20 min). Color development was measured using a micro-plate reader (Beckman Coulter, DTX 880) at 405 nm wavelength.

4.2.1.5 EC surface TF expression

Using solid phase ELISA, EC surface TF expression was measured similarly as described for vWF, in constant shear stress exposed EC, using polyclonal rabbit anti-human TF (1 µg/mL, Abcam for 60 min at 37°C) antibody.

4.2.1.6 Soluble vWF expression

Soluble vWF (released by activated platelets and EC) expression was measured by sandwich ELISA technique using a commercial vWF ELISA kit (Abcam, Cambridge, MA). After shear exposure of 60 min, the fluid phase was collected and centrifuged at 3,000×*g* for 6 min. The supernatant was then collected and applied to a microtiter plate pre-coated with murine monoclonal anti-human antibody against human vWF (2 hr at RT). Biotinylated anti-human secondary antibody (2 hr at RT) was used to bind with the captured vWF for detection. Secondary antibody binding was then detected using streptavidin conjugated peroxidase (30 min in RT), followed by a chromogen substrate (15 min, RT). Color development was measured using a micro-plate reader at 450 nm wavelength.

4.2.1.7 PMP and EMP generation

After shear exposure, the fluid phase (containing platelets, PMP and EMP) was collected and centrifuged at 1,500x*g* for 15 min at RT. Post-centrifugation, supernatant was collected and subjected to a subsequent centrifugation at 17,000x*g* for 2 min at 4ºC. After removing the supernatant, the isolated microparticle pellets were resuspended in 50 µL HBMT. The samples were then incubated with two different antibodies, CD31 (red, 1:12.5 dilution; BD Pharmingen, San Jose, CA) and CD42b (green, 1:12.5 dilution; BD Pharmingen, San Jose, CA) for 30 min at RT. Post-incubation, samples were diluted in HBMT (1:10) and analyzed using flow cytometry. FITC (green fluorochrome) and R-PE (red fluorochrome) conjugated MOPC antibodies (Isotype controls, 1:100 dilution, Ancell Corporation, Bayport, MN) were used to detect non-specific binding.

Suitable gates for platelets (using resting platelets) and MP (smaller than platelets) were established based on the particle size in the density plot (side scatter vs forward scatter). 30,000 events were counted within the MP gate. EMP were distinguished from PMP using CD31 and

CD42b dual staining, as EMP are CD31+/CD42b- and PMP are CD31+/CD42b+. Events occurring in quadrant 1 (CD31+/CD42b-) were counted as EMP; events occurring in quadrant 2 (CD31+/CD42b+) were counted as PMP (Figure 4.6).

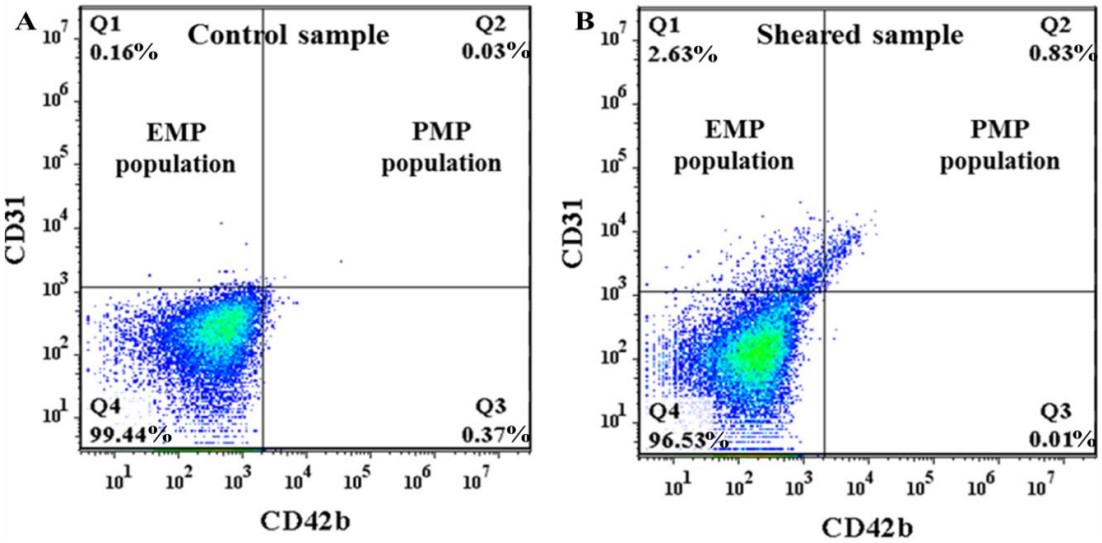

Figure 4.6: Pseudo-color scatter plots (CD31 vs CD42b) showing EMP (Q1 gate) and PMP population (Q2 gate) in A) control and B) sheared sample.

4.2.1.8 Platelet adhesion to EC

Platelet adhesion to EC was observed using optical microscopy. Platelet and EC were co-sheared for 60 min in the cone-plate shearing device under dynamic shear waveforms. After shear exposure, platelet supernatant was aspirated out and EC were fixed with glutaraldehyde (15 min, 37°C). Platelet adhesion to EC was then observed using an optical microscope (Nikon TE 2000U). White light images at 40X magnification were captured by the digital camera (Coolsnap Fast Cooled ES2), connected to the microscope, in each well at 3 different randomized locations. EC treated with TNF-α (to induce activation) were used as a positive control. Using ImageJ software (v1.46, NIH), number of platelets adhering to EC surface in the total image area were counted manually from each images.

4.2.2 *ex vivo* study

Activation and functional changes of EC were examined in rat aortas *ex vivo* using a perfusion flow chamber. Freshly harvested rat aortas were cannulated to the inlet and outlet catheters of the flow chamber. The chamber was connected to a peristaltic pump through silicone tubing and the open ends of the tubing were immersed in a reservoir containing physiological salt solution. The whole setup, except the pump, was placed within an incubator at 37°C. A schematic diagram of the perfusion flow chamber and the setup is shown in Figure 4.7.

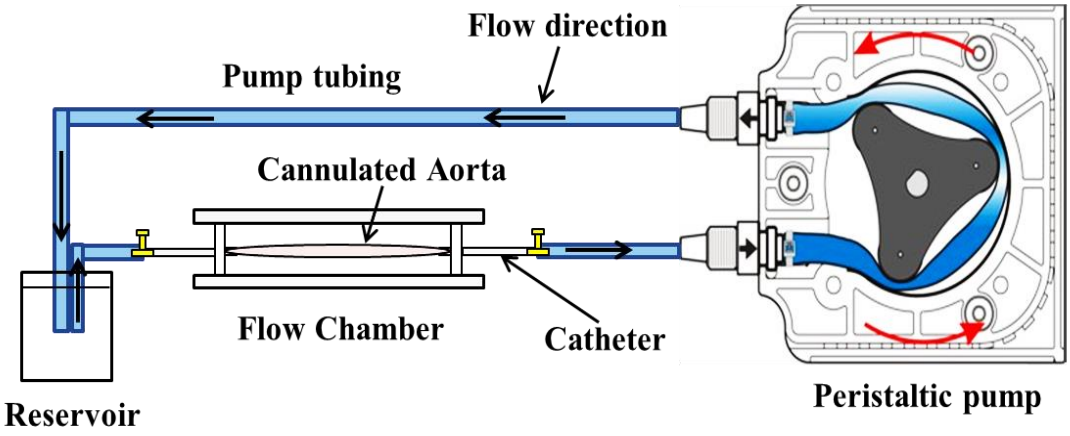

Figure 4.7: Schematic representation of the flow loop of perfusion flow chamber with the cannulated aorta.

Through a tissue sharing plan, abdominal aortas of recently euthanized adult rats (Wistar rats; combination of males and females of 5 to 7 months of age) were collected. Harvested aortas were ~0.15 cm in diameter and 2-3 cm in length. HEPES buffered physiological saline solution was used to preserve the aorta (4ºC) until perfusion. All experiments were conducted within 24 hr of dissection to ensure integrity and proper functionality of the cells and the tissue. The aorta was cleaned and cannulated to the catheters of the flow chamber using 2-0 silk suture. Physiological saline solution was then perfused through the aorta for 2 hr to investigate the effects of shear stress on EC responses. Dynamic wall shear stresses mimicking conditions within the left coronary artery

(normal - 0 to 1 Pa, low - 0 to 0.4 Pa, and elevated - 0 to 6 Pa) were applied to the aorta by adjusting the flow rate of the programmable peristaltic pump (Manostat Varistallic Compulab 3 (RD-1) Modulus Dispensing System, Thermo Scientific, Rockford, IL). Calculations from Hagen-Poiseuille's equation $\left(\tau = \frac{4\mu Q}{\pi r^3}\right)$ indicated that flow rates of 20 mL/min, 8 mL/min, and 124 mL/min could generate normal (1 Pa), low (0.4 Pa), and elevated (6 Pa) shear stress conditions respectively, assuming that perfusate viscosity (μ = 1 cP for saline solution) and abdominal aorta diameter (r = 1.52 mm) were constant. Post-shearing, the shear exposed section of the abdominal aorta was collected and gently washed in phosphate buffer saline (PBS; 9% sodium chloride, 1 M sodium dibasic phosphate, 0.5 M sodium monobasic phosphate; pH = 7.4) to remove any perfusate remaining, then fixed in 4% paraformaldehyde (4°C, overnight). The fixed aorta samples were prepared for paraffin embedding and tissue sectioning (5 μm thickness), as well as haematoxylin and eosin (H&E) staining, at the Oklahoma Animal Disease Diagnostic Laboratory. In parallel, sheared rat aortas were homogenized using a motor pestle, and aorta wall proteins were extracted to run Western blot experiments.

4.2.2.1 Immunostaining of paraffin-embedded tissue sections

To remove the fixative from the tissue sections, the slides were washed through consecutive changes of xylene (2 changes, 5 min each) and alcohol (100% dehydration alcohol and 95% dehydration alcohol, 1 change, 5 min each). After washing with PBS+0.05% Tween 20 for 10 min, tissue sections were blocked with 3% hydrogen peroxide (3 min, RT) and 2% goat serum (25 min, 37°C). After another set of washes, mouse monoclonal anti-rat vWF antibody, mouse monoclonal anti-rat ICAM-1 antibody, and rabbit polyclonal anti-rat TF antibody (all at 1:100 dilution, overnight at 4°C) were used to detect vascular wall vWF, ICAM-1, and TF expressions respectively. Non-specific antibody binding was also detected using MOPC antibody. To detect primary antibody binding, biotinylated secondary antibody (diluted in 2% serum at 1:1000 dilution)

was added to the slides and incubated for 30 min at RT. Immunoreactivity was further enhanced by amplifying the signal intensity using avidin-biotin complex (ABC reagent, Thermo Scientific, Rockford, IL) for 30 min at RT. The tissue sections were then stained with DAB substrate (1:10 dilution in stable peroxide buffer, 10 min at RT; Thermo Scientific), followed by counter staining with haematoxylin (2 min, RT). Using a Nikon TE 2000U microscope, the slides were then examined and the images (at random locations) were captured using a CoolSnap fast cooled digital camera.

4.2.2.2 Sub-cellular protein extraction for Western blotting

Cytoplasmic and membrane proteins of the abdominal aorta wall were extracted using a commercial kit (Thermo Scientific, Rockford, IL). After washing with ice-cold PBS, tissue samples were finely chopped on ice to prevent degradation of proteins and placed in ice-cold cytoplasmic extract buffer (with protease inhibitors). Tissues were then homogenized for 20-30 sec using a motor pestle (vWR international, Batavia, IL). The cytoplasmic extraction buffer released the cytoplasmic contents by permeabilizing the cell membranes. Homogenized samples were centrifuged at 500×*g* for 5 min to separate the tissue debris from the protein extract. Post centrifugation, cytoplasmic protein extract was collected and stored immediately at 4°C. Ice cold membrane extract buffer with protease inhibitors was then added to the tissue pellets and mixed gently for 10 min at 4°C. After proper mixing, the samples were centrifuged at 3,000×*g* for 5 min and the supernatant containing membrane protein extract was collected. Extracted proteins (cytoplasmic and membrane) were stored at -80°C until use. The bicinchoninic acid (BCA) protein assay (Thermo Scientific, Waltham, MA) was used to determine the total protein concentration of the tissue samples. Extracted samples were used to determine the aorta wall vWF, ICAM-1, and TF expressions by Western blotting. A Dual Cool Mini-Vertical Electrophoresis/Blotting System (DCX-700, CBS Scientific, vWR International, Houston, TX) was used for this purpose. Adding

sample buffer (containing Sodium Dodecyl Sulfate (SDS) and beta-mercaptoethanol) to tissue protein extracts, samples were reduced and denatured at 95°C for 5-7 min. Same amounts of denatured samples (cellular and membrane protein extracts) were loaded in each lane of the 4% loading gel (0.83 mL of 30% protogel, 1.57 mL of 2M Tris-Cl^-, pH 8.7, 3.81 mL deionized water, 0.05 mL 10% Ammonium persulfate, 0.031 mL 20% SDS, 0.013 mL Tetramethylethylenediamine) and electrophoretically separated according to their molecular weight in 10% running gel (4.2 mL of 30% protogel, 3.14 mL of 2M Tris-Cl^-, pH 8.7, 5.1 mL deionized water, 0.1 mL 10% Ammonium persulfate, 0.062 mL 20% Sodium dodecyl sulfate, 0.026 mL Tetramethylethylenediamine) at 150 V (constant voltage) for 90 min. Constant voltage was used so that proteins could migrate through the gel at a constant rate without overheating the gel (according to manufacturers' instruction). The protein bands of the gel were transferred and immobilized from gel to nitrocellulose membrane through application of electrical current at 200 mA (constant current) for 3 hr (according to manufacturers' instruction). Care was taken to maintain the electro-blotting buffer temperature below 4°C. Dual color precision plus protein standard (Biorad, Hercules, CA), tagged with recombinant proteins of molecular weight of 10-250 kDa, was used for monitoring electrophoretic separation and efficient blot transfer, and easier identification of the targeted proteins. Running gels were Coomassie blue stained to assess whether protein transfer from gel to membrane was proper or not. Nitrocellulose membranes were then blocked in 5% bovine serum albumin (BSA) for 1 hr at RT and incubated with rabbit polyclonal anti-rat vWF, mouse monoclonal anti-rat ICAM-1, and rabbit monoclonal anti-rat tissue factor primary antibodies separately (all antibodies at 1:1000 dilution, overnight, 4°C, with gentle agitation; Abcam, Cambridge, MA). Primary antibody binding was detected using HRP conjugated goat anti-mouse or goat anti-rabbit secondary antibody (1:1000 dilution, 1 hr, RT; Abcam, Cambridge, MA). An enhanced chemiluminescence (Novex ECL chemiluminescence substrate reagent kit, Invitrogen, Grand Island, NY) substrate was used to bind to the secondary antibody which was detected using the FluorChem system (Cell Bioscience, Santa

Clara, CA). Using spot densitometry (intensity of light within a certain region), the intensity of the developed protein bands was then quantified. In all the experiments, beta actin was used as the loading control. Intensity of each protein expression of the sheared aorta was normalized to the corresponding total protein concentration (from the BCA assay), and to the non-sheared aorta's corresponding protein expression for data analysis purpose.

4.3 Specific aim 2: The goal of this aim was to study signaling pathways involved in endothelial cell responses to dynamic shear stress.

Confluent EC were exposed to dynamic shear stress waveforms (of coronary artery) to investigate if the MAPK pathway and NF-κB activation were involved in EC responses to shear stress. Effect of platelets on EC signaling pathway activation was also examined.

4.3.1 Level of MAPK members' phosphorylation of EC

Protein concentration of phosphorylated ERK1/2, JNK, and p38 were measured using Western blot after EC were exposed to various dynamic shear stress (normal and low) waveforms with or without the presence of platelets for 2, 5, 15, 30, and 60 min.

Post shearing, EC were washed 2X with PBS and detached from the plate using trypsin-ethylenediaminetetraacetic acid (EDTA). EC were then lysed (60 min at 4°C) using lysis buffer (TBS with 1% Triton X-100, supplemented with protease and phosphatase inhibitor cocktail). Based on calculation, volumes of lysis buffer were so adjusted that protein concentration remain same in different samples. Lysed samples were centrifuged at 14,000×*g* for 5 min, and the supernatants (lysate) were collected and stored at -80°C until use.

MAPK pathway activation was assessed through quantification of phosphorylated ERK1/2, JNK, and p38 proteins level using Western blot (following similar procedure mentioned in "Sub-cellular protein extraction for Western blotting" in the previous specific aim). Same

amount of extracted samples was loaded in the gel, separated, and transferred from gel to nitrocellulose membrane. The membranes were then blocked in 5% w/v bovine serum albumin (BSA) solution (dissolved in 1X Tris Buffer Saline Tween 20; 137 mM Sodium Chloride, 20 mM Tris, 0.1% Tween-20, pH = 7.4) for 1 hr at RT. Phosphorylation levels of MAPK proteins were detected using rabbit monoclonal anti-human antibodies against phosphorylated ERK1/2, JNK, and p38 (Cell Signaling Technology, Danvers, MA) (overnight, 4°C, with gentle agitation). Primary antibody binding was detected using HRP conjugated goat anti-rabbit secondary antibody (1:1000 dilution, 1 hr, RT) (Abcam, Cambridge, MA). Enhanced chemiluminescence was used for signal detection as described before. The intensity of the bands was quantified using the spot densitometry technique to measure the level of protein phosphorylation. In all the experiments, beta actin was used as an experimental control and purified ERK1/2, JNK, and p38 proteins (15 µL of each control extract) were used as positive control.

Alternatively, MAPK pathway activation was assessed using immunocytochemical staining. Following shear treatment for 60 min, cells were washed with warm PBS and fixed with 0.5% glutaraldehyde (for 15 min at 37°C). After fixing, the cells were blocked with glycine-0.1% BSA (for 30 min at 37°C) and permeabilized with 0.2% Triton-X for 5 min. Permeabilized cells were then incubated with phosphorylated antibody against ERK1/2 (1:200 dilution, Cell Signaling Technology, Danvers, MA) for 2 hr at RT. Primary antibody binding was detected using a biotinylated secondary antibody (1:4 dilution in blocking serum, 1 hr at RT). Immunoreactivity was further enhanced using avidin-biotin complex (ABC reagent, Thermo Scientific). Cells were then stained with DAB substrate (1:10 dilution in stable peroxide buffer, 10 min at RT; Thermo Scientific), followed by counterstaining with haematoxylin. Level of ERK1/2 phosphorylation at various locations was then examined using an optical microscope (Nikon TE 2000U) and images were captured by the digital camera connected to the microscope. A Matlab program was used to

measure the intensity (in grayscale) of the captured images of sheared and non-sheared EC ERK1/2 phosphorylation level.

4.3.2 NF-κB (p65) activation

The level of phosphorylated NF-κB p65 protein was measured using a commercial sandwich ELISA kit (Cell Signaling Technology, Danvers, MA). After shearing EC with or without platelets for different durations (2, 5, 15, 30, and 60 min), the supernatant was removed and EC were washed with warm PBS. EC were then detached and lysed using lysis buffer as previously mentioned. Cell lysates were applied (for 2 hr at 37°C) to micro-titer plates pre-coated with mouse monoclonal anti-human antibody against phosphorylated NF-κB p65 protein. Post incubation, the captured phosphorylated NF-κB p65 protein was detected using a rabbit NF-κB p65 primary antibody (1 hr, 37°C) followed by an HRP conjugated secondary antibody (30 min, 37°C). Level of NF-κB p65 phosphorylation was detected using tetramethylbenzidine (a choromogenic substrate) for 10 min at 37°C. The magnitude of the optical density (proportional to the level of NF-κB p65 protein phosphorylation) of the developed color was measured using the micro-plate reader at 450 nm.

4.4 Specific aim 3: The goal of this aim was to characterize the uptake/release of endothelial growth factors by platelets, and to test the effect of dynamic shear stress on these processes.

Platelets were exposed to dynamic shear stress of coronary collaterals representing normal shear stress (as found in a healthy collateral) and elevated shear stress (as found in a collateral artery downstream of a 60% stenosed main coronary artery), in a cone-plate shearing device for 1 hr to observe the effects of dynamic shear stress on uptake/release of growth factors (PLGF and VEGF-A) by platelets. The effects of calcium chelator and hyperglycemia on uptake/release were also tested.

4.4.1 Platelet mRNA expression

The reverse transcription polymerase chain reaction (RT-PCR) technique was employed to quantify the mRNA expression of PLGF, VEGF, and β-actin in platelets. Total RNA was collected using RNeasy mini columns (Qiagen, Valencia, CA) following manufacturer provided protocol. The quantity and purity of total RNA was analyzed using Take3 micro volume plate of BioTek Synergy HT Multi-mode Plate Reader (BioTek Instruments, Winooski, VT) at A260/280 ratio. Samples were either directly used or stored in -80°C until use. RNA was reverse transcribed to cDNA using the QuantiTect reverse transcription kit (Qiagen, Valencia, CA) according to the manufacturer's instructions. Forward and reverse primer sequences were: human PLGF, CCTACGTGGAGCTGACGTTCT and TCCTTTCCGGCTTCATCTTCT; human VEGF, ACGAGGGCCTGGAGTGTGT and GATCCGCATAATCTGCATGGT; and human β-actin, TGCCGACAGGATGCAGAAG and CTCAGGAGGAGCAATGATCTTGAT, respectively. Target genes were amplified from cDNA in an ABI 7500 Fast instrument (Life Technologies, Grand Island, NY) using PerfeCTa SYBR Green FastMix, Low ROX (Quanta Biosciences, Gaithersburg, MD) with the appropriate forward and reverse primers. Relative PLGF and VEGF mRNA expression (RQ value) was quantified using the comparative ΔC_t and $\Delta\Delta C_t$ method. All the gene expressions were normalized to the β-actin gene expression for comparison purpose.

4.4.2 Uptake of PLGF and VEGF-A by platelets

Levels of PLGF or VEGF-A protein uptake by platelets were measured using a commercial DuoSet ELISA development kit (R&D Systems, McKinley Place, MN). Equal volumes of washed platelet (250,000/μL) aliquots were incubated with varying concentrations (12, 18, 30, 60, and 120 ng/mL) of recombinant human PLGF and recombinant human VEGF-A (R&D Systems, McKinley Place, MN) for 1 hr at RT with gentle rocking motion. The effect of shear stress on uptake was observed by shearing platelets under normal and elevated shear stress conditions in the presence of

recombinant PLGF or VEGF-A protein. The effect of calcium chelator (EDTA) or beraprost sodium (prostacyclin analogue) or hyperglycemia on uptake of these two growth factors was assessed by incubating platelets with EDTA (2 mg/mL) or beraprost sodium (120 ng/mL), or 250 mg/dL glucose (to induce hyperglycemia), along with recombinant PLGF or VEGF-A. EDTA is a metal ion chelator that diminishes Ca^{2+} ion reactivity by sequestering the ion. Beraprost sodium inhibits increase in intracellular Ca^{2+} level through modulation of cAMP production. Since, Ca^{2+} ion plays major role in most of the platelets functions, EDTA and beraprost sodium was used to see whether PLGF and VEGF-A uptake/release by platelets is Ca^{2+} signaling dependent process or not. Post incubation, samples were centrifuged at 1,100×*g* to pellet the platelets. After aspirating the supernatant, platelet pellets were gently washed with 0.9% NaCl without disturbing the pellets. The samples were then re-centrifuged at 14,000×*g* for 2 min and the supernatants were discarded. Afterwards, the pellets were lysed using lysis buffer (RIPA buffer containing protease and phosphatase inhibitors) and incubated for 60 min on ice. The lysed samples were then centrifuged at 14,000×*g* for 5 min and the supernatants were collected in fresh tubes, discarding any pellet at the bottom of the tubes. Samples were either stored at -80˚C for future use or added to prepared micro-titer plates. Microplates were prepared by applying PLGF or VEGF-A capture antibody (provided in the kit) and incubating overnight on a shaker at RT. The next day, the plate was first blocked with 1% BSA (1 hr at RT) and then incubated with samples and standards for 2 hr at RT. After adding detection antibody (for 2 hr at RT), streptavidin-HRP (for 20 min at RT, in the dark), substrate solution (for 20 min at RT, in the dark), the reaction was stopped using stop solution. The color change was quantified by measuring the optical density of each well using the BioTek Synergy HT Multi-mode Plate Reader (BioTek Instruments, Winooski, VT) at 450 nm wavelength. Plates were washed (3X) with wash buffer in between each step.

4.4.3 Release of PLGF and VEGF-A by platelets

The effect of shear stress on PLGF and VEGF-A release by platelets was measured using the commercial DuoSet ELISA development kit (R&D Systems, McKinley Place, MN). Platelets were initially incubated with 200 ng/mL recombinant human PLGF or 120 ng/mL recombinant human VEGF-A (R&D Systems, McKinley Place, MN) for 1 hr at RT on a rocker. In some experiments, EDTA (2 mg/mL), beraprost-sodium (120 ng/mL), or 250 mg/dL glucose were included in the incubation along with PLGF or VEGF-A. Post-incubation, platelets were centrifuged at 1,100×g for 5 min and the supernatant (containing free recombinant protein) was aspirated. The platelet pellet was then resuspended in HBMT and sheared under normal and elevated dynamic shear waveforms for 1 hr. At the end of shear, the platelet-containing fluid medium was centrifuged at 1,100×g for 5 min. The supernatant was collected, then applied to the micro-titer plates of the ELISA kit following the steps described in the previous section (uptake of PLGF and VEGF-A by platelets) to observe the effects of calcium inhibitors and hyperglycemia on shear-induced release of growth factors (PLGF and VEGF-A) by platelets.

4.5 Specific aim 4: The goal of this aim was to quantify the effect of diabetes-associated major metabolic dysfunction on the expression level of PLGF and vascular endothelial growth factor receptor 1 (VEGFR1, the receptor for PLGF) in mouse and human cell.

Previously conducted studies, in our lab, have demonstrated that, mice consuming Western diet for 24 weeks become diabetic and have reduced PLGF expression in heart and skeletal muscle. Since diabetes has many risk factors such as hyperlipidemia, hyperglycemia, hyperinsulinemia, and oxidative stress associated with it, *in vitro* studies were needed to be conducted to identify which of these risk factors has the greatest impact on PLGF expression inhibition. To achieve this goal and to translate the applicability of the mouse study, mouse and human coronary artery EC (CAEC), cardiac muscle cells (CM), and skeletal muscle cells (SKMC) were subjected to various treatments.

Post treatment, samples were collected for cell synthesized PLGF expression and cell surface VEGFR1 (corresponding PLGF receptor) expression assessment.

4.5.1 Advanced Glycation End Product (AGE) preparation

Glycating bovine serum albumin (BSA) protein in presence of D-(+) glucose or DL-glyceraldehyde, AGE was formed in 8 weeks and 1 week respectively. Glucose derived AGE was prepared dissolving 50 mg/mL BSA (Sigma-Aldrich) and 45 mg/mL D-(+) glucose (Sigma-Aldrich) in phosphate buffered saline (PBS, pH 7.4) and incubating the solution at 37˚C for 8 weeks for full albumin glycation. Glyceraldehyde derived AGE was prepared incubating 25 mg/mL BSA in presence of 20 mM DL-glyceraldehyde (Sigma-Aldrich) in PBS at 37˚C for 1 week. Corresponding controls were prepared incubating 50 mg/mL and 25 mg/mL BSA in PBS at 37˚C for 8 weeks and 1 week respectively. Afterwards, prepared AGE solutions were extensively dialyzed in cold fresh PBS (4˚C, every 2 hr, 4X changes) to remove any free AGEs. To ensure that the solutions were gram-negative bacterial contamination free, endotoxin level was quantified using LAL chromogenic Endotoxin Quantitation Kit (Life Technologies Corporation). If the endotoxin concentration came below 1.0 EU/mL, the solution was considered endotoxin free and used to treat the cells. Protein concentration of the BSA and AGE samples were measured, before treatment, using BCA protein assay kit (Pierce).

4.5.2 Treatments of cells

After confluency was reached, all the cell types (HCAEC, HSKMC, MSKMC, HCM, and MCM), prior to treatment exposure, were serum starved in serum reduced media for 24 hr. To induce diabetes-associated metabolic dysfunctions including hyperlipidemia, hyperglycemia, hyperinsulinemia, and oxidative stress, initially, HCAEC were treated with 50 - 200 µg/mL LDL (Alfa Aesar) or oxidized LDL (ox-LDL, Alfa Aesar), 5 - 20 mM glucose (Sigma Aldrich) or 300 - 1000 µg/mL AGE (glucose or glyceraldehyde derived), 100 - 500 mU/L insulin (Sigma Aldrich),

or 0.05 - 0.3 mM hydrogen peroxide (H_2O_2, vWR International) respectively for 24 hr. Treatments were directly added to the cell culture medium and post treatment, medium supernatant were collected at 4, 8, and 24 hr in protease inhibitors containing microcentrifuge tubes. Along with treatments, untreated cells medium was also collected to use as control sample. Since, cells release synthesized PLGF protein into the medium, only the medium was collected for PLGF protein quantification using sandwich ELISA technique. The most effective concentrations of the metabolic molecules tested were then used to treat the other cell types (HSKMC, MSKMC, HCM, and MCM). After 24 hr time point medium collection, cells were washed (3X with PBS), trypsinized (using 1% TrypleE, Life Technologies Corporation), collected, and lysed using lysis buffer (RIPA buffer containing protease inhibitors) for VEGFR1 quantification. Post 1 hr ice incubation of cells in lysis buffer, sample containing tubes were centrifuged at 14,000×*g* for 5 min to get rid of any cell debris. The supernatants were then collected and used for running VEGFR1 ELISA experiments.

4.5.3 PLGF and VEGFR1 protein quantification

Level of PLGF protein and VEGFR1 protein, produced and expressed on cell surface respectively by different treatment exposed cells, were quantified using solid phase sandwich ELISA technique. Mouse DuoSet ELISAs and human DuoSet ELISAs (R&D Systems) for PLGF and VEGFR1 were purchased for corresponding mouse and human proteins expressions. After exposing cells to different treatment conditions for 24 hr, media samples were collected 4, 8, and 24 hr post treatment and stored at -80°C to use later. At 24 hr, rest of the media were aspirated out and the cells were washed, trypsinized, and lysed using 4°C, protease inhibitor added RIPA lysis buffer. Lysed cells were also stored at -80°C until use. To prepare the plates for protein detection, 96-well microplates were coated and incubated overnight at RT with corresponding capture antibodies on a slow moving shaker. The next day, washing off the capture antibodies, the wells were blocked with reagent diluent (1% BSA, 1 hr, RT) followed by standard/sample incubation (2

hr, RT). Proteins were captured from samples and detected using detection antibody (2 hr, RT), streptavidin HRP (20 min, RT, dark), and substrate solution (20 min, RT, dark). After stopping the reaction using stop solution, the optical density of each well was measured immediately using a Biotek Synergy HT multi-mode plate reader (BioTek Instruments Winooski, VT) at 450 nm wavelength. Values were normalized to total protein concentrations as determined by BCA protein assay (Pierce Biotechnology, Rockford, IL).

4.6 Specific aim 5: The goal of this aim was to investigate the effects of glucose, advanced glycation end products (AGE), and the presence of smooth muscle cells (SMC) on dynamic shear stress-stimulated EC PLGF expression, and to identify the signaling pathways involved.

EC of the co-culture models were exposed to dynamic shear stress of coronary/peripheral collaterals using the cone-plate shearing device in presence/absence of glucose/advanced glycation end product (AGE) treatment to study how hyperglycemic conditions can modulate shear stress induced EC PLGF expression affecting the cell-cell communication. Signal pathways involved in PLGF modulation had also been assessed through quantification of several genes expression.

4.6.1 EC produced PLGF expression

HCAEC/HIAEC (confluent) of the co-culture models were sheared directly, under conditions mimicking normal and elevated dynamic shear stress of healthy and diseased coronary/peripheral collateral artery respectively (as mentioned previously in collateral blood flow induced shear stress section), in the 6 well cone-plate shearing device for 2 hr in presence or absence of glucose/AGE treatments. Culture medium/supernatant samples were collected just pre-shear 0 hr, and post-shear 0 hr, 8 hr, and 24 hr. Using the sandwich ELISA technique, mentioned in the previous section, EC produced PLGF expression was assessed.

4.6.2 EC mRNA expression

The effects of dynamic shear stress (elevated shear stress of coronary collateral arteries) and/or glucose (20 mM)/AGE (1000 μg/mL) on EC RAGE, Nox2, Nox4, HO-1, MCP-1, TNF-α, and β-actin mRNA expressions were examined using reverse transcription polymerase chain reaction (RT-PCR). At the end of 2 hr dynamic shear stress exposure and 24 hr static incubation, EC were gently washed, trypsinized, collected, and resuspended in 1% β-mercaptoethanol added RLT lysis buffer. RT-PCR was then conducted on the targeted genes (RAGE, Nox2, Nox4, HO-1, MCP-1, TNF-α, and β-actin) following the procedure described previously ("Platelet mRNA expression") for the mRNA level quantification. Forward and reverse primer sequences used for targeted genes were: for human RAGE, 5'-ATTGGTGGTGGAGCCAGAAG-3' and 5'-CAGGTCAGGGTTACGGTTCC-3'; for human Nox2, 5'-GGGAACTGGGCTGTGAATGA-3' and 5'-CCAGTGCTGACCCAAGAAGT-3'; for human Nox4, 5'-GGGGTTAAACACCTCTGCCT-3' and 5'-ACACAATCCTAGCCCCAACA-3'; for human HO-1, 5'-CTGCGTTCCTGCTCAACATC-3' and 5'-GGCAGAATCTTGCACTTTGTTG-3'; for human MCP-1, 5'-TGCTCATAGCAGCCACCTTC-3' and 5'-GGGCATTGATTGCATCTGGC-3'; for human TNF-α, 5'-GAATCGGAGCAGGGAGGATG-3' and 5'-AAGTTGGGGACACACAAGCA-3'; and for human β-actin, 5'-AGTTCGCCATGGATGACGAT-3' and 5'-TGCCGGAGCCGTTGTC-3' respectively.

4.7 Specific aim 6: The goal of this aim was to discover the key underlying molecular mechanisms by which a Western diet induces dysfunctional PLGF expression in mouse skeletal muscle.

To understand the underlying molecular mechanisms for the dysfunctional PLGF expression in skeletal muscle tissues of Western diet fed diabetic mice, the protein level of AGE

was quantified (using sandwich ELISA) along with the mRNA level of RAGE, Nox2, Nox4, HO-1, MCP-1, TNF-α, and β-actin (using RT-PCR) in the tissues.

4.7.1 Animals, diets, and metabolic phenotyping

Two different mouse strains (C57BL/6J and ApoE$^{-/-}$) were fed with control diet (TD 120336, Harlan, containing 13% Kcal from fat and cholesterol, 67.9% Kcal from carbohydrate, and 19.2% Kcal from protein) or Western diet (TD 88137, Harlan, containing 3X more sucrose than control diet, 42% Kcal from fat and cholesterol, 42.7% Kcal from carbohydrate, and 15.2% Kcal from protein) to induce healthy/diabetic conditions. The diet program was started at the age of 6-8 weeks of the mice and continued until their sacrifice at 24 weeks. Body weight was recorded weekly for every mouse. Prior to sacrifice, blood samples were collected for total plasma cholesterol and triglyceride level, and plasma 8-isopreostance (biomarker of oxidative stress) level quantification. Plasma level of glucose and insulin level were also measured through intraperitoneal glucose tolerance testing (IPGTT) to confirm metabolic phenotyping. The mouse breeding, raising, feeding, and metabolic phenotyping were conducted by another lab member, Dr. Asitha T Silva.

4.7.2 Tissue Collection

Post sacrifice, control/Western diet fed C57BL/6J and ApoE$^{-/-}$ mice were anesthetized using 5% isoflurane until they were totally sedated (confirmed applying pressure in toes to observe muscle twitch). The thoracic cavity was opened afterwards to ensure lung collapse. Removing the skin layer from the hindlimb, quadriceps femoris (QF) and gastrocnemius/plantaris/soleus (G-P-S) muscles were collected from the thigh and calf respectively. Tissues were divided into two pieces: one for tissue AGE level and the other for tissue mRNA level quantification of several targeted genes. Samples were immediately frozen in liquid nitrogen and then preserved in -80˚C for future use.

4.7.3 AGE protein quantification

Muscle tissues were homogenized, prior to AGE protein quantification, using the Bio-Gen Pro200 homogenizer (PRO Scientific). Submerging the tissues in ice cold 1 mL lysis buffer (RIPA buffer added with protease inhibitors), homogenization was done, three times, going from speed 1 to 5 slowly and then back to speed 1 in 40 sec. A minute interval was given in between each homogenization step to reduce protein degradation due to overheating. The homogenates were then centrifuged at 700×g for 10 min to get rid of tissue debris. Collecting the tissue supernatant in fresh tubes, samples were then either stored in -80˚C or immediately used for running AGE ELISA. OxiSelect AGE competitive ELISA kit from Cell Biolabs was used for quantifying the AGE protein adducts following the manufacturer's instructions. Briefly, the required number of wells of the 96 well plate were coated with 1:1 ratio of AGE conjugate and conjugate diluent and incubated at 4˚C overnight. Next day, removing the AGE conjugate coating solution, the wells were washed and blocked with assay diluent for 1 hr at RT. Then the prepared AGE-BSA standards and unknown samples were added to the AGE conjugate absorbed wells in duplicate. After 10 min incubation on orbital shaker at RT, anti-AGE polyclonal primary antibody was added (1 hr, RT) followed by HRP conjugated secondary antibody (1 hr, RT). Substrate solution was then added for 2 – 20 min, and depending on the color change, the enzyme reaction was stopped adding stop solution to prevent color saturation. The optical density value of the color change was immediately read using the Biotek Synergy HT multi-mode plate reader (BioTek Instruments Winooski, VT) at 450 nm wavelength. Comparing with the AGE-BSA standard curve, the level of AGE protein adducts in the unknown samples were determined, which was normalized to the total protein concentration (quantified using BCA assay). The wells were washed three times and emptied properly in between each step.

4.7.4 mRNA expression of skeletal muscle tissues

Collected muscle tissue sections (QF and G-P-S) were weighed and diced/minced to the smallest pieces possible using very fine surgical scissors. The tissue holding tubes were kept in ice bucket all the time and 1-2 tissue sections were handled each time to reduce tissue mRNA degradation. RLT lysis buffer (1% β-mercaptoethanol added) was then added to the minced tissues at the ratio of 10 µL/mg of tissue. A Bio-Gen Pro200 homogenizer (PRO scientific) was used to homogenize the tissues (three times, 40 sec each), submerged in the RLT buffer, going slowly from low to high level and then back to low level giving interval in between every step. Homogenized tissue supernatants were then centrifuged at 2000×*g* for 10 min to get rid of any tissue debris and the clear supernatants were transferred in new tubes. Total RNA was collected using RNeasy Fibrous tissue mini kit (Qiagen) following the manufacturer's instructions. RNA level of each tissue section was analyzed for quantity and purity using spectrophotometer, reverse transcribed to cDNA, and amplified for targeted genes (mouse RAGE, Nox2, Nox4, HO-1, MCP-1, TNF-α, and β-actin) employing RT-PCR technique mentioned previously in "Platelet mRNA expression" section. Used forward and reverse primer sequences for the targeted genes were: for mouse RAGE, 5'-CAAGGAGGAACCACCCATCC-3' and 5'-CAACCAACAGCTGAATGCCC-3'; for mouse Nox2, 5'-CACACCGCCATCCACACAAT-3' and 5'-GTCACCGATGTCAGAGAGAGC-3'; for mouse Nox4, 5'-TGCCCCAGTGTATCAGCATTAG-3' and 5'-CCGGAATCGTTCTGTCCAGTC-3'; for mouse HO-1, 5'- TCGTGCTCGAATGAACACTCTG-3' and 5'-AGCTCCTCAAACAGCTCAATGT-3'; for mouse MCP-1, 5′-GGCTCAGCCAGATGCAGTTAA-3′ and 5′-CCTACTCATTGGGATCATCTTGCT-3′; for mouse TNF-α, 5'-GACGTGGAACTGGCAGAAGA-3' and 5'-GAGGCTGAGACATAGGCACC-3'; and for mouse β-actin, 5′-AGTTCGCCATGGATGACGAT-3′ and 5'-TGCCGGAGCCGTTGTC-3' respectively. Gene expressions were normalized to the expression of β-actin and the relative gene expressions were quantified using the comparative ΔC_t, $\Delta\Delta C_t$ method.

4.8 Statistical Analysis

Statistical analysis was conducted using Student's *t*-test or ANOVA as appropriate for the experimental design. If a significant difference ($P<0.05$) was detected by ANOVA, the data were further analyzed for multiple comparisons using the Student-Newman-Keuls *post hoc* method. The non-parametric Kruskal-Wallis method was used if a large variance was present. “Primer of Biostatistics” and “Statistical Analysis System” (SAS) software were used for all the statistical analyses.

CHAPTER V

RESULTS

5.1 Specific aim 1: The goal of this aim was to measure platelet and endothelial cell (EC) responses under physiologically relevant dynamic shear stress conditions *in vitro*, and to determine whether the presence of one cell type affects the responses of the other to shear. In addition, the effects of dynamic shear stress on endothelial cell responses *ex vivo*, in a rat aorta model, was also investigated.

Washed platelets and confluent EC were sheared alone or together using the cone-plate shearing device. Dynamic shear stress conditions included normal shear stress, low pulsatile shear stress representing the recirculation zone, and elevated shear stress representing conditions at the stenosis throat of a left coronary artery. Post shearing, platelet responses to flow were measured by assessing platelet surface PECAM-1, GPIbα, and GPIIb expression, and platelet microparticle generation. EC responses to flow were measured by assessing EC surface and released vWF and TF expression, and endothelial microparticle generation.

5.1.1 PECAM-1 expression on the platelet surface

Washed platelets (250,000/µl) were exposed to normal and low pulsatile shear stress for 30 and 60 min with or without the presence of confluent EC. Afterwards, platelet surface PECAM-1 expression was measured with flow cytometry using a PE conjugated anti-human PECAM-1

antibody. All mean fluorescence values were normalized to that of untreated platelets. Figure 5.1 shows that neither shear stress magnitude nor presence of EC affected platelet surface PECAM-1 expression after 30 min shear exposure (n=6/group). However, platelet surface PECAM-1 expression was increased in the presence of EC under both flow conditions after 60 min shear exposure (n=7-8/group), although shear stress magnitude had no effect. Statistical analysis indicated that platelet surface PECAM-1 expression was significantly ($P<0.05$) up-regulated in the presence of EC under dynamic shear stress conditions after 60 min of shear exposure.

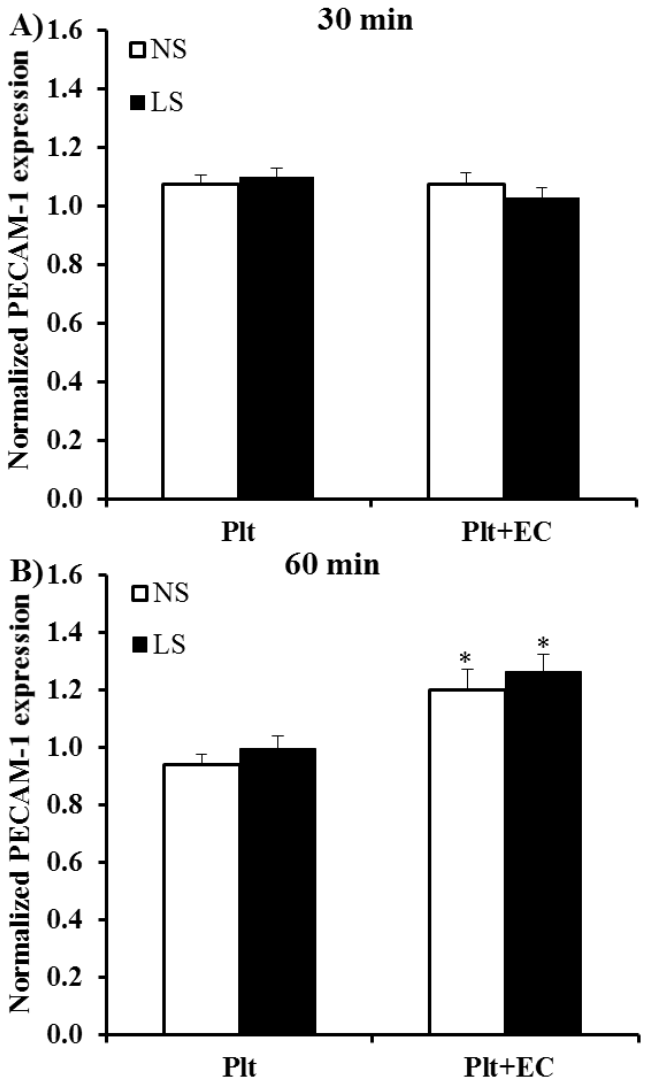

Figure 5.1: PECAM-1 expression of platelets exposed to normal and low pulsatile shear stress for 30 min and 60 min in absence or presence of EC. All mean fluorescence intensity of PECAM-1 expression was normalized to that of control platelets. Values are depicted as Mean+SD. Analysis (from three-way ANOVA) indicated significant increase (P<0.05) in PECAM-1 expression of platelets after 60 min of shear exposure when EC were incorporated into the system (n=7-8/group). However, no significant change in platelet PECAM-1 expression was observed under dynamic shear stress after 30 min of shear exposure even in the presence of EC (n=6/group). (NS: Normal shear, LS: Low shear, Plt: Platelet, *: P<0.05)

These results provided evidence that presence of EC can increase PECAM-1 expression on the platelet surface under dynamic shear stress conditions with prolonged shear exposure.

5.1.2 Platelet surface GPIbα expression

Platelets were exposed to normal (NS), low (LS), and elevated (ES) pulsatile shear stress with or without the presence of EC for 60 minutes. Platelet surface GPIbα expression was then measured by flow cytometry using a FITC conjugated anti-CD42b antibody. All mean fluorescence intensity values were obtained and normalized to those of resting platelets. In the absence of EC, platelets expressed lower level of GPIbα under pathological flow conditions (low and elevated pulsatile shear stress) compared to the normal flow condition (Figure 5.2, n=6/group). In the presence of EC, platelet surface GPIbα expression was reduced under all three dynamic shear stress, significantly under NS and ES (P<0.05) conditions (n=6/group). However, no statistically significant difference was observed, in platelet GPIbα expression between the different dynamic shear stress conditions within each group (absence or presence of EC).

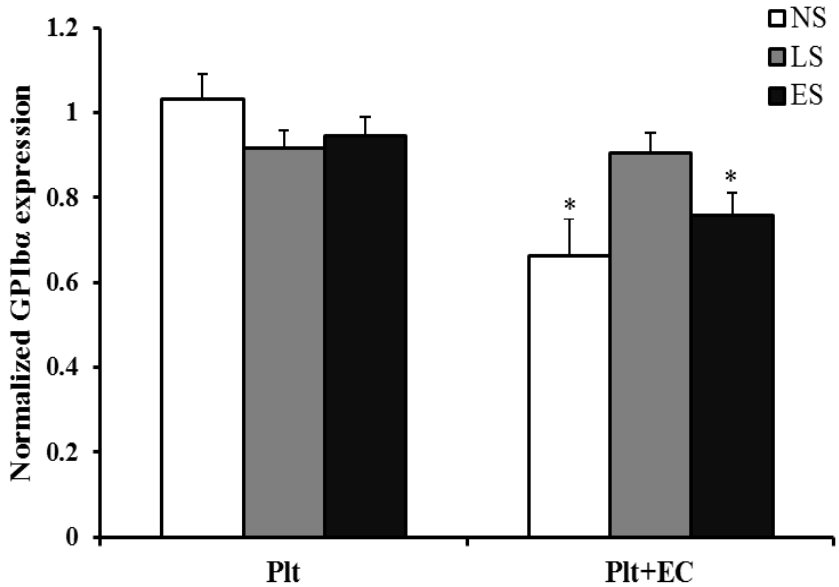

Figure 5.2: Normalized platelet surface GPIbα expression (Mean+SD) under normal (NS), low (LS), and elevated (ES) shear stress conditions, when platelets were sheared (60 min) without or with EC. Normalized values were obtained from the ratio of all mean fluorescence GPIbα expression values of sheared platelets and the corresponding resting platelets (n=6/group). Platelet surface GPIbα expression decreased significantly under NS and ES conditions, when EC were incorporated into the system (*: P<0.05).

Results from these experiments indicated that the presence of EC decreases platelet surface GPIbα expression in response to dynamic flow.

5.1.3 Platelet surface GPIIb expression

Platelets (250,000/μl) were exposed to constant (0.1 Pa, 0.3 Pa, 1 Pa, and 3 Pa) and dynamic shear stress (normal, low, and elevated shear stress) conditions in the presence or absence of confluent healthy or activated (by 1 ng/mL TNF-α) EC for 60 min. Timed sheared samples were collected every 15 min starting at time 0 min. Post-shear, platelet samples were incubated with a FITC conjugated anti-human CD41a antibody (30 min, RT, dark) and analyzed immediately using flow cytometry. All mean fluorescence intensity values were normalized with respect to the signal from non-sheared control platelets. Figure 5.3 shows the normalized mean fluorescence values of platelet GPIIb expression under both constant and dynamic shear stress conditions when platelets were sheared in the absence of EC (n=5-6/group). Platelet GPIIb expression increased slightly after 15 min of constant shear stress exposure, then decreased with shear exposure time. After 60 min shear exposure, GPIIb expression decreased 7.5-20.7% across all shear conditions, compared to the 15 min expression under the same conditions. This effect was strongest in the 3 Pa group, possibly indicating impairment of GPIIb expression under elevated shear condition. Two-way ANOVA analysis indicated that constant shear stress had a significant (P<0.05) effect in downregulation of platelet GPIIb expression. However, no significant change in GPIIb expression was observed under dynamic shear stress when platelets were sheared alone (Figure 5.3, bottom panel). Figure 5.4 illustrates the effect of cellular interaction between platelets and healthy/activated EC on platelet surface GPIIb expression under normal, low, and elevated shear stress, respectively (n=6/group). A decreasing trend was observed in GPIIb expression in presence of EC. Two-way ANOVA analysis indicated that there was a significant difference in GPIIb expression under normal and elevated (P<0.05, in presence of healthy EC), and low and elevated (P<0.05, in presence of activated EC) shear stress conditions.

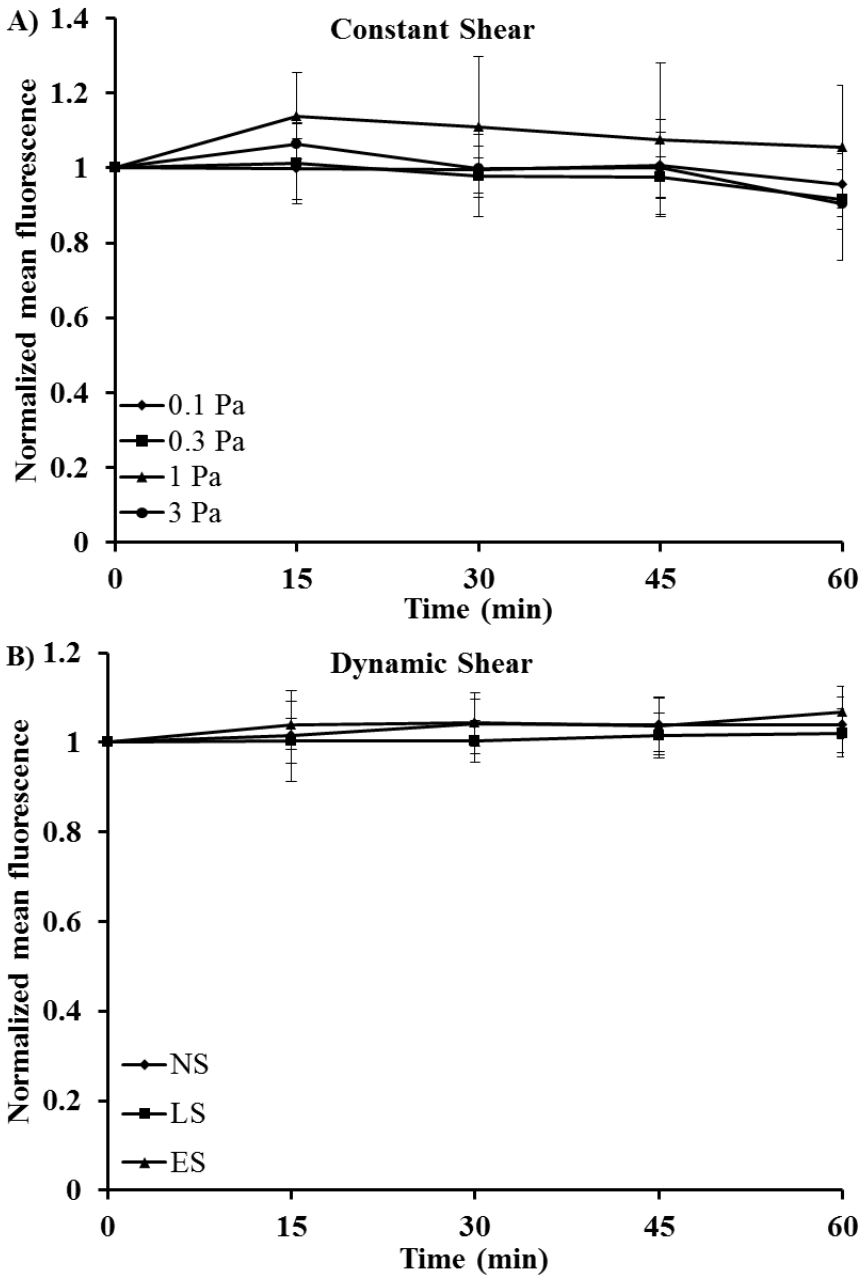

Figure 5.3: Platelets were activated under constant (0.1 Pa, 0.3 Pa, 1 Pa, and 3 Pa) and dynamic (normal, low, and elevated) shear stress for 60 min in a cone-pate shearing device. Platelet surface GPIIb expression was measured in samples collected every 15 min (n=5-6/group). Data are represented as normalized mean fluorescence value (ratio of GPIIb expression of treated timed sample and corresponding control) ± SD. Results indicated significant decrease in GPIIb expression under constant shear exposure (P<0.05), but, not under dynamic shear stress exposure. (Normal shear – NS, low shear – LS, elevated shear – ES).

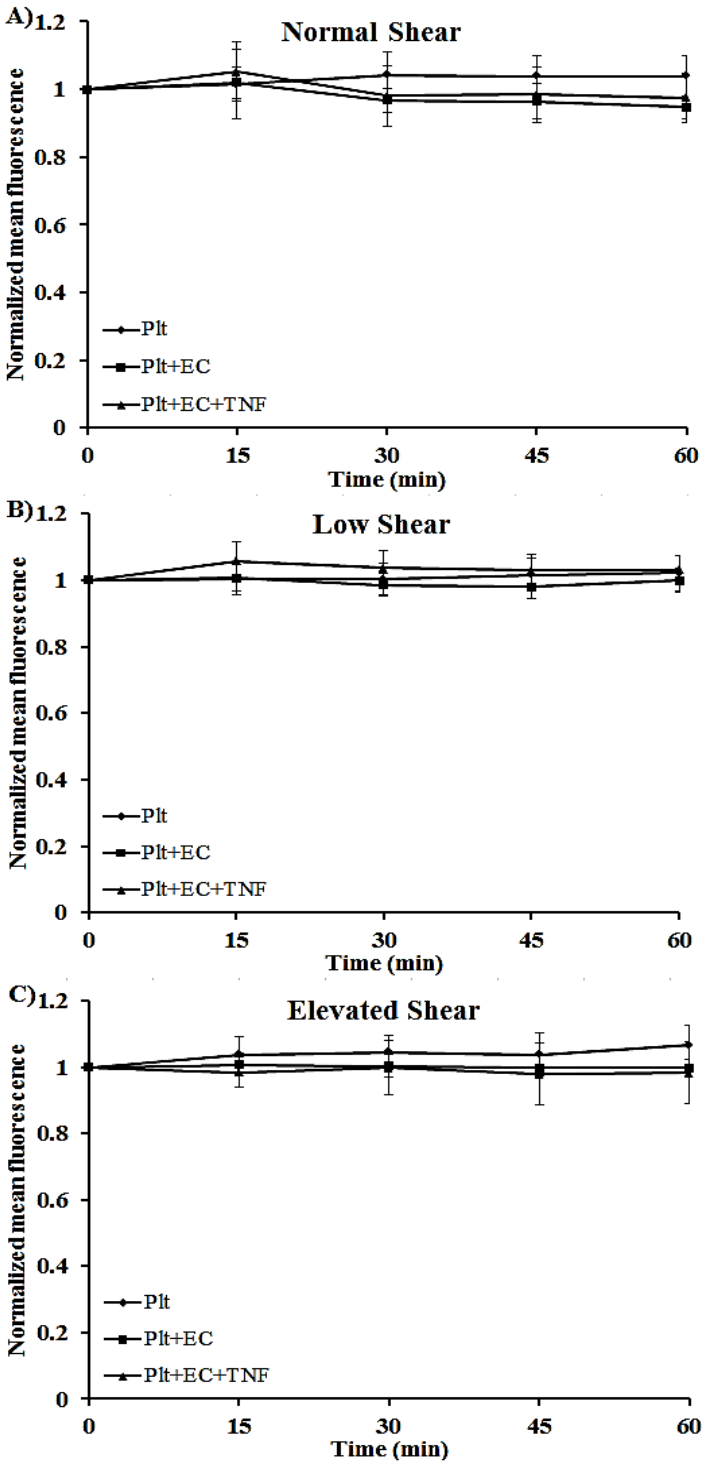

Figure 5.4: Platelets were exposed to dynamic (normal, low, and elevated) shear stress waveforms using a cone-plate shearing device for 60 min in absence/presence of healthy/activated EC and samples were collected every 15 min (n=6/group). Normalized mean fluorescence values of GPIIb expression are represented as Mean±SD. Results indicated decreasing trend in presence of healthy/TNF-α activated EC. Significant difference was observed in GPIIb expression induced by normal and elevated shear stress (P<0.05) in presence of healthy EC, and by low and elevated shear stress (P<0.05) in presence of activated EC.

Using normalized mean fluorescence values for platelet surface GPIIb expression when platelets were exposed to constant shear stress (0.1, 0.3, 1, 3 Pa), as a function of exposed shear stress and shear exposure time, a three dimensional plot (Figure 5.5) was developed using MATLAB. This mathematical model can be used for predicting platelet surface GPIIb expression for different shear stress and exposure time values.

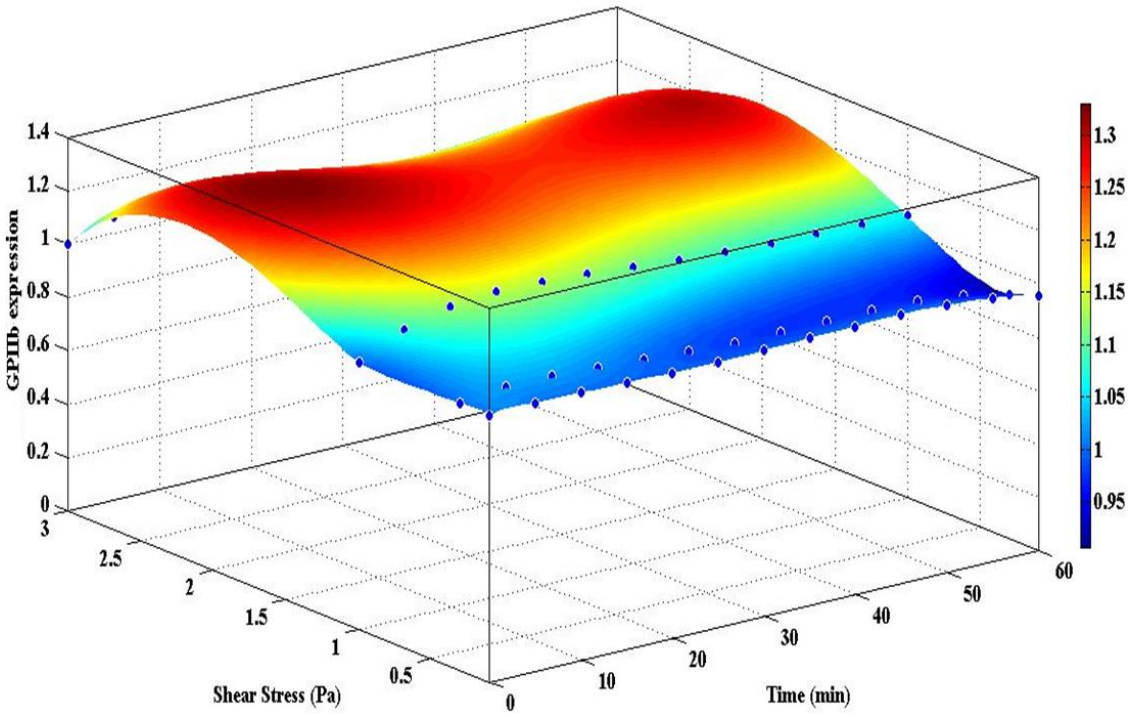

Figure 5.5: A 3D mathematical model for GPIIb expression. Using shear stress magnitude varying between 0 to 3 Pa for exposure duration varying between 0 to 60 min, corresponding platelet surface GPIIb expression can be predicted.

This model was validated using experimental data for platelet GPIIb expression following dynamic shear exposure. Plotting a graph in Excel (Figure 5.6) for GPIIb expression vs shear stress-exposure time integral, a mathematical equation was obtained for constant shear (0.1, 0.3, and 1 Pa) stresses up to 60 min. Since the shear stress-exposure time integral values for dynamic shear stress varies between 828-2088 Pa-s, the excel plot was drawn for 0.1, 0.3, and 1 Pa constant shear stress only. The equation was then used to predict GPIIb expression for dynamic shear stress-time

integral values. Experimental values were close to predicted values (Table 1) and comparison showed minimal % error (below 15%).

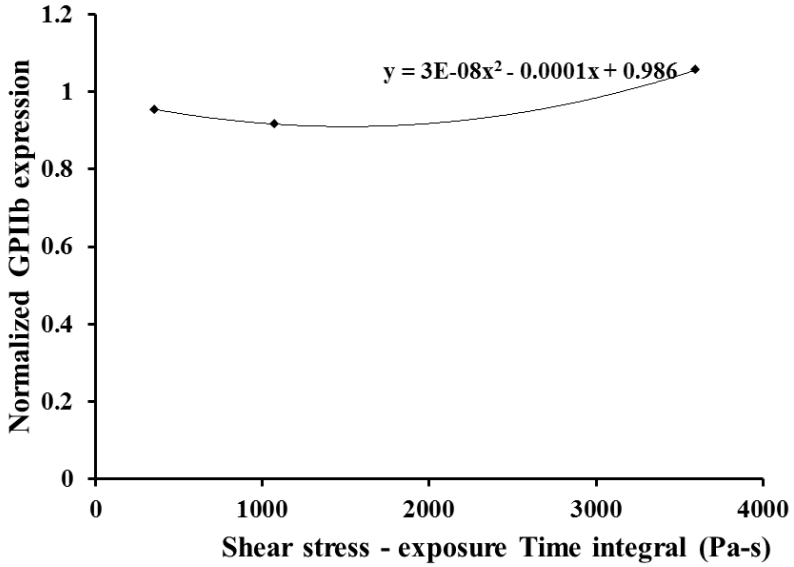

Figure 5.6: Platelet surface GPIIb expression under different constant shear stress-exposure time integrals.

Table 1: Mathematical model validation

Shear Stress	Shear Stress-time integral (Pa-s)	Experimental value	Predicted value	% error
NS	1980	1.039	0.906	12.84
LS	828	1.021	0.924	9.52
ES	2088	1.067	0.908	14.90

For easier comparison of data, normalized GPIIb expression of platelets exposed alone or together with healthy EC for 60 min under dynamic shear stress waveforms were put together in Figure 5.7. Platelet GPIIb expression was significantly decreased (P<0.05) in the presence of EC, under normal and elevated shear stress conditions.

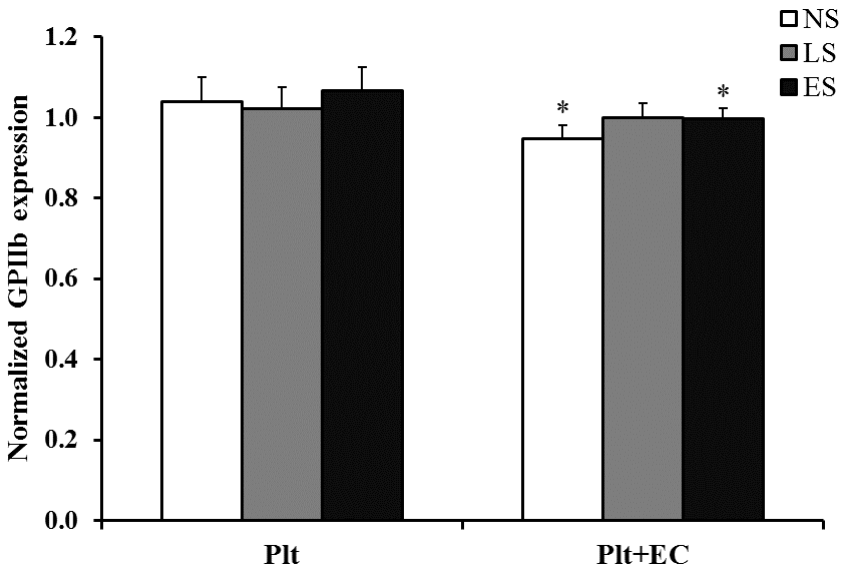

Figure 5.7: GPIIb expression of platelets, sheared alone or together with EC for 60 min, under dynamic shear stress [normal (NS), low (LS), and elevated (ES)] conditions (n=5-6/group). Mean fluorescence values were normalized to those of resting platelets. A significant decrease in GPIIb expression was observed when platelets were sheared in presence of EC under normal and elevated (P<0.05) shear stress conditions. Data are presented as Mean+SD.

These results suggested that dynamic shear stress can decrease platelet surface GPIIb expression in the presence of EC.

5.1.4 Platelet microparticle (PMP) and endothelial microparticle (EMP) generation

Platelets were sheared in presence of EC under dynamic shear stress (normal, low, and elevated) for 30 min. Post shearing, platelet microparticles (PMP) and endothelial microparticles (EMP) were identified by flow cytometry as CD31+/CD42b+ and CD31+/CD42b- respectively. Flow cytometry results indicated an increase in EMP and PMP generation under all shear stress conditions, compared to control. The majority of the microparticles detected were EMP. Figure 5.8 depicts EMP and PMP generation (n=4-6/group) normalized with respect to resting control. Results from the non-parametric Kruskal-Wallis test (used due to the large variance in the number of microparticles across samples) indicated that elevated dynamic shear stress significantly increased EMP (P<0.05) generation, though had no effect on PMP generation. Further comparison

for EMP and PMP generation indicates no significant difference in the generated microparticle numbers under different dynamic shear stress exposure.

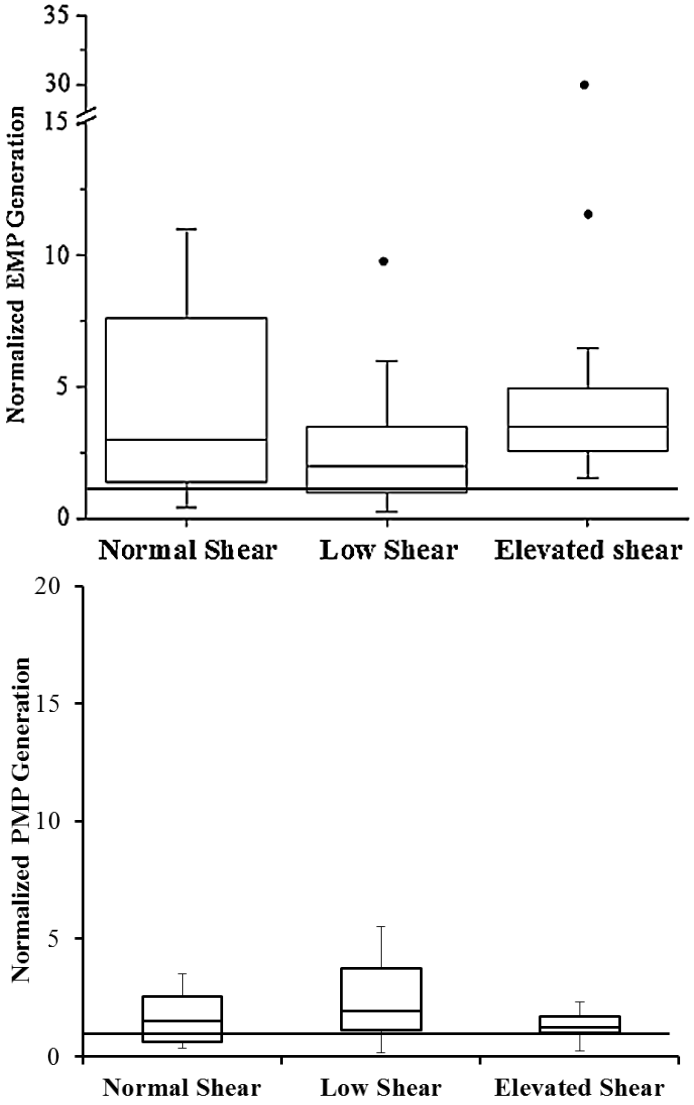

Figure 5.8: Box plot representing normalized (with respect to control) EMP and PMP generation when platelets and EC were co-sheared under dynamic shear stress (NS, LS, and ES) conditions (n=4-6/group). Data are presented as maximum and minimum values along with 75th and 25th percentile (black circles - outliers).

These results indicated that EMP generation can be enhanced by exposure to dynamic shear stress.

5.1.5 EC surface vWF expression

Confluent EC were exposed to constant shear stresses (0.1, 0.3, 1, and 3 Pa) for 60 min. Post-shearing, EC surface vWF expression was measured using solid phase ELISA (n=4-6/group). Figure 5.9 represents the EC surface vWF expression following exposure to constant shear stress at 0.1, 0.3, 1 and 3 Pa. Different shear stress exposure could not induce any significant changes in EC surface vWF expression.

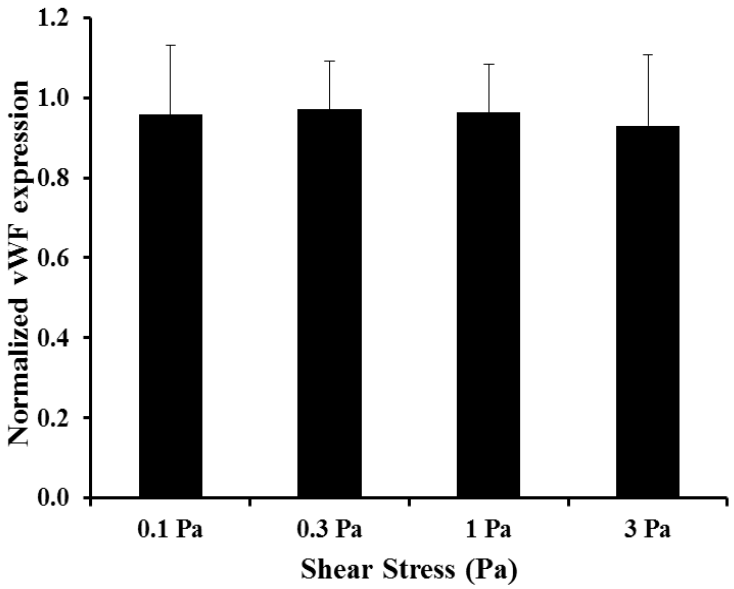

Figure 5.9: Surface expression of sheared (0.1, 0.3, 1, and 3 Pa shear exposure for 60 min) EC vWF expression (n=4-6/group). There was no significant effect of shear stress on EC surface vWF expression. Data are presented as Mean+SD.

EC were also sheared for 60 min in the absence (in a parallel study conducted in our lab) or presence of platelets using dynamic shear waveforms. After shearing, supernatant was removed and EC surface vWF expression was quantified using solid phase ELISA. Figure 5.10 demonstrates the surface vWF expression of EC co-sheared with platelets under dynamic shear exposure (n=5-6/group). There was no significant effect of dynamic shear stress on EC surface vWF factor expression in the presence of platelets. However, compared to EC sheared alone (normal shear, Mean±SD value: 1.00±0.31; low shear, 1.11±0.27; elevated shear, 1.00±0.2), EC co-sheared with

platelets had increased expression of surface vWF (normal shear, 1.104±0.163; low shear, 1.204±0.21; elevated shear, 1.244±0.187)[221].

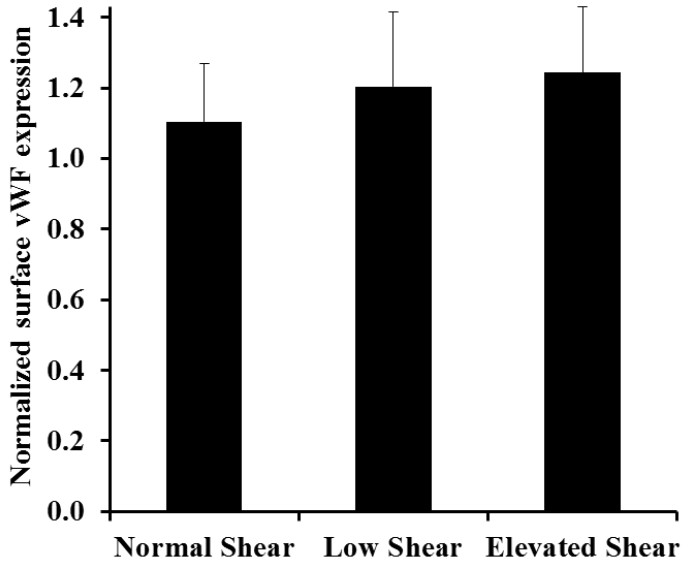

Figure 5.10: vWF expression of EC co-sheared with platelets under normal, low, and elevated shear stress (n=5-6/group). No significant effect of dynamic shear stress on EC surface vWF level was observed. Data are presented as Mean+SD.

Results from the vWF experiments indicated that EC surface vWF expression is unaffected by shear stress exposure.

5.1.6 Soluble vWF expression

The amount of soluble vWF released by EC and platelets following dynamic shear stress exposure was also measured (n=7-8/group). EC released significantly (P<0.05) more soluble vWF under elevated shear stress condition (Figure 5.11). Data analysis (two-way ANOVA) results demonstrated significantly increased soluble vWF expression under elevated shear stress (P<0.05) compared to the normal and low shear stress exposure.

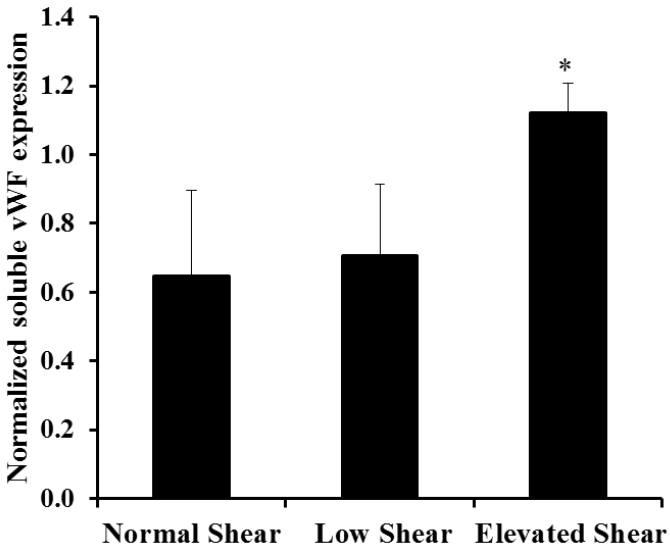

Figure 5.11: Soluble vWF expression of EC in presence of platelets under normal (NS), low (LS), and elevated shear (ES) stress (n=7-8/group). A significantly (P<0.05) increased amount of soluble vWF is released under ES compared to the NS and LS. Data are presented as Mean+SD.

These results indicated that dynamic shear exposure enhance soluble vWF expression.

5.1.7 EC surface TF expression

The effect of shear stress on EC surface TF expression was measured by exposing EC to constant shear stress (0.1, 0.3, 1, and 3 Pa) and dynamic shear stress (normal, low, and elevated; in a parallel study conducted in our lab) for 60 min. The solid phase ELISA technique was utilized for TF measurement. Figure 5.12 represents EC surface TF expression after exposure to constant shear (n=6-7/group). No significant effect of constant shear or dynamic shear stress on EC surface TF expression was observed[221].

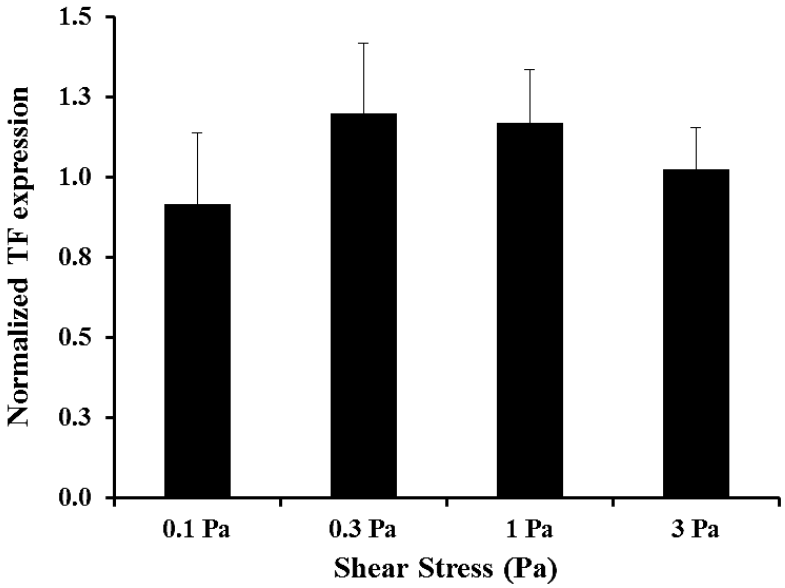

Figure 5.12: TF expression of EC surface, when EC were exposed to 0.1, 0.3, 1, and 3 Pa shear stress waveforms for 60 min (n=6-7/group). No significant effect of constant shear on EC surface TF expression was detected (Data are presented as mean+SD).

All these results indicated that dynamic shear exposure and platelet-EC communication can enhance platelet surface PECAM-1 expression, EC released soluble vWF expression, and EMP generation, and decrease platelet surface GPIbα and GPIIb expression. Overall, these results demonstrated that communication between platelets and EC can modulate functional responses of platelets and EC.

5.1.8 Platelet adhesion to EC

EC were exposed to dynamic (normal and low) shear stress waveforms for 60 min in presence of platelets. TNF-α treated EC were used as positive control. Post-shear exposure or positive control treatment, platelet adhesion to EC was observed using optical microscopy. Figures are attached in appendix which shows platelet-EC interaction under different treatment conditions (TNF-α or shear). Images were consistent with more interaction and attachment of platelets to EC under pathological low shear stress exposure than under normal shear conditions (based on n=2). However, more experiments were needed to be conducted for reaching a definite conclusion.

5.1.9 vWF, ICAM-1, and TF protein expressions of EC in rat aorta model

Physiological relevance was further enhanced by investigating the effects of dynamic shear stress on EC responses in rat aorta model *ex vivo*. Freshly dissected rat abdominal aortas were perfused with physiological salt solution at different flow rates (2 hours at 37°C) to achieve normal, low, and elevated shear stress (shown in Figure 4.2B) at the vessel wall. Cytoplasmic and membrane proteins were extracted from abdominal aortas to assess vessel wall vWF, ICAM-1, and TF expression through Western blot (n=9-13/group). Figure 5.13 represent Western blot results for cytoplasmic and membrane-bound vWF, ICAM-1, and TF for proteins extracted from sheared aortas. Data were first normalized to the total protein (obtained from BCA assay) in the sample, and then to the expression of the same marker in control (unsheared) aortas. Results from Western blots indicated that shear stress significantly reduced (P<0.05) vWF and ICAM-1 protein expressions compared to that of control aortas. Both vWF and ICAM-1 protein level were reduced in the cytoplasmic level of sheared aortas; whereas, ICAM-1 was also reduced in the membrane fraction compared to non-sheared aortas. However, no significant differences were observed in either cytoplasmic or membrane bound TF expression between non-sheared and shear exposed aortas or in vWF, ICAM-1 or TF levels across the three shear stress exposures.

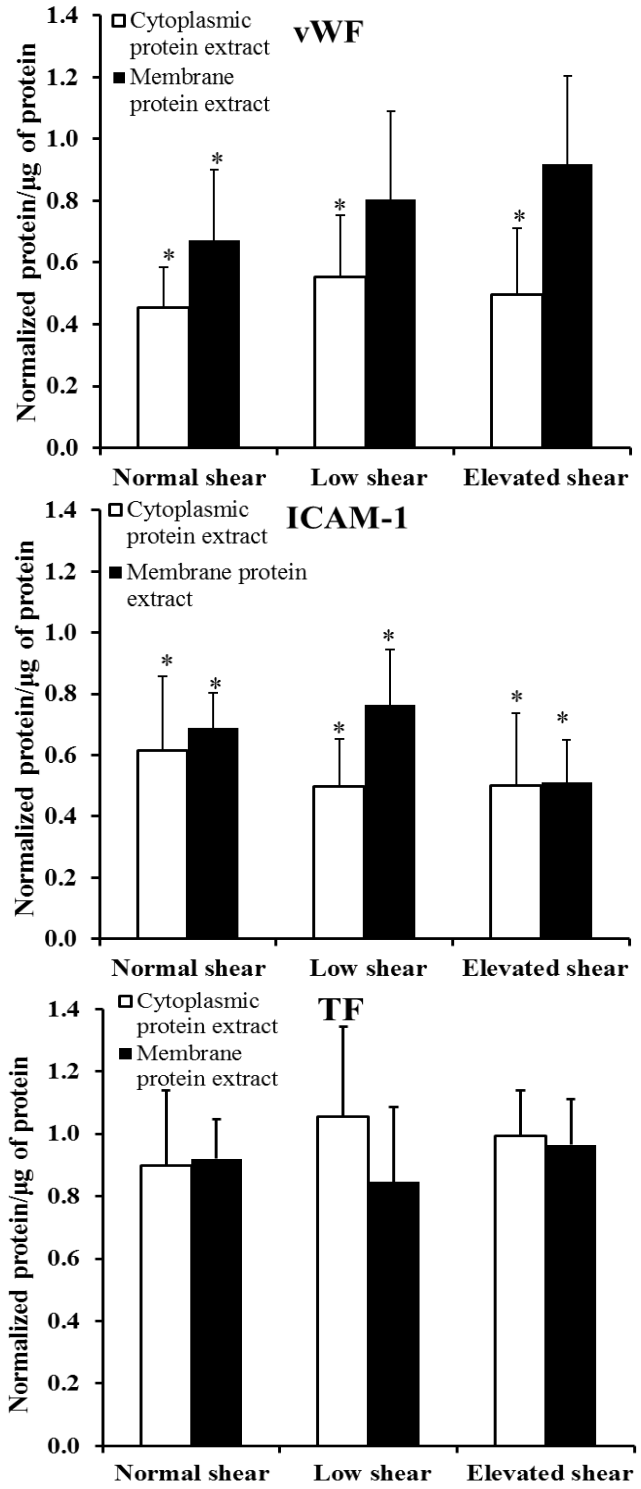

Figure 5.13: Western blot results for cytoplasmic and membrane proteins expression of vWF, ICAM-1, and TF obtained from shear (normal, low, and elevated) exposed aortas (2 hr at 37ºC by perfusing physiological salt solution). Dynamic shear exposure reduced vWF and ICAM-1 expression, compared to the same protein levels in control aortas (n=9-13/group). (* - significantly different compared to non-sheared control aortas' expressions. $P<0.05$, one-way ANOVA).

In parallel, after shearing, the aorta was removed and fixed in 4% paraformaldehyde overnight. The sample was then embedded in paraffin and sectioned (5 μm thickness). Hematoxylin and eosin (H&E) staining was conducted to examine tissue morphology at the vessel wall, and immunostaining against vWF, ICAM-1, and TF was conducted to examine EC activation and injury. Figures are attached in appendix which shows representative H&E and immunostained images of tissue cross-sections of non-sheared (control) and shear stress treated aorta, obtained using a digital camera interfaced with an optical microscope. H&E images of tissue sections from shear stress treated vessels appeared similar to sections from untreated vessels, indicating that shear exposure did not cause tissue damage or affect vascular wall cell morphology. However, immunostained tissue section images were needed to be analyzed for statistical analysis to decide if these changes were significant.

These results indicate that dynamic shear stress can modulate EC responses *ex vivo*, as decrease in cytoplasmic and membrane vWF and ICAM-1 expressions were observed.

5.2 Specific aim 2: The goal of this aim was to study signaling pathways involved in endothelial cell responses to dynamic shear stress.

EC were exposed to various dynamic shear stress (normal and low) of left coronary artery, and MAPK pathway activation was assessed by measuring, ERK1/2, JNK, and p38 phosphorylation levels. Along with the MAPK pathway, NF-κB activation was also quantified. The effect of EC-platelet interaction on MAPK pathway and NF-κB activation was further investigated co-shearing EC with platelets.

5.2.1 Levels of ERK1/2, JNK, and p38 phosphorylation

Level of ERK1/2 phosphorylation under normal (NS) and low (LS) pulsatile shear stress treated EC was measured using Western blot. EC were sheared using the cone-plate shearing device for 2, 5, 15, 30, or 60 min. Band intensity of expressed proteins (obtained from the blots using spot

densitometry) was normalized to that of non-sheared EC. Figure 5.14 shows the band intensity and normalized level of ERK1/2 phosphorylation of EC after 0-60 min exposure to normal and low pulsatile shear stresses. Level of ERK1/2 phosphorylation increased significantly after exposure to shear stress, with a peak at 5 min (P<0.05), and then decreased significantly (P<0.05) with longer shear exposure compared to the non-sheared EC (n=3-4/group).

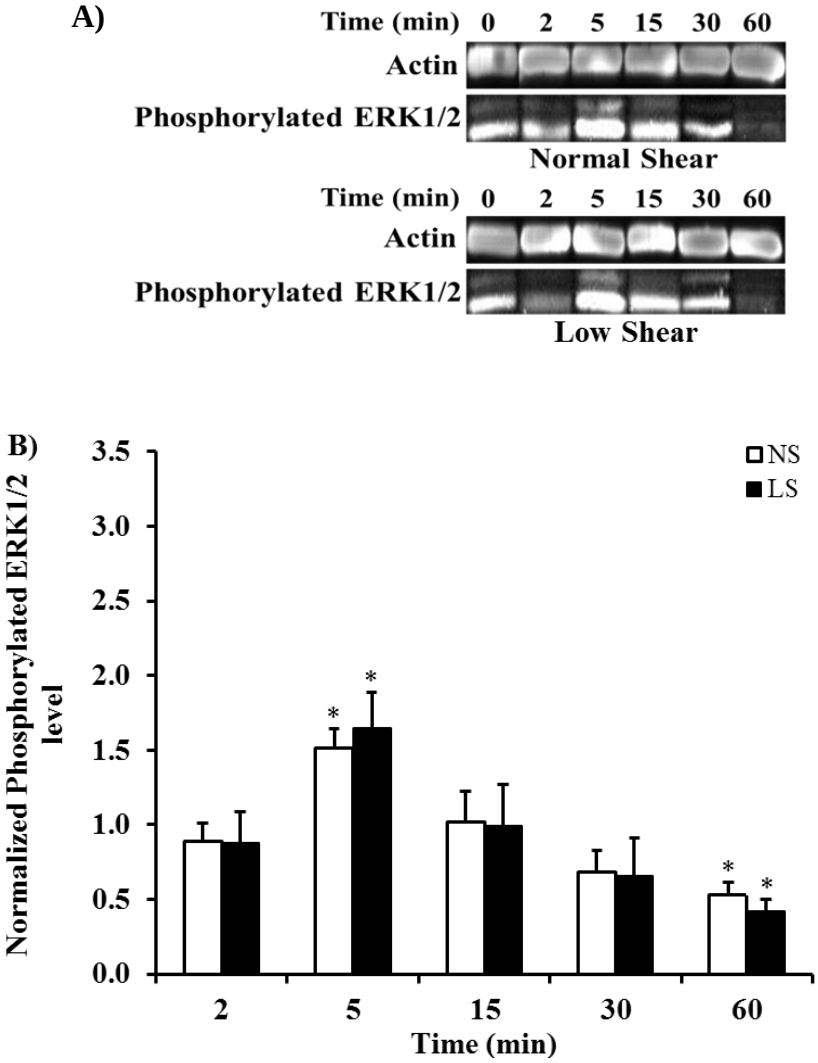

Figure 5.14: Quantification of level of ERK1/2 protein phosphorylation using Western blot. EC were exposed to normal and low shear stress conditions for 0, 2, 5, 15, 30, or 60 min. A) Actin expression and ERK1/2 phosphorylation in EC exposed to normal shear stress (top panel) and low shear stress (bottom panel) respectively. B) Bar graph plot of normalized level of ERK1/2 phosphorylation (normalized to that of non-sheared EC) in EC exposed to normal shear (NS) or low shear (LS) stress (n=3-4/group). Data are presented as Mean+SD. (*- significantly different than the level of phosphorylation of non-sheared control EC. P<0.05, one-way ANOVA).

Phosphorylated ERK1/2 levels were also quantified in EC exposed to normal and low pulsatile shear stresses in the presence of platelets for 2, 5, 15, 30, or 60 min using Western blot. A similar pattern (initial increase and then gradual decrease) in phosphorylated ERK1/2 level following shear exposure was observed in the presence of platelets. An increase in phosphorylated ERK1/2 level was observed at all time points in EC exposed to shear in the presence of platelets vs EC sheared without platelets. However, more experiments were needed for reaching a complete conclusion. Figures are attached in appendix which demonstrated phosphorylated ERK1/2 levels in EC exposed to normal (NS) or low (LS) pulsatile shear stress for 0-60 min in the absence and presence of platelets.

Phosphorylation level of p38 and JNK (two other members of the MAPK family) were also quantified by Western blot in EC exposed to dynamic shear waveforms for 30 min or 60 min in absence (n=3/group) or presence of platelets. Normalized level of p38 and JNK phosphorylation in EC sheared, for 30 min or 60 min, in absence and presence of platelets are presented in Figure 5.15 and in appendix respectively. Significant ($P<0.05$) decrease in phosphorylated p38 level was observed under low shear exposure at 60 min compared to that of non-sheared control EC. However, no significant change was observed in phosphorylated JNK protein level following exposure to shear stress. Presence of platelets induced increase in phosphorylated p38 and JNK levels of EC, compared to that of EC not sheared with platelets (similar to results of phosphorylated ERK1/2 level). However, more experiments were needed for a definite conclusion.

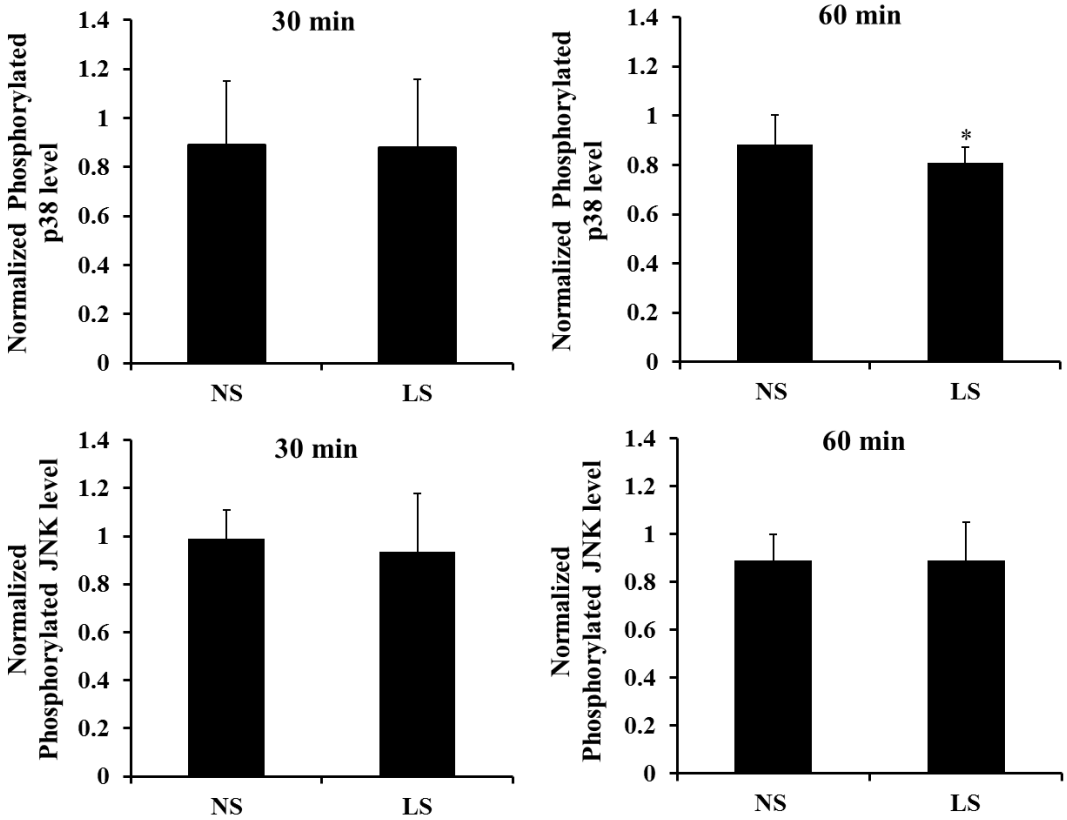

Figure 5.15: Normalized phosphorylated p38 (top panel) and JNK (bottom panel) levels in EC exposed to normal shear (NS) or low shear (LS) stress for 30 min (left panel) or 60 min (right panel) (n=3/group). No significant effect of shear stress on phosphorylated p38 and JNK levels were observed after 30 min shear exposure. Though phosphorylation level of p38 significantly reduced under 60 min LS exposure, such effect was not observed for JNK phosphorylation level at that time point (after 60 min shear exposure). Data are presented as Mean+SD. (*- significantly different than the level of phosphorylation of non-sheared control EC. $P<0.05$, one-way ANOVA).

Immunocytochemical staining for phosphorylated ERK1/2

Phosphorylated ERK1/2 level was measured using immunocytochemical staining, after exposing EC to normal (NS) or low (LS) shear stress conditions (Figure 5.16). After 60 min of shearing, control and sheared EC were fixed, blocked, permeabilized, and incubated with primary antibody against phosphorylated ERK1/2 (n=4-5/group). Qualitative evaluation of the intensity of phosphorylated ERK1/2 indicated that its level decreased following exposure to both NS and LS, compared to control EC phosphorylation level (matching what was observed at 60 min time point from the Western blot experiments). However, the phosphorylated ERK1/2 intensity appeared similar under both shear stress conditions. Quantitative analysis, using a Matlab program, indicated

that dynamic shear exposure for 60 min could not induce any significant difference in level of ERK1/2 phosphorylation between the two shear stress conditions.

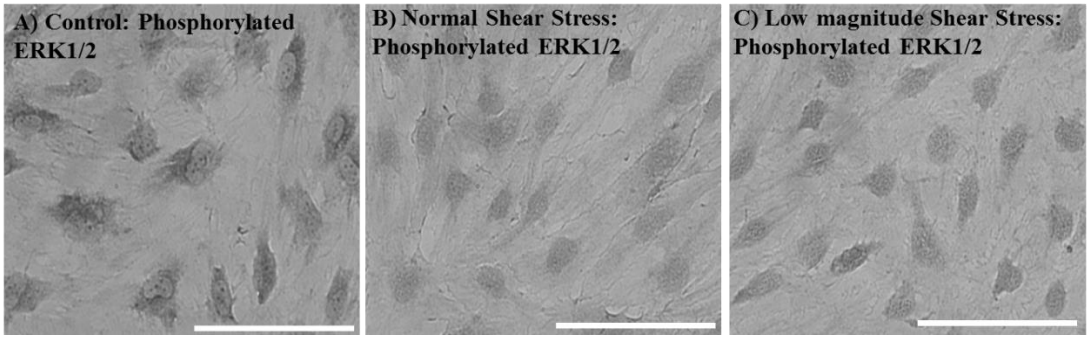

Figure 5.16: Immunocytochemical staining for phosphorylated ERK1/2 (n=4-5/group). Images were taken at 40X magnification. Bars represent 100 μm.

5.2.2 Phosphorylated NF-κB (p65) activation

Level of NF-κB phosphorylation was measured using a sandwich ELISA after exposing EC without/with platelets to normal (NS) or low shear (LS) stress waveforms for 2, 5, 15, 30, and 60 min. Figure 5.17 represents phosphorylated NF-κB levels (normalized to the phosphorylation level of control EC) of EC exposed to dynamic shear waveforms (n=4-5/group). Level of NF-κB phosphorylation followed a similar time course to level of ERK1/2 phosphorylation, but was slightly delayed, with peak level at 30 min post-shear exposure. It began to increase at 15 min (significant for NS exposure, $P<0.05$) and then decreased significantly ($P<0.05$) with prolonged shear exposure. Statistical analysis (ANOVA) indicated significant difference ($P<0.05$) in NF-κB activation level between normal and low shear exposed EC at 30 and 60 min. In the presence of platelets, quick increase in phosphorylation level was observed within 2 min of shear exposure, which then decreased with time (Figure shown in appendix). However, more experiments were needed for reaching a conclusion.

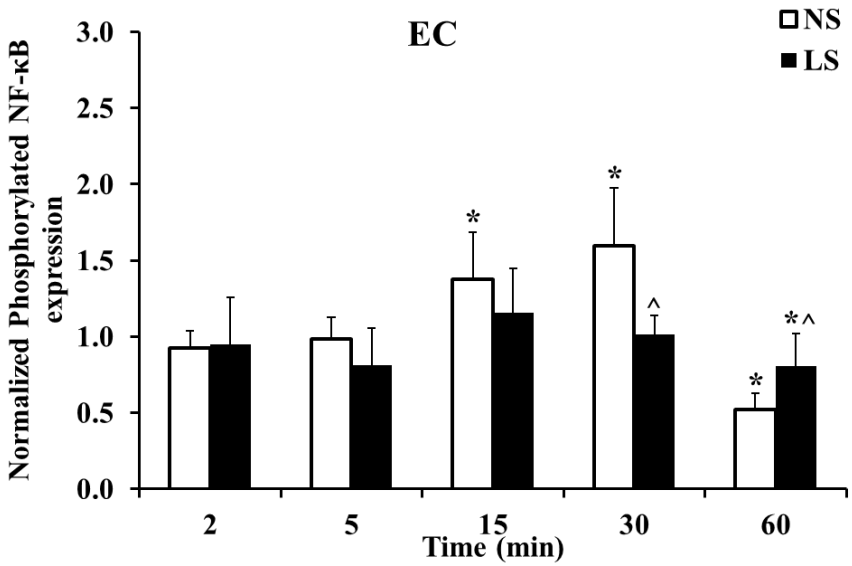

Figure 5.17: Normalized phosphorylated NF-κB level in EC exposed to normal (NS) or low (LS) shear stress (n=4-5/group). Significant difference in NF-κB activation level was observed between normal and low shear exposed EC at 30 min and 60 min time points. Phosphorylation of NF-κB level started to increase significantly at 15 min, reached the peak at 30 min, and then decreased significantly with longer shear exposure duration for shear exposed EC compared to non-sheared control EC. (Data are presented as Mean+SD). (*, ^ - significantly different than the level of phosphorylation of non-sheared control EC and normal shear exposed EC respectively. $P<0.05$, one-way ANOVA).

All these results indicated that dynamic shear stress and platelet-EC communication can modulate activation of MAPK pathway and NF-κB, i.e, signaling pathways.

5.3 Specific aim 3: The goal of this aim was to characterize the uptake/release of endothelial growth factors by platelets, and to test the effect of dynamic shear stress on these processes.

5.3.1 PLGF and VEGF-A mRNA expression by platelets

Platelets were exposed to elevated dynamic shear stress (simulating conditions in a remodeling coronary collateral artery) for 1 hr. Total RNA was isolated from control (unsheared) and shear exposed platelets and RT-PCR was performed for PLGF and VEGF-A quantification to determine whether platelets contain PLGF and VEGF-A mRNA. Results indicated that platelets do not contain PLGF mRNA (undetermined), but do contain VEGF-A mRNA (Average Ct value = 30.8213). A non-significant increase in VEGF-A gene expression in response to dynamic shear

exposure was detected (average RQ value = 1.824) compared to control (average RQ value = 1) platelets.

5.3.2 Uptake of PLGF and VEGF-A by platelets

To characterize the uptake of PLGF and VEGF-A by platelets, platelets were incubated with different concentrations (12, 18, 30, 60, and 120 ng/mL) of recombinant human PLGF or VEGF-A for 1 hr. Platelets were then pelleted, washed gently, lysed, and applied to micro-titer plates to quantify the uptake of the proteins using sandwich ELISA (n=4-5/group). Figure 5.18 depicts PLGF and VEGF-A uptake by platelets. Results indicated that platelets can take up both PLGF (A) and VEGF-A (B) proteins in a dose-dependent manner ($P<0.05$).

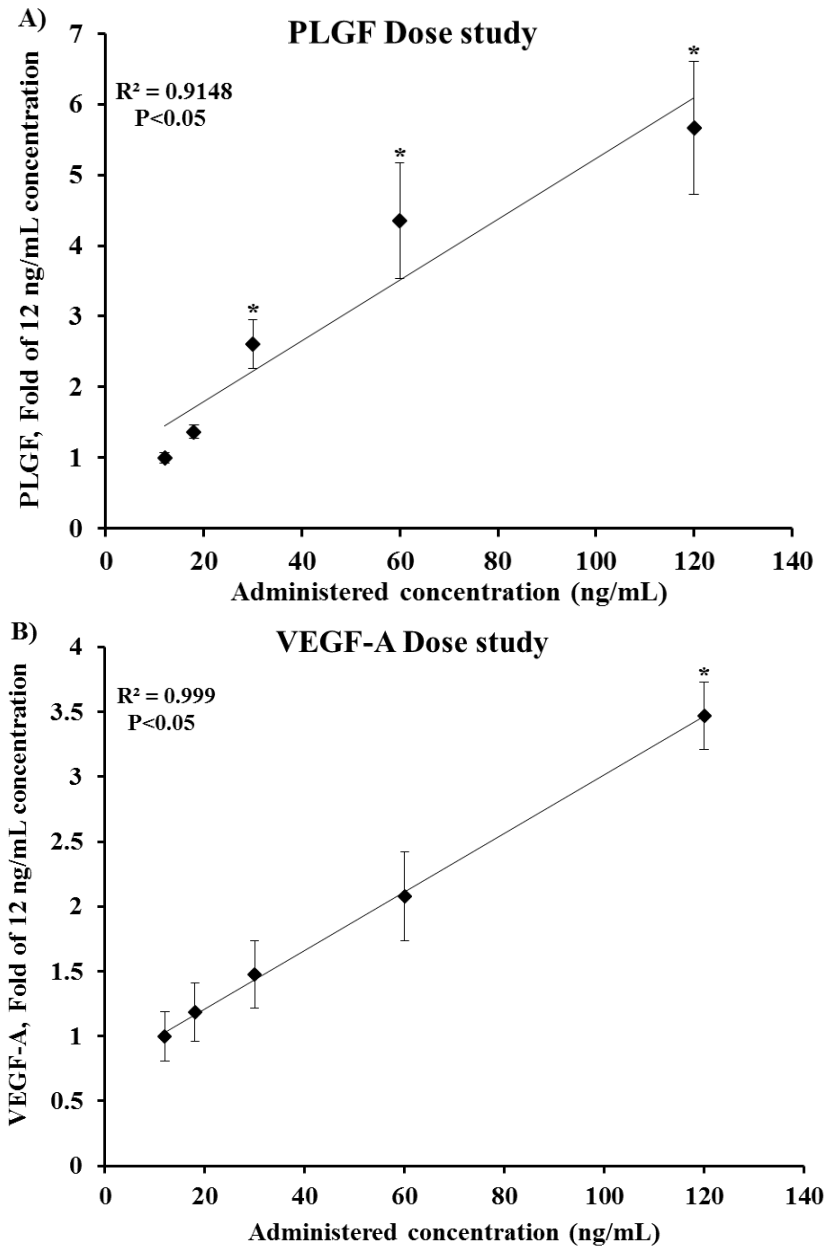

Figure 5.18: PLGF (A) and VEGF-A (B) uptake by platelets after 1 hr incubation with the recombinant proteins (12, 18, 30, 60, and 120 ng/mL). Data (Mean±SEM) are shown as fold increase in the protein concentration relative to 12 ng/mL of the corresponding recombinant protein treatment. Result indicated a significant dose-dependent uptake of the proteins by platelets (n=4-5/group, $P<0.05$).

5.3.3 Effect of beraprost-sodium on uptake of growth factors

The effects of beraprost sodium (a prostacyclin analogue) on uptake of PLGF and VEGF-A by platelets was assessed to determine whether growth factor uptake is passive or an active, Ca^{2+}-dependent process. Beraprost sodium can bind to the G-protein coupled receptors on platelet surface that activate platelet adenyl cyclase to synthesize cyclic adenosine monophosphate (cAMP). cAMP production can inhibit increase in intracellular Ca^{2+} level which plays a major role in most of the platelet activities. Figure 5.19 shows that the presence of beraprost sodium did not affect uptake of either of the growth factors by platelets (n=3/group).

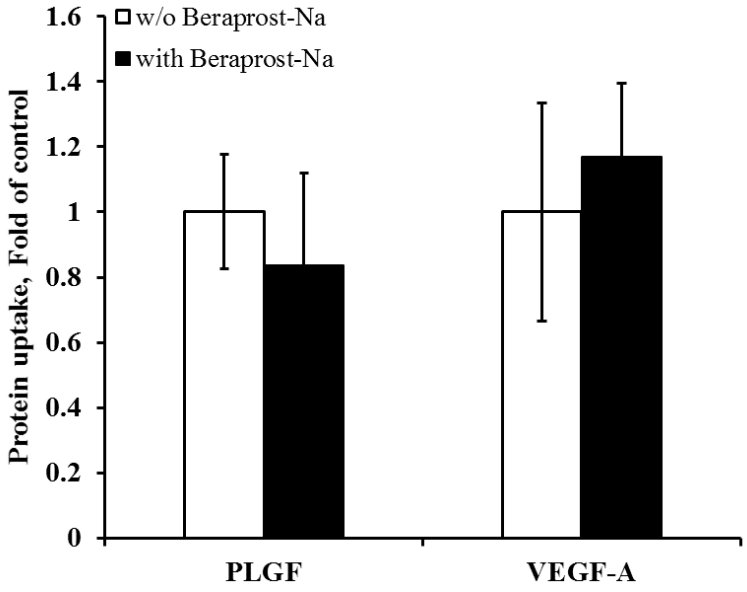

Figure 5.19: Platelets were incubated with recombinant PLGF or VEGF-A for 1 hr with or without beraprost sodium (a prostacyclin analogue). No significant change in the uptake of PLGF or VEGF-A by platelets was observed in the presence of beraprost sodium (n=3/group). Data (Mean±SEM) are presented as fold increase in protein uptake of PLGF or VEGF-A by platelets compared to that of control.

5.3.4 Effect of hyperglycemia on uptake of growth factors

Since diabetes is associated with poor collateral artery growth, we next tested the effect of hyperglycemia (250 mg/dL glucose treatment) on platelet uptake of PLGF and VEGF-A. Results indicated that hyperglycemia did not affect platelets' growth factor uptake (Figure 5.20, n=3/group). However, an increasing trend was observed for platelet PLGF and VEGF-A uptake in presence of hyperglycemic treatment.

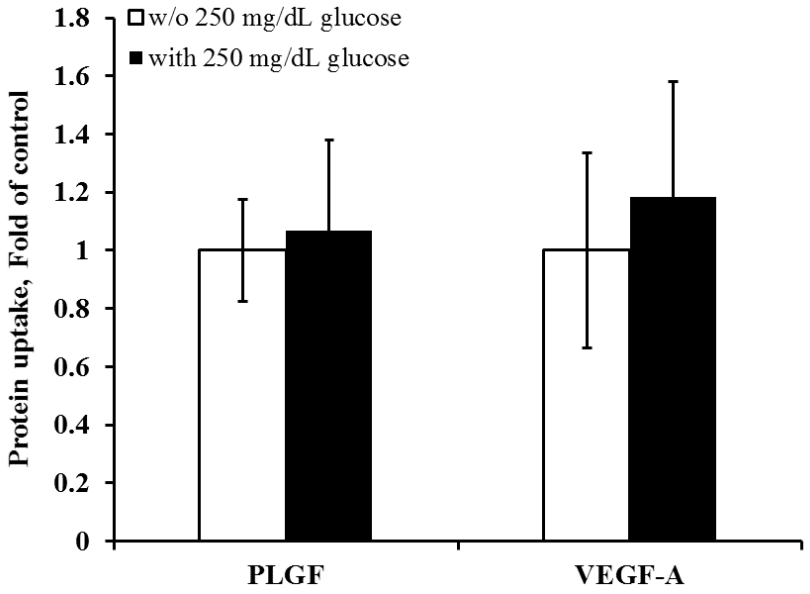

Figure 5.20: Platelets were co-incubated with recombinant PLGF or VEGF-A and 250 mg/dL glucose for 1 hr. Results indicated no significant effect of hyperglycemia on uptake of PLGF or VEGF-A by platelets (n=3/group). Data (Mean±SEM) are presented as fold increase of PLGF or VEGF-A protein uptake compared to that of control.

5.3.5 Combined effects of dynamic shear stress and calcium chelation on uptake of growth factors

To assess the combined effects of dynamic shear stress (simulating conditions within coronary collaterals) and a calcium chelator (ethylenediaminetetraacetic acid, EDTA) on the uptake of growth factors by platelets, platelets were exposed to either normal or elevated shear stress in the absence or presence of EDTA along with either recombinant PLGF or VEGF-A for 1 hr. Figure 5.21 shows PLGF (A) and VEGF-A (B) uptake by platelets following exposure to shear stress with/without EDTA (n=3-5/group). Presence of EDTA could not also induce any significant effect on growth factors uptake by dynamic shear stress exposed platelets.

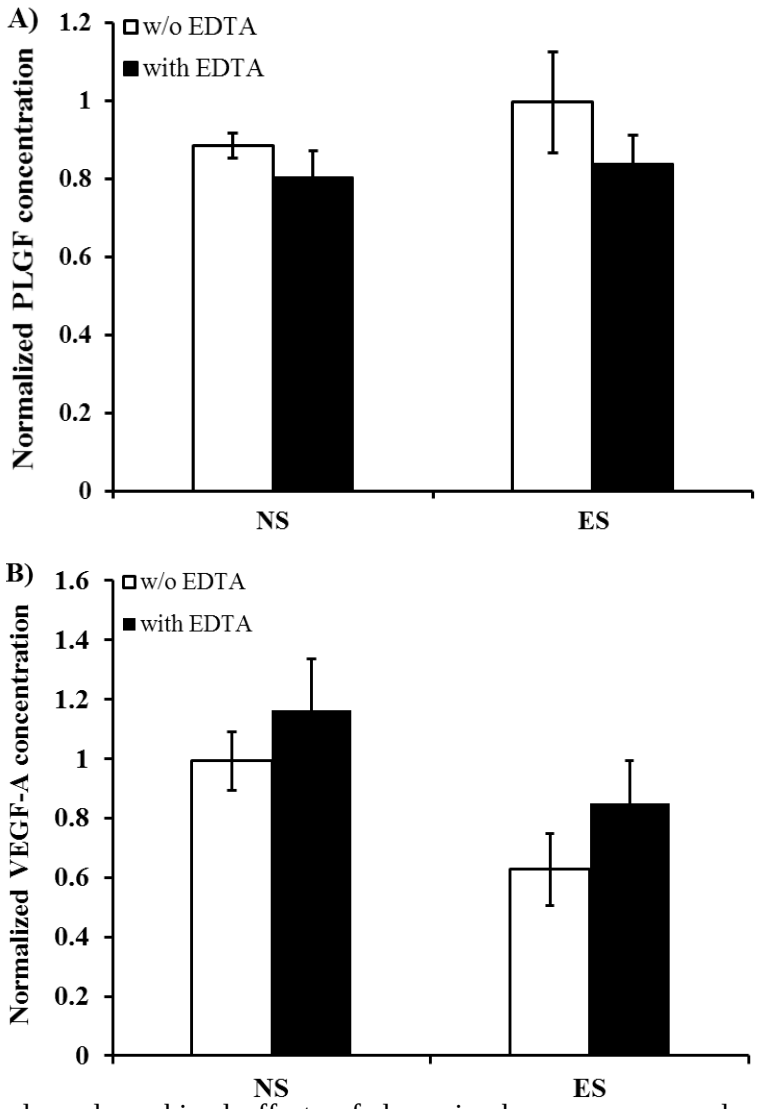

Figure 5.21: Single and combined effects of dynamic shear exposure and calcium chelation (EDTA) on uptake of PLGF or VEGF-A were tested by exposing platelets to normal (NS) and elevated (ES) coronary collateral shear stress for 1 hr in the presence of recombinant PLGF and VEGF-A ± EDTA. Data (Mean±SEM) are presented as normalized (with respect to resting platelet uptake level) PLGF (A) and VEGF-A (B) concentration. Results indicated no significant effect of single or combined treatment of dynamic shear exposure and EDTA on platelets PLGF or VEGF-A uptake (n=3-5/group).

5.3.6 Release of exogenous PLGF and VEGF-A by platelets

Combined effects of dynamic shear stress and beraprost-sodium on release of exogenous growth factors following uptake

Combined effects of dynamic shear stress and beraprost-sodium on release of the growth factors taken up by platelets was also investigated after exposing PLGF/VEGF-A and beraprost-sodium treated platelets to normal and elevated dynamic shear stress (NS and ES) for 1 hr using the cone-plate shearing device. PLGF release had a decreasing trend and VEGF-A release had an increasing trend following dynamic shear stress exposure in the presence of beraprost-sodium (Figure 5.22, n=4/group).

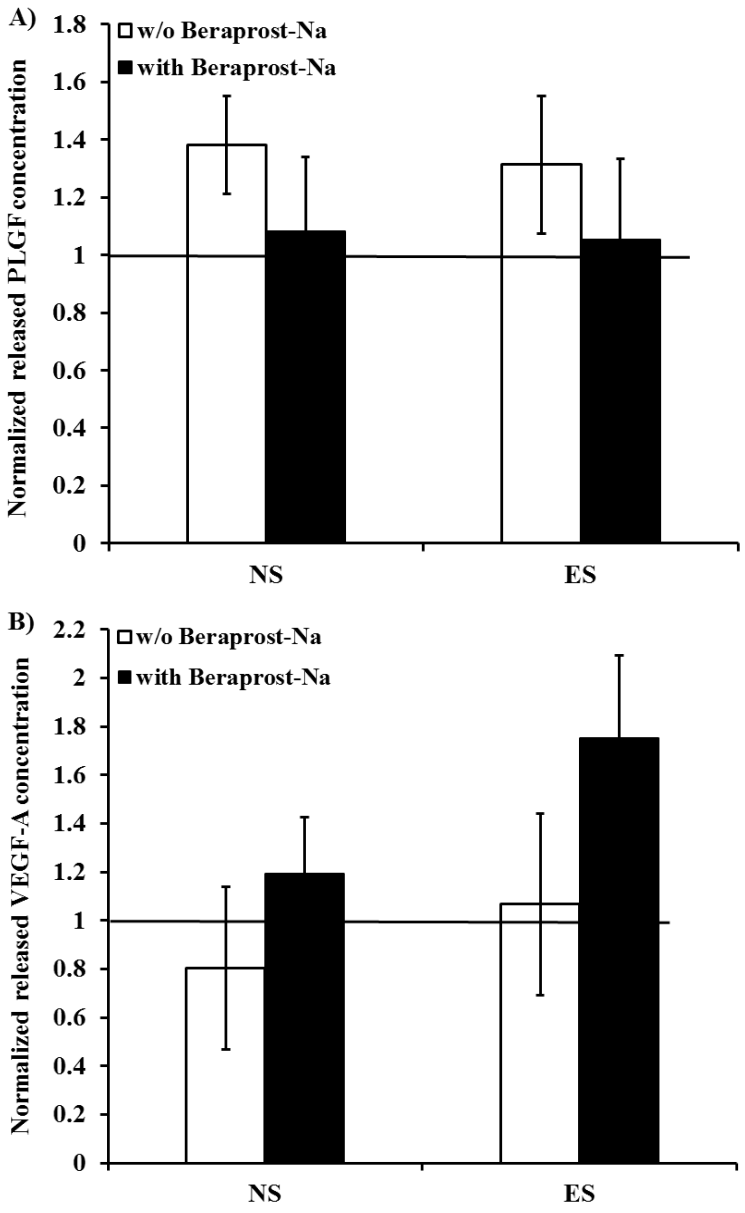

Figure 5.22: Release of PLGF (A) and VEGF-A (B) were observed by exposing PLGF/VEGF-A and beraprost-sodium treated platelets to normal (NS) and elevated (ES) shear stress waveforms. Results indicated no significant effect of beraprost-sodium on shear induced platelet PLGF or VEGF-A release (n=4/group). Released growth factor concentration was normalized to the corresponding value from resting platelets. Data: Mean±SEM.

Combined effects of dynamic shear stress and hyperglycemia on release of growth factors

Recombinant human PLGF or VEGF-A ± 250 mg/dL glucose treated platelets were exposed to normal and elevated shear stress for 1 hr to assess the combined effects of dynamic shear stress and hyperglycemia on release of growth factors previously taken up by platelets. A decreasing trend was observed in PLGF release in presence of hyperglycemic condition. However, no significant change in either of the growth factors (PLGF/VEGF-A) release was observed (Figure 5.23) under dynamic shear and hyperglycemic treatment exposure (n=4/group).

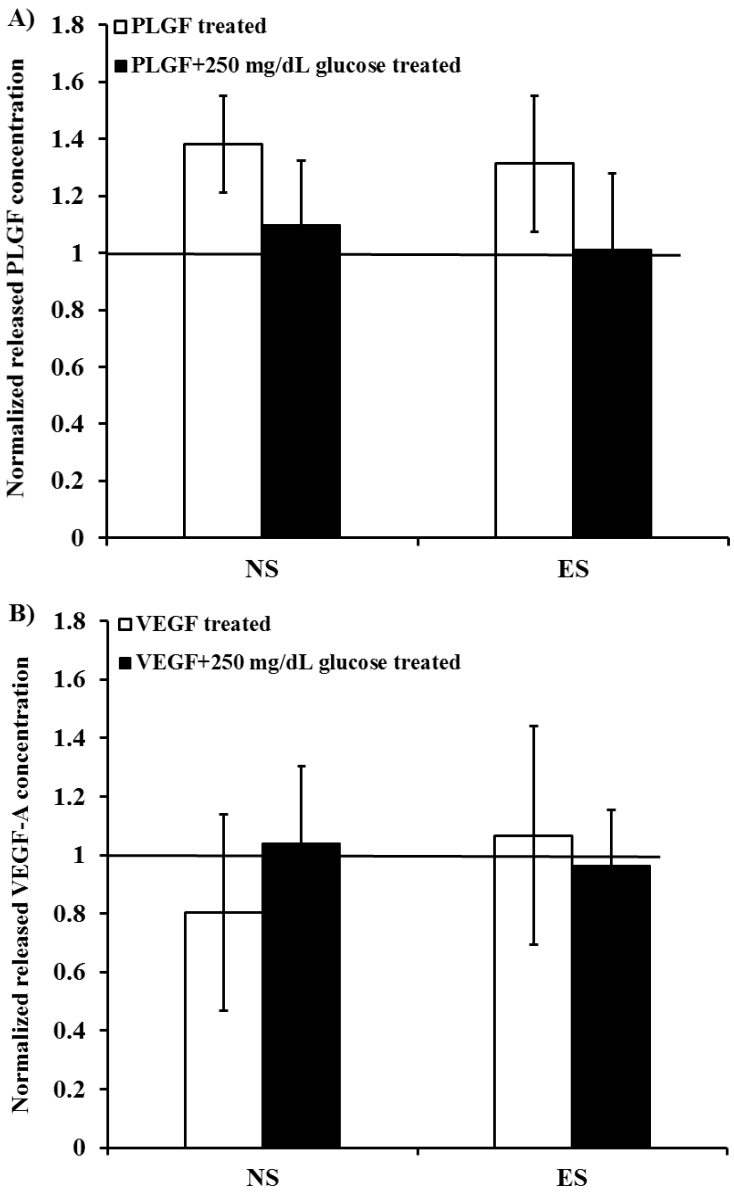

Figure 5.23: PLGF/VEGF-A and/or 250 mg/dL glucose treated platelets were stimulated with dynamic shear (normal and elevated) and the release of PLGF (A) and VEGF-A (B) was quantified using sandwich ELISA. PLGF and VEGF-A protein release was normalized to that of resting platelets release, and presented as Mean±SEM. Combined exposure of platelets to dynamic shear and hyperglycemia did not induce any significant change in PLGF/VEGF-A release by platelets (n=4/group). NS – normal shear stress, ES – elevated shear stress.

All these results indicated that platelets do take up both PLGF and VEGF-A. We were not able to demonstrate a significant effect of Ca^{2+} chelation or hyperglycemia on this process or on release of the growth factors following uptake. However, 1 hr of dynamic shear stress and/or treatment with EDTA, beraprost-sodium, or 250 mg/dL glucose may not be sufficient to induce

significant changes in PLGF/VEGF-A uptake and release. Thus, the short experimental time frame represents one limitation of this study. Low number of experiments (n=3-5) could be another limitation of the study.

5.4 Specific aim 4: The goal of this aim was to quantify the effect of diabetes-associated major metabolic dysfunction on the expression level of PLGF and vascular endothelial growth factor receptor 1 (VEGFR1, the receptor for PLGF) in mouse and human cell.

5.4.1 PLGF and VEGFR1 protein quantification

We wished to identify mechanisms by which diabetes inhibits PLGF expression in heart and skeletal muscle. We utilized both human and mouse cell types for these *in vitro* studies. Cell types tested were human coronary artery endothelial cells (HCAEC), human cardiac muscle cells (HCM), mouse cardiac muscle cells (MCM), human skeletal muscle cells (HSKMC), and mouse skeletal muscle cells (MSKMC). Cells were subjected to different treatments [low density lipoprotein (LDL), oxidized LDL (ox-LDL), glucose, advanced glycation end products (AGE), hydrogen peroxide (H_2O_2), or insulin] to mimic various aspects of diabetes-associated metabolic dysfunction, and cell-produced PLGF protein was quantified. Cell surface VEGFR1 (PLGF receptor) expression was measured as well.

5.4.2 PLGF and VEGFR1 protein expression of HCAEC

Initially, confluent HCAEC were exposed to each of the following for 24 hr: LDL (50-200 μg/mL) or ox-LDL (50-200 μg/mL) to mimic hyperlipidemia; glucose (5-20 mM) to mimic acute hyperglycemia; AGE (glucose or glyceraldehyde derived, 300-1000 μg/mL) to mimic long-term hyperglycemia; hydrogen peroxide (H_2O_2, 0.05-0.3 mM) to simulate oxidative stress, or insulin (100-300 mU/L) to mimic the hyperinsulinemia environment. Post-treatment, cell culture media samples were collected at 4, 8, and 24 hr to quantify PLGF and total protein using commercially

available PLGF ELISA kits and the BCA assay, respectively. The most effective concentrations of the metabolic molecules tested was determined from this HCAEC dose study. These concentrations were then used to treat HCM, MCM, HSKMC, and MSKMC, and media samples were probed for PLGF and total protein as mentioned previously. Cell surface PLGF receptor (VEGFR1) was also quantified post 24 hr treatment using VEGFR1 ELISA. Both PLGF and VEGFR1 protein were normalized to corresponding media and cell total protein respectively, and data analysis was conducted using ANOVA. Figure 5.24 illustrates the PLGF expression of HCAEC treated with LDL (5.24A, n=6/group) or ox-LDL (5.24B, n=4-6/group), figure 5.25 illustrates the PLGF expression of HCAEC treated with glucose (5.25A, n=6/group) or glucose derived-AGE (5.25B, n=4-6/group) or glyceraldehyde derived-AGE (5.25C, n=6/group), and figure 5.26 illustrates the PLGF expression of HCAEC treated with H_2O_2 (5.26A, n=5-6/group) or insulin (5.26B, n=6/group) respectively. Results showed that LDL, ox-LDL, or insulin treatment failed to induce any significant changes in HCAEC PLGF expression. However, glucose, AGE (both glucose and aldehyde derived), and 0.3 mM H_2O_2 significantly ($P<0.05$) reduced PLGF expression. Cell surface expression of VEGFR1 in HCAEC (Figure 5.27, n=4-5/group) exposed to ox-LDL, glyceraldehyde derived-AGE, or H_2O_2 is shown in Figure 5.27A, 5.27B, and 5.27C respectively. Ox-LDL and H_2O_2 treatment did not induce any significant changes in VEGFR1 levels. However, glyceraldehyde derived-AGE significantly ($P<0.05$) increased HCAEC VEGFR1 expression.

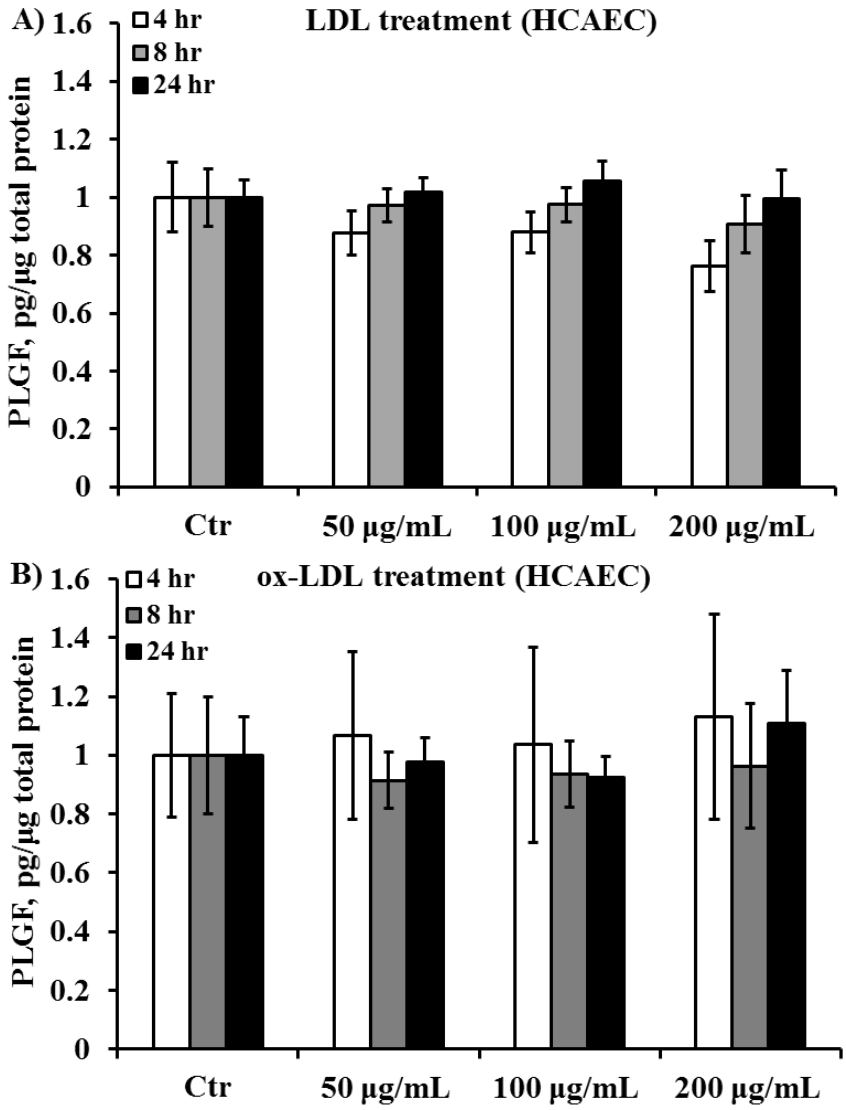

Figure 5.24: PLGF expression level (normalized to total protein), at 4, 8, 24 hr post-treatment, of HCAEC exposed to (A) low density lipoprotein (LDL, 50-200 µg/mL, n=6/group) or (B) oxidized LDL (ox-LDL, 50-200 µg/mL, n=4-6/group) treatment for 24 hr. Data are presented as Mean±SEM. Neither of the treatments had any significant effect on PLGF expression of HCAEC.

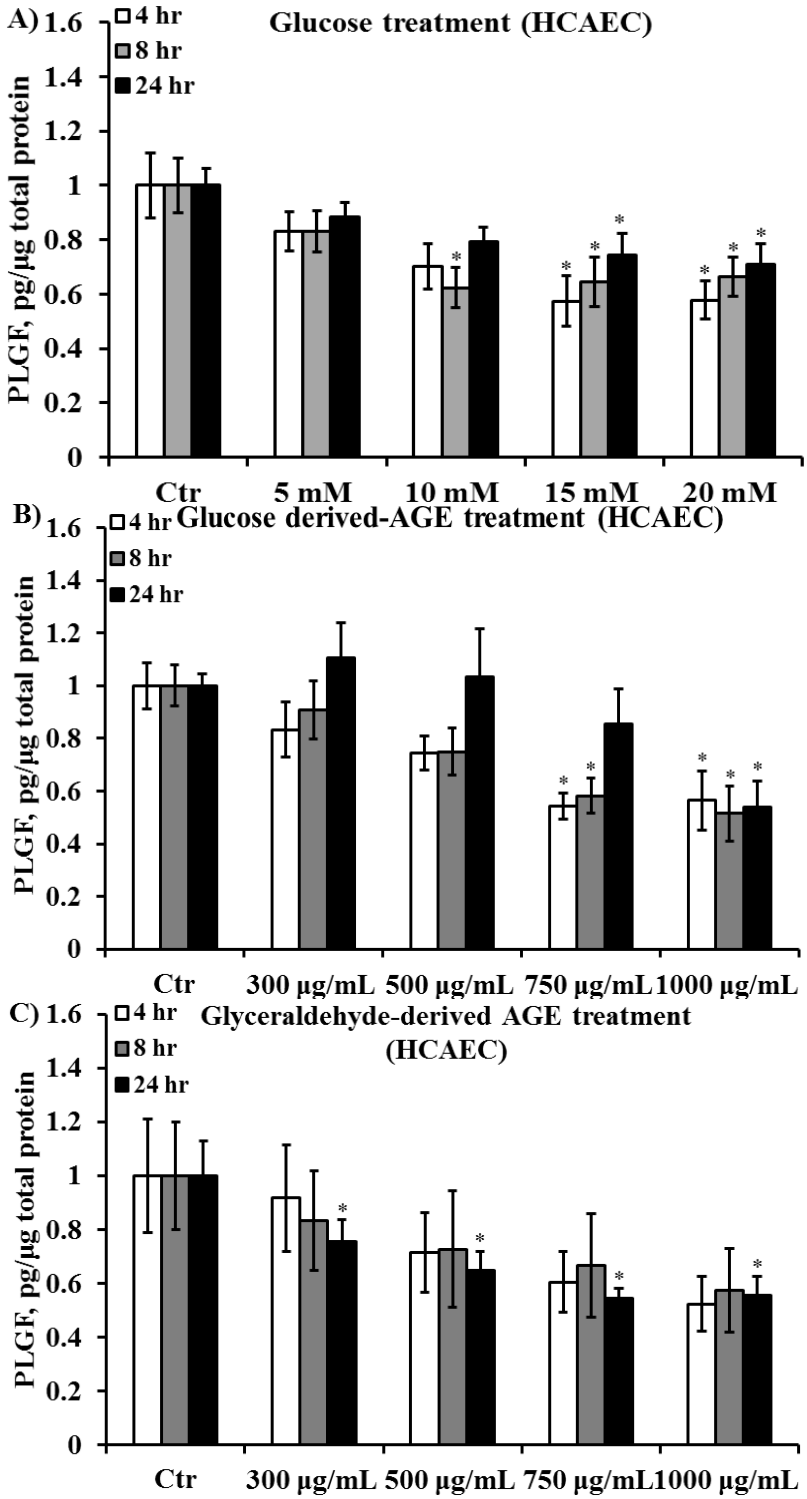

Figure 5.25: Normalized PLGF expression (to total protein) of HCAEC after 4, 8, 24 hr treatment exposure to (A) glucose (5-20 mM, n=6/group), or (B) glucose (n=4-6/group)/(C) glyceraldehyde derived-AGE (300-1000 µg/mL, n=6/group). Treatment with higher concentrations of glucose and AGE all significantly (P<0.05) reduced PLGF expression by HCAEC (Data: Mean±SEM). [*-significantly lower compared to corresponding time point control (Ctr), based on ANOVA analysis].

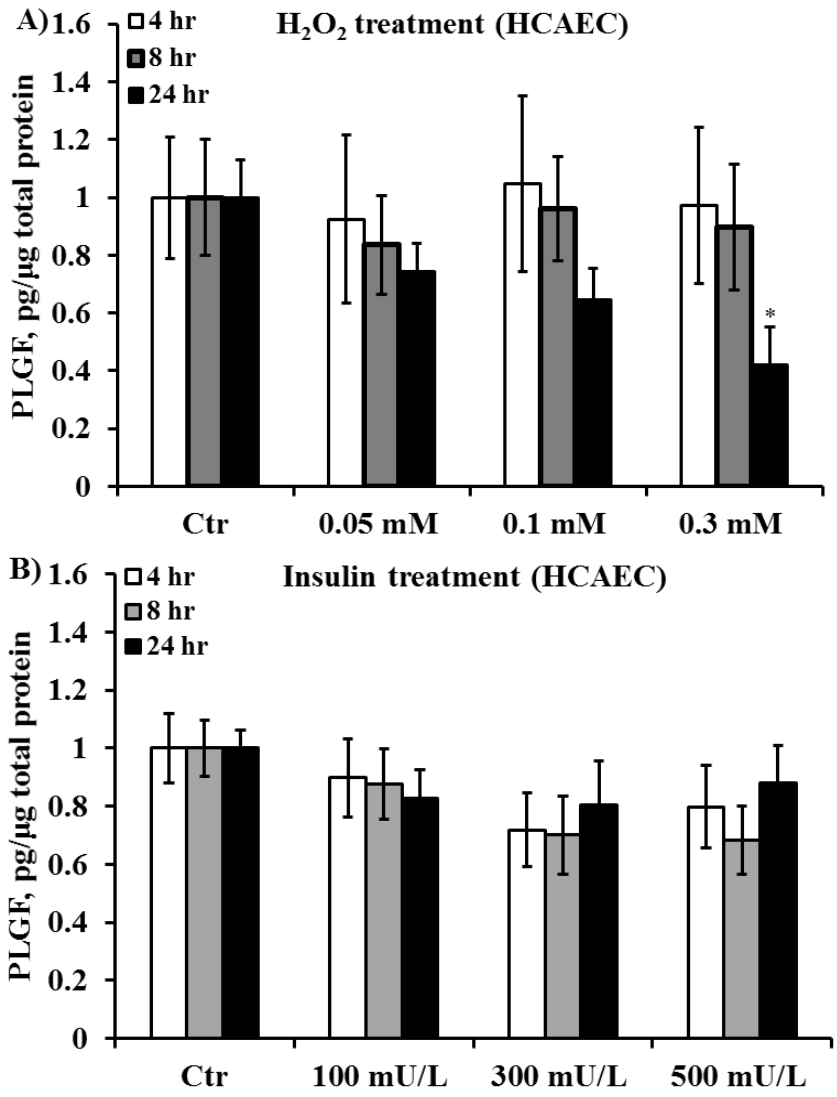

Figure 5.26: Effect of hydrogen peroxide (H_2O_2) and insulin treatment on HCAEC PLGF expression. HCAEC were exposed to (A) 0.05-0.3 mM H_2O_2 (n=5-6/group) or (B) 100-300 mU/L insulin treatment (n=6/group), and media samples were collected and probed for PLGF expression 4, 8, and 24 hr post-treatment. Data are presented as mean normalized PLGF expression (with respect to total protein). Results indicated a significant (P<0.05) reduction in PLGF expression in the presence of 0.3 mM H_2O_2. However, insulin treatment failed to induce any significant effect.

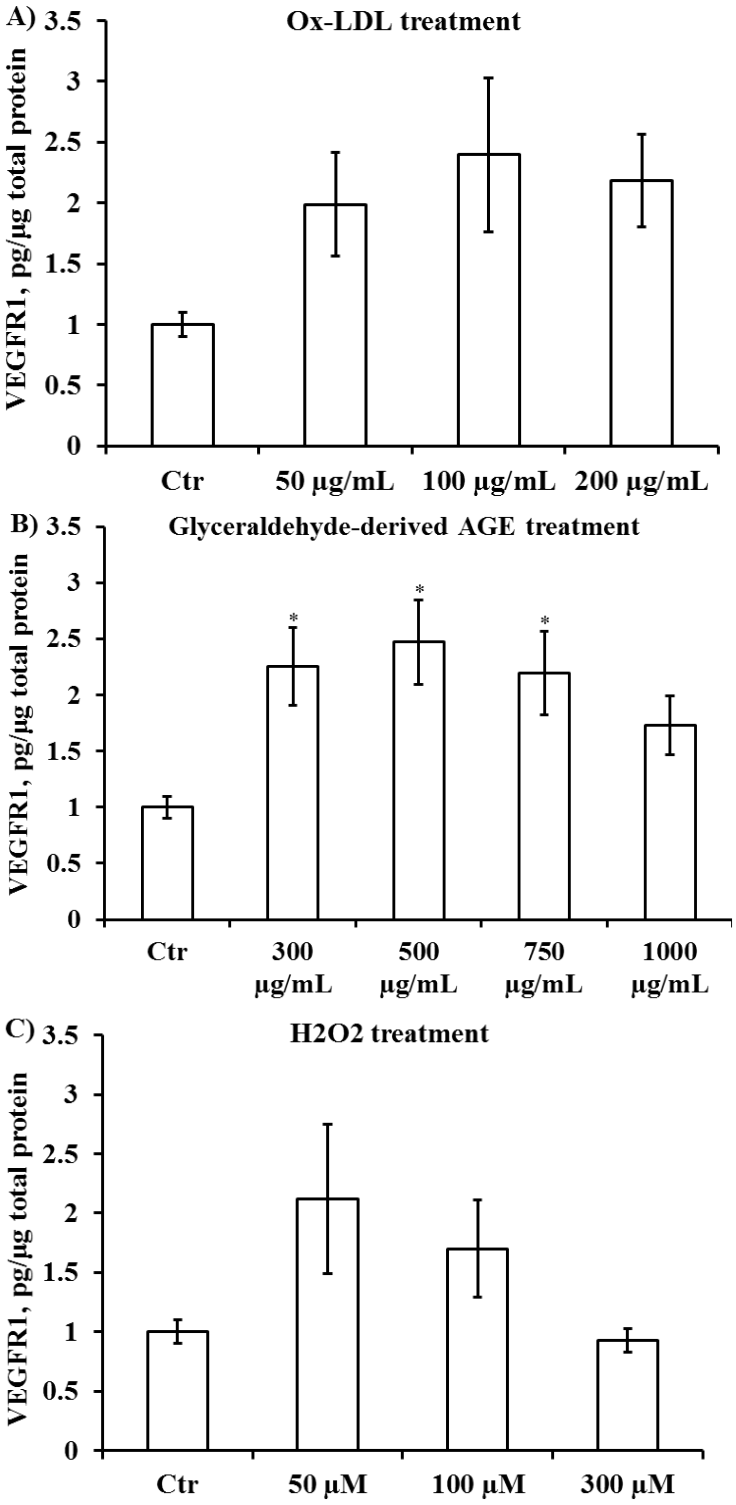

Figure 5.27: Cell surface expression of HCAEC VEGFR1, after 24 hr of (A) ox-LDL (50-200 µg/mL, n=5/group), (B) glyceraldehyde derived AGE (300-1000 µg/mL, n=5/group), or (C) H_2O_2 (0.05-0.3 mM, n=4-5/group) treatment. VEGFR1 expression was normalized to total protein and is represented as Mean±SEM. Glyceraldehyde derived AGE significantly (P<0.05) increased HCAEC surface VEGFR1 expression. The other two treatments (ox-LDL and H_2O_2) had no significant effect.

5.4.3 PLGF and VEGFR1 protein expression of HCM and MCM

Next, HCM and MCM were treated with 200 μg/mL of LDL or ox-LDL, 1000 μg/mL of glucose or glyceraldehyde derived-AGE, or 0.1/0.3 mM of H_2O_2 for 24 hr, and media and cell samples were probed for PLGF and surface VEGFR1 expression respectively, as previously described. Figure 5.28 represents HCM PLGF expression in the presence of LDL/ox-LDL (A), AGE (B), and H_2O_2 (C) treatment (n=5/group). Figure 5.29 illustrates VEGFR1 expression of HCM cells after 24 hr of treatment. Results indicated that LDL treatment had no significant effect on HCM PLGF expression (n=5/group). However, AGE treatment significantly (P<0.05) reduced PLGF expression, whereas 0.3 mM H_2O_2 significantly increased PLGF expression. There was no significant effect of any of the treatments on VEGFR1 expression (n=5/group).

We also compared results from HCAEC and HCM to determine the relative abundance of PLGF in endothelial cells and cardiac myocytes. Figure 5.30 shows that untreated HCAEC produced a significantly higher amount of PLGF (~10-15 times more) than HCM.

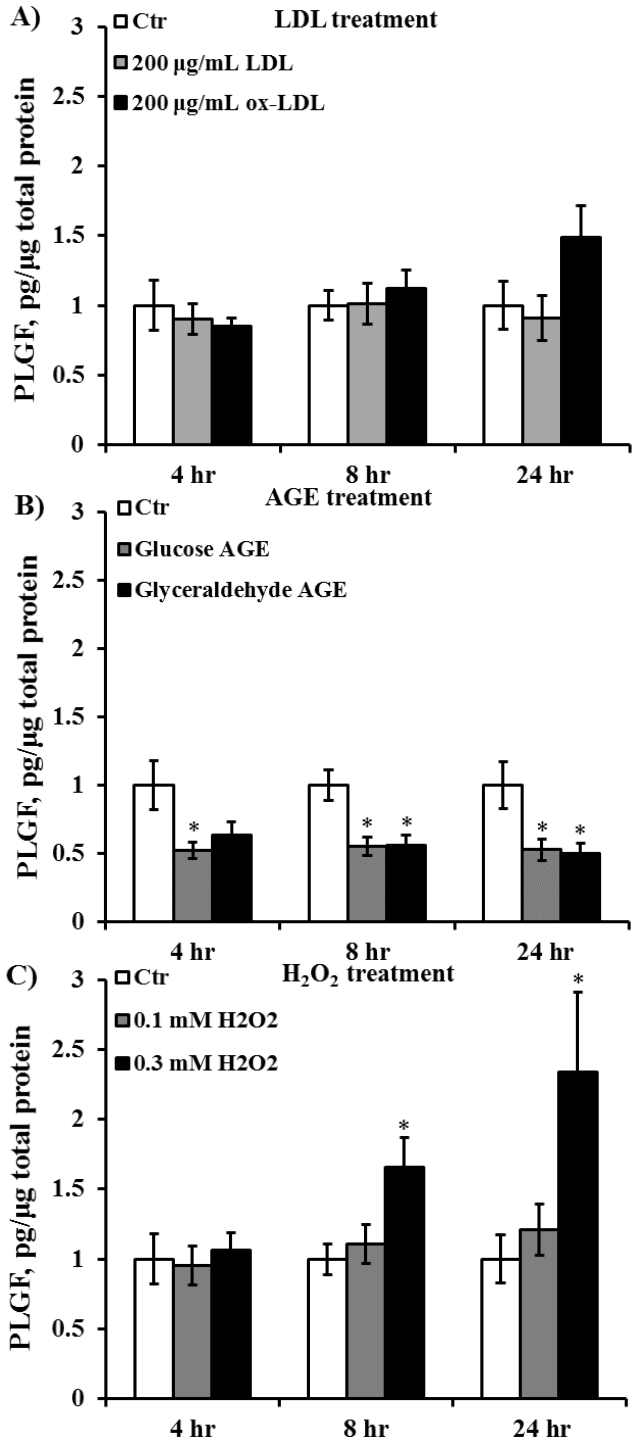

Figure 5.28: Effect of (A) LDL/ox-LDL (200 µg/mL), (B) glucose/glyceraldehyde derived AGE (1000 µg/mL), or (C) H_2O_2 (0.1/0.3 mM) on PLGF production by HCM (n=5/group). PLGF expression was normalized to total protein at 4, 8, and 24 hr post treatment and represented as Mean±SEM. Both of the AGE treatments significantly (P<0.05) reduced PLGF expression at all time points, whereas 0.3 mM H_2O_2 treatment significantly increased HCM produced PLGF level. However, LDL/ox-LDL treatment had no effect. (Ctr – PLGF expression of control cells without any treatment).

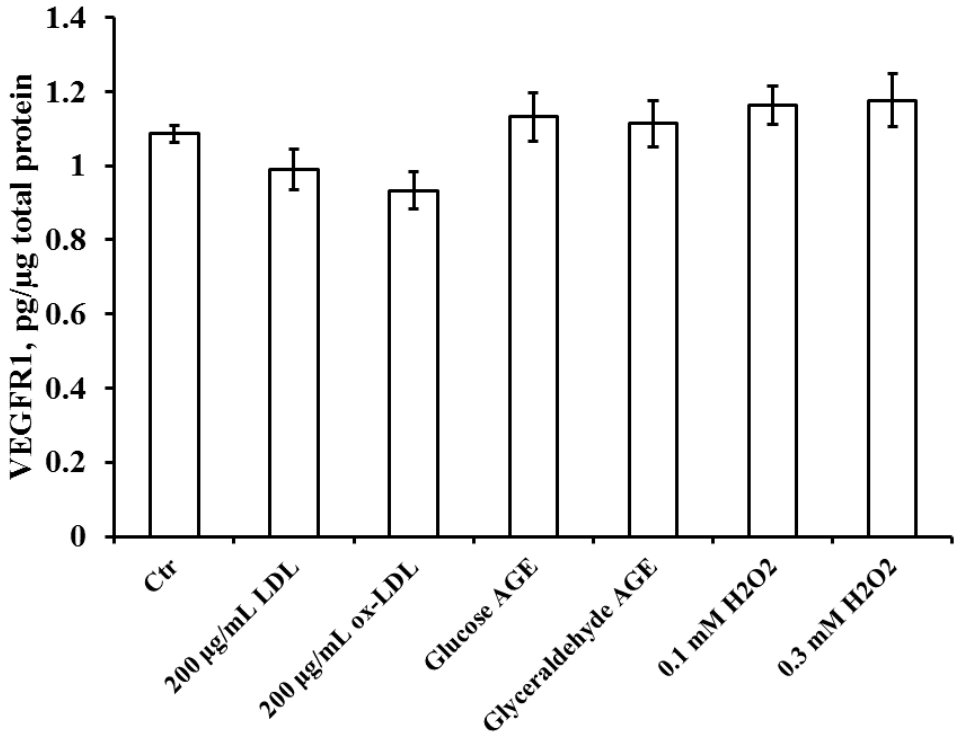

Figure 5.29: Cell surface expression of VEGFR1 by HCM exposed to 200 µg/mL LDL/ox-LDL, 1000 µg/mL glucose/glyceraldehyde derived AGE, or 0.1/0.3 mM H_2O_2 (n=5/group). No significant effect of any of the treatments was found on HCM VEGFR1 expression. (Ctr – VEGFR1 expression of control cells without any treatment).

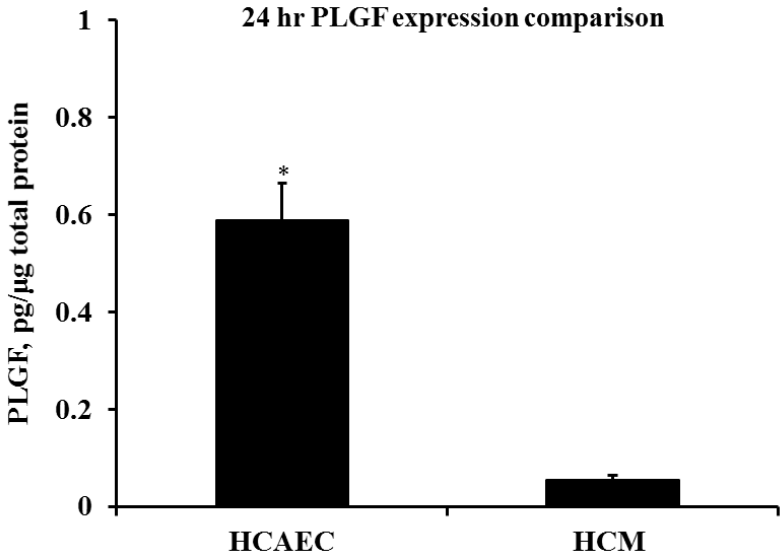

Figure 5.30: Comparative analysis of PLGF expression of untreated HCAEC and untreated HCM. Results identified HCAEC as the major source of PLGF in the heart, as untreated HCAEC produced a significantly (P<0.05) higher amount of PLGF than untreated HCM.

Figure 5.31 and 5.32 represent the produced PLGF level and VEGFR1 expression respectively of MCM exposed to the same treatments as HCM (n=5/group). Results from the MCM study indicated that MCM are more sensitive to the different metabolic treatments, compared to HCM. Both LDL/ox-LDL (5.31A) and glucose/glyceraldehyde derived-AGE (5.31B) significantly (P<0.05) reduced MCM produced PLGF level at different time points (4, 8, and 24 hr), whereas H_2O_2 treatment (5.31C) significantly increased PLGF expression. For VEGFR1 (Figure 5.32), glucose derived-AGE significantly (P<0.05) increased expression, and 0.3 mM H_2O_2 significantly (P<0.05) reduced expression compared to non-treated control (Ctr). However, the other treatments did not produce any significant effects on MCM VEGFR1 expression.

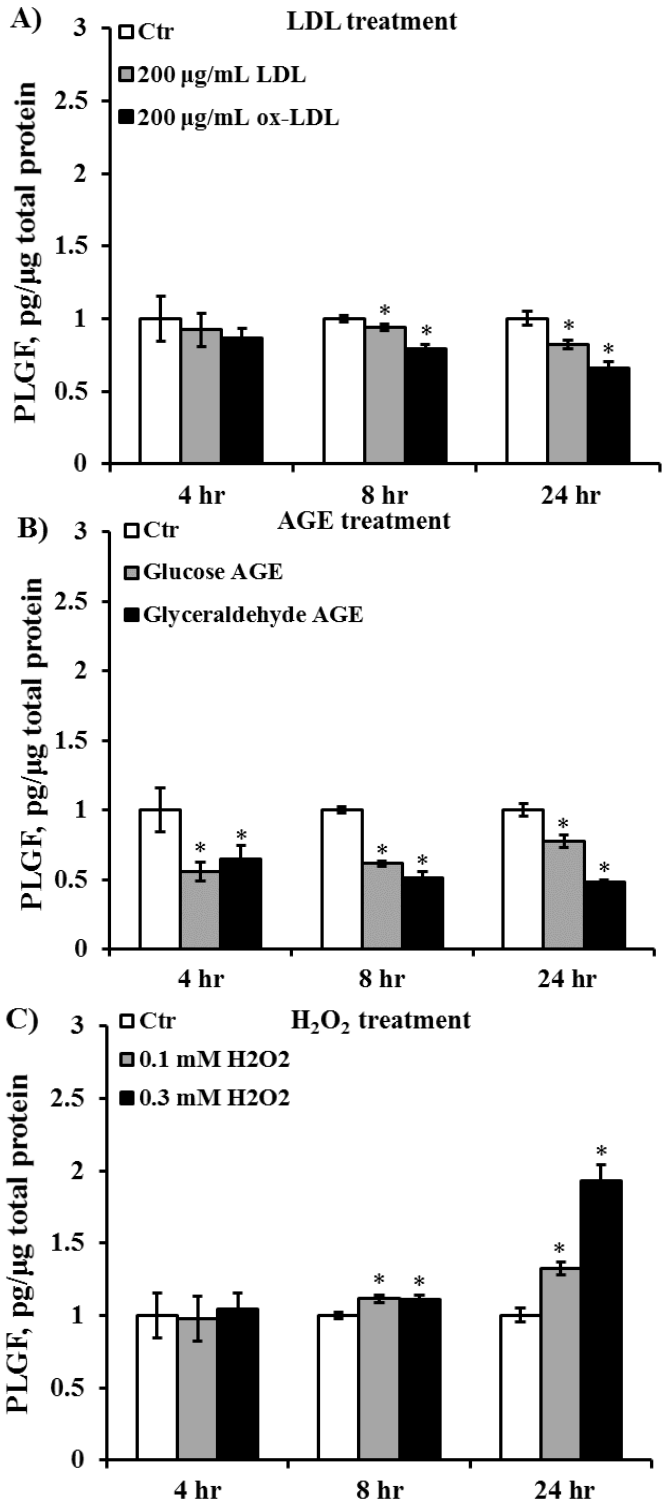

Figure 5.31: PLGF expression (normalized to total protein of corresponding treatment and time point) of MCM exposed to (A) hyperlipidemic (LDL/ox-LDL, 200 µg/mL), (B) long-term hyperglycemic (glucose/glyceraldehyde derived AGE, 1000 µg/mL), or (C) oxidative stress (H_2O_2, 0.1/0.3 mM) environment for 4, 8, or 24 hr (n=5/group). Hyperlipidemic and long-term hyperglycemic treatment significantly (P<0.05) reduced, and oxidative stress treatment significantly (P<0.05) enhanced PLGF expression of MCM.

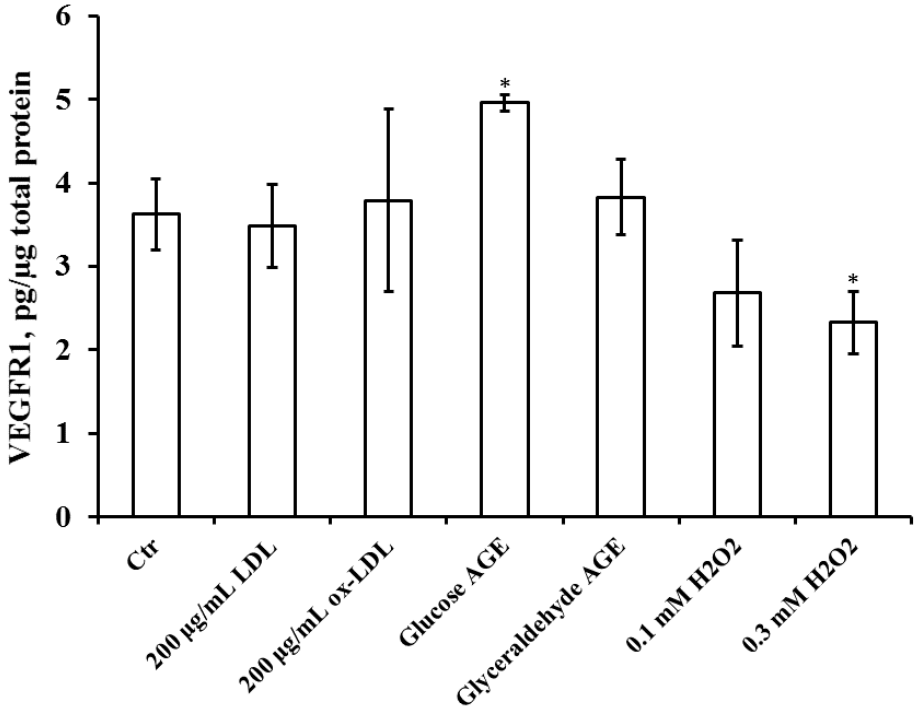

Figure 5.32: VEGFR1 expression (normalized to total protein) of MCM treated with LDL/ox-LDL, glucose/glyceraldehyde derived AGE, or H_2O_2 (n=5/group). Glucose derived AGE and 0.3 mM H_2O_2 significantly increased and decreased cell surface VEGFR1 expression, respectively, by MCM. However, other treatments failed to elicit any significant effect on MCM VEGFR1 expression.

5.4.4 PLGF and VEGFR1 protein expression of HSKMC and MSKMC

Since a previous *in vivo* study conducted in our lab on mouse models of Western diet induced metabolic dysfunction showed that the diet inhibited PLGF expression in skeletal muscle tissue, we treated HSKMC and MSKMC with different compounds as described above to mimic diabetes-associated metabolic dysfunction. Both confluent HSKMC and MSKMC were exposed to 200 μg/mL LDL/ox-LDL (n=6/group), 1000-1500 μg/mL glucose or glyceraldehyde derived-AGE (n=5-10/group), 0.1-0.3 mM H_2O_2 (n=6/group), 5-20 mM glucose (n=6/group), and 100-300 mU/L insulin (n=6/group) for 24 hr. Media samples were assessed for PLGF expression after 4, 8, and 24 hr and cell samples were probed for VEGFR1 expression after 24 hr of treatment using sandwich ELISA. The effects of LDL/ox-LDL (A), glucose/glyceraldehyde derived-AGE (B and C), 0.1/0.3 mM H_2O_2 (D), and glucose/insulin (E) on HSKMC PLGF production is shown in Figure 5.33. LDL/ox-LDL, 0.1/0.3 mM H_2O_2, and insulin treatment had no effect on PLGF expression. The higher concentration (1500 μg/mL) of both glucose and glyceraldehyde derived-AGE significantly reduced PLGF expression at all time points (post 4, 8, and 24 hr); whereas the lower concentration (1000 μg/mL) of glucose and glyceraldehyde derived-AGE reduced PLGF only at 24 hr post treatment. The higher concentrations of glucose (15-20 mM) also inhibited PLGF production by HSKMC. However, none of the treatments elicited any effect on cell surface VEGFR1 expression (n=6/group), as shown in Figure 5.34.

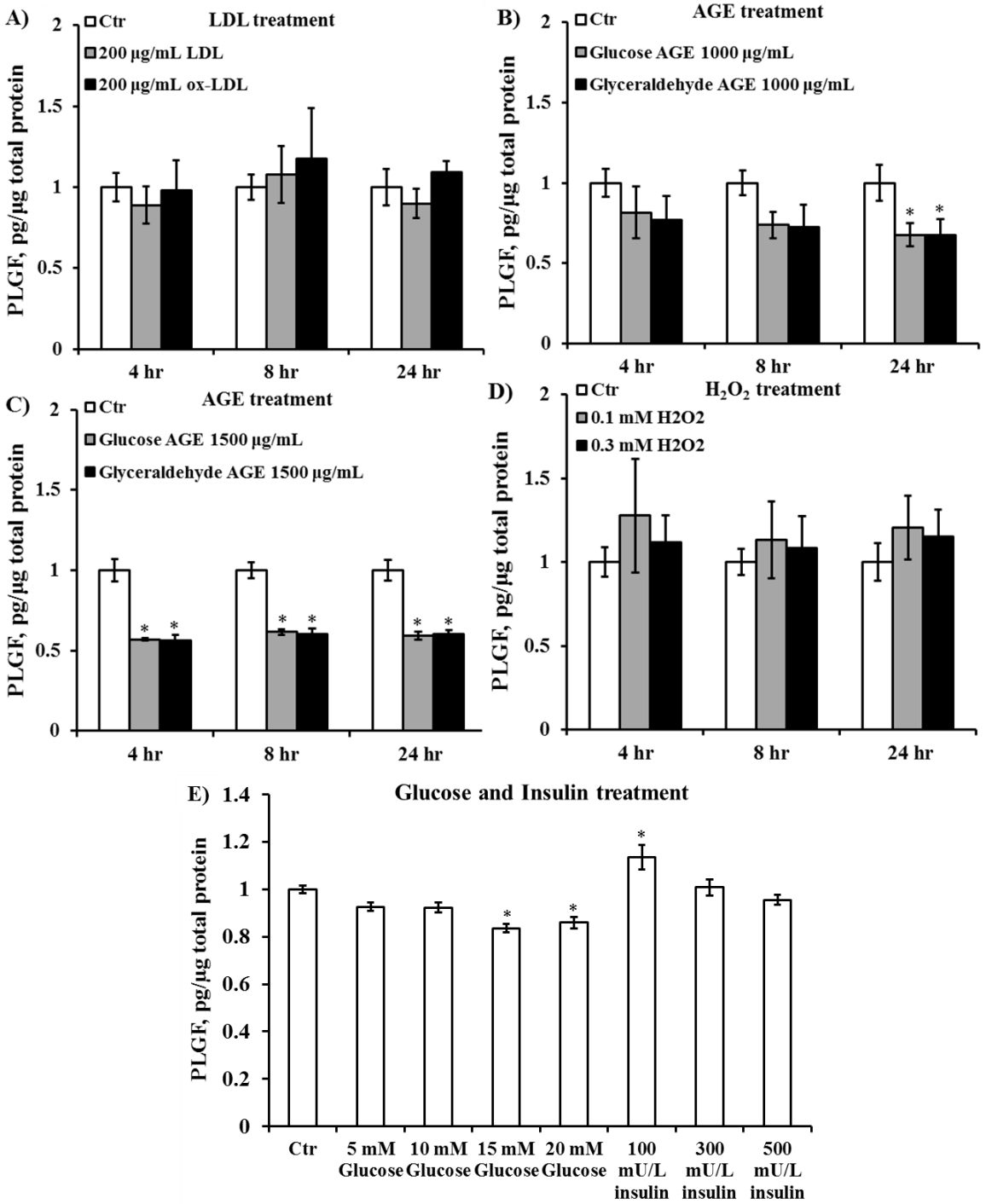

Figure 5.33: PLGF expression in HSKMC following exposure to (A) 200 µg/mL LDL/ox-LDL (n=6/group), (B) 1000-1500 µg/mL glucose or glyceraldehyde derived-AGE (n=5-10/group), (C) 0.1-0.3 mM H_2O_2 (n=6/group), (D) 5-20 mM glucose (n=6/group), or (E) 100-300 mU/L insulin (n=6/group) for 24 hr. Data are presented as Mean±SEM. Results indicated a significant (P<0.05) reduction in PLGF expression in the presence of AGE and glucose, but not in the presence of other treatments.

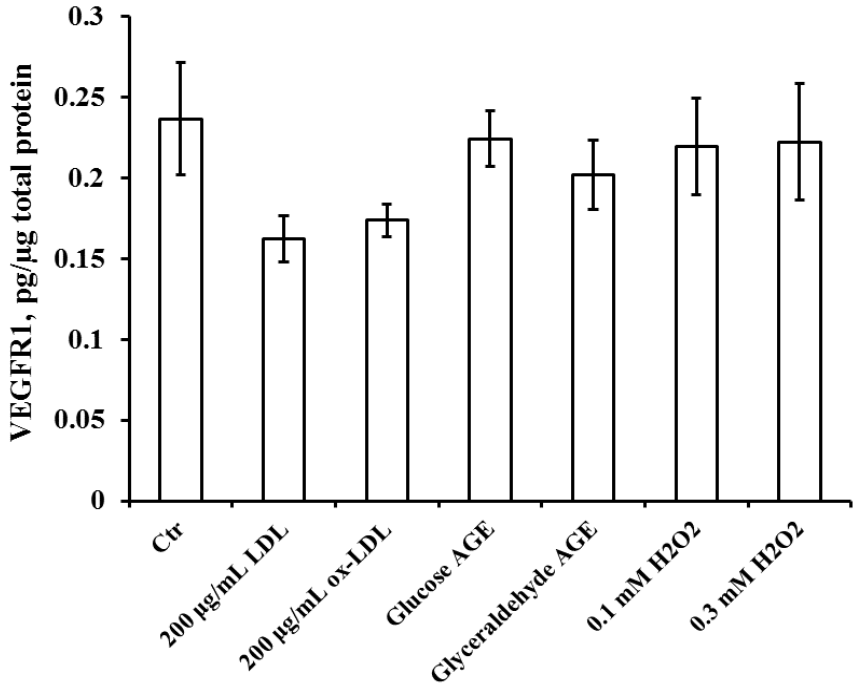

Figure 5.34: Effect of LDL/ox-LDL, glucose/glyceraldehyde derived AGE, and H_2O_2 on HSKMC surface VEGFR1 expression (n=6/group). There was no significant effect of any of the treatments on VEGFR1 expression.

Figure 5.35 illustrates the effect of similar treatments on MSKMC PLGF expression. As in HSKMC, MSKMC were treated with LDL/ox-LDL (A, n=6/group), glucose/glyceraldehyde derived-AGE (B, (n=6/group), 0.1/0.3 mM H_2O_2 (C, n=6/group), or glucose/insulin (D, n=5/group) followed by assessment of PLGF expression. Results indicated a significant change in MSKMC PLGF expression in response to all the treatments except insulin. LDL/ox-LDL, AGE, and H_2O_2 treatment significantly (P<0.05) reduced PLGF expression, whereas glucose induced a significant (P<0.05) increase in PLGF expression in MSKMC. Again, there was no significant effect of any of the treatments on MSKMC surface VEGFR1 expression (Figure 5.36, n=5/group).

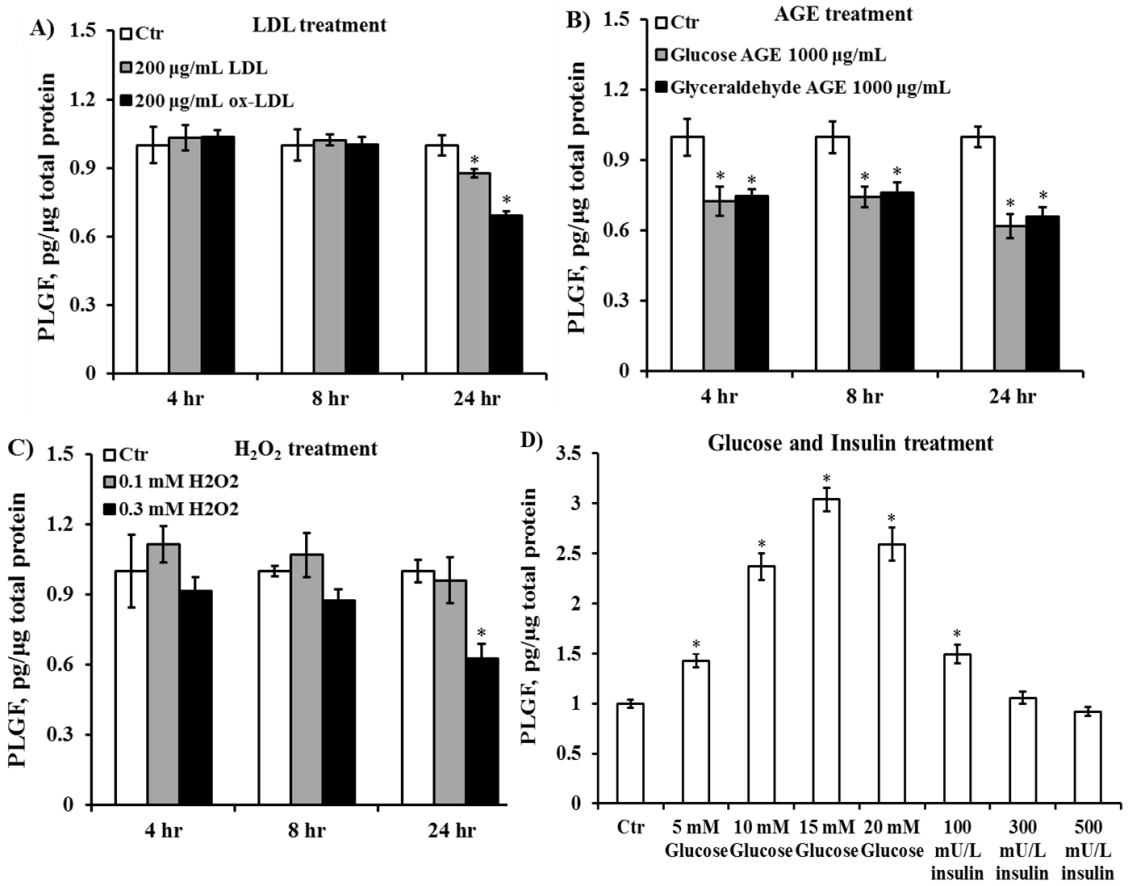

Figure 5.35: Effect of LDL/ox-LDL (A, n=6/group), glucose/glyceraldehyde derived-AGE (B, n=6/group), 0.1/0.3 mM H_2O_2 (C, n=6/group), or glucose/insulin (D, n=5/group) on MSKMC PLGF expression (normalized to total protein) assessed 4, 8, 24 hr after treatment exposure. MSKMC PLGF expression was significantly (P<0.05) downregulated by LDL, ox-LDL, AGE, and H_2O_2 treatment, and significantly (P<0.05) upregulated by glucose treatment.

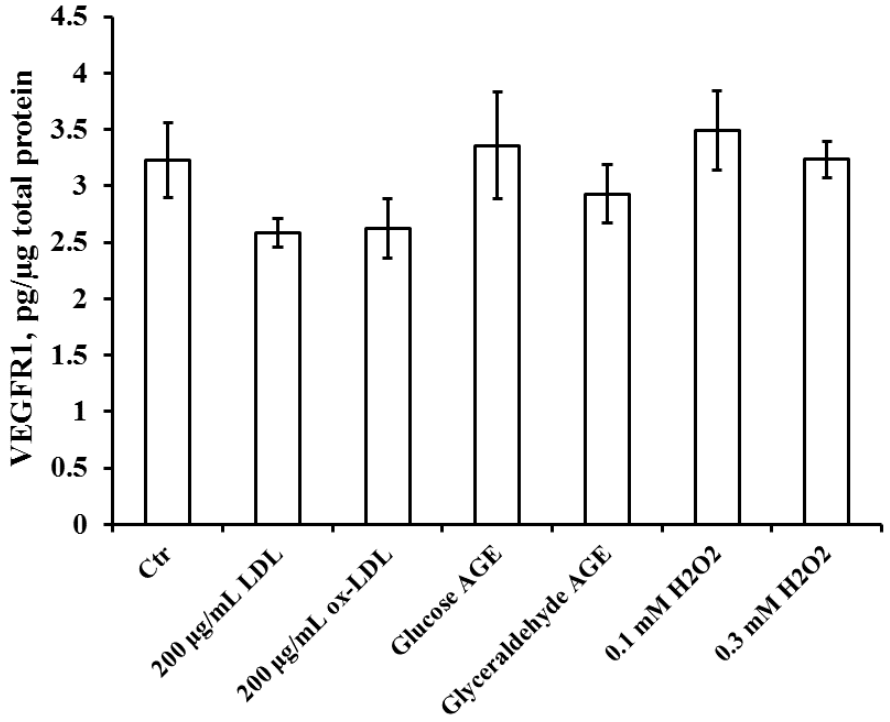

Figure 5.36: Normalized MSKMC cell surface VEGFR1 expression after 24 hr of treatment in the presence of LDL/ox-LDL, glucose/glyceraldehyde derived AGE, or H_2O_2 (n=6/group). None of the treatments could induce any significant change in VEGFR1 expression.

All these results indicated that hyperglycemia and long-term hyperglycemia resulting in AGE formation may be the major contributors to impaired PLGF expression and thus impaired arteriogenesis in diabetic heart and skeletal muscle, as treatment with high concentrations of glucose and AGE had the greatest negative impact on PLGF expression.

5.5 Specific aim 5: The goal of this aim was to investigate the effects of glucose, advanced glycation end products (AGE), and the presence of smooth muscle cells (SMC) on dynamic shear stress-stimulated EC PLGF expression, and to identify the signaling pathways involved.

Human iliac artery EC (HIAEC), co-cultured with human coronary artery SMC (SMC), were exposed to normal (NS) and elevated (ES) shear stress simulating conditions in healthy and remodeling peripheral collateral arteries, and HIAEC PLGF expression was measured.

Human coronary artery EC-SMC co-cultures were exposed to elevated (ES) dynamic shear stress of remodeling coronary collateral artery in the presence or absence of 20 mM glucose or

1000 µg/mL of glucose derived AGE, and EC secreted PLGF was quantified. To identify AGE affected signaling pathways, the gene expression level of EC RAGE, Nox2, Nox4, HO-1, MCP-1, TNF-α, and β-actin were also quantified 24 hr post-elevated shear (ES) exposure.

5.5.1 EC PLGF expression

To investigate how altered dynamic shear stress of diseased peripheral arteries can modulate EC PLGF expression, HIAEC-SMC co-cultures were exposed to normal (NS) and elevated (ES) dynamic shear stress as found in healthy and remodeling peripheral collateral arteries (Figure 4.4) respectively, using the cone-plate shearing device, for 2 hr. Media samples were collected (from HIAEC side) immediately pre-shear and post shear, and also 8 and 24 hr post shear. Samples were assessed for PLGF and total protein level using a PLGF sandwich ELISA and the BCA assay, respectively. The PLGF protein level at the various post-shear time points was double normalized to total protein and to the normalized (to pre-shear total protein) pre-shear value of PLGF expression. Results (Figure 5.37) indicated that ES induced a significant (P<0.05) increase in EC PLGF production compared to NS exposure at 8 hr and a non-significant increase at other time points (at 0 hr, P=0.068; at 24 hr, P=0.089, n=5/group).

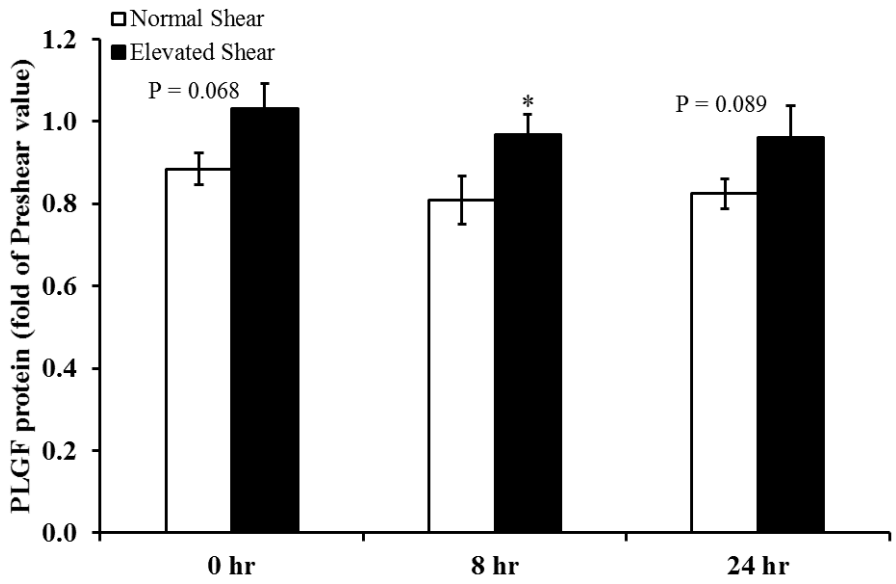

Figure 5.37: Normalized PLGF protein expression by HIAEC exposed to normal (NS) and elevated shear (ES) stress simulating conditions in healthy and remodeling peripheral collateral arteries respectively for 2 hr (n=5/group). ES enhanced PLGF expression significantly at 8 hr and non-significantly at 0 (*P*=0.068) and 24 hr (*P*=0.089) time points compared to NS. Data are presented as Mean±SEM.

The study next focused on how hyperglycemic conditions (simulated by glucose and AGE treatment) could affect shear stress mediated PLGF expression in EC. EC were co-cultured with SMC on two opposite sides of a cell culture insert membrane. EC-SMC co-cultures were then exposed to elevated (ES) pulsatile shear stress mimicking conditions in remodeling coronary collateral arteries for 2 hr in the presence or absence of glucose (20 mM) or glucose derived AGE (1000 µg/mL). Media samples were collected from the EC side immediately pre-shear and again 0, 8, and 24 hr post-shear to assess EC PLGF and total protein using a PLGF sandwich ELISA and the BCA assay, respectively. Data analysis was conducted on PLGF protein normalized to total protein and to the normalized (to pre-shear total protein) pre-shear PLGF protein value using two-way ANOVA. A 2 hr shear exposure time was chosen, as a previously conducted study in our lab had demonstrated that 1 hr shear exposure did not significantly effect PLGF expression. EC-SMC static co-cultures not exposed to any treatment were used as controls (Ctr). Additionally, static co-cultures exposed to 20 mM glucose or 1000 µg/mL of glucose derived AGE were also analyzed to distinguish between the effects of shear stress and metabolic treatments. Figure 5.38 shows the

normalized level of PLGF protein (represented as fold of pre-shear value, n=5/group). Compared to Ctr, AGE treatment significantly (P<0.05) reduced PLGF expression in static culture. Exposure of EC-SMC co-cultures to ES stress significantly (P<0.05) increased PLGF production (~24%). This effect of ES was significantly (P<0.05) blocked by glucose and AGE treatment, with AGE having a greater effect.

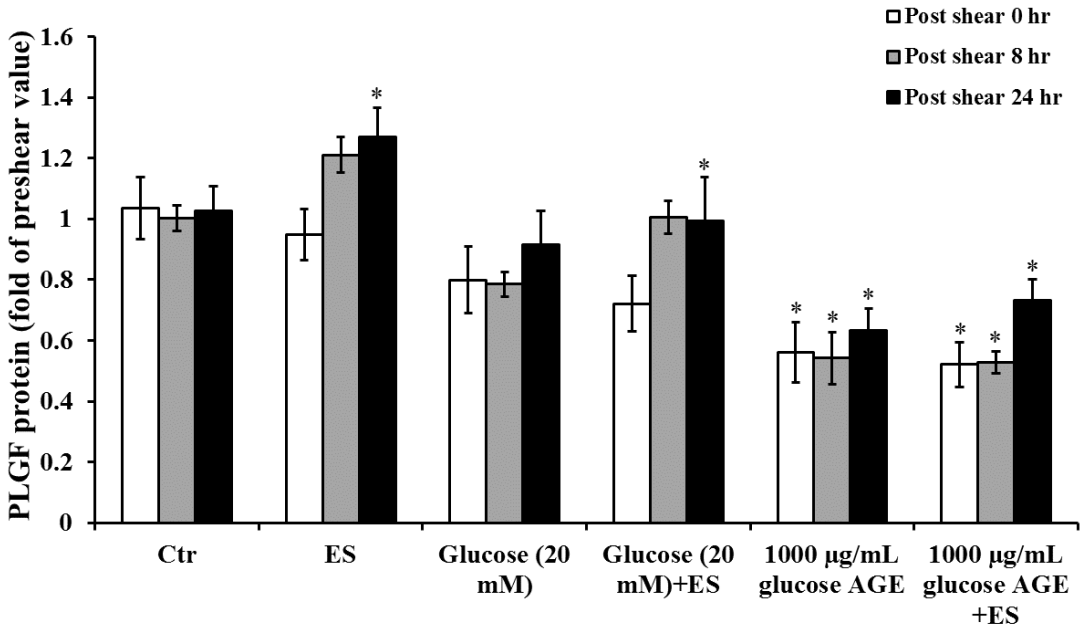

Figure 5.38: Fold change in PLGF expression (with respect to pre-shear PLGF expression) of EC co-cultured with SMC and exposed to elevated (ES) pulsatile shear stress, for 2 hr (n=5/group). ES significantly (P<0.05) enhanced EC PLGF expression. However, this effect was significantly (P<0.05) blocked in the presence of glucose and AGE. AGE treatment, compared to control (Ctr), significantly reduced PLGF expression in static culture. (Data: Mean±SEM, *- significantly different based on ANOVA analysis).

5.5.2 EC mRNA expression

The gene expression level of RAGE, Nox2, Nox4, HO-1, MCP-1, TNF-α, and β-actin in EC was also assessed in shear and glucose/AGE exposed co-cultures using RT-PCR. Twenty-four hr after EC-SMC co-culture exposure to the ES waveform ± 20 mM glucose or 1000 μg/mL AGE treatment, EC were collected, lysed, and probed for the above-mentioned target genes. Figure 5.39 shows gene expression of RAGE, Nox4, HO-1, MCP-1, and TNF-α normalized to β-actin mRNA expression (n=3-5/group). Nox2 gene expression level could not be determined. Results indicated that there was no significant effect of shear, glucose, or AGE treatment on expression of any of the genes, with the exception of TNF-α.

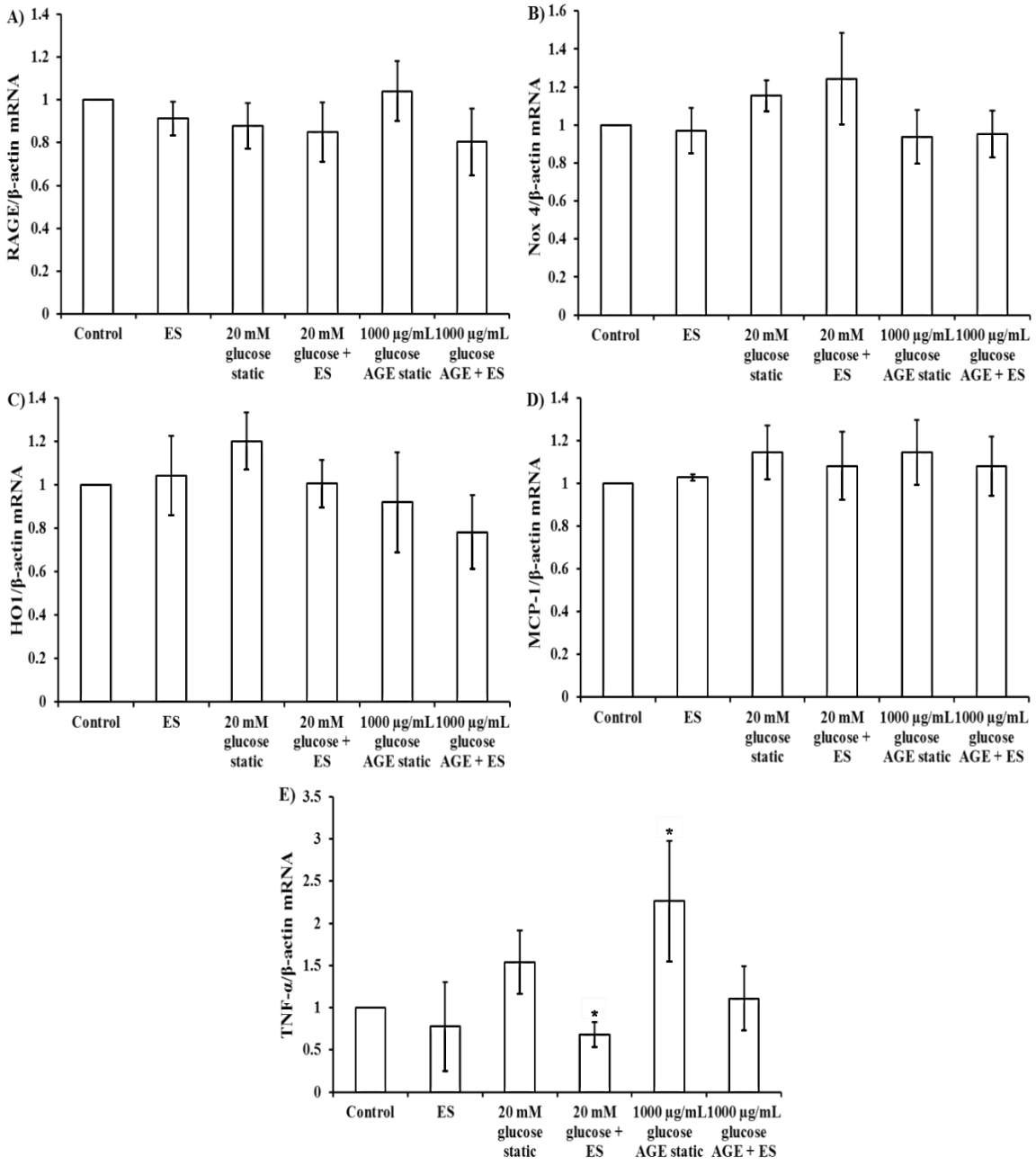

Figure 5.39: Effect of elevated shear stress (ES) ± glucose (20 mM) or advanced glycation end product (1000 µg/mL) treatment on RAGE (A), Nox4 (B), HO-1 (C), MCP-1 (D), and TNF-α (E) gene expression of EC in co-culture (n=3-5/group). Shear, glucose, or AGE treatment had no significant effect on expression of any of the genes except TNF-α. The TNF-α mRNA level was significantly reduced in the presence of glucose + ES treatment, but significantly increased in AGE treated static culture. Data are shown as Mean±SEM. (P<0.05; * - represents significant difference).

These results demonstrated that elevated dynamic shear stress is a major stimulus for PLGF upregulation whose effect can be blocked by glucose and AGE treatment, suggesting that acute and

long term hyperglycemia might inhibit PLGF expression and arteriogenesis by promoting AGE formation[17].

5.6 Specific aim 6: The goal of this aim was to discover the key underlying molecular mechanisms by which a Western diet induces dysfunctional PLGF expression in mouse skeletal muscle.

To better understand the mechanisms by which a Western diet reduces PLGF expression in skeletal muscle, quadriceps femoris (QF) and gastrocnemius/plantaris/soleus (G-P-S) muscles from C57BL/6J and ApoE$^{-/-}$ mice fed a Western diet for 6 mo were collected and probed for levels of advanced glycation end products (AGE) and RAGE, Nox2, Nox4, HO-1, MCP-1, TNF-α, and β-actin mRNA.

5.6.1 AGE protein level quantification

AGE protein level was measured in Western diet fed C57BL/6J and ApoE$^{-/-}$ mouse QF and G-P-S muscle tissues using the sandwich ELISA technique. After homogenizing the tissues, tissue lysate supernatants were collected and added to specially prepared ELISA plates for AGE protein quantification. The AGE protein level was normalized to the total protein level for data analysis. Figure 5.40 shows the normalized AGE protein level of QF and G-P-S muscle tissues of Western diet fed C57BL/6J and ApoE$^{-/-}$ mice (n=8-10/group). Results indicated that the Western diet (WD) significantly (P<0.05) increased the AGE protein level in both QF and G-P-S muscle tissues of C57BL/6J and ApoE$^{-/-}$ mice, compared to control diet (CD) fed mice, with AGE deposition being greater in C57BL/6J mice than in ApoE$^{-/-}$ mice.

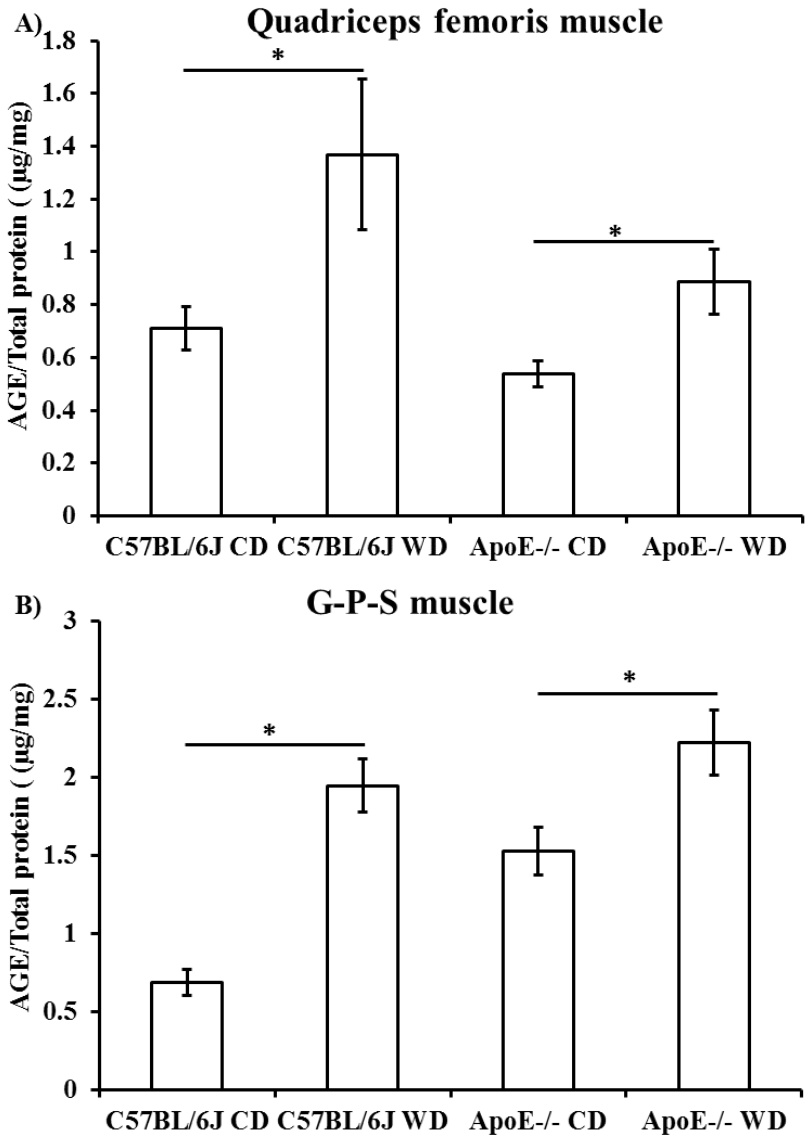

Figure 5.40: Tissue AGE protein quantification in control diet (CD) and Western diet (WD) fed C57BL/6J and ApoE$^{-/-}$ mouse quadriceps femoris (QF) and gastrocnemius/plantaris/soleus (G-P-S) muscles as determined using sandwich ELISA (n=8-10/group). Mouse were fed the diets for 6 mo before sacrifice. AGE protein was normalized to total protein for both QF (A) and G-P-S (B) muscles. Data are presented as Mean±SEM. Results indicated that the WD significantly (P<0.05) increased AGE protein level in QF and G-P-S muscle tissues of both strains, compared to the CD.

5.6.2 mRNA expression of skeletal muscle tissues

To begin defining the pathways through which Western diet induced metabolic dysfunction inhibits skeletal muscle PLGF expression, RAGE, Nox2, Nox4, HO-1, MCP-1, TNF-α, and β-actin mRNA was quantified using RT-PCR. Total RNA was collected from CD and WD fed C57BL/6J and ApoE$^{-/-}$ mouse skeletal muscle tissues (both QF and G-P-S), and was reverse transcribed and amplified for determination of the target gene expression. Target gene expression was normalized to the β-actin level in the corresponding same strain and diet fed tissues. Figure 5.41 and 5.42 show the normalized mRNA level of the target genes in C57BL/6J and ApoE$^{-/-}$ mice QF and G-P-S muscle tissues, respectively (n=3-5/group). Results indicated that in C57BL/6J QF muscle, the WD significantly (P<0.05) reduced the Nox4 mRNA level and increased the RAGE mRNA level; whereas in ApoE$^{-/-}$ QF muscle, the WD significantly reduced (P<0.05) the Nox2 and MCP-1 mRNA level. In C57BL/6J G-P-S muscle, WD consumption was found to significantly (P<0.05) increase the Nox2 and HO-1 mRNA level; whereas in ApoE$^{-/-}$ G-P-S muscle, the WD significantly (P<0.05) reduced the MCP-1 and TNF-α mRNA level compared to CD feeding. No other significant effects of the diets on gene expression were observed.

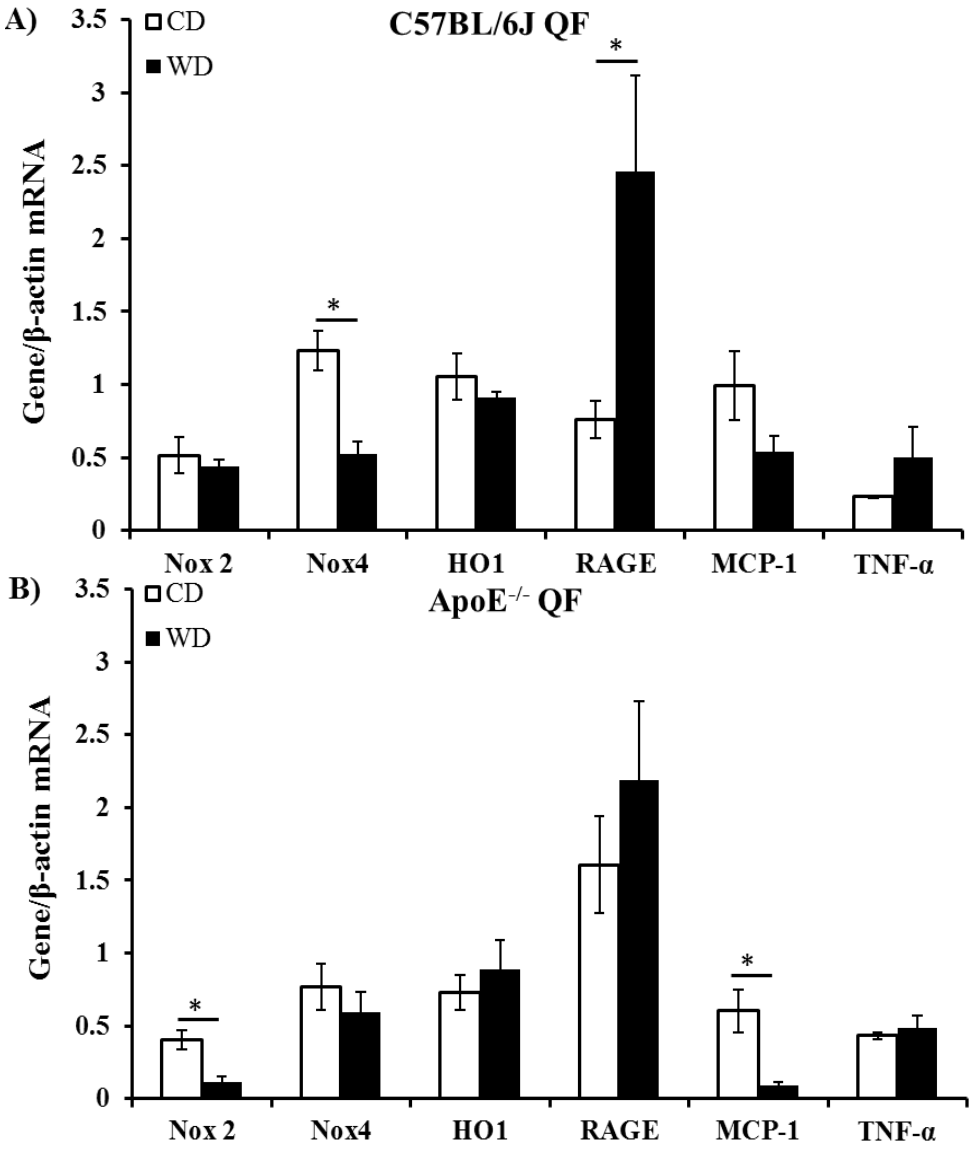

Figure 5.41: mRNA quantification of Nox2, Nox4, HO-1, RAGE, MCP-1, and TNF-α genes using RT-PCR. QF muscle was collected from CD and WD fed C57BL/6J and ApoE$^{-/-}$ mice (n=3-5/group). Gene expression (Data: Mean±SEM) was normalized to the corresponding β-actin mRNA expression. The results demonstrate that Nox4 and RAGE mRNA level was significantly (P<0.05) decreased and increased, respectively, in QF muscle of C57BL/6J mice; whereas, Nox2 and MCP-1 mRNA expression was significantly (P<0.05) reduced in QF muscle of ApoE$^{-/-}$ mice.

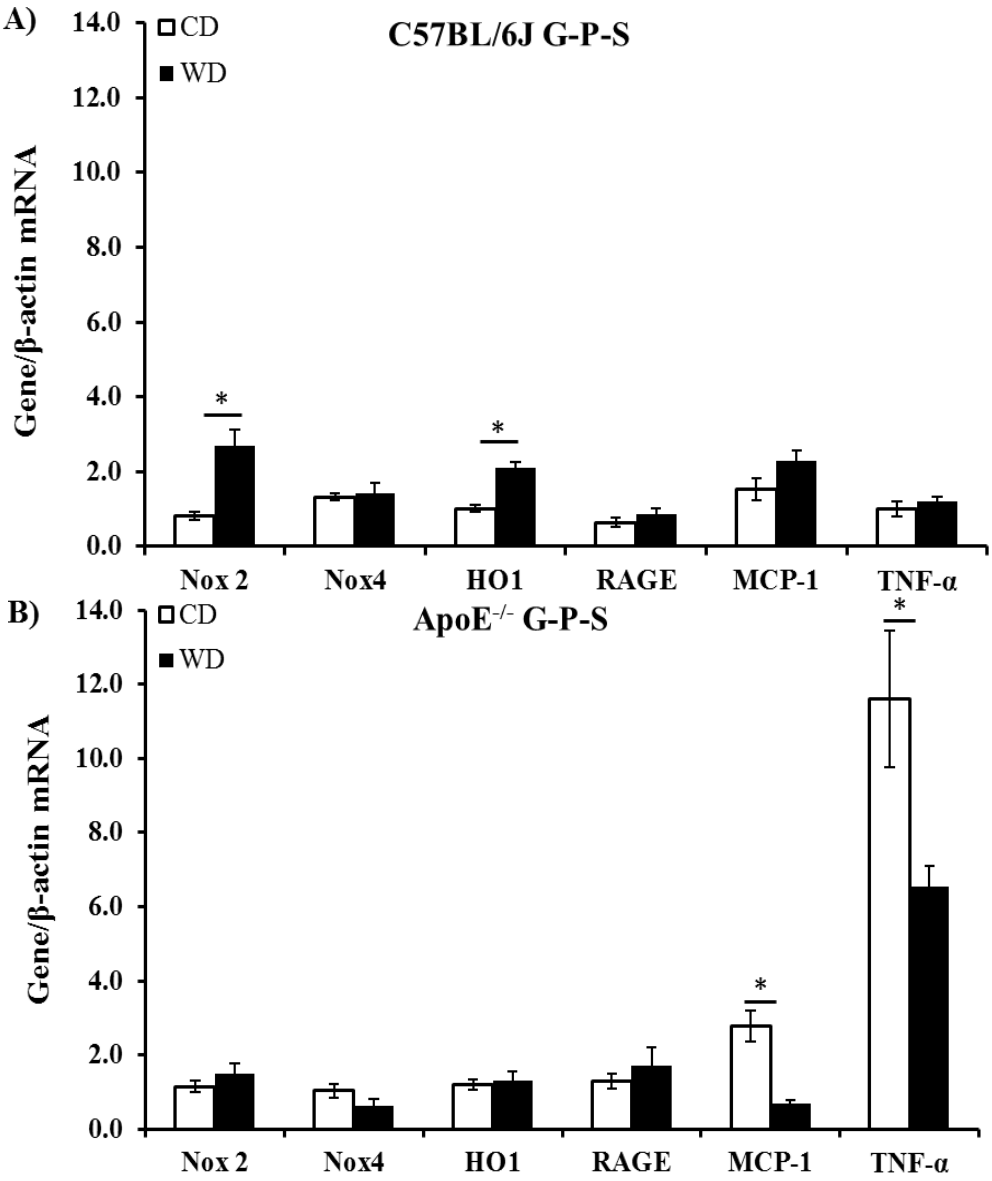

Figure 5.42: Quantification of Nox2, Nox4, HO-1, RAGE, MCP-1, and TNF-α mRNA level in G-P-S skeletal muscle of CD and WD fed C57BL/6J and ApoE$^{-/-}$ mice (n=3-5/group). Target gene expression was normalized to the corresponding β-actin expression value for the same diet and strain. Results indicated that the Nox2 and HO-1 mRNA level was significantly (P<0.05) increased in C57BL/6J mice, and that the MCP-1 and TNF-α mRNA level was significantly (P<0.05) decreased in ApoE$^{-/-}$ mice.

Considered together, these results suggest that the presence of chronic hyperglycemia resulting in AGE formation is one underlying cause for reduced PLGF expression in skeletal muscle of WD fed mice. Along with RAGE, other AGE receptors may play role in AGE-AGE receptor mediated signaling. Our signaling pathway study results may indicate that our hypothesis

of Nox mediated oxidative stress generation and subsequent inflammatory response induction may not be the pathway inducing dysregulated PLGF expression in WD fed mouse skeletal muscle.

CHAPTER VI

DISCUSSION

The onset and pathological progression of cardiovascular disease (CVD), especially coronary artery disease (CAD) and peripheral artery disease (PAD), is greatly modulated by biochemical and biomechanical stimuli. Biomechanical stimuli, such as altered shear stress induced by disturbed blood flow, act as an important regulator of platelet and EC functions. Since EC are the innermost layer of blood vessels, and platelets are freely circulating through the blood, both EC and platelets are continuously exposed to shear stress. Any change in local shear stress may alter their functions and activities significantly. Changes in the shear environment trigger activation of various signaling pathways, resulting in alteration of EC and platelet functional responses (e.g. over-expression of inflammatory and adhesion molecules, and expression of cytokines and growth factors). Activated platelets communicate with the activated EC through various receptor-ligand interactions that can positively or negatively affect each cell type's function.

One of the major goal of this project was therefore to investigate how physiologically relevant dynamic shear stress, along with platelet-endothelial cell interactions, affects function and activation of platelets and endothelial cells. For this purpose, *in vitro* studies were conducted to measure the effects of dynamic shear stress on functional responses of EC through the measurement of cell surface and released von Willebrand factor (vWF) levels and tissue factor (TF) expression,

as well as EC microparticle (EMP) generation. Platelet responses were also monitored under dynamic shear stress conditions by measuring cell surface PECAM-1, GPIbα, and GPIIb expression and platelet microparticle (PMP) generation. In addition, platelets and EC were co-sheared to investigate the combined effects of shear stress and platelet-EC interaction on activation of platelets and EC (Aim 1). Different dynamic (normal, low, and elevated shear stress) shear waveforms were applied for 1 hr to platelets and/or EC (cultured in petri dishes/6 well plates) using a cone-plate viscometer. The shear stresses were obtained through computational fluid dynamics (CFD) modeling conducted previously in our lab that replicated the shear waveforms sensed by EC and platelets in a physiologically realistic left coronary artery (LCA) model under healthy and diseased conditions[46;220]. The LCA was chosen as it is vulnerable to atherosclerotic plaque development due to its complex geometrical structure. *In vitro* studies were further extended to *ex vivo* animal studies to enhance the physiological relevance of the *in vitro* findings. For the *ex vivo* study, freshly harvested rat aortas were exposed to dynamic shear stress (same time average value of shear waveforms as used in the *in vitro* study) and EC activation and inflammatory responses were assessed in terms of ICAM-1, TF, and vWF protein expression (Aim 1). Our goal was to combine *in vitro* and *ex vivo* experimental studies to achieve a better understanding of the role of platelets and EC in the development of cardiovascular diseases. To further evaluate the downstream signaling pathways, involved in modulation of cell functions and various gene expressions, MAPK and NF-κB pathway activation level was quantified through p38, JNK, and ERK1/2, and NF-κB p65 protein phosphorylation after shearing EC under normal and low pulsatile shear stress for 1 hr using the cone-plate shearing device (Aim 2).

Along with contributing to the pathogenesis of cardiovascular diseases, activated platelets and EC also play important roles in the body's compensatory response mechanism to arterial occlusion through arteriogenesis. During arteriogenesis, small arterioles bypassing the obstruction enlarge to accommodate additional blood flow, a process mediated by uptake and release of growth

factors and modulation of growth factor receptor levels. Therefore, the other major goal of the project was to investigate how dynamic shear stress, as found in remodeling coronary collaterals, as well as various metabolic parameters associated with type 2 diabetes, affects platelet and EC behavior related to arteriogenesis. CVD progression (i.e. the presence of atherosclerotic plaque in major arteries) can stimulate arteriogenesis by increasing blood flow and shear stress in collateral arteries. However, as diabetes can inhibit arteriogenesis, diabetes may affect how the shear signal is sensed and/or transduced into an arteriogenic stimulus. Therefore, we focused on studying how platelets, EC, cardiac muscle cells, and skeletal muscle cells take up/release PLGF (an arteriogenesis-specific growth factor) and the related protein VEGF in response to dynamic shear and/or diabetes-associated metabolic parameters. The effect of shear stress and hyperglycemia on PLGF/VEGF uptake/release by platelets was measured after incubating platelets with recombinant PLGF/VEGF protein (Aim 3). Whether the uptake/release of growth factors by platelets is a passive or an active Ca^{2+} signaling dependent process was also assessed in studies using calcium chelators. To identify which type 2 diabetes-associated metabolic parameter has the greatest negative impact on PLGF expression at the cellular level, we exposed coronary artery EC, cardiac muscle cells, and skeletal muscle cells to various simulated metabolic conditions (hyperlipidemia, hyperglycemia, hyperinsulinemia, and oxidative stress) by treating them with low density lipoprotein (LDL), oxidized LDL, glucose, advanced glycation end products (AGE), insulin, and hydrogen peroxide. Following these treatments, PLGF and cell surface VEGFR1 were quantified (Aim 4). To further enhance the physiological relevance of these studies by more completely reproducing conditions within the vascular wall, we tested the effects of simulated acute hyperglycemia (elevated glucose) and long term hyperglycemia (advanced glycation end products AGE) on dynamic shear stress mediated PLGF expression in EC. For these studies, EC from coronary/peripheral vessels were co-cultured with smooth muscle cells (SMC) and exposed to shear stress in the presence or absence of glucose/AGE, followed by quantification of PLGF expression (Aim 5). In addition, underlying signaling mechanisms by which these metabolic parameters could modulate PLGF expression were

assessed through measuring expression of several relevant genes. These *in vitro* studies were again extended to an *ex vivo* animal study, in which skeletal muscle tissues from the thigh and calf of control and Western diet fed mice of two strains were harvested and probed for AGE protein and associated signaling pathway genes. The goal of these experiments was to begin identifying key underlying mechanisms modulating dysfunctional PLGF expression in skeletal muscle in response to feeding of a Western diet (Aim 6).

6.1 Effect of dynamic shear stress and platelet-EC interaction on platelet and endothelial cell responses *in vitro* and *ex vivo*

Since platelets travel through flowing blood and EC are continually exposed to blood flow, both platelets and EC are susceptible to any changes in the blood flow induced shear stress. Therefore, to investigate how these two cell types behave under conditions of dynamic shear exposure, cone-plate shearing devices (Figure 4.1) were used to apply shear stress on platelets and EC. Previous studies have utilized simple constant shear stress to stimulate these cell types; whereas physiologically relevant dynamic shear (physiological and pathological) stress was utilized in this study (shown in Figures 4.2)[21]. Also, to enhance the physiological relevance of the findings, platelets and EC were co-sheared to observe the effects of platelet/EC cross-talk on cellular responses. Using the cone-plate shearing device, platelets and confluent EC were sheared alone/together for 1 hr and activation responses were quantified, for platelets: through cell surface PECAM-1, GPIbα, and GPIIb expression, and platelet microparticle (PMP) generation, and for EC: through cell surface and released von Willebrand factor (vWF) levels, tissue factor (TF) expression, and EC microparticle (EMP) generation.

Platelet endothelial cell adhesion molecule-1 (PECAM-1) is a surface glycoprotein expressed on both platelets and EC. A dual role of PECAM-1 has been reported, in which PECAM-1 acts as an initiator of EC activation but an inhibitor of platelet activation[115;124]. On platelets,

PECAM-1 reduces platelet adhesion or aggregation regulating integrin activation (through inhibition of GPIbα mediated GPIIb activation)[127]. Hence, PECAM-1 can be considered as a potential therapeutic target. Though, several studies have reported activation of PECAM-1 on EC under static shear stress exposure, no studies have yet examined the effect of dynamic shear stress on platelets PECAM-1 expression[31;222]. Therefore, in this study, we quantified the platelet surface PECAM-1 protein after exposing platelets to dynamic shear waveforms (normal and pathological low shear) in either the absence or presence of EC. Interestingly, the presence of EC significantly enhanced platelet PECAM-1 expression (Figure 5.1) after 60 min of shear exposure. Jones *et al.* have shown negative co-relation between platelet surface PECAM-1 expression and platelet function, as expression and clustering of PECAM-1 inhibited multiple signaling pathways resulting in reduced thrombus formation[223]. Therefore, our observations may indicate that platelets which become activated under dynamic shear exposure express more surface PECAM-1, which then acts as a negative regulator to inhibit further platelet activation.

GPIbα, the main binding component of GPIb-IX-V complex, facilitates firm adhesion of activated platelets to suebdothelium through vWF-GPIbα interaction[135]. It has been reported that this interaction can lead to GPIIb/IIIa mediated platelet aggregation as aggregation was attenuated blocking vWF using anti-vWF antibody under high shear stress (10.8 Pa) exposure[224]. Hence in this study, we wanted to see whether dynamic shear exposure (for 1 hr) and EC-platelet communication can affect GPIbα expression of platelets. Our results (Figure 5.2) showed that dynamic shear stress did not have any significant effect on platelet GPIbα expression indicating pulsatile shear stress may initiate some negative regulatory mechanism (such as proteolytic cleavage of GPIbα) that attempts to reduce platelet activation[225]. Another reason could be the variation in shear stress magnitudes over time that has lower shear stress-time integral value, compared to similar level of constant shear stress, that may not be enough to induce any significant effect on platelet GPIbα expression. Exposing platelets to 1-38.8 Pa for 90 s, Leytin *et al.* found no

significant changes in GPIbα expression under low shear stress (1, 4.4, and 11.7 Pa); whereas, found significant downregulation under high shear (20.4 and 38.8 Pa) exposure[226]. When EC were incorporated into our system, dynamic shear (normal and elevated) stress exposure reduced platelet surface GPIbα expression significantly demonstrating role of platelet-EC communication in modulation of platelet responses.

GPIIb is another platelet surface membrane glycoprotein that contributes to platelet aggregation. Upon platelet activation, GPIIb undergoes conformational changes and transforms from inactive state to active state. Reduction in GPIIb expression can decrease shear stress induced pro-coagulant granule secretion and spreading of platelets[227;228]. Though it is unclear how shear stress can affect GPIIb expression, decreased GPIIb expression would mean reduced platelet aggregation eventually[132;229]. In this study, platelets were exposed to constant and dynamic shear stress for 60 min either with or without healthy or activated EC (through TNF-α treatment), and platelet surface GPIIb expression was measured every 15 min (Figure 5.3). Platelet GPIIb responses were observed to vary with different shear loading environments. Platelets were more sensitive in presence of constant shear stress as significant reduction in GPIIb expression was observed under elevated (3 Pa) shear exposure. Time study demonstrated that both normal and elevated constant shear stress (1 and 3 Pa) increased platelet surface GPIIb expression within 15 min of shear exposure that reduced with longer exposure duration (after 60 min). However, dynamic shear stress had no significant effect on platelet GPIIb expression further suggesting that pathological dynamic shear exposure may not necessarily cause damage or activation of platelets. These results indicated that platelets' response to shear stress is dependent on shear stress (constant or dynamic) nature. Platelets tend to have different level of activation under constant shear stress as they are constantly exposed to same level of shear magnitude over a certain period of time. Therefore, they do not get a chance to recover from exposed shear stimulation. However, as dynamic shear stress varies over time, it seems to have a protective effect on platelets[230]. Interestingly, in the presence of healthy

and activated EC, a significant reduction in platelet surface GPIIb expression (Figure 5.4) was observed under dynamic elevated shear exposure, suggesting cross-talk between platelets and EC may have initiated a protective mechanism to reduce aggregation.

Upon activation, platelets and EC also release small vesicles (0.1 to 1.5 μm) known as microparticles that contain most of the platelet and EC surface glycoproteins (PECAM-1, GPIbα, GPIIb), negatively charged surface phospholipids, and binding sites for coagulation factors. Microparticles can induce activation of platelets and EC, facilitating adhesion and platelet aggregation. After exposing platelets to dynamic shear stress in the presence of EC, both platelet (PMP) and EC (EMP) microparticles were quantified in this study based on their size and positive binding for PECAM-1 and GPIbα (Figure 4.6)[231]. PMP are positive for both PECAM-1 and GPIbα; whereas EMP are positive for PECAM-1 and negative for GPIbα. Our results (Figure 5.8) showed an increase in EMP and PMP production under all the dynamic shear exposure conditions compared to static control. Between the two, EMP represented the majority of the detected microparticle population. Further analysis showed that elevated shear exposure significantly increased EMP generation that may have enhanced platelet sensitivity to dynamic shear stress exposure in presence of EC. Applying 1.2 and 10.8 Pa shear stress using a cone plate shearing device for 5 min, Miyazaki *et al*. have found significantly high PMP generation under 10.8 Pa, but, not under 1.2 Pa indicating PMP generation is dependent upon shear stress magnitude as high level of shear stress can enhance PMP release[232]. A positive relationship has been reported to exist between hemodynamic shear stress and EMP generation as both PMP, EMP had been reported to increase during pulmonary hypertension, but only EMP level was associated with the hemodynamic severity of the disease[233].

vWF is a multimeric glycoprotein that is synthesized exclusively by EC and megakaryocytes. vWF is either expressed on the cell surface or released in soluble form into the plasma. Because it is a dimer, vWF can form a bridge between two cells (two platelets or one platelet and one EC) facilitating their interaction and platelet-EC adhesion. vWF binding to GPIbα

plays vital role for activated platelets to adhere to damaged sub-endothelium, whereas GPIIb-vWF interaction for platelet aggregation[28]. Since shear-induced interaction between platelet GPIbα and immobilized vWF can cause GPIbα ectodomain shedding under shear stress exposure, we wanted to see how dynamic shear stress can affect EC vWF expression[225]. Hence, EC were exposed under different constant and dynamic shear exposure, and EC surface and released vWF expression was quantified. Tissue factor (TF) is another membrane bound glycoprotein which has a major role in blood coagulation. During injury, TF forms a complex with coagulation factor (factor VII), resulting in insoluble fibrin formation to stop bleeding. TF is reported to induce an increase in thrombin generation which can down regulate GPIbα expression[234;235]. Therefore, we also investigated the change in TF expression under constant and dynamic shear exposure. Both surface vWF and TF expressions on EC and released soluble vWF was quantified using solid phase and sandwich ELISA technique respectively. Results showed that there was no significant change in EC surface vWF (Figure 5.9 and 5.10) or TF (Figure 5.12) expression under constant or dynamic shear exposure. No change in observed EC surface vWF expression could be due to the applied shear stress magnitude or shear stress exposure duration, or due to the rapid (within seconds to minute) cleavage of EC surface vWF by EC produced metalloproteases (such as ADAMTS13). ADAMTS13 cleaves off the cell surface vWF and reduces the ultra large size of the multimers resulting in soluble vWF expression[54]. Similar result, i.e. no change in EC surface vWF expression, has also been reported in a previous study, when EC were exposed to 1.2 Pa for 6 hr[57]. Interestingly, they found significant increase in vWF expression when EC were sheared for longer duration (15 hr) which demonstrates shear exposure duration as a major modulator of EC surface vWF expression. For TF expression, as EC produce both TF and TF pathway inhibitor (TFPI), no change in EC surface TF expression could be attributed to simultaneous TFPI secretion. Grabowski *et al*., activating HUVEC under 0.068 and 1.32 Pa shear stress for 3 hr, have found direct diminishing effect of flow mediated shear stress on EC TF generation through upregulation of TFPI[236]. In our study, when EC were exposed to dynamic shear stress in the presence of platelets, elevated shear

stress induced a significant increase in soluble vWF expression (Figure 5.11) indicating soluble vWF may be a mediator of enhanced platelet activation under dynamic shear stress exposure. Galbusera *et al*. has also reported significant shear stress magnitude dependent increase in EC released soluble vWF expression after applying 0.2-1.2 Pa shear stress for 6 hr on HUVEC[57].

Interaction between platelets and EC can greatly modulate their functions during physiological and pathological conditions. Both platelets and EC can release different substances that can enhance or inhibit activation of the other cell type. Platelets and EC also communicate via cell surface glycoproteins. To investigate the level of platelet-EC interaction on responses to shear stress, platelets were exposed to dynamic shear stress in the presence of EC. Optical microscopy images showed that dynamic shear exposure enhanced interaction between platelets and EC, as more platelets were observed to adhere to sheared EC. However, more experiments were needed to reach a definite conclusion.

Our results indicated that platelet and EC activation by shear stress is sensitive to the nature of the shear exposure. Constant and dynamic shear can both modulate platelet and EC function, but in different ways. Constant shear stress induced a greater change in protein expression than dynamic shear stress (when compared for platelet surface GPIIb expression). One possible explanation for this observation is that platelets do not get any recovery time from shear stimulation when exposed to constant shear. Another explanation is that the shear stress-exposure time integral value is much higher for constant shear stress (360, 1080, 3600, and 10800 Pa-s for 0.1, 0.3, 1, and 3 Pa shear stress respectively) compared to the dynamic shear waveforms (1980, 828, and 2088 Pa-s for normal, low, and elevated shear stress respectively). Therefore, pathological (low or elevated) dynamic shear stress may not induce as great of a change in expression as constant shear stress. Also, platelet-EC communication plays a vital role in platelet and EC activation[237]. Our results showed that, in the presence of platelets, pathological dynamic shear can induce EC activation (as seen by a significant increase in soluble vWF and EMP generation). Activated EC may engage in

signaling crosstalk with platelets to return activation towards equilibrium levels by increasing/decreasing platelet surface glycoproteins or PMP generation. We conjecture that the increase in platelet surface PECAM-1 (negative modulator for platelets) and decrease in GPIbα and GPIIb and PMP generation which we observed following dynamic shear exposure serves to counteract EC activation by shear stress exposure.

Physiological relevance of *in vitro* EC study has been further enhanced through *ex vivo* animal study. In *ex vivo* study, we have examined activation and injury level of EC, of aorta freshly harvested from rats, following dynamic shear (normal, low, and elevated) exposure in a perfusion flow chamber (Figure 4.5 and 4.7). Total protein expression of vWF, ICAM-1, and TF expression was measured through Western blot. Results from Western blots (Figure 5.13) showed no significant difference in either of the proteins expression (vWF, ICAM-1, or TF) in cytoplasmic or membrane level under different dynamic shear exposure. However, compared to the non-sheared aortas, dynamic shear stress induced significant reduction ($P<0.05$) in vWF and ICAM-1 expression in cytoplasmic level, as well as significant reduction in ICAM-1 expression in membrane protein level. As it has been reported that only ~5% of the synthesized vWF remains stored in the Weibel-Palade bodies of the EC and the remainder gets secreted as soluble vWF, this can cause reduced cytoplasmic vWF expression under dynamic shear exposure[238]. Studies have shown that shear stress magnitude and exposure duration play important role on EC ICAM-1 expression, as significantly increased ICAM-1 level was observed *in vitro* (when HUVEC were subjected to 0.25-4.6 Pa for 48 hr) in time-dependent manner and *in vivo* [when carotid arteries of rabbits were ligated to induce low (0.326±0.058 Pa) and elevated (3.05±0.46 Pa) shear stress for 5 days][13] in shear stress magnitude-dependent manner[239]. Reduction in vWF, ICAM-1 expression might also indicate to a potential protective mechanism that inhibits EC activation. No significant change in either cytoplasmic or membrane TF level was observed under dynamic shear exposure. This could be due to variable expression of EC TF as TF has been identified on activated static

cultured EC surface *in vitro*, whereas has not been found on endothelium *in vivo* indicating the protective effect of flow dependent shear stress on cell synthesized protein expression/release[240;241]. All together the results indicate that dynamic shear stress induce higher activation of EC *in vitro* compared to *ex vivo*. Differences between our *in vitro* and *ex vivo* results could be attributed to some facts: a) EC were exposed to dynamic shear stress *in vitro* for 1 hr, but for 2 hr in *ex vivo* study, b) *in vitro* EC were coronary artery endothelial cell from human (HCAEC); whereas *ex vivo* study EC were abdominal aorta EC of rat, c) total EC lysates were used for *in vitro* study, but tissue lysates were separated as cytoplasmic and membrane protein extracts in *ex vivo* study, and d) the *ex vivo* study is more physiologically relevant than the *in vitro* study. Expression level of a particular protein in EC has been reported to vary not only in different species, but, from different origins as well[196].

6.2 Signal pathways involved in endothelial cell responses to dynamic shear stress

Signal pathways are part of a complex communication system that can modulate different cellular functions such as differentiation, proliferation, and migration. Signals are sensed and converted to intracellular biochemical signals that are passed through the cytoplasm by various signaling pathways. The MAPK pathway is one such pathway (composed of ERK1/2, JNK, and p38 members) that passes the intracellular signal to the nucleus through phosphorylation of its signaling cascade components. NF-κB is an important transcription factor that translocate to the nucleus upon activation and plays an important role in regulating expression of growth factors, cytokines, and other proteins (ICAM-1, E-selectin). Studies have shown that MAPK pathway activation can activate NF-κB and induce its translocation into the nucleus[93;94]. Most studies of the role of shear stress in regulating MAPK and NF-κB activity have utilized constant shear stress to activate EC[79;242]. Therefore, this study was designed to observe the effects of the more physiological stimulus of dynamic shear exposure, as well as platelet-EC interaction, on activation of the MAPK and NF-κB pathway. EC were exposed to normal or low dynamic shear exposure of left coronary

artery, for 1 hr using the cone-plate shearing device, in the absence or presence of platelets, and MAPK and NF-κB pathway activation level was observed through Western blotting. Immunocytochemical staining was also conducted for quantification of ERK1/2 activation. Results from the Western blot (Figure 5.14 and 5.15) experiments indicated that there was no significant effect of dynamic shear exposure on EC MAPK pathway activation (measured through level of ERK1/2, JNK, and p38 phosphorylation) after 30 min, but a significant reduction (P<0.05) in ERK1/2 and p38 phosphorylation level was observed after 60 min shear exposure compared to non-sheared EC (control). Results from immunocytochemical (Figure 5.16) staining images (ERK1/2, 60 min shear exposure, qualitative analysis) were consistent with the Western blot data. In the presence of platelets (more experiments were needed), level of MAPK phosphorylation (ERK1/2, JNK, and p38) of EC increased compared to that of EC sheared in absence of platelets. In the absence of platelets, a significant decrease (P<0.05) in phosphorylated ERK1/2 was observed after 60 min shear exposure (compared to 30 min). Therefore, further experiments were conducted to see whether a shorter dynamic shear exposure duration (2, 5, and 15 min) could activate ERK1/2. As ERK1/2 plays the most prominent role in modulation of cellular and physiological activities among the three members of MAPK family (ERK1/2, JNK, and p38), we were more interested on ERK1/2 activation level. Significant phosphorylation of ERK1/2 occurred during this short exposure duration, with a peak within 5 min followed by a significant decrease with continued shear exposure (at the end of 60 min). Exposing HUVEC to 0.42 Pa shear stress for 0-120 min in a parallel plate flow chamber, Cheng *et al*. also reported increased ERK1/2 phosphorylation level within 10 min of shear exposure that returned to basal level after 60 min[79]. Surapisitchat *et al*. applied 1.2 Pa constant shear stress on HUVEC for 60 min and have found significant increase in ERK1/2 activation within 10 min of shear stress exposure that sustained till the end; whereas, p38 activation level increased slowly reaching the peak after 60 min shear exposure[243]. Their study also indicated no significant effect of shear stress on activation of JNK, similar to what we have found. In the presence of platelets, a similar trend (initial increase followed by a gradual decrease) in

ERK1/2 phosphorylation of EC was observed in our study. Interestingly, an overall higher activation level was observed in the presence of platelets, suggesting that platelet-EC communication enhanced sensitivity of EC to shear stress (more experiments were needed) and activated EC MAPK pathway.

Level of NF-κB phosphorylation was also quantified after exposing EC to dynamic shear stress (normal and low) in the absence or presence of platelets. We observed (Figure 5.17) a similar trend (significant initial increase and gradual decrease, $P<0.05$) in NF-κB phosphorylation as seen for phosphorylation level of ERK1/2. However, the NF-κB response was delayed, as the highest level ($P<0.05$) of phosphorylation reached after 15-30 min of shear exposure. This result suggests that dynamic shear stress first affects MAPK activation, which in turn modulates NF-κB activation. Conducting a time course study on cardiac myocytes, treated with septic plasma, Yang *et al.* found that activation of MAPK members (p38, after 2 min) precedes activation of NF-κB (after 5 min)[244]. Blocking p38 MAPK activity, they also found inhibition of NF-κB phosphorylation and translocation that confirmed the role of MAPK in modulation of NF-κB activities. Therefore, in our study, further investigations were required with MAPK inhibitors in order to test the possibility of dynamic shear stress in such modulation. Other studies have also demonstrated involvement of different MAPK members regulating NF-κB activities[93;245]. Liang *et al*. have reported significantly increased NF-κB staining in nuclei after 30 or 60 min of shear exposure to 0.42 Pa, suggesting activation and translocation of NF-κB from cytoplasm to nuclei under steady shear stress exposure[96]. Interestingly, in our study, the peak activation of NF-κB was observed within 2 min of shear exposure in the presence of platelets, followed by a gradual decrease (more experiments were needed to reach a definite conclusion). However, no significant difference was observed in either ERK1/2 or NF-κB phosphorylation level in response to low shear stress exposure, compared to normal shear. Results from specific aim 1 also indicated that pathological low shear stress does not induce any significant EC activation. Taken together, these data suggest that low dynamic shear

stress may not be harmful for EC, or that low shear exposed EC recovers quickly from shear exposure as the time averaged value of this shear stress waveform is quite low.

6.3 Effect of dynamic shear stress on uptake/release of endothelial growth factors by platelets

PLGF and VEGF-A are two important endothelial growth factors that can contribute to arteriogenesis by modulating various cellular functions (such as cell permeability, survival, proliferation) directly or indirectly (through attraction of inflammatory cells towards EC). Upon activation, EC and SMC produce an abundant amount of PLGF and VEGF-A, respectively[196]. Non-EC secreted VEGF-A then acts on EC in a paracrine manner[246]. However, the mitogenic effect of VEGF-A requires the presence of PLGF to make the greatest impact on EC functions[199]. Studies have shown that PLGF alone does not induce EC migration, but VEGF-A requires PLGF for modulating this function, and PLGF deficiency can hamper responses to VEGF-A[198]. For enhancing the mitogenic response of EC to VEGF-A, a high level of PLGF expression is not necessary; rather, the presence of a low level of PLGF is sufficient to exert the effect[196]. PLGF and VEGF-A bind to their corresponding growth factor receptors (VEGFR1 and VEGFR2) to send different intracellular signals that modulate EC responses[195;212]. Since platelets circulate throughout the body and can take up or release proteins upon activation, platelets can act as effective transporters for carrying PLGF and VEGF-A from the site of protein synthesis to their site of action[247;248]. Therefore, this study investigated the role of platelets in uptake and release of PLGF and VEGF-A. The effects of dynamic shear exposure (simulating conditions in remodeling coronary collateral arteries; Figure 4.3), calcium ion inhibitors (beraprost sodium and EDTA), and metabolic dysfunction (hyperglycemia) on the uptake and release of PLGF and VEGF-A by platelets were also assessed.

Initially, an RT-PCR analysis was conducted to determine whether platelets contain mRNA for PLGF and VEGF-A. Results showed that platelets do contain VEGF-A mRNA. In contrast, no

PLGF mRNA was detected in platelets. The presence of VEGF-A mRNA in platelets has been reported previously, but, no prior studies have reported whether platelets contain PLGF mRNA[249]. We next conducted an uptake study using exogenous PLGF and VEGF-A. Results of this study demonstrated a dose-dependent uptake of both PLGF and VEGF-A by platelets (Figure 5.18), indicating that platelets can take up arteriogenesis-mediating growth factors. Similar to our results for PLGF and VEGF-A, Klement *et al*. also found dose-dependent increase in bFGF uptake by platelets by incubating platelets with different concentrations (0-600 ng/mL) of endostatin and basic fibroblast growth factor (bFGF) for 1 hr[248].

Since most platelet functions are modulated by calcium signaling, and since beraprost sodium (a stable prostacyclin analogue) can inhibit calcium efflux by binding to corresponding prostacyclin receptors present on the platelet surface, we next tested the effect of beraprost sodium on PLGF and VEGF-A uptake by platelets[250]. Beraprost sodium did not affect uptake of PLGF or VEGF-A protein (Figure 5.19), indicating that either the concentration of beraprost sodium or the short treatment duration (1 hr) was insufficient to induce any effect on calcium signaling. A dose-dependent and time-dependent effect of beraprost sodium has been reported by Nony *et al*[251]. The lack of effect of beraprost sodium could also indicate that uptake of the growth factors by resting platelets may not be a calcium dependent process.

Since type 2 diabetes (characterized by insulin resistance of cells) is associated with poor arteriogenesis, we next tested the effect of simulated hyperglycemia on platelet PLGF and VEGF-A uptake[252]. In studies by other groups, induction of hyperglycemia in platelets collected from both non-diabetics and diabetics resulted in increased platelet activation and reactivity *in vitro*[253;254]. Since platelets are known to be hyperreactive in diabetics, we hypothesized that exposure of platelets to simulated hyperglycemic conditions (250 mg/dL glucose treatment) would significantly increase platelet uptake of growth factors. However, acute hyperglycemia (250 mg/dL glucose; 1 hr) had no effect on PLGF and VEGF-A uptake by platelets (Figure 5.20), though an increasing

trend was observed for both the growth factors uptake. The increasing trend suggested that the treatment exposure time frame was probably short to induce any significant effect on platelet growth factor uptake, which is a potential limitation of this study. Another limitation of the study could be low number of experiments. As type 2 diabetes is also characterized by a variety of other abnormal metabolic features (hyperlipidemia, hyperinsulinemia, and oxidative stress) in addition to hyperglycemia, the presence of these conditions could possibly induce defective growth factor uptake by platelets contributing to poor arteriogenesis in diabetics. These conditions were not tested in our present studies. Administration of lipoprotein in diabetic patients has been found to promote calcium efflux leading to reduced platelet activation and aggregation[255]. Hwang *et al*. has reported that hyperinsulinemia induces magnesium efflux in platelets, leading to an increased cAMP level and reduced platelet activation[256]. Therefore, the effects of these parameters on platelet uptake of growth factors should also be examined in future studies.

The effect of a calcium ion chelator (EDTA) on uptake of growth factors by dynamic shear exposed platelets was also assessed. The results showed (Figure 5.21) no significant effect of dynamic shear stress exposure on platelet growth factor (PLGF and VEGF-A) uptake. EDTA treatment also had no significant effect on uptake of growth factors by dynamic shear stress exposed platelets. These results may demonstrate that growth factor uptake by platelets is a process independent of calcium signaling, consistent with what we observed in the beraprost sodium study.

The effect of dynamic shear stress and beraprost-sodium on platelet release of exogenous PLGF and VEGF-A was analyzed by exposing recombinant PLGF/VEGF-A and beraprost-sodium treated platelets to dynamic shear. A decreasing trend for PLGF release and an increasing trend for VEGF-A release was observed under the combined treatment of dynamic shear stress and beraprost-sodium (Figure 5.22). Studies have shown that different types of stimulation (biochemical vs. biomechanical) induce release of angiogenic proteins from activated platelets at different levels based on their release kinetics[247;257]. Since our data analysis indicated no significant

effect of the shear stress or beraprost treatment on growth factor release, these results again suggest that uptake/release of growth factors by platelets is not probably an active Ca^{2+} signaling dependent process.

Next, the combined effect of dynamic shear stress and hyperglycemia on release of PLGF and VEGF-A by platelets was assessed. Results indicated (Figure 5.23) no significant effects of combined exposure to dynamic shear stress and hyperglycemia on growth factor release by platelets. Further studies are necessary to test the effect of other diabetes-associated metabolic features on platelet PLGF and VEGF-A uptake/release. Also, longer dynamic shear stress exposure with/without different metabolic treatments should be considered for future experimental designs.

6.4 Effects of diabetes associated major metabolic dysfunction on PLGF and VEGFR1 expression by human and mouse cardiac and skeletal muscle cell types

PLGF, a major modulator of arteriogenesis, is produced in heart, lungs, skeletal muscles, and abundantly by placenta. PLGF exerts its arteriogenic function through activating VEGFR1 (the PLGF receptor), which is present on the cell surface of EC, SMC and inflammatory cells and sends intracellular signals that modulate EC responses, SMC growth and proliferation, and inflammatory cell migration. Although PLGF has been established as one of the key arteriogenic growth factors, modulation of the PLGF expression level and the mechanisms behind this regulation is not well characterized during disease conditions such as diabetes. Diabetics have a much higher risk of cardiovascular events, as they are more susceptible to develop athero-thrombotic vascular disease and to have impaired angiogenesis/arteriogenesis. These effects are seen in both the cardiac and the peripheral circulation. Together, the increased risk of disease development and the decreased ability to compensate for the disease result in a high risk of heart attack or limb amputation. Therefore, we were interested in studying PLGF expression by myocytes from both cardiac and peripheral origins. We focused on heart and skeletal muscle cells, as diabetic CAD and PAD affect

arteriogenesis in these two regions the most. A previously conducted study in our lab has demonstrated that mice consuming a Western diet for 6 mo exhibit metabolic dysfunction similar to that found in type 2 diabetics (as determined by metabolic phenotyping) and express a reduced level of PLGF in both heart and skeletal muscle. Chou *et al*. reported reduced collateral formation in cardiac tissues of diabetic rats and identified reduced VEGF and VEGFR1/R2 expression as one basis for this impairment[18]. However, diabetes is a complex metabolic disorder characterized by many abnormal metabolic parameters such as hyperlipidemia, hyperglycemia, hyperinsulinemia, and oxidative stress. Therefore, further *in vitro* studies were required to investigate the effect of each of these parameters on PLGF expression and to identify which parameter has the greatest impact on PLGF[258]. Also, we wished to determine the relevance of the mouse study to human physiology. To fulfil this purpose, both human and mouse cell types from heart (human coronary artery endothelial cells, HCAEC and human cardiac myocytes, HCM; and mouse cardiac myocytes, MCM) and skeletal muscle (human skeletal muscle cells, HSKMC and mouse skeletal muscle cells, MSKMC) were subjected to various diabetes-associated treatment conditions mimicking hyperlipidemia (low density lipoprotein, LDL and oxidized LDL, ox-LDL), hyperglycemia (glucose and advanced glycation end products, AGE), hyperinsulinemia (insulin), and oxidative stress (hydrogen peroxide, H_2O_2), followed by PLGF and VEGFR1 quantification. Along with glucose derived AGE, glyceraldehyde derived AGE has been used to treat cells. Glyceraldehyde has the advantage of more rapidly forming AGE than glucose but can evoke similar endothelial cell dysfunction[259]. Endothelial cells form the inner lining of the cardiac chambers and blood vessels and cardiac myocytes constitute the heart wall. Therefore, to identify which of these two major cell types of the heart is the primary source of PLGF in heart, HCAEC and HCM were chosen for the study. Initially, the effect of different metabolic molecules at various concentrations (chosen based on literature survey) was tested on PLGF production by HCAEC. The most effective concentrations were then used to treat the other cell types.

Results from the initial HCAEC dose study showed that hyperlipidemia (LDL/ox-LDL treatment; Figure 5.24) and hyperinsulinemia (insulin treatment; Figure 5.26B) failed to have any effect on HCAEC PLGF expression. No effect of 0.1 mM H_2O_2 (Figure 5.26A) treatment on PLGF production level was expected, as this is considered to be a physiological concentration level for normal cellular activities *in vivo*[176]. However, 0.3 mM H_2O_2 (Figure 5.26A) reduced HCAEC PLGF levels significantly, demonstrating that a pathophysiological level of oxidative stress can inhibit PLGF production by HCAEC. Growth factors such as members from VEGF family appear to be subjected to redox regulation as reduced growth factor (VEGF) expression in the setting of oxidative stress has been reported in epithelial cells that can promote the development of pulmonary disorders[260]. A redox-window hypothesis exists for collateral artery growth, and states that an optimal level of oxidative stress is required above which growth factor dependent signaling and corresponding collateral growth is corrupted. Oxidative stress below the optimal level also results in impaired collateral growth. The results of our oxidative stress study are consistent with this hypothesis[185].

During diabetes, an excess level of glucose is present in the blood. If this condition is maintained for a long duration, the excess glucose begins to interact with proteins, forming AGE. In rodent studies, the presence of high glucose and AGE has been reported to impair angiogenic potential, and this impairment can be reversed by inhibiting AGE's interaction with its receptor (RAGE)[261;262]. Therefore, we next set out to investigate whether PLGF production by HCAEC was inhibited by AGE treatment. Our results indicated that both glucose and AGE significantly reduced PLGF expression (Figure 5.25) demonstrating that acute hyperglycemia and chronic hyperglycemia are both major negative modulators of HCAEC PLGF production. Dose dependent and time dependent effects of glucose and AGE on PLGF were also observed, as the most significant reduction was observed at the highest concentration and the longest treatment duration (24 hr).

Interestingly, lower concentrations of AGE (300-500 µg/mL) significantly and H_2O_2 (0.05 µM) non-significantly increased HCAEC surface VEGFR1 expression after 24 hr of treatment (Figure 5.27), but expression returned to basal levels in the presence of higher concentrations (AGE: 1000 µg/mL and H_2O_2: 0.3 mM). Although PLGF expression was significantly reduced in the presence of AGE and 0.3 mM H_2O_2, a similar level of inhibition was not observed for VEGFR1. This could be due to the reason that VEGFR1 is also a receptor for VEGF-A and the level of VEGF-A was found to be increased in diabetic patients[297]. Therefore, PLGF expression may not correlate with its receptors' (VEGFR1) expression. Another reason could be the generation of soluble variant of VEGFR1 receptor (sVEGFR1) that can bind to PLGF, reducing availability of free and active PLGF protein. Hornig *et al*. has reported sVEGFR1 release by both human microvascular and macrovascular EC[298]. Therefore, along with cell surface VEGFR1, sVEGFR1 level also need to be quantified during different treatment conditions.

Similar to what we observed in the HCAEC study, the results of the HCM study demonstrated that LDL or ox-LDL treatment (Figure 5.28) had no significant effect on HCM PLGF expression. Therefore, hyperlipidemia alone may not be a major contributor to impaired PLGF expression in the heart during diabetes. However, it is possible that hyperlipidemia may act additively or synergistically with other metabolic parameters. Treatment with AGE (Figure 5.28) significantly reduced PLGF, whereas 0.3 mM H_2O_2 (Figure 5.28) significantly increased PLGF expression by HCM. The inhibitory effect of AGE on PLGF inhibition in cardiac cells (both HCAEC and HCM) further supports our hypothesis that AGE formation during long-term hyperglycemia is a key contributor to impaired coronary arteriogenesis during diabetes. The opposite effect of 0.3 mM H_2O_2 on HCAEC (significant decrease) and HCM (significant increase) PLGF expression could be attributed to the metabolic difference of the two cell lines. HCM are the most physically active and highly specialized oxygen content rich cells in the body. Therefore,

though 0.3 mM H_2O_2 level tend to be pathophysiological for HCAEC, the same level of H_2O_2 may be necessary for normal physiological function of HCM.

Comparison of PLGF production by untreated HCAEC and untreated HCM identified HCAEC as the major source of PLGF in the heart, as HCAEC produced ~10-15 times more PLGF than HCM (Figure 5.30). Therefore, although oxidative stress (0.3 mM H_2O_2) induced an increase in PLGF protein by HCM, reduced expression by HCAEC may lead to an overall decrease in cardiac PLGF protein level in the presence of oxidative stress.

Interestingly, PLGF expression was found to be more sensitive to metabolic parameters in MCM than HCM, as a significant change in PLGF expression was observed in response to all of the treatment conditions in MCM (Figure 5.31). In contrast, PLGF levels were affected only by AGE and 0.3 mM H_2O_2 in HCM (Figure 5.28). The various metabolic compounds tested (glucose, AGE, and 0.3 mM H_2O_2), affected MCM VEGFR1 as well (Figure 5.32). This finding suggests that results obtained from mouse studies/cell types should be carefully interpreted, and validated in human tissues and cells.

To investigate the effect of different diabetes-associated metabolic parameters on PLGF expression by skeletal muscle cells (SKMC), HSKMC and MSKMC were also exposed to simulated hyperlipidemic, hyperglycemic, hyperinsulinemic, and oxidative stress conditions as described above. Results from the HSKMC study indicated that skeletal muscle cells were less sensitive to different metabolic treatments, as compared to cardiac cells. This finding could be attributed to the cell-specific differences in protein expression based on the different origins of the cells. For example, even within one species (such as rat), VEGF protein expression and its corresponding receptors have been reported to decrease in cardiac tissue and increase in retina during diabetes[18]. In our study, only the hyperglycemia-associated treatments (glucose and AGE) were able to induce a significant reduction in HSKMC PLGF production (Figure 5.33). Tamarat *et*

al. showed that diabetes associated AGE formation impairs ischemia induced angiogenesis (induced by femoral artery ligation) which was rescued by prohibiting AGE formation using aminoguanidine[263].

A higher sensitivity of mouse skeletal muscle cells (compared to human cells) to the metabolic factors has also been observed. MSKMC PLGF levels were significantly attenuated in the presence of simulated hyperlipidemia, long-term hyperglycemia, and oxidative stress (Figure 5.35). Interestingly, glucose treatment significantly increased PLGF levels in MSKMC. This disparity in results (from mouse and human cells) could be due to the species differences, as mice and humans have many morphological, genetic, and metabolic differences.

No significant change in cell surface VEGFR1 expression was observed under any treatment condition in either HSKMC (Figure 5.34) or MSKMC (Figure 5.36). Summarizing all these results, it can be concluded that hyperglycemia and long-term hyperglycemia resulting in AGE formation may be the major contributors to impaired arteriogenesis in diabetic skeletal muscle as well as in heart; however, other metabolic parameters may also play a role.

A brief overview of the results of this aim is shown in table 2.

Table 2: Effects of different diabetes associated (type 2) metabolic molecules on PLGF expression by different cell types. (N.E. means no effect)

Cell type	Treatments				
	Simulated Hyper-lipidemia	Simulated Hyper-glycemia	Simulated Long-term Hyperglycemia	Simulated Hyper-insulinemia	Simulated Oxidative Stress
HCAEC	N.E.	↓	↓	N.E.	↓
HCM	N.E.	-	↓	-	↑
MCM	↓	-	↓	-	↑
HSKMC	N.E.	↓	↓	N.E.	N.E.
MSKMC	↓	↑	↓	N.E.	↓

6.5 Effects of glucose, AGE, and EC-SMC communication on dynamic shear stress-stimulated EC PLGF expression and related signaling pathways

Increased shear stress is considered to be a major stimulus for arteriogenesis. It is well established that arterial occlusion can increase blood flow induced shear stress in the connecting collateral arteries of proximal areas, affecting EC activation, monocyte adhesion, and subsequent growth factor production by EC in the collaterals[264;265]. Diabetes, a major risk factor for cardiovascular complications, limits both the adaptive response due to arterial obstruction and the number of collaterals that develop. However, the mechanism(s) through which diabetes suppresses arteriogenesis are still not well defined. Our study has identified diabetes associated acute hyperglycemia and chronic hyperglycemia as two of the major modulators that negatively influence the key arteriogenic growth factor PLGF. As experimental hyperglycemia consistently reduced PLGF expression in all of the cell types tested (in the previous specific aim 5), and EC were identified as the major source of PLGF in the heart, the study next focused on how hyperglycemia could affect shear stress mediated PLGF expression in EC. This goal was achieved by exposing

human coronary artery endothelial cells (EC) co-cultured with human coronary artery smooth muscle cells (SMC) to glucose/AGE and/or elevated dynamic shear waveforms mimicking shear stress of coronary collateral arteries undergoing remodeling due to the presence of a 60% blockage in the main artery. Previous studies have shown that co-culturing EC with SMC can affect SMC density and proliferation, as well as EC and SMC gene/protein expression[266;267]. Therefore, we used a co-culture model that mimicked the vascular wall more physiologically due to the presence of direct communication between EC and SMC, allowing them to modulate each other's functions. Also, the co-culture model allowed us to single out the effect of specific treatments on EC PLGF expression since the two cell types can be collected and analyzed separately. Our results (Figure 5.38) indicated that AGE treatment can significantly reduce PLGF production by EC even in co-culture model. Elevated shear stress significantly increased PLGF production ~24% by EC in co-culture. Effects of shear stress on other growth factors have been reported by Gloe *et al*., who found an increase in EC proliferation and differentiation by enhanced basic fibroblast growth factor (bFGF) release during shear exposure[268].

Next, we hypothesized that the increase in PLGF in response to shear stress would be reduced by experimental hyperglycemia. Our results demonstrated that the increase in PLGF expression following exposure to elevated shear stress was blocked by both glucose and AGE treatment, the effect of AGE being greater, suggesting that acute and long term hyperglycemia might inhibit PLGF expression and arteriogenesis by promoting AGE formation during diabetic CAD. Overall, our results are in agreement with previous *in vivo* findings demonstrating that diabetes inhibits arteriogenesis[186;269].

To determine the signal transduction pathway involving AGE-mediated PLGF reduction in the presence of dynamic shear stress, the gene expression level of RAGE, Nox2, Nox4, HO-1, MCP-1, and TNF-α was (Figure 5.39) assessed in EC 24 hr post shear exposure. Our hypothesis was that AGE treatment would inhibit PLGF expression through a RAGE-Nox2/4-TNFα pathway.

RAGE is a receptor for AGE and is present on EC, SMC, and inflammatory cells such as leukocytes. Generally, a low level of RAGE is expressed on quiescent cells, and is upregulated at the site of AGE accumulation[270]. AGE-RAGE interaction has been reported to enhance the activities of NADPH oxidase (Nox) enzyme family members[271]. In presence of AGE, both Nox2 and Nox4 mRNA have been found to be upregulated that can induce sustained ROS production in rat cardiac myocyte and human EC respectively[272;273]. Channon *et al*.'s group has reported increased Nox2 and Nox4 expression in the vascular system (in arteries and veins) of patients suffering from CAD and/or diabetes[274;275]. Nox2 and Nox4 are the major sources of intracellular oxidative stress that generate ROS through superoxide ($O_2^{\cdot-}$) and H_2O_2 production[276]. When produced at low levels (in the μM range; the optimum level for arteriogenesis), H_2O_2 plays an important role in physiological cellular signaling. However, increased levels of H_2O_2 have been found to amplify ROS generation in vascular cells, increasing iron uptake and enhancing Nox and xanthine oxidase activities. This acts as a positive feedback mechanism to further enhance and sustain H_2O_2 production[277]. Increased pathological level of H_2O_2 can then lead to dysregulated cellular functions through instigation of inflammatory responses (cytokine production such as TNF-α). Valen *et al*. reported that treatment of HUVEC with 0.2 mM H_2O_2 (which is considered as pathological level of oxidative stress for cultured HUVEC) enhances TNF-α mRNA level about four-fold, which can induce an inflammatory environment[277;278]. An increased serum level of TNF-α has been associated with endothelial dysfunction in type 2 diabetic patients[279]. Chen *et al*. has reported that Nox generated H_2O_2 can potentiate TNF-α induced MCP-1 gene expression in EC[280]. MCP-1 is a chemoattractant protein that plays an important role in arteriogenesis by mediating monocyte recruitment. An increased level of MCP-1 has been found in plasma of type 2 diabetics[281]. Though MCP-1 had been reported to modulate expression of growth factors such as VEGF-A, the effect of MCP-1 on PLGF levels in diabetes has not been defined yet[282]. Therefore, we also analyzed MCP-1 gene expression in this study. Gene expression of HO-1 was studied as well. HO-1 protects cells from oxidative stress injury by controlling iron metabolism, which is a

potential source of oxidative stress. Interestingly, HO-1 can generate H_2O_2 during its catalytic reaction. If present at high concentration levels, this H_2O_2 can inhibit iron degradation by HO-1[283].

Our results indicated that the Nox2 gene expression was below detection level in EC. Previous studies also have demonstrated that Nox4 is the most abundant Nox isoform present in the EC and the level of Nox2 is very low (~1000 times) compared to Nox4[17;284]. The results from our other gene expression study demonstrated that there was no significant effect of shear stress, glucose or AGE treatment on expression of any of the genes studied, except for TNF-α. One possible explanation for this finding could be that gene expression was quantified 24 hr post shear. Results from previously conducted studies in our lab have indicated that EC PLGF gene expression in response to shear stress was transient, as the PLGF mRNA expression level increased significantly within 4 hr but had returned to basal levels by post 24 hr shear exposure. Though the change in PLGF protein level was detected 8 hr post-shear exposure, there was no change in gene expression at a similar time point (10 hr). Also, PLGF upregulation was found to be dependent on the Nox4 signaling pathway, and Nox4 gene expression was elevated within 4 hr of shear exposure[17]. Therefore, to more conclusively identify the involvement of different signaling molecules, expression of the target genes should have been quantified at earlier time points (at 0-2 hr).

6.6 Underlying molecular mechanisms inducing dysfunctional PLGF expression in skeletal muscle of Western diet fed mice

Diabetes can impair arteriogenesis through inhibition of growth factor production and release. From the results of our two previous specific aims, we concluded that advanced glycation end products (AGE) formed during long-term hyperglycemia reduces placental growth factor (PLGF) expression *in vitro*. To further enhance the physiological relevance of these findings, we next studied whether these results could be confirmed in an animal model. We focused on the

quadriceps femoris (QF, from thigh) and gastrocnemius/plantaris/soleus (G-P-S, from calf) skeletal muscle tissues, where two distinct types of vascular remodeling occur that are relevant to disease conditions such as PAD. Arteriogenesis is the main type of remodeling in the QF, whereas angiogenesis (capillary growth) is predominant in the G-P-S. Mice of two strains (C57BL/6J and $ApoE^{-/-}$) were fed a Western diet (WD, high fat diet) for 6 mo to mimic diet-induced type 2 diabetes, followed by collection of the QF and G-P-S muscles[285]. In previously conducted studies in our lab, PLGF expression was found to be down-regulated in both the muscle types of both the strains. Therefore, based on these findings and the results of our *in vitro* experiments on skeletal muscle cells, we set out to determine whether tissue AGE could account for the reduced PLGF expression in skeletal muscle of WD fed mice. Our *ex vivo* study results (Figure 5.40) demonstrated that the WD did significantly increase AGE protein levels in both QF and G-P-S muscle tissues of C57BL/6J and $ApoE^{-/-}$ mice, compared to the control diet fed mice, with AGE deposition being greater in C57BL/6J mice than in $ApoE^{-/-}$ mice. Similar results showing increased level of AGE following high fat/high sugar diet feeding have been reported in aorta and skeletal muscle by different groups, and linked to aortic stiffening and muscle fiber atrophy, respectively[286;287]. AGE has also been reported to modulate the expression level of growth factors such as VEGF[288]. Therefore, these results are consistent with our hypothesis that AGE deposition could be the underlying cause of dysfunctional PLGF expression in skeletal muscle tissues of WD fed mice.

We next tried to further identify underlying molecular mechanisms by which AGE could induce dysfunctional PLGF expression. We hypothesized that the RAGE-Nox2/4-TNFα pathway mentioned in the discussion section of the previous specific aim could be involved in AGE mediated signaling in skeletal muscle. We were interested in MCP-1 and HO-1 gene expression as well for the same reasons mentioned in the previous specific aim's discussion section. Though we investigated gene expression in both muscles (QF and G-P-S), we were primarily interested in the QF, since vascular growth in the QF in response to vascular occlusion happens primarily by

arteriogenesis (whereas the G-P-S mainly undergoes angiogenesis). Our results indicated that the Nox4 mRNA level was significantly reduced, while the RAGE mRNA level was significantly increased in QF muscle of WD fed C57BL/6J mice (Figure 5.41A). However, in QF muscle of WD fed ApoE$^{-/-}$ mice (Figure 5.41B), the only significant change was a reduction in both Nox2 and MCP-1 mRNA. A non-significant increase in RAGE mRNA was observed as well. In the G-P-S muscle of C57BL/6J mice (Figure 5.42A), the Nox2 and HO-1 mRNA level was significantly increased, whereas in the G-P-S muscle of ApoE$^{-/-}$ mice (Figure 5.42B), the MCP-1 and TNF-α mRNA level was significantly reduced following long-term WD consumption.

Though we were expecting an increase in RAGE mRNA in all the muscle types, due to the observed increase in tissue AGE level, we found a significant increase in RAGE only in the QF muscle of C57BL/6J mice, with a non-significant increase in ApoE$^{-/-}$ mice. Since there are several other receptors for AGE, one possible reason for this result could be that one or more of these other receptors (which were not examined in our study) was affected by the diet. Though RAGE is the most studied AGE receptor, several studies have also reported the existence of other cellular AGE receptors, such as oligosaccharyl transferase-48 (AGE-R1), protein kinase C (AGE-R2), and substrate galectin-3 (AGE-R3) whose expression level may have varied with the WD consumption[169;289]. The lack of change in RAGE expression in G-P-S muscle is consistent with possible involvement of other AGE receptors in our model.

As described above, the Nox2, Nox4, and MCP-1 mRNA level was significantly reduced, while the expression of other genes (HO-1, TNF-α) was not significantly changed in QF muscle of either of the mouse strains. This results may indicate that our proposed signaling pathway of Nox mediated oxidative stress generation leading to inflammatory cytokines (TNF-α and MCP-1) production does not mediate dysregulated PLGF expression in WD fed mice QF muscle. AGE has been found to modulate the activities of xanthine oxidase (XO) and uncoupled endothelial nitric oxide synthase (eNOS) through AGE receptor interaction, both of which are other potential sources

of oxidative stress[171;172]. AGE also induces expression of several other inflammatory molecules and chemokines such as interleukin (IL)-6, -8, CCL-3, and -4[290;291]. IL-6 and CCL-4 have been reported to modulate expression of growth factors such as VEGF[292;293]. Therefore, the involvement of other signaling pathways not tested in the current study could be a possibility.

In G-P-S muscle of C57BL/6J mice, although expression of pro-oxidant Nox2 increased, anti-oxidant HO-1 expression also increased. HO-1 is a cytoprotective enzyme that can inhibit Nox activity, thereby reducing oxidative stress[294;295]. In G-P-S muscles of ApoE$^{-/-}$ mice, neither Nox2 nor Nox4 gene expression was affected, but expression of mRNA for the inflammatory molecule TNF-α and chemoattractant protein MCP-1 was significantly reduced after WD consumption, compared to CD. These results of G-P-S muscle may indicate the existence of an inhibitory pathway that acts to limit Nox generated oxidative stress and subsequent inflammation.

The differing results from QF and G-P-S muscle are consistent with the different types of vascular growth that occur within each tissue in response to vascular occlusion. QF is composed of four muscles, whereas G-P-S consists of three separate muscles. The capillary distribution or vascular growth is different in each section of these muscles. This could be a reason for differing gene expression in QF and G-P-S muscle. Another possible reason could be the low number of experiments (n=3-5/group) conducted for gene analysis. However, as it was difficult to identify a clear pattern of gene expression overall, analysis of protein levels for the target factors could provide more clear insights into the involvement of these factors in mediating WD-induced inhibition of PLGF expression. Further studies are also needed to examine other candidate signaling pathways that could contribute to this response.

CHAPTER VII

CONCLUSION

The major goals of this study were to investigate the effects of physiologically relevant dynamic shear stress, cell-cell communication, and type 2 diabetes-associated metabolic factors on platelet and EC activities. This study was divided into two parts: study 1 and study 2. Study 1 focused on understanding how changes in platelet and EC behavior (expression of adhesion ligands and inflammatory molecules) during dynamic shear exposure can contribute to CAD progression. Study 2 focused on the role of platelets and EC in arteriogenesis during diabetic CAD/PAD (in terms of their production, uptake, and/or release of key arteriogenic growth factors). Associated signaling pathways and the underlying molecular mechanisms modulating these processes were investigated as well.

Results from *in vitro* and *ex vivo* study of stimulation of endothelial cells (EC) in the absence/presence of platelets under physiologically relevant dynamic shear stress (simulating conditions in both healthy and diseased left coronary arteries) showed that presence of both the cell types can greatly affect each other's activities. Our results further demonstrated that shear stress type (constant or dynamic), magnitude (low or elevated), and exposure duration are important modulators of the cellular activation level. Platelet surface PECAM-1 expression was increased in the presence of EC, while platelet surface GPIbα and GPIIb expression was decreased by dynamic shear exposure. The presence of platelets significantly increased EC soluble vWF expression and

microparticle (EMP) generation. Overall, these results demonstrated that platelet-EC interaction can modulate platelet and EC activation level *in vitro*. Platelets enhance dynamic shear induced EC activation, which then through platelet-EC signaling crosstalk tries to return the activation level towards the equilibrium level by modulating platelet activation. This result was further confirmed through an *ex vivo* study, where EC activation (vWF, ICAM-1) was found to be modulated by dynamic shear exposure compared to non-sheared controls.

Next, the study addressed the question of whether the EC activation response was mediated through MAPK and NF-κB pathway activation. Our findings indicated the involvement of the MAPK and NF-κB pathways modulating EC responses to dynamic shear exposure. However, further experiments with inhibitors are needed to confirm the involvement of the MAPK pathway in modulation of NF-κB activities.

In study 2, the first goal was to characterize the uptake/release of key endothelial growth factors (PLGF and VEGF) by platelets, and to test whether these processes could be modulated by dynamic shear (simulating conditions in quiescent and remodeling coronary collateral arteries) exposure. Our results indicated that platelets do take up endothelial growth factors. However, we could not demonstrate any effect of dynamic shear stress, calcium chelation, or hyperglycemia on platelet uptake or release of exogenous growth factors. The relatively low concentration level of these treatments, low number of experiments, and/or the relatively short time frame are potential limitations of this study.

The next aim was to quantify the effect of major metabolic dysfunctions associated with type 2 diabetes (such as hyperlipidemia, acute hyperglycemia, chronic hyperglycemia, hyperinsulinemia, or oxidative stress) on modulation of PLGF and VEGFR1 expression by mouse and human cardiac and skeletal muscle cells. The goal of these studies was to identify which of the tested metabolic parameters had the greatest negative influence on PLGF expression at the cellular

level. Results from this study identified acute hyperglycemia and chronic hyperglycemia (resulting in AGE formation) as the major contributors to impaired PLGF expression in diabetic cardiac and skeletal muscle cells, suggesting that this phenomenon could contribute to impaired arteriogenesis in diabetic patients. Also, this study identified human coronary artery endothelial cell (EC) as the major source of PLGF in the heart. Based on our results, we hypothesized that oxidative stress could lead to an overall PLGF reduction in heart, since oxidative stress reduced PLGF expression in EC. In type 2 diabetics, this decrease could be additive to the decrease in PLGF produced by hyperglycemia/AGE. Lastly, comparison between mouse and human cell results yielded the interesting observation that PLGF expression is more sensitive to metabolic dysfunction in mouse cells than in human cells.

Next, the effect of acute and chronic hyperglycemia (simulated by glucose and AGE administration) on dynamic shear stress stimulated EC PLGF expression was assessed. We also attempted to identify signaling pathways involved in this response. Results from this aim demonstrated that elevated shear stress of coronary collateral arteries significantly increases PLGF production by co-cultured EC and the presence of glucose or AGE negatively modulate dynamic shear stress enhanced PLGF expression, further supporting our hypothesis that glucose and AGE are the major inhibitors of cardiac arteriogenesis through inhibition of PLGF expression. However, the involvement of the specific signaling pathway which we hypothesized would contribute to this effect (RAGE-Nox2/4-TNF-α) could not be confirmed through gene expression analysis.

In the final part of our study, validation of the above *in vitro* study results was taken to the next level through an *ex vivo* study. The goal of this aim was to discover underlying mechanisms that contribute to dysfunctional PLGF expression in Western diet (WD) fed mouse skeletal muscle. Based on *in vitro* results, we quantified the AGE protein level in skeletal muscle tissues. Our findings showed a significantly increased level of AGE in skeletal muscle tissues of WD fed mice, compared to control diet (CD) fed mice. Assessment of pathways potentially involved in AGE

mediated signaling suggested that AGE receptors not tested in the present study (such as AGER1 and AGER2) may act in conjunction with RAGE to mediate activation of downstream AGE-induced signal transduction pathways leading to decreased PLGF expression. Our gene expression results testing potential involvement of Nox2, Nox4, TNF-α, and MCP-1 were inconsistent and study of these factors at the protein level, along with investigation of additional possible signaling mechanisms, is needed.

Summarizing all these results, it can be concluded that platelet and EC interaction under conditions of dynamic shear stress exposure can modulate both platelet and EC functions. Dynamic shear exposure can increase platelet surface PECAM-1 expression in the presence of EC, which can initiate an inhibitory mechanism that reduces platelet surface GPIbα and GPIIb expression. Activated platelets can enhance shear-induced EC activation, as an increased level of EC-released soluble vWF and EMP generation was observed in the presence of platelets. Our *ex vivo* study showed downregulation of EC activation through reduced EC vWF and ICAM-1 expression following dynamic shear exposure. In addition, dynamic shear stress has been found to modulate EC signaling pathways, i.e. the MAPK and NF-κB pathways. All these results demonstrate that dynamic shear stress exposure and platelet-EC crosstalk can induce platelet activation, which in turn enhances shear induced EC activation. Activated platelets and EC then work together to attempt to return the activation level towards its equilibrium level by inhibiting each other's activation. These interactions may contribute to CAD development. Additionally, activated platelets and EC can also modulate arteriogenesis. Platelets can take up growth factors (PLGF and VEGF-A) in a dose-dependent manner, making them potential transporters of growth factors. Activated EC can produce PLGF, as shear stress stimulated EC were found to express a significantly higher level of PLGF compared to static control EC. However, the presence of conditions simulating type 2 diabetes was found to reduce PLGF production by stimulated EC. Among the different metabolic dysfunctions (hyperlipidemia, hyperglycemia, hyperinsulinemia,

and oxidative stress) associated with diabetes, simulated acute (glucose treatment) and chronic (AGE treatment) hyperglycemia, and oxidative stress were found to be the major negative modulators of EC PLGF production. Along with EC, these metabolic parameters (acute and chronic hyperglycemia) also modulated PLGF expression by cardiac myocytes and skeletal muscle cells (both mouse and human). These findings suggest that hyperglycemia and long-term hyperglycemia resulting in AGE formation can contribute to impaired arteriogenesis in both diabetic cardiac and skeletal muscles through reduction of PLGF expression during CAD/PAD. *Ex vivo* study of mouse skeletal muscle tissues (QF and G-P-S) further supports our hypothesis that deposition of AGE is the underlying reason for dysfunctional PLGF expression in diabetic skeletal muscle.

Overall, the results obtained from this study have advanced our knowledge of how platelets and EC interact with each other in various physiological and pathophysiological settings, including dynamic shear stress and diabetes associated metabolic dysfunction. Our results suggest that these interactions can contribute to both CAD development and arteriogenesis. Thus, this study has the potential to lead to eventual therapeutic innovations.

REFERENCES

1. Mozaffarian D, Benjamin EJ, Go AS et al. Heart disease and stroke statistics-2015 update: a report from the american heart association. Circulation 2015;131:e29-e322.
2. Heidenreich PA, Trogdon JG, Khavjou OA et al. Forecasting the future of cardiovascular disease in the United States: a policy statement from the American Heart Association. Circulation 2011;123:933-944.
3. Shaaban AM, Duerinckx AJ. Wall shear stress and early atherosclerosis: a review. AJR Am.J.Roentgenol. 2000;174:1657-1665.
4. THE SAGE GROUP Releases New Estimates for the United States Prevalence of Peripheral Artery Disease (PAD) and Critical Limb Ischemia (CLI). 9-30-2010.
   Ref Type: Report
5. Rouf F, Lloyd PG. Effect of Diabetes-Associated Metabolic Factors on Placental Growth Factor in Skeletal Muscle Cells. The FASEB Journal 2016;30:766.
6. Center for Disease Control and Prevention. More than 29 million Americans have diabetes; 1 in 4 doesn't know. 6-10-2014.
   Ref Type: Report
7. Pipp F, Heil M, Issbrucker K et al. VEGFR-1-selective VEGF homologue PlGF is arteriogenic: evidence for a monocyte-mediated mechanism. Circ.Res. 2003;92:378-385.
8. Sheehan P. Peripheral arterial disease in patients with diabetes. In: Abela G, ed. Peripheral Vascular Disease: Basic Diagnostic and Therapeutic Approaches.: Lippincott Williams

and Wilkins; 2016:62-75.

9. van Gils JM, Zwaginga JJ, Hordijk PL. Molecular and functional interactions among monocytes, platelets, and endothelial cells and their relevance for cardiovascular diseases. J.Leukoc.Biol. 2009;85:195-204.
10. Murata M, Matsubara Y, Kawano K et al. Coronary artery disease and polymorphisms in a receptor mediating shear stress-dependent platelet activation. Circulation 1997;96:3281-3286.
11. Yin W, Shanmugavelayudam SK, Rubenstein DA. 3D numerical simulation of coronary blood flow and its effect on endothelial cell activation. Conf.Proc.IEEE Eng Med.Biol.Soc. 2009;2009:4003-4006.
12. Anderson GH, Hellums JD, Moake JL, Alfrey CP, Jr. Platelet lysis and aggregation in shear fields. Blood Cells 1978;4:499-511.
13. Nagel T, Resnick N, Atkinson WJ, Dewey CF, Jr., Gimbrone MA, Jr. Shear stress selectively upregulates intercellular adhesion molecule-1 expression in cultured human vascular endothelial cells. J.Clin.Invest 1994;94:885-891.
14. Sampath R, Kukielka GL, Smith CW, Eskin SG, McIntire LV. Shear stress-mediated changes in the expression of leukocyte adhesion receptors on human umbilical vein endothelial cells in vitro. Ann.Biomed.Eng 1995;23:247-256.
15. Seiler C. The human coronary collateral circulation. Eur.J.Clin.Invest 2010;40:465-476.
16. Conklin BS, Zhong DS, Zhao W, Lin PH, Chen C. Shear stress regulates occludin and VEGF expression in porcine arterial endothelial cells. J.Surg.Res. 2002;102:13-21.
17. Rashdan NA, Lloyd PG. Fluid shear stress upregulates placental growth factor in the vessel wall via NADPH oxidase 4. Am.J.Physiol Heart Circ.Physiol 2015;309:H1655-H1666.
18. Chou E, Suzuma I, Way KJ et al. Decreased cardiac expression of vascular endothelial growth factor and its receptors in insulin-resistant and diabetic States: a possible

explanation for impaired collateral formation in cardiac tissue. Circulation 2002;105:373-379.

19. Rouf F, Lloyd PG. Placental Growth Factor Expression is Inhibited by Hyperglycemia in Cardiac Cells. The FASEB Journal 2016;30:734.
20. Lin MC, Almus-Jacobs F, Chen HH et al. Shear stress induction of the tissue factor gene. J.Clin.Invest 1997;99:737-744.
21. Ramstack JM, Zuckerman L, Mockros LF. Shear-induced activation of platelets. J.Biomech. 1979;12:113-125.
22. NIH, NHLBI. What Is a Heart Attack? NIH,NHLBI NIH,NHLBI. 2012.
    Ref Type: Online Source
23. Uchida Y, Ichimiya S, Ishii H et al. Impact of plaque burden in the left main coronary artery determined by intravascular ultrasound on cardiovascular events in a Japanese population undergoing percutaneous coronary intervention. Am.J.Cardiol. 2012;109:352-358.
24. Malek AM, Alper SL, Izumo S. Hemodynamic shear stress and its role in atherosclerosis. JAMA 1999;282:2035-2042.
25. Chatzizisis YS, Coskun AU, Jonas M et al. Role of endothelial shear stress in the natural history of coronary atherosclerosis and vascular remodeling: molecular, cellular, and vascular behavior. J.Am.Coll.Cardiol. 2007;49:2379-2393.
26. Kazmierski R. [Biomechanic shear stress in carotid arteries and atherosclerosis development]. Postepy Hig.Med.Dosw. 2003;57:713-725.
27. Brakemeier S, Kersten A, Eichler I et al. Shear stress-induced up-regulation of the intermediate-conductance Ca(2+)-activated K(+) channel in human endothelium. Cardiovasc.Res. 2003;60:488-496.
28. Kroll MH, Hellums JD, McIntire LV, Schafer AI, Moake JL. Pletelets and Shear Stress. The journal of the American Society of Hematology 1996;88:1525-1541.

29. Wu KK, Thiagarajan P. Role of endothelium in thrombosis and hemostasis. Annu.Rev.Med. 1996;47:315-331.

30. Gudi SR, Clark CB, Frangos JA. Fluid flow rapidly activates G proteins in human endothelial cells. Involvement of G proteins in mechanochemical signal transduction. Circ.Res. 1996;79:834-839.

31. Harada N, Masuda M, Fujiwara K. Fluid flow and osmotic stress induce tyrosine phosphorylation of an endothelial cell 128 kDa surface glycoprotein. Biochem.Biophys.Res.Commun. 1995;214:69-74.

32. Olesen SP, Clapham DE, Davies PF. Haemodynamic shear stress activates a K+ current in vascular endothelial cells. Nature 1988;331:168-170.

33. Wang Y, Miao H, Li S et al. Interplay between integrins and FLK-1 in shear stress-induced signaling. Am.J.Physiol Cell Physiol 2002;283:C1540-C1547.

34. Bhullar IS, Li YS, Miao H et al. Fluid shear stress activation of IkappaB kinase is integrin-dependent. J.Biol.Chem. 1998;273:30544-30549.

35. Girard PR, Nerem RM. Shear stress modulates endothelial cell morphology and F-actin organization through the regulation of focal adhesion-associated proteins. J.Cell Physiol 1995;163:179-193.

36. Liu Y, Chen BP, Lu M et al. Shear stress activation of SREBP1 in endothelial cells is mediated by integrins. Arterioscler.Thromb.Vasc.Biol. 2002;22:76-81.

37. Tseng H, Peterson TE, Berk BC. Fluid shear stress stimulates mitogen-activated protein kinase in endothelial cells. Circ.Res. 1995;77:869-878.

38. Wang Y, Flores L, Lu S et al. Shear Stress Regulates the Flk-1/Cbl/PI3K/NF-kappaB Pathway Via Actin and Tyrosine Kinases. Cell Mol.Bioeng. 2009;2:341-350.

39. Jalali S, Li YS, Sotoudeh M et al. Shear stress activates p60src-Ras-MAPK signaling pathways in vascular endothelial cells. Arterioscler.Thromb.Vasc.Biol. 1998;18:227-234.

40. Li YS, Shyy JY, Li S et al. The Ras-JNK pathway is involved in shear-induced gene expression. Mol.Cell Biol. 1996;16:5947-5954.

41. Collins T, Read MA, Neish AS et al. Transcriptional regulation of endothelial cell adhesion molecules: NF-kappa B and cytokine-inducible enhancers. FASEB J. 1995;9:899-909.

42. Libermann TA, Baltimore D. Activation of interleukin-6 gene expression through the NF-kappa B transcription factor. Mol.Cell Biol. 1990;10:2327-2334.

43. Tsuboi H, Ando J, Korenaga R, Takada Y, Kamiya A. Flow stimulates ICAM-1 expression time and shear stress dependently in cultured human endothelial cells. Biochem.Biophys.Res.Commun. 1995;206:988-996.

44. Morigi M, Zoja C, Figliuzzi M et al. Fluid shear stress modulates surface expression of adhesion molecules by endothelial cells. Blood 1995;85:1696-1703.

45. Tsou JK, Gower RM, Ting HJ et al. Spatial regulation of inflammation by human aortic endothelial cells in a linear gradient of shear stress. Microcirculation. 2008;15:311-323.

46. Yin W, Shanmugavelayudam SK, Rubenstein DA. The effect of physiologically relevant dynamic shear stress on platelet and endothelial cell activation. Thromb.Res. 2011;127:235-241.

47. Davies MJ, Gordon JL, Gearing AJ et al. The expression of the adhesion molecules ICAM-1, VCAM-1, PECAM, and E-selectin in human atherosclerosis. J.Pathol. 1993;171:223-229.

48. Chu AJ. Tissue factor, blood coagulation, and beyond: an overview. Int.J.Inflam. 2011;2011:367284.

49. Houston P, Dickson MC, Ludbrook V et al. Fluid shear stress induction of the tissue factor promoter in vitro and in vivo is mediated by Egr-1. Arterioscler.Thromb.Vasc.Biol. 1999;19:281-289.

50. Reininger AJ. Function of von Willebrand factor in haemostasis and thrombosis. Haemophilia. 2008;14 Suppl 5:11-26.

51. Rand JH, Badimon L, Gordon RE, Uson RR, Fuster V. Distribution of von Willebrand factor in porcine intima varies with blood vessel type and location. Arteriosclerosis 1987;7:287-291.

52. Yamamoto K, de W, V, Fearns C, Loskutoff DJ. Tissue distribution and regulation of murine von Willebrand factor gene expression in vivo. Blood 1998;92:2791-2801.

53. Nachman RL, Jaffe EA. Subcellular platelet factor VIII antigen and von Willebrand factor. J.Exp.Med. 1975;141:1101-1113.

54. Dong JF, Moake JL, Nolasco L et al. ADAMTS-13 rapidly cleaves newly secreted ultralarge von Willebrand factor multimers on the endothelial surface under flowing conditions. Blood 2002;100:4033-4039.

55. Ruggeri ZM. Mechanisms initiating platelet thrombus formation. Thromb.Haemost. 1997;78:611-616.

56. Ruggeri ZM, Ruggeri ZM. Platelet and von Willebrand factor interactions at the vessel wall. Hamostaseologie. 2004;24:1-11.

57. Galbusera M, Zoja C, Donadelli R et al. Fluid shear stress modulates von Willebrand factor release from human vascular endothelium. Blood 1997;90:1558-1564.

58. Banfi C, Brioschi M, Wait R et al. Proteome of endothelial cell-derived procoagulant microparticles. Proteomics. 2005;5:4443-4455.

59. Combes V, Simon AC, Grau GE et al. In vitro generation of endothelial microparticles and possible prothrombotic activity in patients with lupus anticoagulant. J.Clin.Invest 1999;104:93-102.

60. Kushak RI, Nestoridi E, Lambert J et al. Detached endothelial cells and microparticles as sources of tissue factor activity. Thromb.Res. 2005;116:409-419.

61. del C, I, Shrimpton CN, Thiagarajan P, Lopez JA. Tissue-factor-bearing microvesicles arise from lipid rafts and fuse with activated platelets to initiate coagulation. Blood 2005;106:1604-1611.

62. Dignat-George F, Boulanger CM. The many faces of endothelial microparticles. Arterioscler.Thromb.Vasc.Biol. 2011;31:27-33.

63. Sabatier F, Roux V, Anfosso F et al. Interaction of endothelial microparticles with monocytic cells in vitro induces tissue factor-dependent procoagulant activity. Blood 2002;99:3962-3970.

64. Chironi GN, Boulanger CM, Simon A et al. Endothelial microparticles in diseases. Cell Tissue Res. 2009;335:143-151.

65. Hunter MP, Ismail N, Zhang X et al. Detection of microRNA expression in human peripheral blood microvesicles. PLoS.One. 2008;3:e3694.

66. Yuan A, Farber EL, Rapoport AL et al. Transfer of microRNAs by embryonic stem cell microvesicles. PLoS.One. 2009;4:e4722.

67. Sapet C, Simoncini S, Loriod B et al. Thrombin-induced endothelial microparticle generation: identification of a novel pathway involving ROCK-II activation by caspase-2. Blood 2006;108:1868-1876.

68. Simoncini S, Njock MS, Robert S et al. TRAIL/Apo2L mediates the release of procoagulant endothelial microparticles induced by thrombin in vitro: a potential mechanism linking inflammation and coagulation. Circ.Res. 2009;104:943-951.

69. Curtis AM, Edelberg J, Jonas R et al. Endothelial microparticles: sophisticated vesicles modulating vascular function. Vasc.Med. 2013;18:204-214.

70. Vion AC, Ramkhelawon B, Loyer X et al. Shear stress regulates endothelial microparticle release. Circ.Res. 2013;112:1323-1333.

71. Boulanger CM, Amabile N, Guerin AP et al. In vivo shear stress determines circulating levels of endothelial microparticles in end-stage renal disease. Hypertension 2007;49:902-908.

72. Koga H, Sugiyama S, Kugiyama K et al. Elevated levels of VE-cadherin-positive endothelial microparticles in patients with type 2 diabetes mellitus and coronary artery disease. J.Am.Coll.Cardiol. 2005;45:1622-1630.

73. Mallat Z, Benamer H, Hugel B et al. Elevated levels of shed membrane microparticles with procoagulant potential in the peripheral circulating blood of patients with acute coronary syndromes. Circulation 2000;101:841-843.

74. Preston RA, Jy W, Jimenez JJ et al. Effects of severe hypertension on endothelial and platelet microparticles. Hypertension 2003;41:211-217.

75. Berk BC, Corson MA, Peterson TE, Tseng H. Protein kinases as mediators of fluid shear stress stimulated signal transduction in endothelial cells: a hypothesis for calcium-dependent and calcium-independent events activated by flow. J.Biomech. 1995;28:1439-1450.

76. Dimmeler S, Assmus B, Hermann C, Haendeler J, Zeiher AM. Fluid shear stress stimulates phosphorylation of Akt in human endothelial cells: involvement in suppression of apoptosis. Circ.Res. 1998;83:334-341.

77. Shepherd RD, Kos SM, Rinker KD. Long term shear stress leads to increased phosphorylation of multiple MAPK species in cultured human aortic endothelial cells. Biorheology 2009;46:529-538.

78. Kolch W. Meaningful relationships: the regulation of the Ras/Raf/MEK/ERK pathway by protein interactions. Biochem.J. 2000;351 Pt 2:289-305.

79. Cheng M, Wu J, Li Y, Nie Y, Chen H. Activation of MAPK participates in low shear stress-induced IL-8 gene expression in endothelial cells. Clin.Biomech.(Bristol., Avon.) 2008;23 Suppl 1:S96-S103.

80. Cuschieri J, Maier RV. Mitogen-activated protein kinase (MAPK). Crit Care Med. 2005;33:S417-S419.

81. Zhang H, Shi X, Hampong M, Blanis L, Pelech S. Stress-induced inhibition of ERK1 and ERK2 by direct interaction with p38 MAP kinase. J.Biol.Chem. 2001;276:6905-6908.

82. Paumelle R, Tulasne D, Leroy C et al. Sequential activation of ERK and repression of JNK by scatter factor/hepatocyte growth factor in madin-darby canine kidney epithelial cells. Mol.Biol.Cell 2000;11:3751-3763.

83. Vega-Ostertag M, Casper K, Swerlick R et al. Involvement of p38 MAPK in the up-regulation of tissue factor on endothelial cells by antiphospholipid antibodies. Arthritis Rheum. 2005;52:1545-1554.

84. Miho N, Ishida T, Kuwaba N et al. Role of the JNK pathway in thrombin-induced ICAM-1 expression in endothelial cells. Cardiovasc.Res. 2005;68:289-298.

85. Watanabe N, Shikata K, Shikata Y et al. Involvement of MAPKs in ICAM-1 expression in glomerular endothelial cells in diabetic nephropathy. Acta Med.Okayama 2011;65:247-257.

86. Tamura DY, Moore EE, Johnson JL et al. p38 mitogen-activated protein kinase inhibition attenuates intercellular adhesion molecule-1 up-regulation on human pulmonary microvascular endothelial cells. Surgery 1998;124:403-407.

87. Curtis AM, Wilkinson PF, Gui M et al. p38 mitogen-activated protein kinase targets the production of proinflammatory endothelial microparticles. J.Thromb.Haemost. 2009;7:701-709.

88. Grugel S, Finkenzeller G, Weindel K, Barleon B, Marme D. Both v-Ha-Ras and v-Raf stimulate expression of the vascular endothelial growth factor in NIH 3T3 cells. J.Biol.Chem. 1995;270:25915-25919.

89. Hayden MS, Ghosh S. Signaling to NF-kappaB. Genes Dev. 2004;18:2195-2224.

90. Li YS, Haga JH, Chien S. Molecular basis of the effects of shear stress on vascular endothelial cells. J.Biomech. 2005;38:1949-1971.

91. Schulze-Osthoff K, Ferrari D, Riehemann K, Wesselborg S. Regulation of NF-kappa B activation by MAP kinase cascades. Immunobiology 1997;198:35-49.

92. Yang M, Wu J, Martin CM, Kvietys PR, Rui T. Important role of p38 MAP kinase/NF-kappaB signaling pathway in the sepsis-induced conversion of cardiac myocytes to a proinflammatory phenotype. Am.J.Physiol Heart Circ.Physiol 2008;294:H994-1001.

93. Tuyt LM, Dokter WH, Birkenkamp K et al. Extracellular-regulated kinase 1/2, Jun N-terminal kinase, and c-Jun are involved in NF-kappa B-dependent IL-6 expression in human monocytes. J.Immunol. 1999;162:4893-4902.

94. Vanden Berghe W, Plaisance S, Boone E et al. p38 and extracellular signal-regulated kinase mitogen-activated protein kinase pathways are required for nuclear factor-kappaB p65 transactivation mediated by tumor necrosis factor. J.Biol.Chem. 1998;273:3285-3290.

95. Lan Q, Mercurius KO, Davies PF. Stimulation of transcription factors NF kappa B and AP1 in endothelial cells subjected to shear stress. Biochem.Biophys.Res.Commun. 1994;201:950-956.

96. Liang F, Huang N, Wang B, Chen H, Wu L. Shear stress induces interleukin-8 mRNA expression and transcriptional activation in human vascular endothelial cells. Chin Med.J.(Engl.) 2002;115:1838-1842.

97. Mohan S, Mohan N, Sprague EA. Differential activation of NF-kappa B in human aortic endothelial cells conditioned to specific flow environments. Am.J.Physiol 1997;273:C572-C578.

98. Read MA, Whitley MZ, Williams AJ, Collins T. NF-kappa B and I kappa B alpha: an inducible regulatory system in endothelial activation. J.Exp.Med. 1994;179:503-512.

99. Costanzo A, Moretti F, Burgio VL et al. Endothelial activation by angiotensin II through NFkappaB and p38 pathways: Involvement of NFkappaB-inducible kinase (NIK), free oxygen radicals, and selective inhibition by aspirin. J.Cell Physiol 2003;195:402-410.

100. Rahman A, Anwar KN, True AL, Malik AB. Thrombin-induced p65 homodimer binding to downstream NF-kappa B site of the promoter mediates endothelial ICAM-1 expression and neutrophil adhesion. J.Immunol. 1999;162:5466-5476.

101. Tak PP, Firestein GS. NF-kappaB: a key role in inflammatory diseases. J.Clin.Invest 2001;107:7-11.

102. Neeves KB, Onasoga AA, Hansen RR et al. Sources of variability in platelet accumulation on type 1 fibrillar collagen in microfluidic flow assays. PLoS.One. 2013;8:e54680.

103. White JG. Anatomy and structural organization of platelets. In: RW Colman JHVMES, ed. Hemostasis and Thrombosis: Basic principles and chemical practice. 1994:397-413.

104. Reed GL, Fitzgerald ML, Polgar J. Molecular mechanisms of platelet exocytosis: insights into the "secrete" life of thrombocytes. Blood 2000;96:3334-3342.

105. Yin W, Bond K, Rouf F, Rubenstein DA. Altered Flow Changes Thrombin Generation Rate of Circulating Platelets. Ann.Biomed.Eng 2015;43:2827-2837.

106. Kulkarni S, Dopheide SM, Yap CL et al. A revised model of platelet aggregation. J.Clin.Invest 2000;105:783-791.

107. Phillips DR, Charo IF, Parise LV, Fitzgerald LA. The platelet membrane glycoprotein IIb-IIIa complex. Blood 1988;71:831-843.

108. Jackson SP, Mistry N, Yuan Y. Platelets and the injured vessel wall-- "rolling into action": focus on glycoprotein Ib/V/IX and the platelet cytoskeleton. Trends Cardiovasc.Med. 2000;10:192-197.

109. Nomura S, Tandon NN, Nakamura T et al. High-shear-stress-induced activation of platelets and microparticles enhances expression of cell adhesion molecules in THP-1 and endothelial cells. Atherosclerosis 2001;158:277-287.

110. Brown CH, III, Leverett LB, Lewis CW, Alfrey CP, Jr., Hellums JD. Morphological, biochemical, and functional changes in human platelets subjected to shear stress. J.Lab Clin.Med. 1975;86:462-471.

111. Yin W, Rubenstein DA. Dose Effect of Shear Stress on Platelet Complement Activation in a Cone and Plate Shearing Device. Cellular and Molecular Bioengineering 2009;2:274-280.

112. Sheriff J, Bluestein D, Girdhar G, Jesty J. High-shear stress sensitizes platelets to subsequent low-shear conditions. Ann.Biomed.Eng 2010;38:1442-1450.

113. DeLisser HM, Newman PJ, Albelda SM. Molecular and functional aspects of PECAM-1/CD31. Immunol.Today 1994;15:490-495.

114. Newman PJ. The role of PECAM-1 in vascular cell biology. Ann.N.Y.Acad.Sci. 1994;714:165-174.

115. Metzelaar MJ, Korteweg J, Sixma JJ, Nieuwenhuis HK. Biochemical characterization of PECAM-1 (CD31 antigen) on human platelets. Thromb.Haemost. 1991;66:700-707.

116. Wu XW, Lian EC. Binding properties and inhibition of platelet aggregation by a monoclonal antibody to CD31 (PECAM-1). Arterioscler.Thromb.Vasc.Biol. 1997;17:3154-3158.

117. Cramer EM, Berger G, Berndt MC. Platelet alpha-granule and plasma membrane share two new components: CD9 and PECAM-1. Blood 1994;84:1722-1730.

118. Tzima E, Irani-Tehrani M, Kiosses WB et al. A mechanosensory complex that mediates the endothelial cell response to fluid shear stress. Nature 2005;437:426-431.

119. Jackson DE, Ward CM, Wang R, Newman PJ. The protein-tyrosine phosphatase SHP-2 binds platelet/endothelial cell adhesion molecule-1 (PECAM-1) and forms a distinct signaling complex during platelet aggregation. Evidence for a mechanistic link between PECAM-1- and integrin-mediated cellular signaling. J.Biol.Chem. 1997;272:6986-6993.

120. Osawa M, Masuda M, Harada N, Lopes RB, Fujiwara K. Tyrosine phosphorylation of platelet endothelial cell adhesion molecule-1 (PECAM-1, CD31) in mechanically stimulated vascular endothelial cells. Eur.J.Cell Biol. 1997;72:229-237.

121. Harry BL, Sanders JM, Feaver RE et al. Endothelial cell PECAM-1 promotes atherosclerotic lesions in areas of disturbed flow in ApoE-deficient mice. Arterioscler.Thromb.Vasc.Biol. 2008;28:2003-2008.

122. Stevens HY, Melchior B, Bell KS et al. PECAM-1 is a critical mediator of atherosclerosis. Dis.Model.Mech. 2008;1:175-181.

123. Gumina RJ, El SJ, Yao Z et al. Antibody to platelet/endothelial cell adhesion molecule-1 reduces myocardial infarct size in a rat model of ischemia-reperfusion injury. Circulation 1996;94:3327-3333.

124. Patil S, Newman DK, Newman PJ. Platelet endothelial cell adhesion molecule-1 serves as an inhibitory receptor that modulates platelet responses to collagen. Blood 2001;97:1727-1732.

125. Cicmil M, Thomas JM, Leduc M, Bon C, Gibbins JM. Platelet endothelial cell adhesion molecule-1 signaling inhibits the activation of human platelets. Blood 2002;99:137-144.

126. Falati S, Patil S, Gross PL et al. Platelet PECAM-1 inhibits thrombus formation in vivo. Blood 2006;107:535-541.

127. Rathore V, Stapleton MA, Hillery CA et al. PECAM-1 negatively regulates GPIb/V/IX signaling in murine platelets. Blood 2003;102:3658-3664.

128. Plow EF, D'Souza SE, Ginsberg MH. Ligand binding to GPIIb-IIIa: a status report. Semin.Thromb.Hemost. 1992;18:324-332.

129. Perutelli P, Marchese P, Mori PG. [The glycoprotein IIb/IIIa complex of the platelets. An activation-dependent integrin]. Recenti Prog.Med. 1992;83:100-104.

130. Gawaz M, Neumann FJ, Schomig A. Evaluation of platelet membrane glycoproteins in coronary artery disease : consequences for diagnosis and therapy. Circulation 1999;99:E1-E11.

131. Woods VL, Jr., Wolff LE, Keller DM. Resting platelets contain a substantial centrally located pool of glycoprotein IIb-IIIa complex which may be accessible to some but not other extracellular proteins. J.Biol.Chem. 1986;261:15242-15251.

132. Feng S, Lu X, Resendiz JC, Kroll MH. Pathological shear stress directly regulates platelet alphaIIbbeta3 signaling. Am.J.Physiol Cell Physiol 2006;291:C1346-C1354.

133. Ikeda Y, Handa M, Kawano K et al. The role of von Willebrand factor and fibrinogen in platelet aggregation under varying shear stress. J.Clin.Invest 1991;87:1234-1240.

134. Ikeda Y, Handa M, Kamata T et al. Transmembrane calcium influx associated with von Willebrand factor binding to GP Ib in the initiation of shear-induced platelet aggregation. Thromb.Haemost. 1993;69:496-502.

135. Chow TW, Hellums JD, Moake JL, Kroll MH. Shear stress-induced von Willebrand factor binding to platelet glycoprotein Ib initiates calcium influx associated with aggregation. Blood 1992;80:113-120.

136. Goto S, Ikeda Y, Saldivar E, Ruggeri ZM. Distinct mechanisms of platelet aggregation as a consequence of different shearing flow conditions. J.Clin.Invest 1998;101:479-486.

137. Ferguson JJ, Vaisman D. Therapeutic potential of GP IIb/IIIa receptor antagonists in acute myocardial infarction. Expert.Opin.Investig.Drugs 2001;10:1965-1976.

138. Labinaz M, Ho C, Banerjee S et al. Meta-analysis of clinical efficacy and bleeding risk with intravenous glycoprotein IIb/IIIa antagonists for percutaneous coronary intervention. Can.J.Cardiol. 2007;23:963-970.

139. Holme PA, Brosstad F, Solum NO. The difference between platelet and plasma FXIII used to study the mechanism of platelet microvesicle formation. Thromb.Haemost. 1993;70:681-686.

140. Wolf P. The nature and significance of platelet products in human plasma. Br.J.Haematol. 1967;13:269-288.

141. George JN, Pickett EB, Saucerman S et al. Platelet surface glycoproteins. Studies on resting and activated platelets and platelet membrane microparticles in normal subjects, and observations in patients during adult respiratory distress syndrome and cardiac surgery. J.Clin.Invest 1986;78:340-348.

142. Sinauridze EI, Kireev DA, Popenko NY et al. Platelet microparticle membranes have 50- to 100-fold higher specific procoagulant activity than activated platelets. Thromb.Haemost. 2007;97:425-434.

143. Merten M, Pakala R, Thiagarajan P, Benedict CR. Platelet microparticles promote platelet interaction with subendothelial matrix in a glycoprotein IIb/IIIa-dependent mechanism. Circulation 1999;99:2577-2582.

144. Owens MR, Holme S, Cardinali S. Platelet microvesicles adhere to subendothelium and promote adhesion of platelets. Thromb.Res. 1992;66:247-258.

145. Yano Y, Kambayashi J, Shiba E et al. The role of protein phosphorylation and cytoskeletal reorganization in microparticle formation from the platelet plasma membrane. Biochem.J. 1994;299 (Pt 1):303-308.

146. Nomura S, Komiyama Y. [Shear stress and platelet-derived microparticles]. Rinsho Byori 1997;45:927-933.

147. Miyoshi H, Umeshita K, Sakon M et al. Calpain activation in plasma membrane bleb formation during tert-butyl hydroperoxide-induced rat hepatocyte injury. Gastroenterology 1996;110:1897-1904.

148. Wiedmer T, Sims PJ. Participation of protein kinases in complement C5b-9-induced shedding of platelet plasma membrane vesicles. Blood 1991;78:2880-2886.

149. Rouf, F. The effects of physiologically relevant shear stress and platelet-endothelial cell interaction on platelet activation and platelet microparticle generation. 7-7-2011. Oklahoma State University.

Ref Type: Thesis/Dissertation

150. Holme PA, Orvim U, Hamers MJ et al. Shear-induced platelet activation and platelet microparticle formation at blood flow conditions as in arteries with a severe stenosis. Arterioscler.Thromb.Vasc.Biol. 1997;17:646-653.

151. Gawaz M, Neumann FJ, Ott I, Schiessler A, Schomig A. Platelet function in acute myocardial infarction treated with direct angioplasty. Circulation 1996;93:229-237.

152. Lee YJ, Jy W, Horstman LL et al. Elevated platelet microparticles in transient ischemic attacks, lacunar infarcts, and multiinfarct dementias. Thromb.Res. 1993;72:295-304.

153. Yin W, Rouf F, Rubenstein DA. Activated endothelial cells enhance platelet responses to dynamic shear stress conditions [abstract]. The FASEB Journal 2011;637.7:

154. Siegel-Axel DI, Gawaz M. Platelets and endothelial cells. Semin.Thromb.Hemost. 2007;33:128-135.

155. da Costa MP, Garcia-Vallejo JJ, van Thienen JV et al. P-selectin glycoprotein ligand-1 is expressed on endothelial cells and mediates monocyte adhesion to activated endothelium. Arterioscler.Thromb.Vasc.Biol. 2007;27:1023-1029.

156. Senden NH, Jeunhomme TM, Heemskerk JW et al. Factor Xa induces cytokine production and expression of adhesion molecules by human umbilical vein endothelial cells. J.Immunol. 1998;161:4318-4324.

157. Chen CH, Walterscheid JP. Plaque angiogenesis versus compensatory arteriogenesis in atherosclerosis. Circ.Res. 2006;99:787-789.

158. Mack PJ, Zhang Y, Chung S et al. Biomechanical Regulation of Endothelium-dependent Events Critical for Adaptive Remodeling. J.Biol.Chem. 2009;284:8412-8420.

159. Wahlberg E. Angiogenesis and arteriogenesis in limb ischemia. J.Vasc.Surg. 2003;38:198-203.

160. Wang B, Han YL, Li Y et al. Coronary collateral circulation: Effects on outcomes of acute anterior myocardial infarction after primary percutaneous coronary intervention. J.Geriatr.Cardiol. 2011;8:93-98.

161. Center for Disease Control and Prevention. 2014 National Diabetes Statistics Report. 5-15-2015. Ref Type: Report

162. Dall TM, Yang W, Halder P et al. The economic burden of elevated blood glucose levels in 2012: diagnosed and undiagnosed diabetes, gestational diabetes mellitus, and prediabetes. Diabetes Care 2014;37:3172-3179.

163. Yamagishi S, Nakamura K, Imaizumi T. Advanced glycation end products (AGEs) and diabetic vascular complications. Curr.Diabetes Rev. 2005;1:93-106.

164. Uribarri J, Woodruff S, Goodman S et al. Advanced glycation end products in foods and a practical guide to their reduction in the diet. J.Am.Diet.Assoc. 2010;110:911-916.

165. Vlassara H, Palace MR. Diabetes and advanced glycation endproducts. J.Intern.Med. 2002;251:87-101.

166. Neumann A, Schinzel R, Palm D, Riederer P, Munch G. High molecular weight hyaluronic acid inhibits advanced glycation endproduct-induced NF-kappaB activation and cytokine expression. FEBS Lett. 1999;453:283-287.

167. Yan SD, Schmidt AM, Anderson GM et al. Enhanced cellular oxidant stress by the interaction of advanced glycation end products with their receptors/binding proteins. J.Biol.Chem. 1994;269:9889-9897.

168. Goldin A, Beckman JA, Schmidt AM, Creager MA. Advanced glycation end products: sparking the development of diabetic vascular injury. Circulation 2006;114:597-605.

169. Ahmed N. Advanced glycation endproducts--role in pathology of diabetic complications. Diabetes Res.Clin.Pract. 2005;67:3-21.

170. Stern DM, Yan SD, Yan SF, Schmidt AM. Receptor for advanced glycation endproducts (RAGE) and the complications of diabetes. Ageing Res.Rev. 2002;1:1-15.

171. Afanas'ev I. Signaling of reactive oxygen and nitrogen species in Diabetes mellitus. Oxid.Med.Cell Longev. 2010;3:361-373.

172. Shi L, Yu X, Yang H, Wu X. Advanced glycation end products induce human corneal epithelial cells apoptosis through generation of reactive oxygen species and activation of JNK and p38 MAPK pathways. PLoS.One. 2013;8:e66781.

173. Abo A, Pick E, Hall A et al. Activation of the NADPH oxidase involves the small GTP-binding protein p21rac1. Nature 1991;353:668-670.

174. Bedard K, Krause KH. The NOX family of ROS-generating NADPH oxidases: physiology and pathophysiology. Physiol Rev. 2007;87:245-313.

175. Vieceli Dalla SF, Zambonin L, Fiorentini D et al. Specific aquaporins facilitate Nox-produced hydrogen peroxide transport through plasma membrane in leukaemia cells. Biochim.Biophys.Acta 2014;1843:806-814.

176. Thomas SR, Chen K, Keaney JF, Jr. Hydrogen peroxide activates endothelial nitric-oxide synthase through coordinated phosphorylation and dephosphorylation via a phosphoinositide 3-kinase-dependent signaling pathway. J.Biol.Chem. 2002;277:6017-6024.

177. Nowotny K, Jung T, Hohn A, Weber D, Grune T. Advanced glycation end products and oxidative stress in type 2 diabetes mellitus. Biomolecules. 2015;5:194-222.

178. Deshmane SL, Kremlev S, Amini S, Sawaya BE. Monocyte chemoattractant protein-1 (MCP-1): an overview. J.Interferon Cytokine Res. 2009;29:313-326.

179. Kuhad A, Chopra K. Attenuation of diabetic nephropathy by tocotrienol: involvement of NFkB signaling pathway. Life Sci. 2009;84:296-301.

180. Yoshida LS, Tsunawaki S. Expression of NADPH oxidases and enhanced H(2)O(2)-generating activity in human coronary artery endothelial cells upon induction with tumor necrosis factor-alpha. Int.Immunopharmacol. 2008;8:1377-1385.

181. Osterud B, Bjorklid E. Role of monocytes in atherogenesis. Physiol Rev. 2003;83:1069-1112.

182. Fuhrman B, Partoush A, Volkova N, Aviram M. Ox-LDL induces monocyte-to-macrophage differentiation in vivo: Possible role for the macrophage colony stimulating factor receptor (M-CSF-R). Atherosclerosis 2008;196:598-607.

183. Abaci A, Oguzhan A, Kahraman S et al. Effect of diabetes mellitus on formation of coronary collateral vessels. Circulation 1999;99:2239-2242.

184. Yan J, Tie G, Park B et al. Recovery from hind limb ischemia is less effective in type 2 than in type 1 diabetic mice: roles of endothelial nitric oxide synthase and endothelial progenitor cells. J.Vasc.Surg. 2009;50:1412-1422.

185. Pung YF, Chilian WM. Corruption of coronary collateral growth in metabolic syndrome: Role of oxidative stress. World J.Cardiol. 2010;2:421-427.

186. Ruiter MS, van Golde JM, Schaper NC, Stehouwer CD, Huijberts MS. Diabetes impairs arteriogenesis in the peripheral circulation: review of molecular mechanisms. Clin.Sci.(Lond) 2010;119:225-238.

187. Sena CM, Pereira AM, Seica R. Endothelial dysfunction - a major mediator of diabetic vascular disease. Biochim.Biophys.Acta 2013;1832:2216-2231.

188. van Golde JM, Ruiter MS, Schaper NC et al. Impaired collateral recruitment and outward remodeling in experimental diabetes. Diabetes 2008;57:2818-2823.

189. Waltenberger J, Lange J, Kranz A. Vascular endothelial growth factor-A-induced chemotaxis of monocytes is attenuated in patients with diabetes mellitus: A potential predictor for the individual capacity to develop collaterals. Circulation 2000;102:185-190.

190. Heil M, Schaper W. Influence of mechanical, cellular, and molecular factors on collateral artery growth (arteriogenesis). Circ.Res. 2004;95:449-458.

191. Heil M, Eitenmuller I, Schmitz-Rixen T, Schaper W. Arteriogenesis versus angiogenesis: similarities and differences. J.Cell Mol.Med. 2006;10:45-55.

192. dela Paz NG, Walshe TE, Leach LL, Saint-Geniez M, D'Amore PA. Role of shear-stress-induced VEGF expression in endothelial cell survival. J.Cell Sci. 2012;125:831-843.

193. Abumiya T, Sasaguri T, Taba Y, Miwa Y, Miyagi M. Shear stress induces expression of vascular endothelial growth factor receptor Flk-1/KDR through the CT-rich Sp1 binding site. Arterioscler.Thromb.Vasc.Biol. 2002;22:907-913.

194. De FS. The discovery of placenta growth factor and its biological activity. Exp.Mol.Med. 2012;44:1-9.

195. Autiero M, Luttun A, Tjwa M, Carmeliet P. Placental growth factor and its receptor, vascular endothelial growth factor receptor-1: novel targets for stimulation of ischemic tissue revascularization and inhibition of angiogenic and inflammatory disorders. J.Thromb.Haemost. 2003;1:1356-1370.

196. Xiang L, Varshney R, Rashdan NA, Shaw JH, Lloyd PG. Placenta growth factor and vascular endothelial growth factor a have differential, cell-type specific patterns of expression in vascular cells. Microcirculation. 2014;21:368-379.

197. Park JE, Chen HH, Winer J, Houck KA, Ferrara N. Placenta growth factor. Potentiation of vascular endothelial growth factor bioactivity, in vitro and in vivo, and high affinity binding to Flt-1 but not to Flk-1/KDR. J.Biol.Chem. 1994;269:25646-25654.

198. Carmeliet P, Moons L, Luttun A et al. Synergism between vascular endothelial growth factor and placental growth factor contributes to angiogenesis and plasma extravasation in pathological conditions. Nat.Med. 2001;7:575-583.

199. Luttun A, Tjwa M, Moons L et al. Revascularization of ischemic tissues by PlGF treatment, and inhibition of tumor angiogenesis, arthritis and atherosclerosis by anti-Flt1. Nat.Med. 2002;8:831-840.

200. Carmeliet P, Conway EM. Growing better blood vessels. Nat.Biotechnol. 2001;19:1019-1020.

201. Bottomley MJ, Webb NJ, Watson CJ et al. Placenta growth factor (PlGF) induces vascular endothelial growth factor (VEGF) secretion from mononuclear cells and is co-expressed with VEGF in synovial fluid. Clin.Exp.Immunol. 2000;119:182-188.

202. Mac GF, Popel AS. Systems biology of vascular endothelial growth factors. Microcirculation. 2008;15:715-738.

203. Tammela T, Enholm B, Alitalo K, Paavonen K. The biology of vascular endothelial growth factors. Cardiovasc.Res. 2005;65:550-563.

204. Li W, Shen W, Gill R et al. High-resolution quantitative computed tomography demonstrating selective enhancement of medium-size collaterals by placental growth factor-1 in the mouse ischemic hindlimb. Circulation 2006;113:2445-2453.

205. Takeda Y, Uemura S, Iwama H et al. Treatment with recombinant placental growth factor (PlGF) enhances both angiogenesis and arteriogenesis and improves survival after myocardial infarction. Circ.J. 2009;73:1674-1682.

206. Scholz D, Elsaesser H, Sauer A et al. Bone marrow transplantation abolishes inhibition of arteriogenesis in placenta growth factor (PlGF) -/- mice. J.Mol.Cell Cardiol. 2003;35:177-184.

207. Gerber HP, McMurtrey A, Kowalski J et al. Vascular endothelial growth factor regulates endothelial cell survival through the phosphatidylinositol 3'-kinase/Akt signal transduction pathway. Requirement for Flk-1/KDR activation. J.Biol.Chem. 1998;273:30336-30343.

208. Kroll J, Waltenberger J. The vascular endothelial growth factor receptor KDR activates multiple signal transduction pathways in porcine aortic endothelial cells. J.Biol.Chem. 1997;272:32521-32527.

209. Ferrara N. Role of vascular endothelial growth factor in regulation of physiological angiogenesis. Am.J.Physiol Cell Physiol 2001;280:C1358-C1366.

210. Kroll J, Waltenberger J. VEGF-A induces expression of eNOS and iNOS in endothelial cells via VEGF receptor-2 (KDR). Biochem.Biophys.Res.Commun. 1998;252:743-746.

211. Wheeler-Jones C, Abu-Ghazaleh R, Cospedal R et al. Vascular endothelial growth factor stimulates prostacyclin production and activation of cytosolic phospholipase A2 in

endothelial cells via p42/p44 mitogen-activated protein kinase. FEBS Lett. 1997;420:28-32.

212. Olsson AK, Dimberg A, Kreuger J, Claesson-Welsh L. VEGF receptor signalling - in control of vascular function. Nat.Rev.Mol.Cell Biol. 2006;7:359-371.

213. Roeckl W, Hecht D, Sztajer H et al. Differential binding characteristics and cellular inhibition by soluble VEGF receptors 1 and 2. Exp.Cell Res. 1998;241:161-170.

214. Barleon B, Sozzani S, Zhou D et al. Migration of human monocytes in response to vascular endothelial growth factor (VEGF) is mediated via the VEGF receptor flt-1. Blood 1996;87:3336-3343.

215. Translational Stroke Research: From Target Selection to Clinical Trials.; 2012.

216. Urbich C, Stein M, Reisinger K et al. Fluid shear stress-induced transcriptional activation of the vascular endothelial growth factor receptor-2 gene requires Sp1-dependent DNA binding. FEBS Lett. 2003;535:87-93.

217. Kavey RE, Daniels SR, Lauer RM et al. American Heart Association guidelines for primary prevention of atherosclerotic cardiovascular disease beginning in childhood. Circulation 2003;107:1562-1566.

218. Saydah SH, Miret M, Sung J et al. Postchallenge hyperglycemia and mortality in a national sample of U.S. adults. Diabetes Care 2001;24:1397-1402.

219. Blackman BR, Barbee KA, Thibault LE. In vitro cell shearing device to investigate the dynamic response of cells in a controlled hydrodynamic environment. Ann.Biomed.Eng 2000;28:363-372.

220. Shanmugavelayudam SK, Rubenstein DA, Yin W. Effect of geometrical assumptions on numerical modeling of coronary blood flow under normal and disease conditions. J.Biomech.Eng 2010;132:061004.

221. Shanmugavelayudam, S. K. Effects of dynamic shear stress on endothelial cells, platelets, and their interactions. 5-13-0013.

Ref Type: Thesis/Dissertation

222. Fleming I, Fisslthaler B, Dixit M, Busse R. Role of PECAM-1 in the shear-stress-induced activation of Akt and the endothelial nitric oxide synthase (eNOS) in endothelial cells. J.Cell Sci. 2005;118:4103-4111.

223. Jones CI, Garner SF, Moraes LA et al. PECAM-1 expression and activity negatively regulate multiple platelet signaling pathways. FEBS Lett. 2009;583:3618-3624.

224. Iijima K, Murata M, Nakamura K et al. High shear stress attenuates agonist-induced, glycoprotein IIb/IIIa-mediated platelet aggregation when von Willebrand factor binding to glycoprotein Ib/IX is blocked. Biochem.Biophys.Res.Commun. 1997;233:796-800.

225. Cheng H, Yan R, Li S et al. Shear-induced interaction of platelets with von Willebrand factor results in glycoprotein Ibalpha shedding. Am.J.Physiol Heart Circ.Physiol 2009;297:H2128-H2135.

226. Leytin V, Allen DJ, Mykhaylov S et al. Pathologic high shear stress induces apoptosis events in human platelets. Biochem.Biophys.Res.Commun. 2004;320:303-310.

227. Goto S, Tamura N, Li M et al. Different effects of various anti-GPIIb-IIIa agents on shear-induced platelet activation and expression of procoagulant activity. J.Thromb.Haemost. 2003;1:2022-2030.

228. Oda A, Yokoyama K, Murata M et al. Protein tyrosine phosphorylation in human platelets during shear stress-induced platelet aggregation (SIPA) is regulated by glycoprotein (GP) Ib/IX as well as GP IIb/IIIa and requires intact cytoskeleton and endogenous ADP. Thromb.Haemost. 1995;74:736-742.

229. Goncalves I, Nesbitt WS, Yuan Y, Jackson SP. Importance of temporal flow gradients and integrin alphaIIbbeta3 mechanotransduction for shear activation of platelets. J.Biol.Chem. 2005;280:15430-15437.

230. Rubenstein DA, Yin W. Quantifying the effects of shear stress and shear exposure duration regulation on flow induced platelet activation and aggregation. J.Thromb.Thrombolysis. 2010;30:36-45.

231. Mirikova N, Casciari J, Hunninghake R, Riordan N. Increased level of circulating endothelial microparticles and cardiovascular risk factors. Clinical and experimental cardiology 2011;2:1-6.

232. Miyazaki Y, Nomura S, Miyake T et al. High shear stress can initiate both platelet aggregation and shedding of procoagulant containing microparticles. Blood 1996;88:3456-3464.

233. Amabile N, Heiss C, Real WM et al. Circulating endothelial microparticle levels predict hemodynamic severity of pulmonary hypertension. Am.J.Respir.Crit Care Med. 2008;177:1268-1275.

234. Butenas S, Brummel KE, Branda RF, Paradis SG, Mann KG. Mechanism of factor VIIa-dependent coagulation in hemophilia blood. Blood 2002;99:923-930.

235. Michelson AD. Thrombin-induced down-regulation of the platelet membrane glycoprotein Ib-IX complex. Semin.Thromb.Hemost. 1992;18:18-27.

236. Grabowski EF, Reininger AJ, Petteruti PG, Tsukurov O, Orkin RW. Shear stress decreases endothelial cell tissue factor activity by augmenting secretion of tissue factor pathway inhibitor. Arterioscler.Thromb.Vasc.Biol. 2001;21:157-162.

237. Yin W, Rouf F, Shanmugavelayudam SK, Rubenstein DA. Endothelial cells modulate platelet response to dynamic shear stress. Cardiovascular Engineering and Technology 2014

238. Senis YA, Richardson M, Tinlin S, Maurice DH, Giles AR. Changes in the pattern of distribution of von Willebrand factor in rat aortic endothelial cells following thrombin generation in vivo. Br.J.Haematol. 1996;93:195-203.

239. Walpola PL, Gotlieb AI, Cybulsky MI, Langille BL. Expression of ICAM-1 and VCAM-1 and monocyte adherence in arteries exposed to altered shear stress. Arterioscler.Thromb.Vasc.Biol. 1995;15:2-10.

240. Brox JH, Osterud B, Bjorklid E, Fenton JW. Production and availability of thromboplastin in endothelial cells: the effects of thrombin, endotoxin and platelets. Br.J.Haematol. 1984;57:239-246.

241. Drake TA, Morrissey JH, Edgington TS. Selective cellular expression of tissue factor in human tissues. Implications for disorders of hemostasis and thrombosis. Am.J.Pathol. 1989;134:1087-1097.

242. Jo H, Sipos K, Go YM et al. Differential effect of shear stress on extracellular signal-regulated kinase and N-terminal Jun kinase in endothelial cells. Gi2- and Gbeta/gamma-dependent signaling pathways. J.Biol.Chem. 1997;272:1395-1401.

243. Surapisitchat J, Hoefen RJ, Pi X et al. Fluid shear stress inhibits TNF-alpha activation of JNK but not ERK1/2 or p38 in human umbilical vein endothelial cells: Inhibitory crosstalk among MAPK family members. Proc.Natl.Acad.Sci.U.S.A 2001;98:6476-6481.

244. Yang M, Wu J, Martin CM, Kvietys PR, Rui T. Important role of p38 MAP kinase/NF-kappaB signaling pathway in the sepsis-induced conversion of cardiac myocytes to a proinflammatory phenotype. Am.J.Physiol Heart Circ.Physiol 2008;294:H994-1001.

245. Schulze-Osthoff K, Ferrari D, Riehemann K, Wesselborg S. Regulation of NF-kappa B activation by MAP kinase cascades. Immunobiology 1997;198:35-49.

246. Maharaj AS, Saint-Geniez M, Maldonado AE, D'Amore PA. Vascular endothelial growth factor localization in the adult. Am.J.Pathol. 2006;168:639-648.

247. Battinelli EM, Markens BA, Italiano JE, Jr. Release of angiogenesis regulatory proteins from platelet alpha granules: modulation of physiologic and pathologic angiogenesis. Blood 2011;118:1359-1369.

248. Klement GL, Yip TT, Cassiola F et al. Platelets actively sequester angiogenesis regulators. Blood 2009;113:2835-2842.

249. Wartiovaara U, Salven P, Mikkola H et al. Peripheral blood platelets express VEGF-C and VEGF which are released during platelet activation. Thromb.Haemost. 1998;80:171-175.

250. Melian EB, Goa KL. Beraprost: a review of its pharmacology and therapeutic efficacy in the treatment of peripheral arterial disease and pulmonary arterial hypertension. Drugs 2002;62:107-133.

251. Nony P, Ffrench P, Girard P et al. Platelet-aggregation inhibition and hemodynamic effects of beraprost sodium, a new oral prostacyclin derivative: a study in healthy male subjects. Can.J.Physiol Pharmacol. 1996;74:887-893.

252. Rocic P. Why is coronary collateral growth impaired in type II diabetes and the metabolic syndrome? Vascul.Pharmacol. 2012;57:179-186.

253. Yngen M, Ostenson CG, Li N, Hjemdahl P, Wallen NH. Acute hyperglycemia increases soluble P-selectin in male patients with mild diabetes mellitus. Blood Coagul.Fibrinolysis 2001;12:109-116.

254. Yngen M, Norhammar A, Hjemdahl P, Wallen NH. Effects of improved metabolic control on platelet reactivity in patients with type 2 diabetes mellitus following coronary angioplasty. Diab.Vasc.Dis.Res. 2006;3:52-56.

255. Calkin AC, Drew BG, Ono A et al. Reconstituted high-density lipoprotein attenuates platelet function in individuals with type 2 diabetes mellitus by promoting cholesterol efflux. Circulation 2009;120:2095-2104.

256. Hwang DL, Yen CF, Nadler JL. Insulin increases intracellular magnesium transport in human platelets. J.Clin.Endocrinol.Metab 1993;76:549-553.

257. Schar MO, Diaz-Romero J, Kohl S, Zumstein MA, Nesic D. Platelet-rich concentrates differentially release growth factors and induce cell migration in vitro. Clin.Orthop.Relat Res. 2015;473:1635-1643.

258. Ansley DM, Wang B. Oxidative stress and myocardial injury in the diabetic heart. J.Pathol. 2013;229:232-241.

259. Kitahara Y, Takeuchi M, Miura K et al. Glyceraldehyde-derived advanced glycation end products (AGEs). A novel biomarker of postprandial hyperglycaemia in diabetic rats. Clin.Exp.Med. 2008;8:175-177.

260. Kanazawa H, Yoshikawa J. Elevated oxidative stress and reciprocal reduction of vascular endothelial growth factor levels with severity of COPD. Chest 2005;128:3191-3197.

261. Goova MT, Li J, Kislinger T et al. Blockade of receptor for advanced glycation end-products restores effective wound healing in diabetic mice. Am.J.Pathol. 2001;159:513-525.

262. Teixeira AS, Andrade SP. Glucose-induced inhibition of angiogenesis in the rat sponge granuloma is prevented by aminoguanidine. Life Sci. 1999;64:655-662.

263. Tamarat R, Silvestre JS, Huijberts M et al. Blockade of advanced glycation end-product formation restores ischemia-induced angiogenesis in diabetic mice. Proc.Natl.Acad.Sci.U.S.A 2003;100:8555-8560.

264. Schaper W, Scholz D. Factors regulating arteriogenesis. Arterioscler.Thromb.Vasc.Biol. 2003;23:1143-1151.

265. van RN, Piek JJ, Buschmann I et al. Stimulation of arteriogenesis; a new concept for the treatment of arterial occlusive disease. Cardiovasc.Res. 2001;49:543-553.

266. Chiu JJ, Chen LJ, Lee PL et al. Shear stress inhibits adhesion molecule expression in vascular endothelial cells induced by coculture with smooth muscle cells. Blood 2003;101:2667-2674.

267. Fillinger MF, Sampson LN, Cronenwett JL, Powell RJ, Wagner RJ. Coculture of endothelial cells and smooth muscle cells in bilayer and conditioned media models. J.Surg.Res. 1997;67:169-178.

268. Gloe T, Sohn HY, Meininger GA, Pohl U. Shear stress-induced release of basic fibroblast growth factor from endothelial cells is mediated by matrix interaction via integrin alpha(v)beta3. J.Biol.Chem. 2002;277:23453-23458.

269. De VS, Palmer-Kazen U, Kalin B, Wahlberg E. Risk factors for poor collateral development in claudication. Vasc.Endovascular.Surg. 2005;39:519-524.

270. Chavakis T, Bierhaus A, Nawroth PP. RAGE (receptor for advanced glycation end products): a central player in the inflammatory response. Microbes.Infect. 2004;6:1219-1225.

271. Basta G, Lazzerini G, Del TS et al. At least 2 distinct pathways generating reactive oxygen species mediate vascular cell adhesion molecule-1 induction by advanced glycation end products. Arterioscler.Thromb.Vasc.Biol. 2005;25:1401-1407.

272. Rodino-Janeiro BK, Gonzalez-Peteiro M, Ucieda-Somoza R, Gonzalez-Juanatey JR, Alvarez E. Glycated albumin, a precursor of advanced glycation end-products, up-regulates NADPH oxidase and enhances oxidative stress in human endothelial cells: molecular correlate of diabetic vasculopathy. Diabetes Metab Res.Rev. 2010;26:550-558.

273. Zhang M, Kho AL, Anilkumar N et al. Glycated proteins stimulate reactive oxygen species production in cardiac myocytes: involvement of Nox2 (gp91phox)-containing NADPH oxidase. Circulation 2006;113:1235-1243.

274. Guzik TJ, Mussa S, Gastaldi D et al. Mechanisms of increased vascular superoxide production in human diabetes mellitus: role of NAD(P)H oxidase and endothelial nitric oxide synthase. Circulation 2002;105:1656-1662.

275. Guzik TJ, Sadowski J, Guzik B et al. Coronary artery superoxide production and nox isoform expression in human coronary artery disease. Arterioscler.Thromb.Vasc.Biol. 2006;26:333-339.

276. Nisimoto Y, Diebold BA, Cosentino-Gomes D, Lambeth JD. Nox4: a hydrogen peroxide-generating oxygen sensor. Biochemistry 2014;53:5111-5120.

277. Cai H. NAD(P)H oxidase-dependent self-propagation of hydrogen peroxide and vascular disease. Circ.Res. 2005;96:818-822.

278. Valen G, Erl W, Eriksson P et al. Hydrogen peroxide induces mRNA for tumour necrosis factor alpha in human endothelial cells. Free Radic.Res. 1999;31:503-512.

279. Makino N, Maeda T, Sugano M et al. High serum TNF-alpha level in Type 2 diabetic patients with microangiopathy is associated with eNOS down-regulation and apoptosis in endothelial cells. J.Diabetes Complications 2005;19:347-355.

280. Chen XL, Zhang Q, Zhao R, Medford RM. Superoxide, H2O2, and iron are required for TNF-alpha-induced MCP-1 gene expression in endothelial cells: role of Rac1 and NADPH oxidase. Am.J.Physiol Heart Circ.Physiol 2004;286:H1001-H1007.

281. Panee J. Monocyte Chemoattractant Protein 1 (MCP-1) in obesity and diabetes. Cytokine 2012;60:1-12.

282. Varney ML, Olsen KJ, Mosley RL, Singh RK. Paracrine regulation of vascular endothelial growth factor--a expression during macrophage-melanoma cell interaction: role of monocyte chemotactic protein-1 and macrophage colony-stimulating factor. J.Interferon Cytokine Res. 2005;25:674-683.

283. Huber WJ, III, Marohnic CC, Peters M et al. Measurement of membrane-bound human heme oxygenase-1 activity using a chemically defined assay system. Drug Metab Dispos. 2009;37:857-864.

284. van Buul JD, Fernandez-Borja M, Anthony EC, Hordijk PL. Expression and localization of NOX2 and NOX4 in primary human endothelial cells. Antioxid.Redox.Signal. 2005;7:308-317.

285. Winzell MS, Ahren B. The high-fat diet-fed mouse: a model for studying mechanisms and treatment of impaired glucose tolerance and type 2 diabetes. Diabetes 2004;53 Suppl 3:S215-S219.

286. Henson GD, Walker AE, Reihl KD, Donato AJ, Lesniewski LA. Dichotomous mechanisms of aortic stiffening in high-fat diet fed young and old B6D2F1 mice. Physiol Rep. 2014;2:e00268.

287. Mastrocola R, Collino M, Nigro D et al. Accumulation of advanced glycation end-products and activation of the SCAP/SREBP Lipogenetic pathway occur in diet-induced obese mouse skeletal muscle. PLoS.One. 2015;10:e0119587.

288. Mamputu JC, Renier G. Advanced glycation end products increase, through a protein kinase C-dependent pathway, vascular endothelial growth factor expression in retinal endothelial cells. Inhibitory effect of gliclazide. J.Diabetes Complications 2002;16:284-293.

289. Yamada Y, Ishibashi K, Ishibashi K et al. The expression of advanced glycation endproduct receptors in rpe cells associated with basal deposits in human maculas. Exp.Eye Res. 2006;82:840-848.

290. Rasheed Z, Akhtar N, Haqqi TM. Advanced glycation end products induce the expression of interleukin-6 and interleukin-8 by receptor for advanced glycation end product-mediated activation of mitogen-activated protein kinases and nuclear factor-kappaB in human osteoarthritis chondrocytes. Rheumatology.(Oxford) 2011;50:838-851.

291. Yang K, Wang XQ, He YS et al. Advanced glycation end products induce chemokine/cytokine production via activation of p38 pathway and inhibit proliferation and migration of bone marrow mesenchymal stem cells. Cardiovasc.Diabetol. 2010;9:66.

292. Huang SP, Wu MS, Shun CT et al. Interleukin-6 increases vascular endothelial growth factor and angiogenesis in gastric carcinoma. J.Biomed.Sci. 2004;11:517-527.

293. Yoshiji H, Kuriyama S, Yoshii J et al. Vascular endothelial growth factor and receptor interaction is a prerequisite for murine hepatic fibrogenesis. Gut 2003;52:1347-1354.

294. Datla SR, Dusting GJ, Mori TA et al. Induction of heme oxygenase-1 in vivo suppresses NADPH oxidase derived oxidative stress. Hypertension 2007;50:636-642.

295. Taille C, El-Benna J, Lanone S et al. Induction of heme oxygenase-1 inhibits NAD(P)H oxidase activity by down-regulating cytochrome b558 expression via the reduction of heme availability. J.Biol.Chem. 2004;279:28681-28688.

296. Watanabe SM, Blanco PJ, Feijoo RA et al. Mathematical Model of Blood Flow in an Anatomically Detailed Arterial Network of the Arm. EDP Sciences. 2013; 47: 961-985.

297. Kakizawa H, Itoh M, Itoh Y et al. The relationship between glycemic control and plasma vascular endothelial growth factor and endothelin-1 concentration in diabetic patients. Metabolism 2004;53:550-555.

298. Hornig C, Barleon B, Ahmad S et al. Release and complex formation of soluble VEGFR-1 from endothelial cells and biological fluids. Lab Invest 2000;80:443-454.

APPENDICES

Platelet adhesion to EC

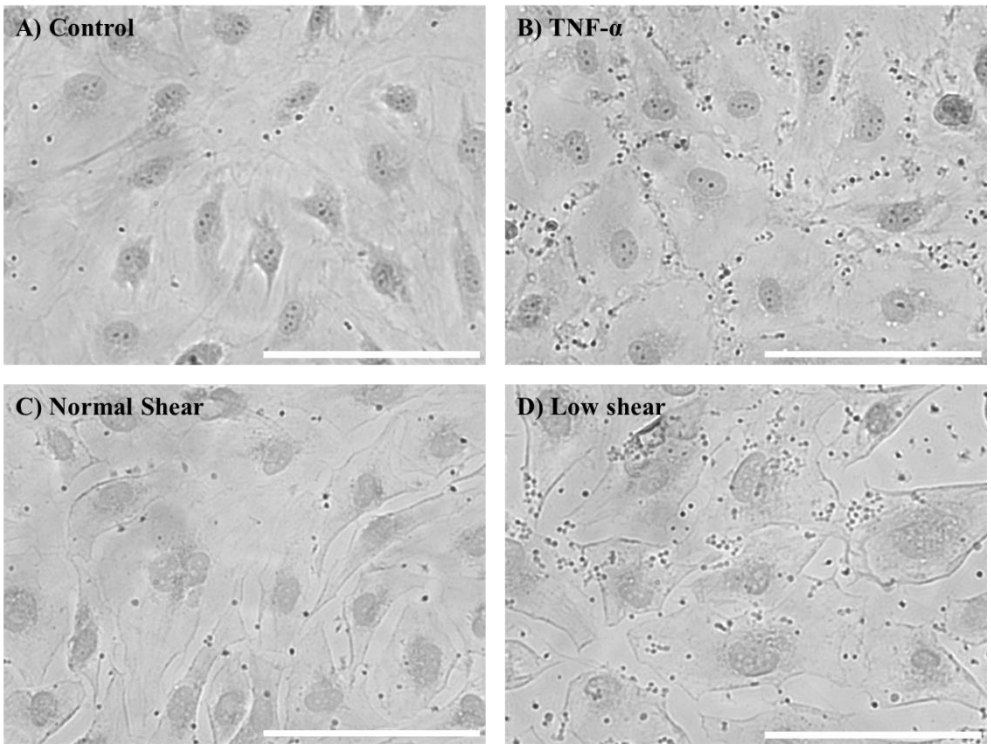

Figure: White light images of platelets adhering to EC. Platelets and EC were exposed to dynamic shear stress waveforms of left coronary artery and TNF-α treatment for 1 hr. Small black dots are the platelets. Images were taken in 40X magnification. Bars represent 100 μm.

vWF, ICAM-1, and TF protein expression

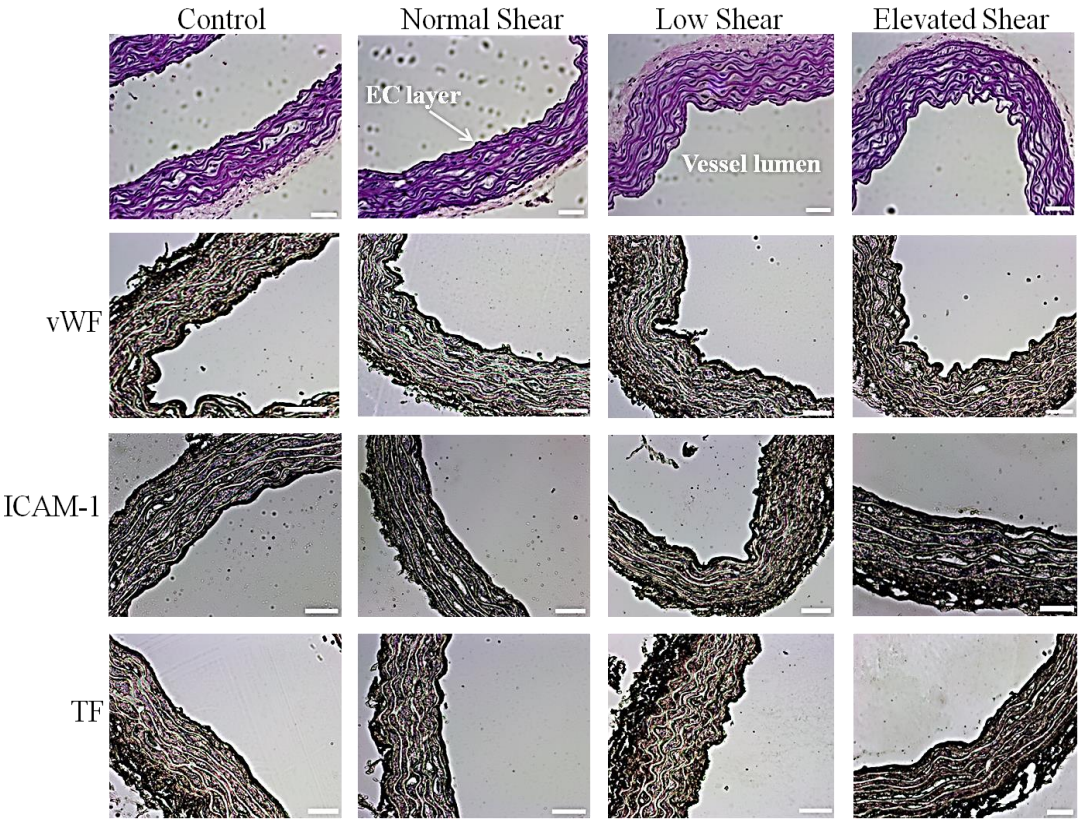

Figure: Top panel: H&E stained cross sections of control and sheared (exposed under dynamic shear stress waveforms of left coronary artery) aorta. Images indicate that shear stress exposure did not damage the aorta wall, as the vessel wall morphology looks intact. Bottom three panels: EC activation visualized through vWF, ICAM-1, and TF immunostaining on cross sections of control and shear stress (normal, low, and elevated) exposed (for 2 hr) aortas. All images were taken at 10X magnification. (Scale bar: 100 μm).

Levels of ERK1/2, JNK, and p38 phosphorylation of EC in presence of platelets

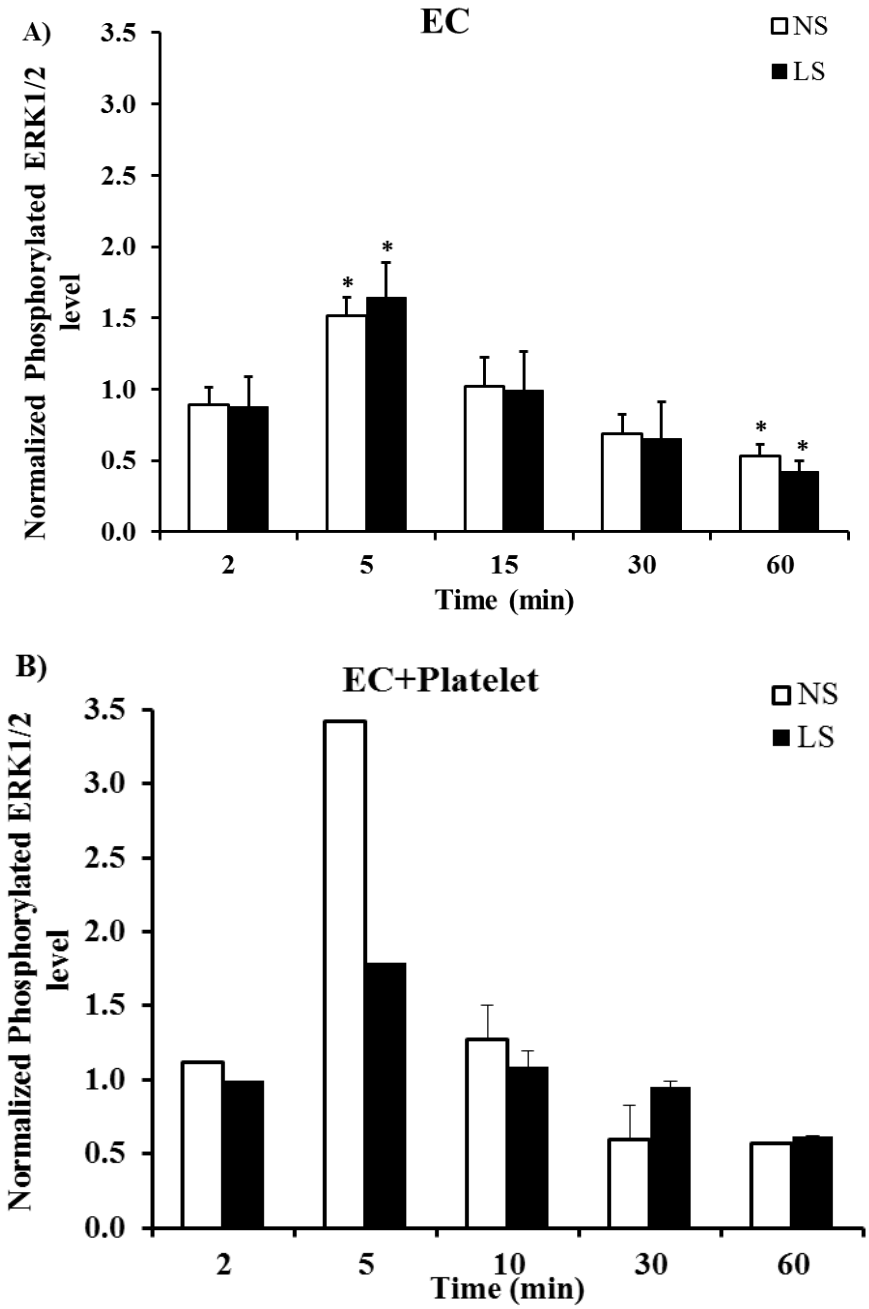

Figure: Normalized phosphorylated ERK1/2 levels in EC exposed to normal or low shear stress without (A) or with (B) platelets. Increased level of phosphorylated ERK1/2 was observed in the presence of platelets. A decreasing phosphorylation trend was also observed in the presence of platelets with increasing shear exposure time. Data are presented as Mean+SD. (*- significantly different than the level of phosphorylation of non-sheared control EC. $P<0.05$, one-way ANOVA).

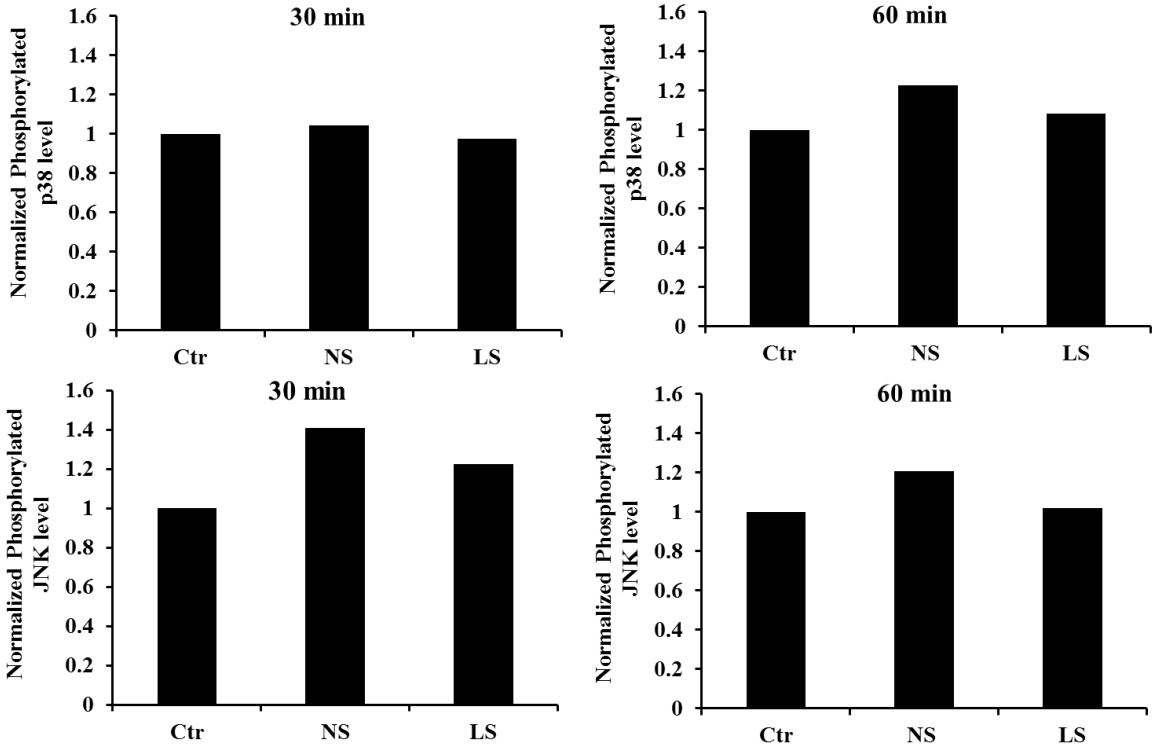

Figure: Normalized phosphorylated p38 (top panel) and JNK (bottom panel) levels in EC exposed to normal shear (NS) or low shear (LS) stress for 30 min or 60 min in presence of platelets. Presence of platelets increased p38 and JNK phosphorylation level in EC at both time points compared to the corresponding expressions of EC sheared in absence of platelets. Data are presented as Mean+SD. (*- significantly different than the level of phosphorylation of non-sheared control EC incubated in presence of platelets. $P<0.05$, one-way ANOVA).

Phosphorylated NF-κB (p65) activation of EC in presence of platelets

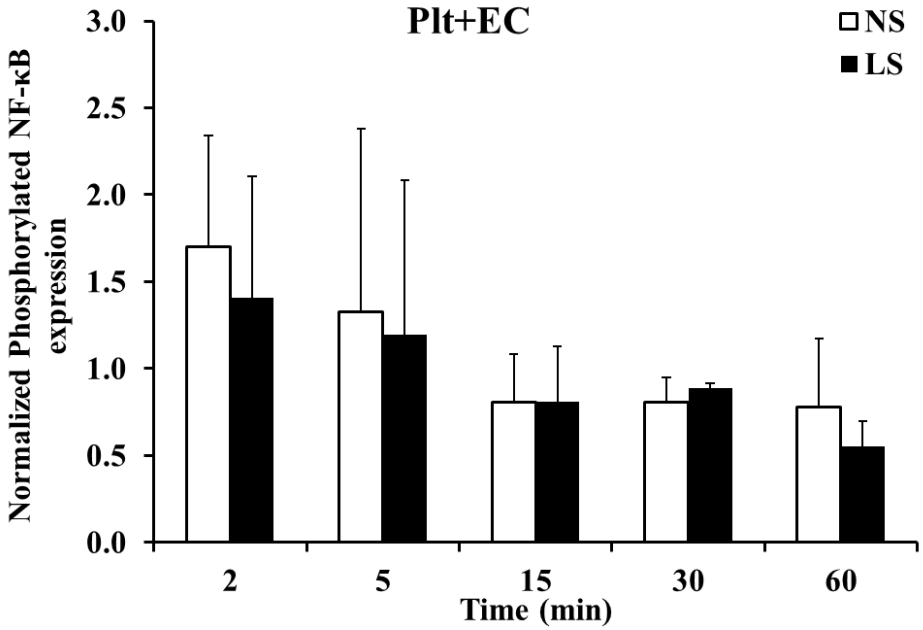

Figure: Normalized phosphorylation level of NF-κB of EC exposed to dynamic [normal (NS) or low (LS)] shear stress in presence of platelets (Plt). NF-κB phosphorylation level reached the peak within 2 min of shear exposure and decreased with further shear exposure duration. Data are presented as Mean+SD. More experiments were needed to reach a definite conclusion.

EC surface VEGFR1 and VEGFR2 expression

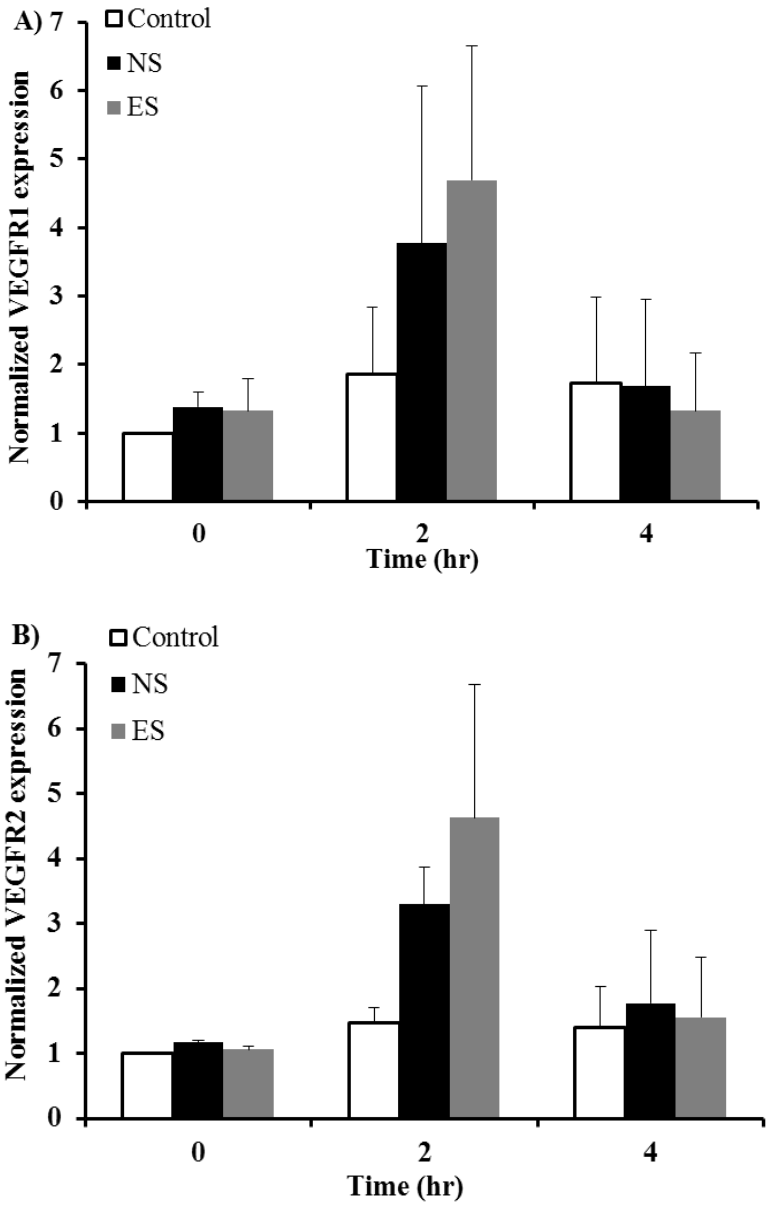

Figure: VEGFR1 and VEGFR2 expression on EC surface following exposure to normal (NS) or elevated (ES) dynamic shear waveforms of coronary collateral artery for 1 hr. Post-shear, samples were incubated for 0, 2, or 4 hr prior to quantification of VEGFR1 and VEGFR2 expression. All mean fluorescence intensity values were normalized to the 0 hr static control sample. Data are presented as Mean+SD.

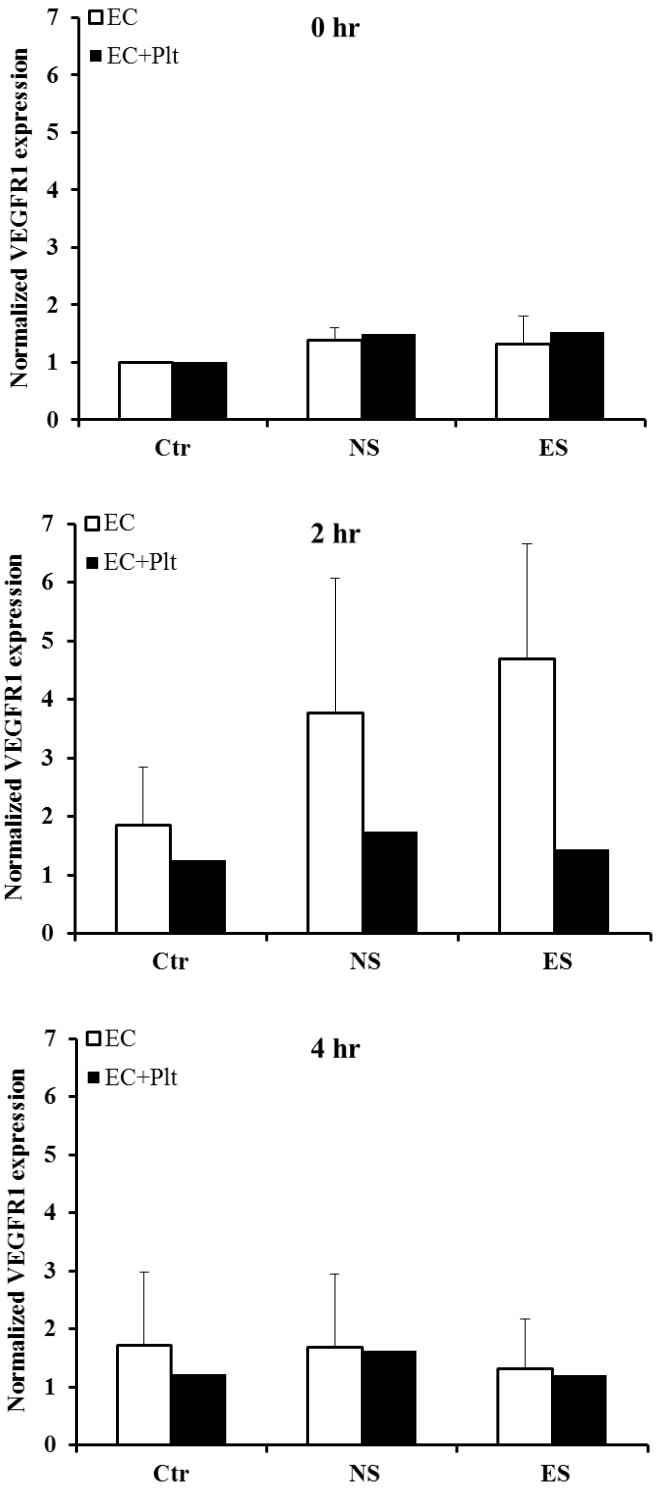

Figure: Effect of normal (NS) and elevated (ES) dynamic shear stress of coronary collateral artery on EC surface VEGFR1 expression in the absence or presence of platelets (Plt), assessed 0, 2, or 4 hr after shear exposure. EC surface VEGFR1 expression was not upregulated by dynamic shear stress in the presence of platelets. Data were normalized to the 0 hr static control EC and are presented as Mean+SD.

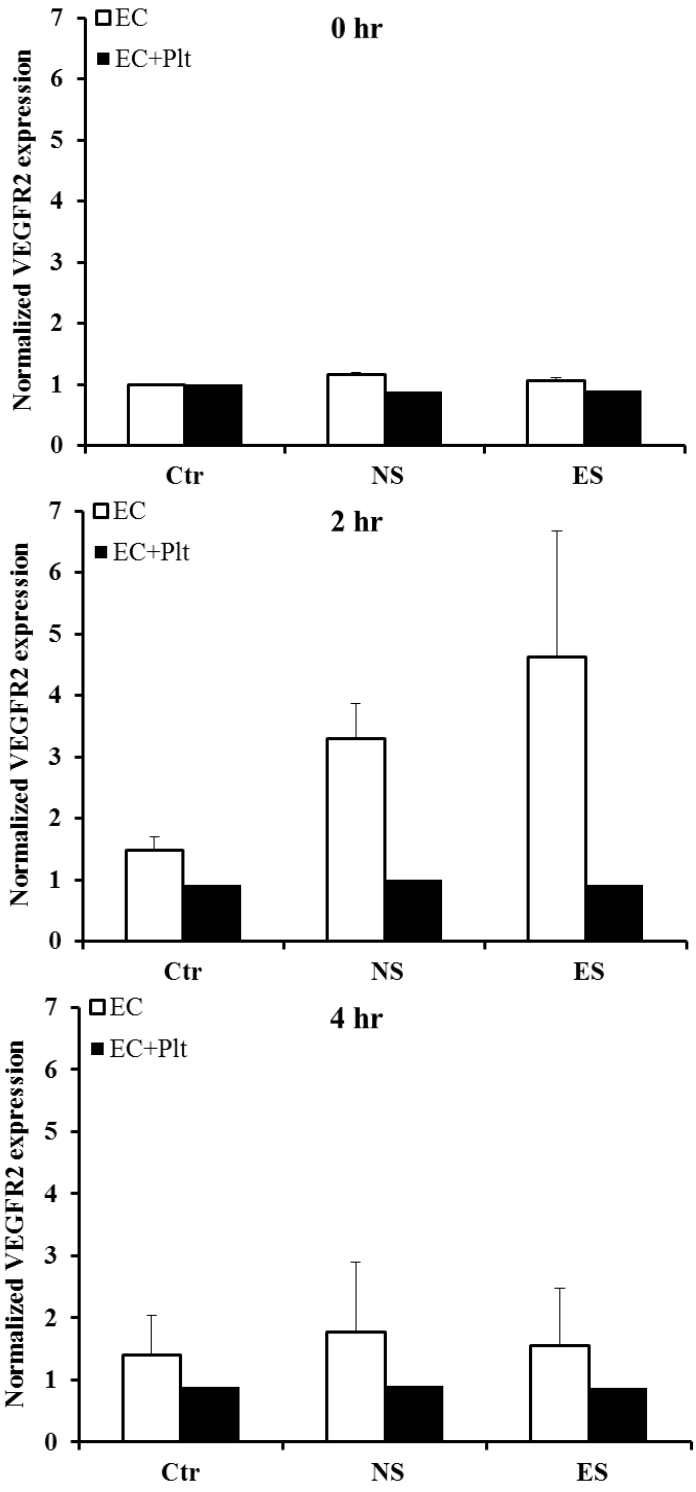

Figure: Effect of normal (NS) and elevated (ES) dynamic shear stress of coronary collateral artery on EC surface VEGFR2 expression (normalized to 0 hr static EC expression) assessed 0, 2, or 4 hr after 1 hr shear exposure without or with platelets (Plt). EC surface VEGFR2 expression was not upregulated by shear in the presence of platelets. Data are presented as Mean+SD.

VITA

Farzana Rouf

Candidate for the Degree of

Doctor of Philosophy

Thesis: RESPONSES OF VASCULAR CELLS TO SHEAR STRESS AND DIABETES-ASSOCIATED METABOLIC DYSFUNCTION

Major Field: Mechanical and Aerospace Engineering

Biographical:

Education:
Completed the requirements for the Doctor of Philosophy in Mechanical and Aerospace Engineering specializing in Biomedical Engineering, Vascular remodeling, Biofluidics, and Biomechanics at Oklahoma State University, Stillwater, Oklahoma in December, 2016.

Completed the requirements for the Master of Science in Mechanical and Aerospace Engineering at Oklahoma State University, Stillwater, Oklahoma in May, 2011.

Completed the requirements for the Bachelor of Science in Mechanical Engineering at Bangladesh University of Engineering and Technology (BUET), Dhaka, Bangladesh in February 2008.

Experience:
Research Assistant - Vascular Remodeling lab (Jan 2014 – July 2016)
Department of Physiological Science, Oklahoma State University, Stillwater
Research Assistant - Biomedical engineering lab (Jan 2010 – July 2013)
Department of Mechanical and Aerospace Engineering, Oklahoma State University, Stillwater, Oklahoma
Teaching Assistant – Department of Mechanical and Aerospace Engineering, Oklahoma State University, Stillwater, Oklahoma
Fluid Mechanics (Jan 2016 – May 2016)
Engineering Analysis (Jan 2014 – May 2016)
Biomechanics (Jan 2012 – May 2012, Jan 2013 – May 2013)
Instrumentation and Measurement (Aug 2009–Dec 2011, Aug 2013–Dec 2013)

Professional Memberships:
American Physiological Society (APS)
Biomedical Engineering Society (BMES)
The Institution of Engineers in Bangladesh (IEB)